

Alma Mater Studiorum – Università di Bologna

DOTTORATO DI RICERCA IN:

ARCHITETTURA

Ciclo XXXI

Settore Concorsuale: 08/E1 – DISEGNO

Settore Scientifico Disciplinare: ICAR/17 – DISEGNO

ALGORITHMIC MODELLING OF FOLDED SURFACES.

**Analysis and Design of Folded
Surfaces in Architecture and Manufacturing.**

Presentata da: Riccardo Foschi

Coordinatore Dottorato:

Annalisa Trentin

Supervisore:

Fabrizio Ivan Apollonio

Co-supervisor:

Federico Fallavollita

Tomohiro Tachi

Esame finale anno 2019

Abstract

Both in the field of design and architecture origami is often taken as a reference for its kinetic properties and its elegant appearance. Dynamic facades, fast deployment structures, temporary shelters, portable furniture, retractile roofs, are some examples which can take advantage of the kinetic properties of the origami. While designing with origami, the designer needs to control shape and motion at the same time, which increases the complexity of the design process. This complexity of the design process may lead the designers to choose a solution where the patterns are mere copies of well-known patterns or to reference to the origami only for ornamental purposes. The origami-inspired projects that we gathered and studied in the fields of architecture, manufacturing and fashion, confirmed this trend. We observed that the cause of this lack of variety could also be attributed to insufficient knowledge, or to inefficiency of the design tools. Many researchers studied the mathematical implications of origami, to be able to design specific patterns for precise applications. However, this theoretical knowledge is hard to apply directly to different practical projects without a deep understanding of these theorems. Thus, in this thesis, we aim to narrow the gap between potentialities of this discipline and limits of the available designing tools, by proposing a simplified synthetic constructive approach, applied with a parametric modeller, which allows the designers to bypass scripting and algebraic formulations and, at the same time, it increases the design freedom. Among the cases studies, we propose some fabrication-aimed examples, which introduce the subjects of thick-origami, distribution of stresses and analysis of deformations of the folded models.

Nei campi dell'architettura e dell'industrial design, l'origami è spesso preso come riferimento per le sue proprietà cinetiche e le sue forme eleganti. Facciate dinamiche, strutture pieghevoli, rifugi temporanei, arredi portatili, tetti retrattili, sono alcuni esempi di progetti che potrebbero beneficiare delle proprietà cinetiche dell'origami. Progettare con l'origami richiede di controllare forma e movimento contemporaneamente; ciò aumenta la complessità del processo progettuale. Questa difficoltà progettuale può portare i progettisti a scegliere soluzioni che non sono altro che mere copie di pattern noti o a considerare l'origami come riferimento solo per ragioni ornamentali. I progetti ispirati all'origami che abbiamo raccolto ed analizzato nei campi di architettura, industria manifatturiera, e moda, confermano questo trend. Abbiamo osservato che la causa di questo mero utilizzo potrebbe essere attribuibile a preparazione insufficiente del progettista o a inefficienza degli strumenti progettuali. Diversi ricercatori hanno studiato le implicazioni matematiche dell'origami, per poter progettare specifici pattern per precise applicazioni. Nonostante ciò, questa conoscenza teorica è difficile da applicare direttamente ad altri progetti pratici senza una profonda comprensione di questi teoremi. Questa tesi punta quindi a ridurre il divario tra potenzialità di questa disciplina e limiti imposti dagli strumenti progettuali disponibili, proponendo un approccio sintetico e costruttivo semplificato, che permetta ai progettisti di evitare scripting e formulazioni algebriche, aumentando allo stesso tempo la libertà progettuale. Tra i casi studio, proponiamo anche alcuni esempi mirati alla fabbricazione che introducono il tema dell'origami a spessore non nullo, della distribuzione delle forze e dell'analisi delle deformazioni sui modelli piegati.

Acknowledgements

This thesis was possible thanks to the Department of Architecture of Bologna University, the Marco Polo grant and the School of Arts and Science of the Tokyo University. I want to thank all the persons that followed me in this journey into applied origami, in particular, the professors: Fabrizio Ivan Apollonio, Federico Fallavollita, Tomohiro Tachi that guided me for these three intense years, and the professor Yasushi Yamaguchi that allowed me to join his research team in Tokyo. I want also to thank professors Yoshinobu Miyamoto and Graziano Mario Valenti who revised the thesis precisely and gave me important suggestions to improve its form and clarity. Special thanks to all my PhD mates and research colleagues with whom I passed the last three years sharing sweat and joy, in particular, Kai Suto for the profitable time we passed together at Komaba campus in Tokyo, without whom I could not achieve certain results on degree-4 vertices and prototyping. I also want to thank my dear friend Marco Mandia who helped me thinking with a programmer point of view and handling delicate mathematics and Carolina Gelsomini who helped me with some English forms and took me up when I was down. Last but not least, I want to thank my family who helped me economically and humanly during these three years without whom this thesis would not be possible.

Summary

1. CHAPTER I: Aims, Tools and Background	11 -
1.1. Introduction.....	- 11 -
1.2. Aims of the Research	- 11 -
1.3. Research Field.....	- 12 -
1.4. Structure of the Thesis	- 13 -
1.5. Tools	- 13 -
1.5.1. Comparing “Synthetic” and “Analytical” Methods	- 14 -
1.5.2. Conclusions About the “Synthetic method”.....	- 18 -
1.5.3. Existing Software for Designing Origami.....	- 18 -
1.6. Background.....	- 20 -
1.6.1. Brief History of Origami	- 20 -
1.6.2. Origami in Education – Art, Design and Math	- 22 -
1.6.3. Math Meets Art - Most Known Methods to Design Origami	- 24 -
1.7. References – CHAPTER I	- 26 -
2. CHAPTER II: Origami-Inspired Designs	29 -
2.1. Classification Criteria	- 29 -
2.2. Permanent Architecture - Synoptic Tables	- 30 -
2.3. Temporary Architecture - Synoptic Tables.....	- 33 -
2.4. Installations - Synoptic Tables.....	- 34 -
2.5. Goods and Furniture - Synoptic Tables	- 35 -
2.6. Fashion and Clothing - Synoptic Tables.....	- 40 -
2.7. Data Processing – Trend of Each Field.....	- 41 -
2.8. Designing with Folded Surfaces - Critical Observations.....	- 43 -
2.9. References - CHAPTER II.....	- 44 -
3. CHAPTER III: Definitions and Theorems.....	46 -
3.1. Fold Angle	- 46 -
3.1.1. Fold Angle Over Time - From Plot Analysis.....	- 46 -
3.2. Developability.....	- 49 -
3.3. Degree of Freedom (DOF).....	- 50 -
3.4. Rigid-Foldability.....	- 51 -
3.4.1. Reciprocal Diagram to Judge the First-Order Rigid-Foldability.....	- 52 -
3.5. Flat-Foldability	- 53 -
3.5.1. Four Rules of Flat-Foldability - Kawasaki and Maekawa Conditions	- 53 -
3.5.2. Flat-Foldable Degree-4 Single Vertex – Relations Between Fold Angles.....	- 54 -
3.5.3. Flat-Foldable Degree-4 Single Vertex – Reciprocal Diagram and Fold Angles.....	- 56 -

3.5.4.	Calculating k Through Reciprocal Diagram – Proved by Experimental Method.....	- 57 -
3.6.	Non-Flat-Foldability	- 58 -
3.6.1.	Non-Flat-Foldable Degree-4 Single Vertex - Huffman’s Formulations.....	- 58 -
3.6.2.	The Blocking Crease	- 61 -
3.6.3.	Understanding the Kinematics of a Non-Flat-Foldable Developable Degree-4 Vertex	- 61 -
3.6.4.	First Blocking Crease in a Developable Degree-4 Vertex.....	- 63 -
3.6.5.	Other Fold Angles at Blocked State – With the Spherical Law of Cosine.....	- 65 -
3.7.	Conclusions – Relation Between Origami Functionality and Real Applications.....	- 66 -
3.8.	References – CHAPTER III.....	- 66 -
4.	CHAPTER IV: Constructive Methods for Solving the Kinematics of Origami.....	- 68 -
4.1.	Families of Folded Surfaces	- 68 -
4.2.	Operative Tools.....	- 69 -
4.3.	Analogy with Computer Programming and Terminology Clarification	- 69 -
4.3.1.	Clustering and Nesting	- 69 -
4.3.2.	Definition of “Algorithm”	- 70 -
4.4.	Single Linear Crease	- 70 -
4.4.1.	Single Linear Crease Between Equal Rectangular Faces, Two Edges Slide on Construction Plane – Intersecting Circles	- 70 -
4.4.2.	Single Linear Crease Between Asymmetric Rectangular Faces, Two Edges Slide on Construction Plane – Intersecting Circles	- 72 -
4.4.3.	Single Linear Crease Between Rectangular Faces, Crease on Construction Plane – Varying Fold Angle	- 72 -
4.4.4.	Single Linear Crease Between Triangular Faces, Crease on Construction Plane – Varying Fold Angle	- 73 -
4.4.5.	Single Linear Crease Between Triangular Faces, Two Edges Slide on Construction Plane – Intersecting Circles.....	- 74 -
4.4.6.	Single Linear Crease Between Trapezoidal Faces, Two Edges Slide on the Construction Plane – Intersecting Circles.....	- 75 -
4.5.	Patterns with Multiple (Non-Intersecting) Linear Creases.....	- 76 -
4.5.1.	Straight Accordion – Array of “Single Linear Crease Between Rectangular Faces” Molecules.	- 77 -
4.5.2.	Straight Accordion Sliding on a Rail – Intersecting Circles.....	- 77 -
4.5.3.	Straight Accordion on a Rail with Non-Uniform Fold Angle Distribution – Intersecting Circles and “Graph Mapper”	- 79 -
4.5.4.	Accordion on Two Circular Rails – Intersecting Circles.....	- 80 -
4.5.5.	Triangulated Accordion – Joining Multiple “Single Linear Crease Between Triangular Faces” Molecules	- 81 -
4.6.	Single Degree-4 Vertex.....	- 83 -
4.6.1.	Symmetric Reverse Fold – Reflecting a Single Linear Crease.....	- 84 -
4.6.2.	Asymmetric Reverse Fold – Reflection and Collision Detection.....	- 85 -

4.6.3.	Generic Degree-4 Vertex – Intersecting Cones.....	- 86 -
4.7.	Multiple Degree-4 Vertices.....	- 88 -
4.7.1.	Joining “Symmetric Reverse Fold” Molecules – Critical Observations About Global Rigid-Flat-Foldability.....	- 88 -
4.7.2.	Joining “Asymmetric Reverse Fold” Molecules	- 90 -
4.7.3.	Reverse Fold on Triangulated Accordion – Joining “Symmetric Reverse Fold” Molecules.....	- 91 -
4.7.4.	The Miura Pattern – Planar Rectangular Array of “Symmetric Reverse Fold” Molecules – Intersecting Circle with Plane of Symmetry	- 94 -
4.7.5.	The sink fold – Reflecting the tip of a degree-4 vertex.....	- 96 -
4.8.	Patterns with Single or Multiple Degree>4 Vertices	- 98 -
4.8.1.	Degree>4 Vertices – Physical Simulation.....	- 99 -
4.8.2.	Testing the Algorithm with Different Patterns.....	- 101 -
4.8.3.	Limits of the Algorithm and Known Problems – Pop-Up and Pop-Down.....	- 103 -
4.9.	References – CHAPTER IV	- 104 -
5.	CHAPTER V: Pattern Design from a Given Shape	- 106 -
5.1.	Lampshade – Vertices Extrusion and Reflection.....	- 106 -
5.2.	Folded Facade – Vertices Extrusion from Reference Curved Rails	- 108 -
5.3.	Building Envelope – Reflection of a Creased Developable Surface.....	- 110 -
5.4.	Curve-Folded Table	- 112 -
5.4.1.	Reflection of a Developable Curved Surface	- 112 -
5.4.2.	Discretization of the Curved Crease.....	- 113 -
5.5.	Conformable Corrugated Suspended Ceiling	- 114 -
5.5.1.	Conformation of a Rigid Creased Surface to a Curved Surface.....	- 115 -
5.5.2.	Conformation of a Flexible Miura-Ori to a Curved Surface	- 117 -
5.5.3.	Optimization of Supporting Cables and Anchor Points	- 119 -
5.5.4.	Changing shape to the Surface - Adjusting Cables Lengths	- 121 -
5.6.	References – CHAPTER V.....	- 122 -
6.	CHAPTER VI: Fabrication-Aimed Designs	- 123 -
6.1.	Known Origami Thickening Methods – State of the Art.....	- 123 -
6.1.1.	Offset Panels	- 124 -
6.1.2.	Hinge Shifting	- 124 -
6.1.3.	Tapered Panels	- 124 -
6.1.4.	Constant Thickness Attached Panels.....	- 125 -
6.1.5.	Membrane Hinges	- 125 -
6.1.6.	Rolling Contact or “SOURCE” Technique.....	- 126 -
6.1.7.	Strained Joint.....	- 126 -
6.1.8.	Double Hinge	- 127 -
6.1.9.	Symmetric Miura-Ori Vertex by Shifted Hinges and Carved Panels.....	- 127 -

6.1.10.	Slidable Hinges.....	- 127 -
6.1.11.	Double Line.....	- 128 -
6.2.	Case Study - One-DOF, Developable, Non-Flat Rigid-Foldable Ladder	- 129 -
6.2.1.	Preliminary Paper Prototype and Digitalization.....	- 129 -
6.2.2.	Fine-Tuning the Dimensions of the Ladder with Trigonometry	- 130 -
6.2.3.	Thickening – “Offset Panels” Method.....	- 131 -
6.2.4.	Thickening – “Tapered Panels” Method	- 132 -
6.2.5.	Thickening – “Double Line” Method.....	- 134 -
6.2.6.	Stability Problems and Possible Solutions	- 136 -
6.3.	Case Study - One-DOF, Developable, Non-Flat Rigid-Foldable Chair	- 138 -
6.3.1.	Preliminary Paper Prototype.....	- 138 -
6.3.2.	Thickening – “Double Line” Method.....	- 140 -
6.3.3.	Blocked Degree-4 Vertex – From a Non-Developable Corner of 3 Faces.....	- 142 -
6.3.4.	Adjusting Shape and Dimensions to Improve ergonomics and Stability	- 143 -
6.3.5.	Human-Size Prototype of the Chair - Critical Observations	- 144 -
6.4.	References – CHAPTER VI.....	- 146 -
	Conclusions.....	- 148 -
	Outlook	- 149 -
	Bibliography.....	- 150 -
	Appendix A. Definitions and Theorems – Generative Algorithms	- 156 -
	Appendix B. Constructive Methods for Solving the Kinematics of Origami -Generative Algorithms	- 165 -
	Appendix C. Pattern Design from a Given Shape – Generative Algorithms.....	- 188 -
	Appendix D. Fabrication-aimed designs – Generative algorithms	- 203 -
	Appendix E. Glossary.....	- 206 -

1. CHAPTER I: Aims, Tools and Background

1.1. Introduction

Both in the fields of manufacturing and architecture, origami was taken as a reference for its kinetic properties, its elegant and geometric shapes, for its capability to rationalize the creative process following precise geometric rules and specific spatial references and its capacity to combine shape and motion in a functional way. If the crease is replaced with a hinge and the paper with a panel of a rigid material, or the hands of the origami artist with a CNC machine, it is not hard to imagine the numerous possible application of this art and technique. Dynamic facades, deployable structures, temporary shelters, portable furniture, retractile roofs, unfoldable boxes, are some examples of kinetic designs that can take advantage of origami constructions. Differently from structures with bars and panels, the origami can be used to obtain continuous surfaces without assembling different parts, optimizing the constructive process, the transportation, and the cost, at the expense of the designing time, in fact designing with origami makes the shape and movement harder to control with the contemporary professional computer applications.

“In the design process of such applied origami, it is very difficult for the designer to control the form to fit design contexts while preserving the necessary functionalities of the original patterns. Therefore, without sufficient knowledge or intelligent design systems, the result designs would end up in either just a mere copy and paste of an existing origami pattern or an ‘origami-inspired’ design which is not using the properties of origami in functional ways” (Demaine & Tachi, 2010).

In this research, we analysed many existing origami-inspired designs, and we noticed that the major part of these projects uses mere copies of well-known origami patterns. In accordance with Tachi and Demaine’s studies, we observed that the cause of this lack of variety could be attributed to insufficient knowledge, or to the inefficiency of the design tools. When designing with these types of surfaces it is necessary to control both shape and motion at the same time without losing the developability, consequently, some mathematical or geometrical rules must be considered. This increases complexity and time consumption when designing with origami.

1.2. Aims of the Research

Many researchers studied the mathematical implications of origami, but they are hardly directly applicable to a creative process. In this research, we propose simplified methods to design origami-like geometries, using a synthetic approach¹ based on constructions typical of the descriptive geometry, applied with a parametrical node-based application. Working with geometrical constructions and spatial references is more natural for most of the professionals that operate in the fields of manufacturing and architecture because it is related to the representation method, which is the synthetic method² usually used by architects and designers.

We are going to use the visual parametric node-based modeller called Grasshopper (and relative add-ons) as a tool to construct all the algorithms³. We chose to solve all the presented cases with the same tool because we wanted to limit as much as possible the problems generated by the file conversion between different software, which is not recommended in a professional workflow.

The variety of possibilities that the origami offers is boundless, for this reason, the aim is not to produce a specific command or a piece of software that performs specific tasks, because this would limit the designer’s freedom. Contrariwise, we want to present a series of case studies and operative guidelines which will help optimizing the design process that involves origami geometries.

All these materials are aimed at those professionals interested in origami design but without a specific background in mathematics or computer science, thus we minimize the use of scripting and algebraic formulations as much as possible.

¹ The meaning of “Synthetic method” is reported in section 1.5.1.

² A comprehensive comparison between the synthetic and the analytical methods is made in section 1.5.1 and 1.5.2

³ A detailed definition of “Algorithm” is stated in section 4.3.2.

1.3. Research Field

The origami world for his capability to combine technique and art, static nature and dynamism, straight lines and curves, recursive patterns and sculpted figures, planar configurations and three-dimensional objects, stiffness and flexibility, is versatile and applicable in a vast number of fields like engineering, manufacturing, astronomy, medicine, chemistry, architecture, robotics, computer science, art, fashion, design. The application fields are innumerable as well as the researchers that use origami constructions to improve some aspect of their projects.

One of the most influential researchers in the field of applied origami is Tomohiro Tachi. He investigates the paper folding since the first decade of the 21st century (Tachi, n.d.-a). He developed some of the most versatile and powerful computer applications focused on the design of origami, his aim is to simplify the origami design process to make it accessible to a vaster number of designers. He developed several mathematical theorems about origami, and he demonstrated their usefulness applying them in many practical applications, such as the “Rigid-origami table” which folds and unfolds in a single rigid motion or the “Vault structure” designed with rigid-foldable⁴, curved tubular arches. He also developed some techniques to thicken the zero-thickness study model while preserving the kinematics of the original pattern (Tachi, 2011b).

With similar aims and approaches, in the last few years, some researches in the “Sapienza” University of Rome in Italy explored the kinematic proprieties of origami from the point of view typical of the descriptive geometry, and they searched for solutions suitable to be applied to the field of kinetic architecture (Casale & Calvano, 2012; Casale, Valenti, & Calvano, 2013)

Erik Demaine, computer scientist, mathematician, artist and professor at MIT, has a pluriannual experience into origami science, he is nowadays one of the most active and influential theorists in the field of computational origami, he contributed to the development of some computer applications that solve some specific origami problems related to pattern design, rigid-foldability, flat-foldability and curve-folding.

Because computer applications for designing origami are lacking, many different researchers started developing their own digital tools, such as Tomohiro Tachi, Jun Mitani, Ke Liu and Glaucio H Paulino, Zhonghua Xi, only to name a few⁵. However, the first who developed a computer application to help the designers to optimize and create their own origami patterns was Robert J. Lang.

Lang is considered one of the most important origami scientist and artist of all times. He contributed to refine and extend some of the most advanced techniques still used by scientists and artists to design complex origami patterns. He also worked on several projects for aerospace applications which represent probably the most interesting and advanced frontier of this art and technique. For example, he contributed to the design of the “Eyeglass” telescope for Lawrence Livermore National Laboratory and to the “Starshade” project for NASA, which are respectively a foldable lens for a space-based telescope and an occulter for the sunlight that will be used to look for planets orbiting faraway stars (Feder, 2018). He also contributed developing an algorithm to optimize the air-bag flattening in collaboration with the EASi airbag company (Lang, 2015a).

Some other interesting uses of origami into practical applications are the “Origami-Based Deployable Ballistic Barrier” by Seymour et al. (Seymour et al., 2018); the “Deployable Locomotive Fairing” designed to improve the aerodynamics of the locomotives by Tolman et al. (Tolman, Crampton, Stucki, Mayenes, & Howell, 2018); and the origami stent by Kuribayashi et al., that facilitate the insertion of the stent inside the human body by folding it in a specific way (Kuribayashi et al., 2006). All these applications were possible also thanks to Thomas Hull, Toshikazu Kawasaki, Humiaki Huzita, Koshiro Hatori, Koryo Miura and many others who contributed to set the basis and extended the fundamental theorems of the origami mathematics.

This thesis wants to add a small contribution in this vast landscape of projects and theories, trying to narrow the gap between theories and applications, and opening this field full of possibilities to all those professionals and designers, without a specific background in engineering, mathematics and computer science, who want to use origami functionalities in their projects.

⁴ A detailed definition of rigid-foldability is given into section 3.4.

⁵ A more comprehensive analysis of existing computer applications for origami design can be found in section 1.5.3

1.4. Structure of the Thesis

CHAPTER I: Aims, Tools and Background

In the first part of this chapter, we discuss the aims of the research, the structure of the thesis, the tools that we will use, and we introduce the research field. Then we present the background of the field of the applied origami, starting from a synthesis of the origami history and its implications in mathematics, education and art. This part is aimed at those readers who have no background in applied or traditional origami, and it briefly traces the state of art of this field. This chapter is also aimed to clarify the whole philosophy of the thesis, and the storyline we want to tell. Furthermore, we try to outline clearly the connections between the different parts.

CHAPTER II: Origami-Inspired Designs

This part is focused on gathering and analysing projects inspired by origami to outline a trend for many different application fields. We divide the gathered projects into five different groups: “Permanent architecture”, “Temporary architecture”, “Installations”, “Goods and Furniture” “Fashion and Clothing”. We catalogued and characterized each project specifying which aspects are inspired by origami and why. As a result of this analysis, we highlight possible problems and potentialities about using origami-like solutions in each field.

CHAPTER III: Definitions and Theorems

In this chapter, we deal with the following topics: Fold-angle, Developability, Degree of Freedom (DOF), Rigid-foldability, Flat-foldability, Non-flat-foldability. We define every term, and for each one of them, we introduce the main known mathematical theorems. In the subsequent chapters of the thesis, we will refer to these terms and theories widely.

CHAPTER IV: Constructive Method for Solving the Kinematics of Origami

In this section, we propose a set of procedures aimed to animate some given creased unfolded patterns. We start analysing the easier cases such as patterns with a single crease, up to patterns with multiple internal vertices with several converging creases. These algorithms could help designers who need to animate rigidly known patterns preserving their initial shape, thus they are particularly useful for kinetics applications.

CHAPTER V: Pattern Design from a Given Shape

This part of the thesis is focused on design-aimed algorithms. It contains a catalogue of case studies, which aim to exemplify some applications starting from given environmental, framework or background conditions. These algorithms do not return the fold animation, but they are aimed to return always developable patterns following precise generative processes by using strict rules, applied in a precise order, which guarantee the creation of an already folded surface which is developable.

CHAPTER VI: Fabrication-Aimed Designs

In this chapter, we present Two case studies: a foldable chair and a foldable ladder. Their design processes are presented from start to finish, trying to highlight the design thinking behind each one of them, which is different case by case depending on the aim and boundary conditions. The fabrication of an origami-like geometry raises the issues of the thickening of the conceptual zero-thickness model and the problems of stability and structural stiffness under certain loads.

1.5. Tools

To model folded surfaces in a three-dimensional digital environment and to integrate them into the design of a building or a piece of furniture, it is highly preferred the use of computer applications which can exchange files with the software used by architects and designer. The less the exchanges between different computer programs the better. This is important to limit time consumption and conversion problems.

Parametric modelling is the widespread solution that is usually used to control such type of complex geometries and integrate them into the projects while speeding up the shape-finding process at the same time. Traditional 3D modelling computer programs can produce parametrical models through the integrated scripting interface, which is usable by users that can script in the programming language that the software requires. This kind of applications are tricky to use, and the programming language usually changes from one software to the other, complicating the portability between different applications. Thus, they are usually harder to learn than the logic environment of a graphical parametric node-based modeller, such as Dynamo, a plug-in for Autodesk Revit (Autodesk, n.d.), or Grasshopper, a plug-in for Rhinoceros (Rutten, n.d.). This kind of applications converts code strings in visual “nodes” that can be connected reciprocally to compose complex algorithms for documentation, fabrication, coordination, simulation and analysis. The research of the tools has been carried out analysing the international professional and academic landscape. Grasshopper has been chosen for this research for many reasons. The choice has been influenced by the capacity of being integrated with software used by both architects and designers, the versatility, the price, the usability, the number of add-ons, the active online community, the efficient assistance, the possibility to integrate missing nodes by scripting. Although, any other software can be used to achieve similar results. In this thesis, we will try to explain the procedures in the most general way, explaining them systematically, so that they can be easily transposed in a different software with a different interface.

According to the initial statement, the generative algorithms in this thesis will be carried out trying to limit as much as possible scripting and mathematical formulations, thus we will base all the definitions on geometric constructive procedures, using visual references and geometric primitives as construction tools.

This approach is comparable to the “Synthetic method”. The synthetic method has been used for centuries by mathematicians and scientists as an alternative to the analytical method and it can be compared to the field known today as “Descriptive geometry” extensively studied and disseminated by the geometer and mathematician Gaspard Monge (1746-1818) (Cardone, 2017). From that time, where ruler and compass were the most used tools, the methods and the solutions are greatly improved. Riccardo Migliari et al. into the book “Geometria descrittiva” (Migliari, 2009b, 2009a) proposes several methods to solve some old and new problems of descriptive geometry with three-dimensional modelling applications. Today we can work into three-dimensional space, and we can move the point of view in space to verify spatial relations easier. We can also measure distances and angles without needing to project them into auxiliary planes, which does not only simplify the visualization of the problems, but it also may simplify the actual constructions needed to solve those problems. Furthermore, nowadays, the accuracy when drawing with this kind of applications is incredibly high, this gives to the synthetic method great possibilities when looking for new problems and new solutions.

The researchers of the Roman school, to which Migliari belong, studied for many decades, until nowadays, the synthetic method and its implications, and they use it to study and solve complex modern geometrical problems or to verify problems from the past (Carlevaris, De Carlo, & Migliari, 2012; Fallavollita, 2008; Fallavollita & Salvatore, 2013; Migliari, 2008b, 2008a, 2012; Salvatore, 2012). An interesting contribution from the Roman school, related to the topic of this thesis, is the book “Architettura delle superfici piegate” written by Andrea Casale and Graziano Mario Valenti (Casale et al., 2013) who use geometric constructions applied with the computer to solve the kinematics of origami. Our contribution is strictly related to this school of thinking, thus, the case studies that we will present will be carried out with the synthetic method applied with parametric 3D-applications.

In the following section, we will clarify the meaning of the word “Synthetic” and we will show that the synthetic method has the same dignity as the analytical method, and it can be considered as a research tool capable of proving and visualizing things with the same power (and for some aspects even more) as the analytical method. We will report the definitions of both methods clarifying them with examples, and we will conclude by reporting the pros and cons of both.

1.5.1. Comparing “Synthetic” and “Analytical” Methods⁶

The word “Synthetic” has many different meanings depending on the field where it is used. The Oxford English dictionary and the Merriam Webster American dictionary reports the following definitions:

- *“Having truth or falsity determinable by recourse to experience. Compare with analytic”*,

⁶ In this section we translated reported and commented the contents of the chapter X of the book by Gino Loria “*Metodi matematici: essenza, tecnica, applicazioni*”; and some extracts from the book “*Dei due metodi analitico e sintetico discorso dell'abate*” by Federico Maria Zanelli (Loria, 1935)

- “Relating to or involving synthesis: not analytic”,
- “Attributing to a subject something determined by observation rather than analysis of the nature of the subject and not resulting in self-contradiction if negated”.

The word “Method” means:

- “A particular procedure for accomplishing or approaching something, especially a systematic or established one.”,
- “A way, technique, or process of or for doing something”.

The IGI global dissemination of knowledge gives very exhaustive definitions of the two words combined “Synthetic method”:

- “The synthetic method starts like induction from the observed facts and the inferred theory (but it can also start like deduction from a set of assumptions). On this basis, the synthetic method engineers an artificial system, the objective being that, while operating, this system will behave like the real one, thus confirming the tested theory”.

Considering these definitions, we can say that a synthetic method is the counterpart of the analytical method. Thus, to fully understand what synthetic method means, we also need to define the analytical method. An interesting comparison between the analytical and the synthetic methods was made by Federico Maria Zinelli in the book “Dei due metodi Analitico e Sintetico Discorso dell’Abate”⁷ (Zinelli, 1832) (Figure 1).

Definizione del metodo sintetico.

Questo metodo naturale di procedere dal cognito all'ineognito, nel quale abbiamo già fatto dimostro, come si ritrovino tutte le note caratteristiche attribuite si dagli antichi, come dai moderni filosofi al metodo sintetico, si può definire così: Quando dati certi principii o per se conosciuti, o per esperienza, o per ragionamento, quelli combinando per le sole leggi della associazione delle idee, se ne deducono delle conseguenze per mezzo della ragione, si procede per metodo sintetico.

Figure 1: definition of the Synthetic method written by Federico Maria Zanelli, from the book “Dei due metodi analitico e sintetico discorso dell’abate” 1832.

Zinelli asserts that the synthetic method is: “A natural way to proceed from known to unknown... given some principles, taken from our knowledge or from experience, or from reasoning, combining them with association of ideas, we can deduct some consequences with logic, this is the synthetic method.”

⁷ “Abbot’s speech about the two methods Analytical and Synthetic”

Questo metodo opportuno a ricercare la verità, che non si conosce; nel quale si ritrovano tutte le note caratteristiche attribuite sì dagli antichi, come da' moderni filosofi al metodo analitico, si può definire così: Quando una cosa non si conosce in se stessa, ma bensì nel rapporto complesso, ch'essa ha ad altre cose ben conosciute, si va sciogliendo questa relazione in una più semplice, e così via via; fino a che si giunga ad una sì semplice, per cui si discopra la cosa ignota, si procede alla scoperta della verità col metodo analitico.

Definizione del metodo analitico.

Figure 2: definition of the Analytical method written by Federico Maria Zanelli, from the book "Dei due metodi analitico e sintetico discorso dell'abate" 1832.

He defines the analytic method as "A method suitable to find an unknown truth... when a thing is not known, but it is known the relations between that thing and other known things. The unknown thing can be understood by going from a relation to an easier one and so on, so we proceed to the discovery of the truth with the analytic method".

Mentre poi il metodo analitico porge questa utilità in confronto del sintetico, che senza avere i principii, dai quali dipende una verità, si può procedere alla investigazione; perchè il metodo stesso va suggerendoli, e dimostrandoli all'uopo; d'altra parte si dee confessare, che perciò appunto egli allunga le dimostrazioni; sebbene questo difetto potrebbe essere con arte diminuito, quando altri non dica ancora affatto tolto e levato. Richiamiamoci alla memoria l'ultima conchiusione di quell'esempio geometrico, trattato con metodo analitico, e vedremo che la quistione si riduce a divider AB in due parti in modo, che il quadrato di una parte sia eguale al rettangolo di tutta AB nell'altra parte. Siccome ciò si sapea eseguire; abbiamo colà posto fine all'Analisi. Che se ciò non fosse stato insegnato anteriormente, saremmo andati sciogliendo questa relazione col metodo analitico fino a che fosse ridotta a' primi principii.

Differenza fra l'uno e l'altro metodo in riguardo ai principii generali.

Figure 3: comparison between the two methods written by Federico Maria Zanelli, from the book "Dei due metodi analitico e sintetico discorso dell'abate" 1832.

He also compares the two methods saying that in the analytical method if we want to use a fact as a base to prove another fact, if it is not proved previously, we must proceed to prove it in the first place. Therefore, it may make the analytical demonstration longer than the synthetic one.

To further clarify the differences between the two methods, we report an example proposed by Gino Loria into the book "Metodi Matematici: essenza, tecnica, applicazioni"⁸. He asserts that to analytically prove the existence of the regular convex polyhedra we can use the following formulation, which is known as the Euler's polyhedron formula:

$$F + V = E + \chi. \quad (1)$$

where F is the number of the faces, V is the number of vertices, E is the number of edges and χ is the Euler's characteristic, which is a number that describes topological shape and structure of a polyhedron. This equation is known as the Euler's polyhedron formula. For every convex polyhedron we have:

$$F + V - E = 2. \quad (2)$$

⁸ "Mathematical methods: essence, technique, applications"

and if we call n the number of the edges of every face and m the number of edges connected to each solid angle, we will have:

$$nF = 2S, \quad mV = 2S. \tag{3}$$

Then if we combine these with the previous formulation we will have:

$$S = \frac{1}{\frac{1}{m} + \frac{1}{n} - \frac{1}{2}}, \quad F = \frac{\frac{2}{n}}{\frac{1}{m} + \frac{1}{n} - \frac{1}{2}}, \quad V = \frac{\frac{2}{m}}{\frac{1}{m} + \frac{1}{n} - \frac{1}{2}}. \tag{4}$$

These numbers must be positive, and integers and m and n must satisfy the relations:

$$\frac{1}{m} + \frac{1}{n} - \frac{1}{2} > 0 \quad \text{or} \quad (m - 2)(n - 2) < 4. \tag{5}$$

Thus, the only possible values for m and n are the ones that satisfy the following relations:

$$(m - 2)(n - 2) = 1, \quad (m - 2)(n - 2) = 2, \quad (m - 2)(n - 2) = 3. \tag{6}$$

And because $m, n \geq 3$ the only possible solutions of m and n are given by the following pair of numbers:

$$3,3 \qquad 3,4 \qquad 4,3 \qquad 3,5 \qquad 5,3$$

Now if we calculate F, V, S they will be all integer and positive numbers as reported in the following table:

Table 1: regular polyhedra geometrical properties.

	F	V	S
Tetrahedron	4	4	6
Hexahedron (Cube)	6	8	12
Octahedron	8	6	12
Dodecahedron	12	20	30
Icosahedron	20	12	30

From that, we can say that the only possible regular polyhedra are five and they are: the tetrahedron, the hexahedron (cube), the octahedron, the dodecahedron and the icosahedron.

To prove the existence of platonic solids with the Synthetic method, Loria proposes the following example by using only geometrical constructions.

Tetrahedron – Construct an equilateral triangle ABC given the edge l and the centre O ; the perpendicular line to the plane of the triangle from the point O is the set of points equidistant to the vertices; thus if we draw a sphere with centre O and radius l and we call D the point of intersection between the sphere and the perpendicular line, the four triangles DBC, DCA, DAB and ABC will be equal, and they will define a regular tetrahedron.

Hexahedron – Construct a square $ABCD$ with edge l ; from its vertices trace the lines perpendicular to its lying plane. From the same side of the plane draw the four segments AA_1, BB_1, CC_1, DD_1 , all the segments are equal to l . The points A_1, B_1, C_1, D_1 belong to the same plane and with the points, A, B, C, D they are the vertices of a polyhedron defined by 6 equal squares as we wanted.

Octahedron – Construct a square $ABCD$ with edge l ; find the centre O by drawing the diagonals; draw the perpendicular line to its lying plane passing from O ; this line is the set of points equidistant from the vertices of the square; then we call

E, F the intersections of that perpendicular line to the sphere centred in A and with radius l ; the eight resultant triangles $EAB, EBC, ECD, EDA, FAB, FBC, FCD, FDA$ are the faces of the regular octahedron.

Dodecahedron – $ABCDE$ is a regular pentagon with each edge equal to l ; we call $\alpha (=108^\circ)$ each angle of the Pentagon. From A , trace a line which makes with the edges AB and AE angles equal to α ; on that line mark the segment $AA_1=l$. Draw the segments BB_1, CC_1, DD_1, EE_1 in the same way all on the same side of the plane where the Pentagon lies; we close the polyline A_1ABB_1 with two new segments B_1P and A_1P so that they form a regular planar pentagon. In the same way, we draw the regular pentagons $BB_1QC_1C, CC_1LD_1D, DD_1ME_1E, EE_1NA_1A$; in this way we have obtained a poly-surfaces formed by six regular equal pentagons which end with a decagonal skewed polyline $A_1PB_1QC_1LD_1ME_1N$ that does not lie on a plane. Now if we construct another poly-surface equal to the first one, and we place it so that their decagonal naked edges match, we will obtain a regular polyhedron with twelve equal pentagonal faces with all the characteristics of the regular dodecahedron whose existence we wanted to prove.

Icosahedron – $ABCDE$ is again a regular pentagon with edge l and centre O . The perpendicular line to the plane passing from O is the set of points equidistant from the vertices of the Pentagon. If F is the intersection of that perpendicular line with the sphere centred in A with radius l , we will be able to construct five equal triangles around the point F . Now, because from the point B we can see starting three segments BA, BF, BC , that makes angles of 60° one to each other, we can add two new segments BG and BH that forms angles of 60° one to each other and with the pre-existent segments starting from B . In this way we will be able to draw three new equilateral triangles that share the vertex B . Now, if we draw a segment with length l from C that forms with the segments CD and CH angles of 60° and we will be able to draw two new equilateral triangles equal to all the other triangles. In total, we have ten triangles that make an open polysurface. Construct a new open polysurface equal to the first one and place it so that the naked edges match perfectly; in this way, we obtained a regular polyhedron that possesses all the characteristics of an Icosahedron. Thus, also the existence of the icosahedron is proved.

1.5.2. Conclusions About the “Synthetic method”

In conclusion, using Loria’s words, we can say that if we want to prove something with the analytical approach we start from the solution and walking backwards we reduce the problem to minimal components that we compare to other easier problems already proved before or with already known solutions. Contrariwise, with the synthetic method, we build a series of considerations that step by step leads to the desired purpose. We can say that the analytical method is a process of research as well as the synthetic method, and the synthetic method by no means have to be considered less scientific or accurate than the analytical method, in fact, using Loria’s words, “*It is the classical process to present any truth from an ordered series of facts*”. Nevertheless, we can say that the analytical method is usually longer than the synthetic method, but for those who know the mathematical language, it is clear and straight. Contrariwise, the synthetic method is easy to transmit and understand when it is visualized with physical models, or by drawing, but when it is explained using only words it may become difficult to follow.

1.5.3. Existing Software for Designing Origami

Architects, designers, engineers, and artists interested in origami, have until today developed their own tools for designing origami. Ron Resh was the pioneer of computer science applied to origami:

“... *the design is a kind of feedback loop between the artist and the environment... the computer can really speed up this kind of loop, (design) and I think it greatly aid creativity... the excitement for me is to try to develop the computer as a medium for exploration and as a medium for expression.*” (Resh, 1992).

As Resh stated, the computer does not only speed up the creative process, but it becomes a medium for expression and exploration. Kostas Terzidis shares the same point of view when he says:







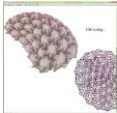


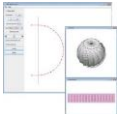

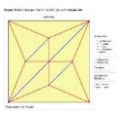
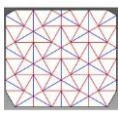
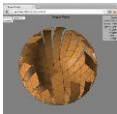

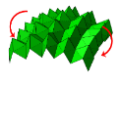
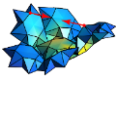
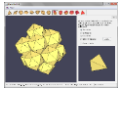
“*We shouldn’t consider the computer as an extension of the mind, but rather as a partner in the design process with fundamentally different aptitudes and ways to reason*” (Terzidis, 2006). And “*Computers should be acknowledged not only as machines for imitating and appropriating what is understood but also as vehicles for exploring and visualizing what is not (yet) understood.*” (Terzidis, 2009)

Thus, using the computer not only optimizes and speed up our design processes but also opens new unexpected possibilities. In fact, at the beginning of the twenty-first century, when computer applications for the design of origami started spreading, the complexity of the new origami models increased rapidly.

Robert J. Lang was the first to develop a stand-alone computer application to generate origami crease patterns called Treemaker (Lang, 2015c). This software was made for designing crease patterns using the circle river packing

technique⁹. In 1998 with version 4.0 this software was released outside the academic sector. Tomohiro Tachi developed several pieces of software to analyse and design origami-like geometries. Some of them are aimed to design non-flat foldable patterns or aimed to analyse the folding motion of any rigid-foldable pattern. The software developed until now by Tachi are: Freeform Origami, Origamizer, Rigid Origami Simulator, which allow the users to develop modify and analyse origami models with intuitive 2D and 3D interfaces (Tachi, n.d.-b). Jun Mitani developed: Oriref and Orirevo, made to design origami with reflections (Mitani & Igarashi, 2011) and revolutions (Mitani, 2009), and Oriipa, which is a software to design planar origami patterns and returns their collapsed flat-folded configuration. All these apps can be found on Mitani’s official web page (Mitani, n.d.). Tess is a software aimed to design origami tessellations developed by Bateman (Bateman, n.d.). Pepakura is not properly an origami software for purists, but it is somehow related to origami, because it works with folds, other than cuts, to make 2D pattern starting from a generic three-dimensional mesh (Tamasoft, n.d.). Another interesting recent application that returns the folding animation of a given origami pattern is the Origami Simulator by Amanda Ghassaei (Ghassaei, n.d.), which run directly on the internet browser. We want also to cite Merlin 2 by Ke Liu and Glucio. H. Paulino which is a versatile powerful tool for the analysis of origami structures (Kawaguchi, Ohsaki, Takeuchi, Liu, & Paulino, 2016; Liu & Paulino, 2018).

In the following table, we report some of the most important applications that concern origami and folding, at the present moment.

	1998 Treemaker Robert J. Lang		(Unknown date, probably around 2000) Pepakura Tama Software		2003 Reference finder Robert J. Lang
	2007 Tess Alex Bateman		2007 Rigid Origami Simulator Tomohiro Tachi		2008 Origamizer Tomohiro Tachi
	2010 Freeform Origami Tomohiro Tachi		2011 Oriipa Jun Mitani		2011 Oriref Jun Mitani
	2011 Orirevo Jun Mitani		2011 Orirevo Morph Jun Mitani		2013 Single Vertex Rigid Origami Simulator Zhonghua Xi
	2014 Origami Pattern Designer Zhonghua Xi		2014 Tes Generator Zhonghua Xi		2014 Rigid Origami Folder Zhonghua Xi
	2015 Origami Folder Zhonghua Xi		2017 Origami Simulator Amanda Ghassaei		2017 Merlin Ke Liu and Glucio. H. Paulino
	2018 Merlin 2 Ke Liu and Glucio. H. Paulino		2018 DeltaMod Naoya Tsuruta		

These applications (and many others not reported here), simplify the design of origami-inspired geometries and mechanisms to be used in architecture and manufacturing, but a deep theoretical origami knowledge is needed to properly use most of them. Furthermore, some applications often absolve only one single task. They are useful tools, nevertheless, they require numerous exporting and importing operations to be able to use them into a real professional workflow. These file conversions may cause loss of data while moving the model from one software to another, e.g. the mountain valley assignments, the folded or unfolded state, the folding animation, the overlapping sequence of the layers, the colour or the shader of the surface. Some researchers are already working trying to partially solve this problem through the creation of a file extension specific for origami. This innovation could revolutionize the design of these folded patterns. The file extension is called “.fold” from the GitHub repository by E. Demaine, it is defined as follows: “*FOLD (Flexible Origami*

⁹ Refer to section 1.6.3 for a brief explanation of the circle river packing technique.

List Data-structure) is a file format (with extension .fold) for describing origami models: crease patterns, mountain/valley patterns, folded states, etc. Mainly, a FOLD file can store a mesh with vertices, edges, faces, and links between them, with optional 2D or 3D geometry, plus the topological stacking order of faces that overlap geometrically. A mesh can also easily store additional user-defined data." (Demaine, n.d.).

While we wait for the enhancing of the interoperability between these applications, the solution that this thesis proposes is trying to clarify how a designer needs to think while designing with origami and what strategies he needs to follow to make a creative and interesting origami-based design. To do so we will propose a variety of algorithms and case studies using a parametric modelling software so that any designer would be able to work in the same platform without needing to move the file from one software to the other saving time and preventing data loss.

1.6. Background

1.6.1. Brief History of Origami ¹⁰

Origami has no certain origins. The paper degrades easily, for this reason, it is probably impossible to know who was the first who folded a piece of paper or when origami has been invented. The implications of the origin of traditional origami on the field of origami applied to architecture and manufacturing are minimal because the origami as we know today is very different from the one practised in ancient times. Despite that, we chose to start from here to give a wider point of view and to understand where this art came from.

There are many theories about origami origins. Someone says that origami originated in China concurrently with the paper invention around 2000 years ago, this theory is based on the fact that many believe that paper was born in 105 BCE, when the Chinese official of Han dynasty, Cai Lun, wrote a document that explained the procedure to produce paper used at the time. Koshiro Hatori in his article "History of Origami in the East and the West before Interfusion" (Hatori, 2011) states that all these assumptions are wrong, because there is no evidence of origami from that period and, furthermore, the paper wasn't invented in China in that period. Hatori reports recent studies, by Imami Sakamoto, which dates high-quality foldable bark paper around 5000 years BCE, and there are proves of a similar type of rough paper found in different parts of the world at that time (Meso-America, Hawaii, Southeast Asia). Furthermore, even if they folded the paper in half or more it is hard to consider that as an actual origami. This philosophical observation about the number of folds needed to consider a folded sheet as a proper origami makes even harder trying to date its origins. This does not mean that an independent Chinese origami tradition does not exist. For example, the "Yuan bao" is a traditional Chinese origami representing a golden nugget which was invented by an unknown probably earlier than the tenth century CE when it was already a tradition folding it and burn it at funerals (Mitchell, n.d.). There is also who believe that origami originated in Japan in the Heian era (794-1192). The theory is based on traditional anecdote where Abe-no Seimei took a piece of paper and he transmuted it into a real heron. However, even this hypothesis is not sufficient to prove that they were talking about origami as we know them nowadays, because, according to what Hatori reports, some version of the stories says that the heron was made by knotting the paper or drawing or cutting it instead of folding it. In addition, Hatori explains that the Japanese paper strips, "Shade" and "Heisoku", used in Shinto rituals and the paper dolls, "hitogata", were not made of paper in ancient Japan, and they are not necessarily folded even now. The word "origami", came from "oru" meaning "to fold" and "kami" meaning "paper" or "divinity". This leads us to think that there is a strict relationship between Japanese religion and the art of paper folding, but in ancient Japanese language the pronunciation of those words were different, so Hatori believe that it is hard to see a connection even between the traditional origami and the Japanese religion.

¹⁰ The main reference that we used to trace the ancient history of origami was the paper "History of Origami in the East and the West before Interfusion" by Koshiro Hatori.

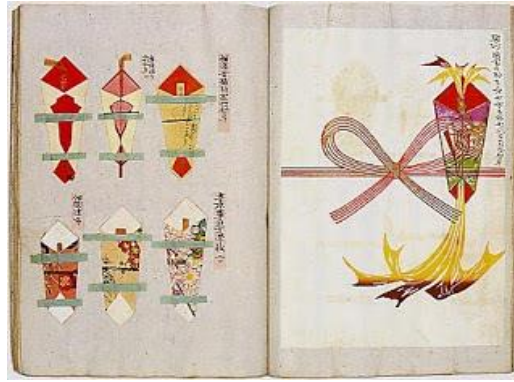


Figure 4: different type of Noshi. Source: noshi collection by Yamanaka Kyoko (1850-1928).



Figure 5: Mecho and Ocho models used as decorations on sake bottles.

The oldest unequivocal document about origami in Japan is a short poem composed by Ihara Saikaku in 1680, where he speaks about “*Origami butterflies in Rosei’s dreams*”. He refers to origami “Ocho” and “Mecho” which are male and female butterflies, Japanese people still use those folded paper models to ornate bottles at weddings. This means that origami was already deep-rooted in Japanese culture when the poem was written, in fact, the samurai warriors between 1603 and 1868 were supposed to fold wrapping paper, shaping it in a symmetric regular figure. Such type of folded figure named “Noshi” is probably dated between 1333-1573 and it was gifted as a token of good luck. What is surprising is that an older document reported by Vicente Palacios where we can recognize an origami boat was probably edited in Venice for the first time in the 13th century. It is the “*Tractatus de Sphaera Mundi*” by Giovanni Sacrobosco, according to Vicente, the image of the boat on the bottom has been found in the 1490 edition, but it could have been present even in an earlier edition. However, even in this case, Hatori discourages to take it as a certain clue because there is no written evidence of origami in Europe in that period, and the picture could also have represented a simple stylized boat instead of an accurate origami boat.

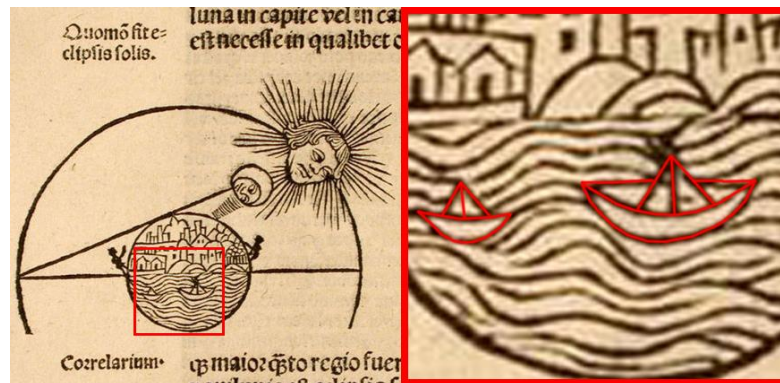


Figure 6: “*Tractatus de Sphaera Mundi*” written by Giovanni Sacrobosco, paper boats zoom. (Source: History of origami. Origami resource centre. <http://www.origami-resource-center.com/history-of-origami.html>).

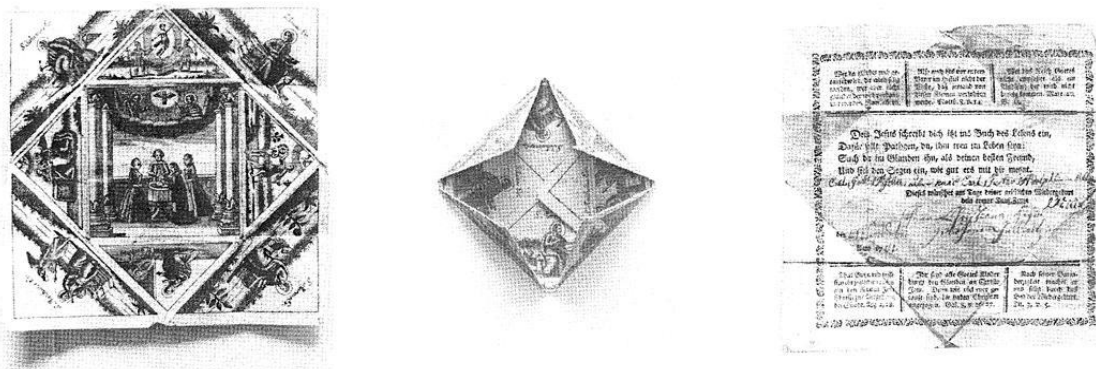


Figure 7: German baptismal certificate from the eighteenth century. Source “History of Origami in the East and the West before Interfusion” (Hatori, 2011).

Another European document that proves that origami was present in Europe in ancient times, which is probably unrelated to Japanese origami tradition, was the baptismal certificate which was folded in a way that is known today as the “double blintz base”, and it can be dated back to the sixteenth century before the protestant reformation. In addition, there are several examples of love letters dating back to the early nineteenth century folded in a similar way which could be related to an autonomous European tradition of paper folding.

What is almost certainly true is that there is not a univocal place or time where and when origami was born, but it probably had a concurrent diffusion in many different countries and ages because the paper by its nature invites to folding it. Nevertheless, it is still an open problem, which we probably will never be able to solve due to the lack of evidence.

What is certain is that the origami, even if it could not be born exclusively in Japan, nowadays is considered strictly related to Japanese culture. The reason for this can be related, on the one hand, to the higher number of references to origami in the ancient and modern Japanese art compared to other countries; for example the first known book about ornamental origami is the Japanese book “Hiden Senbazuru Orikata” first published in 1797; and on the other hand, it can be related to the work of many Japanese artists who lived in 20th to 21st century such as Akira Yoshizawa (1911, 2005) who is considered the father of modern origami and the one who redefined the graphical system which is used today to represent the folding procedures of origami, known as “Yoshizawa-Randlett system”. He probably created more than 50.000 original models, of which only a small amount was published in his 18 books. For his contribution, as an ambassador of the Japanese culture in the world, he has been awarded from Emperor Hirohito with the “Order of the Rising Sun”, which is the highest honour conferred in Japan.

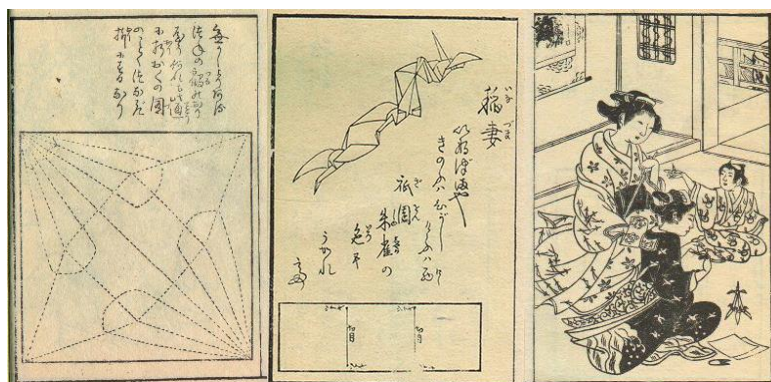


Figure 8: “Hiden Senbazuru Orikata”, the first known book about origami, first published in 1797.

1.6.2. Origami in Education – Art, Design and Math¹¹

In the past, origami was not only used for artistic or ceremonial purposes. Thanks to its intrinsic geometrical properties, it was often used for educational purposes. One of the first well-documented examples of origami used in classes was

¹¹ This section could have been divided in two distinct parts: education for art and design, education for math, and it could have been interesting to study it more in depth; although we decided to synthesize and unify these topics into

the experience of Joseph Albers who used origami as a tool to experience construction at Bauhaus in the 1920s. Quoting the artist Hans Beckmann words on his experience in Joseph Albers's basic design course at Bauhaus *"I remember vividly the first day of Vorkurs, Josef Albers entered the room, carrying with him a bunch of newspapers. ... he then addressed us saying: Ladies and gentlemen, we are poor, not rich. We cannot afford to waste materials or time. We have to make the most out of the least. All art starts with a material, and therefore we have first to investigate what our material can do. So, at the beginning, we will experiment without aiming at making a product. At the moment, we prefer cleverness to beauty. ... Our studies should lead to constructive thinking. ... I want you now to take the newspapers ... and try to make something out of them that is more than you have now. I want you to respect the material and use it in a way that makes sense — preserve its inherent characteristics. If you can do without tools like knives and scissors, and without glue, the better."* (Roth, Pentak, & Lauer, 2013).



Figure 9: Josef Albers Discussing Paper Sculptures presented by his students during the basic design course at the Bauhaus (retrieved from Bauhaus archives).

In the book "Geometric folding algorithms: linkages, origami, polyhedra" by Demaine and O'Rourke, the authors report an interesting and extensive research about the history of origami in math. They report a contribution precedent to the Bauhaus experience that used origami with educational purposes, which was the geometry essay by Rev. Dionysius Lardner written in 1840. This book illustrates several geometric concepts using paper folding. Furthermore, Sundara Row in 1893 wrote a contribute where origami has been used as a tool to make geometrical constructions and they have been compared to ruler and compass constructions. These writings can also be considered as the firsts known contributions to origami in the field of mathematics, even if in these cases the origami is used as a tool and not as the focus of the study (Demaine & O'Rourke, 2007). In 1936 is dated the first known contribute signed by Margherita Piazzola Beloch, which considers origami as the focus of a research about mathematics. In this book, she starts the investigation of the origami axioms, which later will be investigated further by Humiaki Huzita, the Japanese-Italian mathematician who, in 1985, presented the first 6 of the 7 axioms which define the operation that can be made with a single piece of paper, folded with linear creases with no cuts and completed on a plane. Someone believed that the 7th axiom was discovered in 2002 by Koshiro Hatori, a Japanese folder who found a new type of single fold alignment which could not be attributed to any of the Huzita axioms. From that moment, the 7 axioms started to be known as "Huzita-Haori" axioms, but according to Robert J. Lang's point of view¹², the seven axioms should have been named "Huzita-Justin axioms" (Lang, 2016), because in fact it turned out later that all the 7 axioms were already been completed by a French researcher Jacques Justin in 1989, who published the paper "Resolution par le pliage de l'equation du troisieme degre et applications geometriques" in which he enumerated 7 possible combinations of one single fold alignments. This fact instilled the doubt in Lang that the axioms could have been not concluded, thus a few years later he proved their completeness mathematically (Lang, 2015b). The full set of axioms is reported in Table 2.

Table 2: Huzita-Justin Axioms

one single section for the sake of brevity and in order to not compare it with the other more relevant sections which are more pertinent and related to the area of study of the thesis.

¹² This point of view has now been accepted from the scientific community.

HUZITA-JUSTIN AXIOMS	
01	Given two points p_1 and p_2 we can fold a line connecting them.
02	Given two points p_1 and p_2 we can fold p_1 onto p_2
03	Given two lines l_1 and l_2 , we can fold line l_1 onto l_2
04	Given as point p_1 and a line l_1 , we can make a fold perpendicular to l_1 passing through the point p_1
05	Given two points p_1 and p_2 and a line l_1 , we can make a fold that places p_1 onto l_1 and passes through the point p_2
06	Given two points p_1 and p_2 and two lines l_1 and l_2 we can make a fold that places p_1 onto line l_1 and places p_2 onto line l_2
07	Given a points p_1 and two lines l_1 and l_2 , we can make a fold perpendicular to l_2 that places p_1 onto line l_1

For those who are interested to study further the origami axioms, more details can be found in the following contributes by different authors: “Origami and geometric constructions” and “Huzita-Justin axioms” by Robert J. Lang (Lang, 2015b, 2016), “The mathematics of origami” by Sheri Yin (Yin, 2009), “Some results to the Huzita axioms” by H. R. Khademzadeh and H. Mazaheri (Khademzadeh & Mazaheri, 2007), “Résolution par le pliage de l'équation du troisième degré et applications géométriques” by J. Jaques (Jacques, 1989), and “Geometric folding algorithms: linkages, origami, polyhedra” by E. Demaine and J. O'Rourke (Demaine & O'Rourke, 2007). A lot of studies about axioms, and about geometrical constructions that are possible thanks to the origami axioms, can be also found on Thomas Hull's web page and other publications by him (Hull, n.d., 2003b, 2003a, 2006).

Even if the seven axioms of origami are not easily directly applicable to practical designs in the field of engineering, manufacturing and architecture, they are the basics of the “mathematics of paper folding”. Starting from these basic axioms, the scientific community became more and more interested in origami mathematics. The studies were extended to many different problems, such as the flat-foldability, the definition of generalized techniques to design any shape only by folding, the degree of freedoms of a pattern and so on. There are many theorems about flat-foldability, extensively studied by Jun Maekawa, Toshikazu Kawasaki, Jacques Justin¹³. Later Thomas Hull continued their work on flat-foldability from the early nineties until today. Contrariwise, there is not a large bibliography about non-flat foldable patterns, one of the few references is the paper written by David A. Huffman “Curvature and Creases: A Primer on Paper” (Huffman, 1976). One of the first examples of computational origami is attributable to by Ronald Resh. Between the late 1950s and early 1970s, he worked with paper folding both artistically and computationally. In the 70s he developed a computer program at the University of Huta that converted any space curve in a curve-folded edge (Schmidt & Statmann, 2009).

Robert J. Lang developed around 1993 an algorithm, which became later a standalone software, to design crease patterns, this contribution determines a conjunction point between the origami intended as an art and the origami intended as a technique, but probably the most important Lang's contribution is his book “Origami design secrets” (Lang, 2003, 2011). The first edition dates back to 2003 re-edited in 2011. His “magnum opus” on origami design methods was extended by another recent publication “Twists, Tilings and Tessellations. Mathematical methods for Geometric Origami.” (Lang, 2018) which extends the previous publications with new methods to design tessellations, twists and corrugations. Erik Demaine asserted that “Lang's work may be viewed as the start of the recent trend to explore computational origami” (Demaine & O'Rourke, 2007).

The next frontier of the origami mathematics will probably be focused on the curved folding, which has already been approached by Tachi and Demaine et al. (Demaine, Demaine, Huffman, Koschitz, & Tachi, 2015, 2018; Demaine, Demaine, Koschitz, & Tachi, 2011; Tachi, 2011a, 2013) but it still has a lot of open problems. Lang also asserted that he is interested in studying further this topic, which is still mostly unexplored.

1.6.3. Math Meets Art - Most Known Methods to Design Origami

All the theorems developed since the second half of the twentieth century until today were not only a matter of mathematicians, engineers and scientists, also the artistic community started applying some of those theorems to increase their design possibilities. The result of that was a surprising increase in the complexity of the figurative origami models. This gave birth to a new artistic design approach based on mathematical rules.

Before this revolution, the traditional method to design origami usually consisted of a trial-and-error process. This method is still used by the most part of origami designers, and it starts by fixing the subject to design; then the designers try to get a schematic geometric figure by using their experience and a trial-and-error method. The geometrical base

¹³ That we will discuss later in section 3

must be as much close to the desired subject as possible so that they can shape and sculpt it to achieve a more realistic look. The design method is focused on finding clear folding steps and reference easy points in spite of looking for an optimized crease pattern (CP).

Sometimes the process can also be reversed, the artist folds a random base without having in mind a particular subject searching for the inspiration while folding it, and only after folded the base he/she searches for a figure that could match the base and he/she starts shaping it accordingly.

The most recent mathematically-based approach is characterized by applying mathematical or graphical rules to draw an accurate crease pattern before even folding a single crease, only after the pattern is finished the artist will find the folding sequence. Sometimes there is not an easy step by step process to collapse complex patterns, and sometimes it is necessary to collapse it all at once making it way more difficult to fold than a traditional step-by-step sequence. The first approach is usually used for simple models, the second one is necessary for very complex models because the design time would be too long if approached with the trial-and-error method.

Ryujin by Kamiya Satoshi, for example, is one of the most complex models ever created. It is folded from a 2m x 2m single square sheet of paper and represents an eastern style scaled dragon with several claws horns and fangs. It took Kamiya many months to design and fold its final version, and without a precise design strategy, and solid mathematical basis, Kamiya would not probably be able to realize it.



Figure 10: Ryujin 3.5, designed by Kamiya Satoshi folded by Atilla Yurtkul.

Many different widespread mathematically-based approaches exist, some of them aim to optimize the paper usage, others aim to simplify the design process, others want to push to another level the possibilities of origami even if the method is not convenient for the folders, some of them want to be as flexible and reliable as possible. The most known are explained in Lang's book "Origami design secrets" (Lang, 2011), most of them come from the analysis of traditional techniques, enriched by Lang's experience. He explains how to design any origami figure, just by modifying a traditional known pattern, or by assembling different pieces of known patterns that he calls "tiles" or "molecules".

To understand how to mate two tiles it is necessary to understand the rivers and circle rules, which will not be explained in depth here. Suffice it to say that circles represent flaps and points, and rivers represent connectors between flaps and points in the folded geometric base model. To obtain a flat foldable origami composed by different tiles it is necessary to line up all the rivers and the circles of the adjacent tiles. The natural consequence of a tiles-based method (molecule method) is to investigate all the possible ways to arrange the tiles (thus the river and the circles) on the plane (the sheet of paper). The answer to this problem is a geometrical well-known problem called circle packing, which is defined as the study of the arrangement of circles on a given surface such that no overlapping occurs and so that all circles touch one another.

The tree theory explained by Lang is an evolution of the circle packing and molecule technique, and it consists in drawing a schematic figure where the lengths of the limbs are the lengths of the flaps, and thus, they are the radii of the circles which have to be arranged on the unfolded sheet as a guide to draw the crease pattern. Once drawn all the creases the verse of each crease must be assigned (valley or mountain) which can be done through the rules of flat foldability that we are going to explain in section 3.5. When connecting with creases the packed circles, the angles between creases are often odds, and thus it can be very hard to find references just by folding.

The box pleating technique became famous between origami artists to avoid this problem, due to its simplicity both in terms of designability and foldability. This technique was born to design box-like origami and evolved becoming a self-standing technique which can be used to design any kind of flat-foldable or non-flat-foldable origami. In the "box pleating" method, angles which are not multiple of 45° are not allowed thus it solves the problem of odd angles greatly simplifying the pre-creasing process. However, it partially limits the design freedom; Lang says "*Because of their simple angles, box-pleated crease patterns can be much easier to develop linear folding sequences for. They come with a cost, however; not all circle patterns possess box-pleatable molecules.*" (Lang, 2011).

In architecture, manufacturing and engineering, the design processes differ from the ones used by artists. Usually, the shape-finding process starts from the context or it is aimed at finding particular movements to be applied in particular situations instead of finding a specific shape. The necessity to control the movement makes the design process longer and harder. In these fields, it is not easy to identify a set of known approaches because they usually differ case by case. However, for sure the common ground is the use of computer applications and/or math, to generate, control, modify and analyse the behaviour of rigid-foldable surfaces.

1.7. References – CHAPTER I

- Autodesk. (n.d.). Dynamo. Accessed February 4, 2019, from <https://dynamobim.org/>
- Bateman, A. (n.d.). Tess. Accessed September 6, 2016, from <http://www.papermosaics.co.uk/software.html>
- Cardone, V. (2017). *Gaspard Monge, padre dell'ingegnere contemporaneo*. Rome: DEI Tipografia del genio civile.
- Carlevaris, L., De Carlo, L., & Migliari, R. (2012). *Attualità della geometria descrittiva*. Gangemi editore.
- Casale, A., & Calvano, M. (2012). House of cards. The fold for the construction of articulated surfaces. *Disegnarecon*, 9, 289–300.
- Casale, A., Valenti, G. M., & Calvano, M. (2013). *Architettura delle superfici piegate: le geometrie che muovono gli origami*. Roma: Edizioni K.
- Demaine, E. D. (n.d.). .Fold file format. Accessed February 4, 2019 from <https://github.com/edemaine/fold>
- Demaine, E. D., & O'Rourke, J. (2007). *Geometric folding algorithms: linkages, origami, polyhedra*. New York: Cambridge University Press.
- Demaine, E. D., & Tachi, T. (2010). Lecture 23 Video, Architectural Origami. Retrieved October 1, 2018, from <http://courses.csail.mit.edu/6.849/fall10/lectures/L23.html>
- Demaine, E. D., Demaine, M. L., Koschitz, D., & Tachi, T. (2011). Curved crease folding: a review on art, design and mathematics. *Proceedings of the IABSE-IASS Symposium: Taller, Longer, Lighter (IABSE-IASS2011)*, 20–23.
- Demaine, E. D., Demaine, M. L., Huffman, D. A., Koschitz, D., & Tachi, T. (2015). Characterization of curved creases and rulings: design and analysis of lens tessellations. *Origami 6*, 209–230.
- Demaine, E. D., Demaine, M. L., Huffman, D. A., Koschitz, D., & Tachi, T. (2018). Conic crease patterns with reflecting rule lines. *Origami 7: Mathematics*, 573–589.
- Fallavollita, F. (2008). L'estensione del problema di Apollonio nello spazio e L'Ecole Polytechnique. *Ikhnos*, 1, 29–42.
- Fallavollita, F., & Salvatore, M. (2013). La costruzione degli assi principali delle superfici quadriche. *Disegnare Idee Immagini*, 46, 42–51.
- Feder, T. (2018). Q&A: Robert Lang, origami master. *Physics Today, People and History*, (January). <https://doi.org/10.1063/PT.6.4.20180108a>
- Ghassaei, A. (n.d.). Origami Simulator. Accessed July 31, 2018, from <http://apps.amandaghassaei.com/OrigamiSimulator/>
- Hatori, K. (2011). History of Origami in the East and the West before Interfusion. *Origami 5: Fifth International Meeting of Origami Science, Mathematics, and Education*, 3–11.
- Huffman, D. A. (1976). Curvature and Creases: A Primer on Paper. *IEEE Transactions on Computers*, C-25(10), 1010–1019. <https://doi.org/10.1109/TC.1976.1674542>

- Hull, T. C. (n.d.). Tom Hull's page. Accessed February 4, 2019, from <http://mars.wne.edu/~thull/>
- Hull, T. C. (2003a). Counting mountain/valley assignments for flat folds. *Ars Combinatoria*, 67, 175–187.
- Hull, T. C. (2003b). Origami and Geometric Constructions: a comparison between straight edge and compass constructions and origami. Accessed February October 10, 2018, from <http://mars.wne.edu/~thull/omfiles/geoconst.html>
- Hull, T. C. (2006). *Project origami*. New York: A K Peters/CRC Press.
- Jacques, J. (1989). Résolution par le pliage de l'équation du troisième degré et applications géométriques. *Proceedings of the First International Meeting of Origami Science and Technology*. Ferrara, Italy.
- Kawaguchi, K., Ohsaki, M., Takeuchi, T., Liu, K., & Paulino, G. H. (2016). MERLIN: A MATLAB implementation to capture highly nonlinear behavior of non-rigid origami. *Proceedings of IASS Annual Symposia (International Association for Shell and Spatial Structures)*, 2016(13), 1–10.
- Khademzadeh, H. R., & Mazaheri, H. (2007). Some results to the Huzita axioms. *International Mathematical Forum*, 2(14), 699–704.
- Kuribayashi, K., Tsuchiya, K., You, Z., Tomus, D., Umemoto, M., Ito, T., & Sasaki, M. (2006). Self-deployable origami stent grafts as a biomedical application of Ni-rich TiNi shape memory alloy foil. *Materials Science and Engineering A*, 419(1–2), 131–137. <https://doi.org/10.1016/j.msea.2005.12.016>
- Lang, R. J. (2003). *Origami design secrets: mathematical methods for an ancient art*. Wellesley: A.K. Peters.
- Lang, R. J. (2011). *Origami design secrets: mathematical methods for an ancient art, (Second ed.)*. Boca Raton, FL, USA: CRC Press.
- Lang, R. J. (2015a). Air Bag Folding. *Self-Published*. Accessed April 10, 2018, from <https://langorigami.com/article/airbag-folding/>
- Lang, R. J. (2015b). Origami and geometric constructions. *Self-Published*, 1–55. Accessed April 10, 2018 from http://langorigami.com/science/hha/origami_constructions.pdf
- Lang, R. J. (2015c). Treemaker. Accessed April 10, 2018, from <https://langorigami.com/article/treemaker/>
- Lang, R. J. (2016). Huzita-Justin Axioms. Accessed January 1, 2017, from <http://www.langorigami.com/article/huzita-justin-axioms>
- Lang, R. J. (2018). *Twists, Tilings and Tessellations. Mathematical methods for Geometric Origami. (First ed.)*. Boca Raton, FL, USA: K Peters/CRC Press.
- Liu, K., & Paulino, G. H. (2018). Highly efficient nonlinear structural analysis of origami assemblages using the MERLIN2 software. *Origami* 7, 4, 1167–1182.
- Loria, G. (1935). *Metodi matematici: essenza, tecnica, applicazioni*. (U. Hoepli, Ed.). Milano.
- Migliari, R. (2008). Il problema di Apollonio e la Geometria descrittiva. *Disegnare Idee Immagini*, 36, 22–37.
- Migliari, R. (2008). Rappresentazione come sperimentazione. *Ikhnos, Analisi gr*, 11–28.
- Migliari, R. (2009a). *Geometria Descrittiva - metodi e costruzioni (Vol. 1)*. Novara: Città Studi edizioni.
- Migliari, R. (2009b). *Geometria Descrittiva - tecniche e applicazioni (Vol. 2)*. Novara: Città Studi edizioni.
- Migliari, R. (2012). Descriptive Geometry: From its Past to its Future. *Nexus Network Journal*, 14(3), 555–571. <https://doi.org/10.1007/s00004-012-0127-3>

- Mitani, J. (n.d.). Jun Mitani's page. Accessed March 12, 2018, from <http://mitani.cs.tsukuba.ac.jp/en/>
- Mitani, J. (2009). A design method for 3D origami based on rotational sweep. *Computer-Aided Design and Applications*, 6(1), 69–79. <https://doi.org/10.3722/cadaps.2009.69-79>
- Mitani, J., & Igarashi, T. (2011). Interactive Design of Planar Curved Folding by Reflection. *Pacific Conference on Computer Graphics and Applications - Short Papers*, 77–81. <https://doi.org/10.2312>
- Mitchell, D. (n.d.). A brief outline of origami design history. Accessed April 10, 2017, from <http://www.origamiheaven.com/origamidesignhistory.htm>
- Resh, R. (1992). *The Ron Resch Paper and Stick Film*. Accessed April 10, 2017, from <http://www.ronresch.org/ronresch/gallery/paper-and-stick-film/>
- Roth, R., Pentak, S., & Lauer, D. A. (2013). *Design Basics: 2D and 3D* (Eighth ed.). Boston: Wadsworth.
- Rutten, D. (n.d.). Grasshopper official page. Accessed July 31, 2018, from <http://www.grasshopper3d.com/>
- Schmidt, P., & Stattmann, N. (2009). *Unfolded: Paper in Design, Art, Architecture and Industry*. Birkhäuser.
- Salvatore, M. (2012). *La stereotomia scientifica in Amédée François Frézier*. Firenze University Press.
- Seymour, K., Burrow, D., Avila, A., Bateman, T., Morgan, D. C., Maglebay, S. P., & Howell, L. L. (2018). Origami-Based Deployable Ballistic Barrier. *Origami 7: Engineering 1*, 763–777.
- Tachi, T. (n.d.-a). Tachi's web Page. Accessed September 6, 2017 from <http://www.tsg.ne.jp/TT/>
- Tachi, T. (n.d.-b). Tachi's Software. Accessed September 6, 2017 from <http://www.tsg.ne.jp/TT/software/>
- Tachi, T. (2011a). One-DOF rigid foldable structures from space curves. *Proceedings of the IABSE-IASS Symposium*, 20–23.
- Tachi, T. (2011b) Rigid-Foldable Thick Origami. *Origami 5: Fifth International Meeting of Origami Science Mathematics and Education*, 253–264.
- Tachi, T. (2013). Composite rigid-foldable curved origami structure. *1st International Conference on Transformable Architecture*, 18–20.
- Tamasoft. (n.d.). Pepakura designer. Accessed September 6, 2016, from www.tamasoft.co.jp
- Terzidis, K. (2006). *Algorithmic architecture*. Amsterdam [etc.]: Routledge.
- Terzidis, K. (2009). *Algorithms for visual design using the processing language*. Indianapolis: John Wiley & Sons.
- Tolman, K., Crampton, E., Stucki, C., Mayenes, D., & Howell, L. L. (2018). Design of an Origami-Inspired Deployable Aerodynamic Locomotive Fairing. *Origami 7: Engineering 1*, 669–684.
- Yin, S. (2009). The Mathematics of Origami. Accessed January 16, 2018, from www.math.washington.edu.
- Zinelli, F. M. (1832). *Dei due metodi analitico e sintetico discorso dell'abate*. Venezia: Nella tipografia di Giuseppe Picotti.

2. CHAPTER II: Origami-Inspired Designs

In this chapter, we report the study of existent projects that take inspiration from origami for a diversity of aspects. This study has the aim to outline the general trend of the selected application fields that are the focus of this thesis.

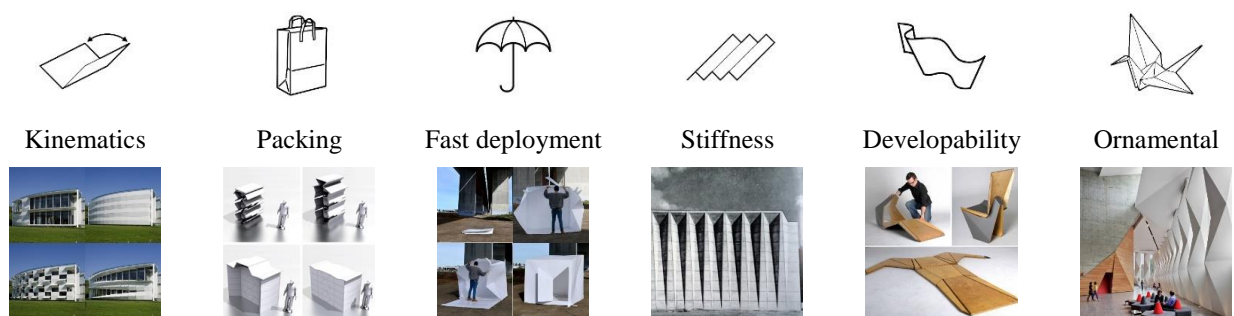
To collect the projects sorted into the following synoptic tables we analysed the fields of permanent architecture, temporary architecture, artistic installations, furniture and manufacturing, and fashion. In the conclusions of this chapter, we will formulate some critical observations.

The catalogue of projects does not in any way claim to provide a comprehensive and exhaustive cataloguing of all the existing origami-related projects because the number of objects suitable with regards to the assumed criteria would be too wide to be listed in this context. Therefore, we decided to narrow the collection of references to a limited number of objects, but vast enough to make some robust considerations.

In accordance to all of these assumptions, the gathered projects will be subdivided into the 5 sub-groups: “Permanent Architecture”, “Temporary Architecture”, “Installations”, “Goods and Furniture”, “Fashion and Clothing”.



2.1. Classification Criteria












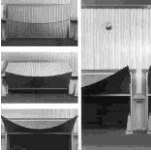
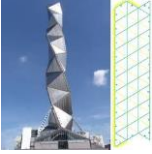







In the next sections, we will present some synoptic tables where the collected project have been sorted, and we will analyse each project and highlight for each one of them the characteristics inspired by origami. According to this principle, we defined six main classes of origami-related functions: “Ornamental”, “Stiffness”, “Kinematics”, “Packing”, “Fast Deployment” and “Developability”. Every project will be described by one or more of them.

The “Ornamental” class includes all the designs which take inspiration from origami for aesthetical reasons. This class will be organized in 2 columns: one will count all the works inspired to origami, the other one will count the works inspired by origami exclusively for ornamental reasons. We make this distinction only for this class because the projects that take the origami as a reference exclusively for aesthetical reasons do not need origami theories to be designed and they do not follow origami rules, thus their design workflows are free of geometrical constraints and they would not benefit from the design methods that we are going to propose next. For “Stiffness” are intended those works which use

folds to get a stronger structure. The “Kinematics” class includes those works that use origami rules to achieve specific movements. In the “Packing” class are included those works that exploit origami mechanisms to reduce their dimensions for transportation stocking or for space optimization. The “Fast deployment” class includes all those works where the origami mechanisms are used to pack and deploy rapidly the structure. The “Developability” class include all those works which use a developable pattern to build the final object starting from a single sheet of a specific material or from a modular composition of single folded pieces. It does not necessarily need to be unfoldable after being folded the first time to be included in this class. The developability characteristic is often used to optimize the cutouts and the scraps during the production and to optimize the assembling time.

To classify the selected projects, we tried to be as objective as possible, although some cases are hard to be assigned to one or the other class univocally. However, the objective of this analysis is not to extract a precise number of projects in one or the other class, but it is to trace a trend, thus even if a small number of projects may be not univocally classifiable, the high number of case studies considered will globally flatten out this uncertainty, and the outlined trend of each group of projects will not lose relevance.

2.2. Permanent Architecture - Synoptic Tables

 <p>🏠 1923 -Hangars of the Orly Airport -Paris, FR -Eugène Freyssinet www.arquiscopio.com</p>	 <p>🏠 1953-1958 -Assembly Hall of the UNESCO Headquarters -Paris, FR -Pierluigi Nervi and Zehruss www.archimaps.tumblr.com</p>	 <p>🏠 1958 -American Concrete Institute Building -Detroit, US -Minoru Yamasaki www.michiganmodern.org</p>
 <p>🏠 1962 -Steel Pre-Fab Houses -Palm Springs, CA, US -Donald Wexler www.archdaily.com</p>	 <p>🏠 1962 -USFA Cadet Chapel -El Paso, CO, US -Walter Netsch of Skidmore, Owings, & Merrill www.archdaily.com</p>	 <p>🏠 1963 -Miami Marine Stadium -Miami, US -Hilario Candela www.archdaily.com</p>
 <p>🏠 1966 -Shelter for sulphur factory -Pomezia, IT -Renzo Piano Studio www.archdaily.com</p>	 <p>🏠 1966-68 -St. Paulus Neuss Church -Mito, Ibaraki, JP -Fritz Schaller and Stefan Polonyi www.baukunst-nrw.de</p>	 <p>🏠 1973 -Teatro Regio di Torino -Torino, IT -Carlo Mollino www.italianways.com</p>
 <p>🏠 1985 -Ernstings Warehouse -Coesfeld-Lette, DE -Santiago Calatrava www.archi-pedia.blogspot.it</p>	 <p>🏠 1990 -Art Tower Mito -Mito, Ibaraki, JP -Arata Isozaki www.arttowermito.or.jp</p>	 <p>🏠 2000 -M-house -Gorman, California, USA -Michael Jantzen www.arcspac.com</p>
 <p>🏠 2002 -Meguro Persimmon Hall -Tokio, JP -Nihon Sekkei www.nagata.co.jp</p>	 <p>🏠 2002 -Rehearsal room in Tannhausen -Stuttgart, DE -Regina Schineis www.forum-holzbau.ch/</p>	 <p>🏠 2003 -Bengt Sjostrom Starlight Theatre -Rockford, IL, US -Studio Gang Architects www.archdaily.com</p>
 <p>🏠 2007 -CaixaForum -Madrid, ES -Herzog & de Meuron www.archdaily.com</p>	 <p>🏠 2007 -Dom mieszkalny w Doktorgässchen -Niemy, Augsburg, DE -Regina Schineis Architecten BDA www.equitone.pl</p>	 <p>🏠 2007 -Fuji television wangan studio -Tokyo, JP -Kajima design www.kajima.co.jp</p>



2007
 -Monaco House
 -Melbourne VIC, AU
 -McBride Charles Ryan
www.archdaily.com



2007
 -Nestlé Chocolate Museum
 -Toluca de Lerdo, MX
 -Rojkind Arquitectos
www.archdaily.com



2007
 -Spertus Institute of Jewish Studies
 -Chicago, Illinois, US
 -Krueck & Sexton Architects
www.archdaily.com



2008
 -Klein Bottle house
 -Morningside Peninsula, VIC, AU
 -McBride Charles Ryan
www.archdaily.com



2008
 -Café-Restaurant OPEN
 -Amsterdam, NL
 -De Architekten Cie
www.architecturelist.com



2008
 -Karuizawa Museum Complex
 -Karuizawa, JP
 -YASUI HIDEO ATELIER
www.archdaily.com



2009
 -Autobahn Church Siegerland
 -Wilnsdorf, DE
 -Schneider+Schumacher
www.archdaily.com



2009
 -Horten Headquarters
 -Copenhagen, DK
 -3XN
www.archdaily.com



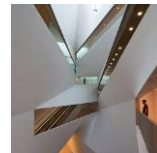
2009
 -Neo Solar Power Corporation
 -Hsinchu City, TW
 -J. J. Pan & Partners, Architects & Planners (JPPP)
www.solaripedia.com



2010
 -Arthouse
 -Hangzhou, Zhejiang, CN
 -Joey Ho Design
www.archdaily.com



2010
 -Kiefer Technic Showroom
 -Bad Gleichenberg, AT
 -Ernst Giselbrecht + Partner
www.e-architect.co.GB



2010
 -Museum of Art Amir Building
 -Tel Aviv, IL
 -Preston Scott Cohen
www.archdaily.com



2010
 -Office Building in Istanbul
 -Istanbul, TR
 -Tago Architects
www.archdaily.com



2010
 -Q1, ThyssenKrupp Quarter
 -Essen, DE
 -JSWD Architekten, Chaix & Morel et Associés
www.archdaily.com



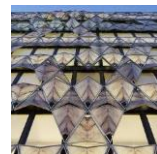
2011
 -CIB, Biomedical Research Center
 -Pamplona, ES
 -Vaíllo & Irigaray & Galar
www.archilovers.com



2011
 -Glasgow Riverside Museum of Transport
 -Glasgow, GB
 -Zaha Hadid Architects
www.archdaily.com



2011
 -House 77
 -Póvoa de Varzim, PT
 -dIONISO LAB
www.archdaily.com



2011
 -Origami
 -Paris, FR
 -Manuelle Gautrand Architecture
www.e-architect.co.GB



2011
 -Perry and Marty Granoff Center for the Creative Arts
 -Providence, Rhode Island, US
 -Diller Scofidio + Renfro
www.archdaily.com



2011
 -Stadshuis Nieuwegein
 -Nieuwegein, NL
 -3XN
www.archdaily.com



2011
 -Vivida
 -Hawthorn, Melbourne, AU
 -ROTHELOWMAN
www.archdaily.com



2012
 -Al Bahar Towers
 -Abu Dhabi, AE
 -Aedas Architects
www.architizer.com



2012
 -Dalian International Conference center
 -Dalian, CN
 -Coop Himmelb(l)au
www.archdaily.com



2012
 -Factory Building on the Vitra Campus
 -Weil am Rhein, DE
 -SANAA
www.archdaily.com





2012
-FECHAC Regional Office
-Ciudad Juarez, MX
-Grupo ARKHOS
www.archdaily.com



2012
-Festival Hall of the Tiroler Festsche
-Erl, AT
-Delugan Meissl Associated Architects
www.archdaily.com



2012
-Hooke Park Big Shed
-Dorset, GB
-AA Design & Make
www.archdaily.com



2012
-Kilden
-Kristiansand, NO
-ALA Architects
www.archdaily.com



2012
-Mülimatt Sports Education and Training Centre in Windisch
-Brugg, CH
-Studio Vacchini Architetti
www.archdaily.com



2012
-Naturum Kosterhavet
-Ekenäs, SE
-White Arkitekter
www.archdaily.com



2012
-Roberto Cantoral Cultural Center
-Coyoacán México DF, MX
-Broissin Architects
www.archdaily.com



2012
-Salon Urbain
-Montreal, QC, CA
-Ædifica + Sid Lee Architecture
www.coloribus.com



2013
-Aix en Provence Conservatory of Music
-Aix-en-Provence, FR
-Kengo Kuma and Associates
www.archdaily.com



2013
-Assemble Studio
-Northcote, VIC, AU
-Assemble
www.archdaily.com



2013
-Dear Ginza
-Chuo, Tokyo, JP
-Amano design office
www.archdaily.com



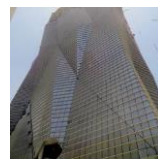
2013
-High School Crinkled Wall
-Kufstein, AT
-Wiesflecker Architecture
www.archdaily.com



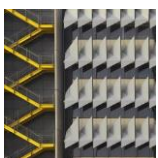
2013
-HygroSkin - Meteorosensitive pavilion.
-FRAC Centre Orleans, FR
-Achim Menges, Oliver David Krieg and Steffen Reichert
icd.uni-stuttgart.de/?p=9869



2013
-Innovation and Technical and Technological Transfer Park
-Chihuahua, MX
-Grupo ARKHOS
www.archdaily.com



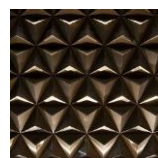
2013
-Muqarnas Tower
-Riyadh SA
-Skidmore, Owings & Merrill, SOM
www.archdaily.com



2013
-Siemens HQ in Masdar City
-Masdar City - Abu Dhabi - AE
-Sheppard Robson
www.archdaily.com



2013
-Textilmacher
-Munich, DE
-tillicharchitektur
www.archdaily.com



2014
-Commercial Foyer Space, 105 Wigmore Street
-London, GB
-Paul Nulty Lighting Design
www.illumni.co



2014
-New Wave Architecture
-Designs Rock Gym for Polur
-Polur, IN
-New Wave Architecture
www.archdaily.com



2014
-SDU Campus Kolding
-Kolding, DK
-Henning Larsen Architects
www.archdaily.com



2014
-Velenje Car Park
-3320 Velenje, SI
-ENOTA
www.archdaily.com



2014
-Yokohama International Passenger Terminal
-Yokohama, JP
-Foreign Office Architects (FOA)
www.archdaily.com



2015
-Bespoke Theatre
-Xishuangbanna, Yunnan, CN
-Stufish Entertainment Architects
www.archdaily.com



2015
-Cozzarelli price stage, National Academy of Science
- Washington DC
www.paulino.ce.gatech.edu/cozzarelli2015.html





2015
-Qingdao Cruise Terminal
-Qingdao, Shandong, CN
-CCDI - Mozhao Studio & Jing Studio
www.archdaily.com



2016
-Poly International Plaza
-Beijing Shi, CN
-Skidmore, Owings & Merrill
www.som.com



2016
-Széll Kálmán Square
-Budapest, HU
-Építész Stúdió, Lépték-Terv
www.archdaily.com



2016
-Tokyu plaza
-Tokyo, JP
-Nikken Sekkei
<http://www.archdaily.com>



2017
-Low Carbon Energy Centre
-London, GB
-C.F. Møller Architects
www.archdaily.com



2013
-Kyushu Geibunkan
-Fukuoka, JP
-Kengo Kuma
www.talfriedman.com

2.3. Temporary Architecture - Synoptic Tables



1964
-Pavillon Wehrhafte Schweiz
-Lausanne, CH
-Carl Fingerhuth
www.eda.admin.ch



1967
-Plydome at Flash Peak camp
-Indio, CA
-Herbert Yates, Hirshen Van der Ryn Architects
<https://goo.gl/YYYYZx5>



2000
-Origami Shelter sculpture
-JP
-Yuko Nishimura
www.yukonishimura.com



2005
-Jumbo Origamic Arch White
-Jakarta (Indonesia, Pescara, IT)
-Atelier Bow-Wow
www.bow-wow.jp



2005
-Jumbo Origamic Arch Orange
-Kobe Art Village Center, Hyogo, JP
-Atelier Bow-Wow
www.bow-wow.jp



2006
-dB folding disco
-BR
-Fernanda Dolabella Dubal
www.designboom.com



2008
-Embedded Project
-Shanghai, CN
-HHD_FUN + Xu Wenkai
www.dezeen.com



2008
-Chapel for the Deaconesses
-Hôpital de St-Loup, CH
-Localarchitecture + Danilo Mondada
www.archdaily.com



2009
-Cardboard banquet paper pavilion
-Cambridge, GB
-Cambridge University
www.iconeye.com



2011
-Bloomberg Pavilion
-Tokyo, JP
-Akihisa Hirata
www.designboom.com



2011
-Winnipeg Skating Shelters
-Winnipeg, MB, CA
-Patkau Architects
www.archdaily.com



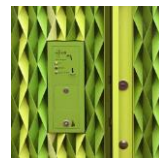
2012
-Burning Man yurt
-Black Rock City, US
-Joerg Student - ideoLABS
www.labs.ideo.com



2012
-Canary Wharf Kiosk
-London, GB
-Make Architects
www.makearchitects.com



2012
-Instant Flat-Pack Origami Shelter
-Stuttgart, DE
-Doowon Suh, KR
weburbanist.com



2012
-Public Toilets
-Uster, CH
-Gramazio & Kohler
www.archdaily.com




2012
-The Bowooss Temporary Pavilion
-Saarbrücken, DE
-The School of Architecture at Saarland University
www.arch2o.com





2013
-ArboSkin Pavilion
-Stuttgart, DE
-ITKE
www.inhabitat.com




2013
-Cardborigami, temporary cardboard shelter
-Santa Monica, California, US
-Callison LLC
www.cardborigami.org



▲ 2013
-Emergency Shelter
-Melbourne, AU
-Woods Bagot
www.notesontheroad.com

▲ 2013
-Ferrocement Shelter
-IN
-Anupama Kundoo
www.cusp-design.com




▲ 2013
-Indo-German Urban Mela pavillions
-Pune, IN
-Markus Heinsdorff
www.DE-and-IN.com




▲ 2013
-Plate house
-Oxford, GB
-Jo Gattas and Zhong You
joe.gattas.com/plate-house




▲ 2013
-Pop-up Dome Prototype
-Delft, DE
-University of Technology
www.designplaygrounds.com




▲ 2014
-FFolded Bamboo + Paper House concept
-CN
-Ming Tang
www.archdaily.com




▲ 2014
-Flat-pack disaster housing
-AU
-Alastair Pryor
www.mnn.com




▲ 2014
-Ha-Ori Shelter
-Bolinas, CA
-Joerg Student - ideoLABS
www.labs.ideo.com




▲ 2017
-Look! Look! Look!
-Herefordshire, GB
-Studio Morison
www.archdaily.com




2.4. Installations - Synoptic Tables




▲ 2000
-La Patata
-DE
-Volker Flamm & Wolfgang Ohnmacht
www.detail.de




▲ 2002
-Your spiral view
-Fondation Beyeler, Basel, CH
-Olafur Wliasson
<https://olafureliasson.net/>

▲ 2008
-Life Tunnel
-The Hayward, London, UK
-Atelier Bow Wow
www.edgeofthep plank.com




▲ 2009
-Ecological Installations
-Greenmeme
www.ponoko.com




▲ 2010
-Move: Choreographing You
-exhibition design
-London, UK
-Amanda Levet ARchitects
www.dezeen.com




▲ 2011
-Le Fabrique Sonore
-Reims, FR
-Hyung-Gul Kook, Ali Momeni and Robin Meier
www.design-afterhours.blogspot.it




▲ 2011
-Overliner
-MIT, US
-Joel Lamere, Cynthia Gunadi
www.arts.mit.edu




▲ 2011
-Resonant chamber
-University of Michigan, US
-RVTR
www.archdaily.com




▲ 2011
-Tessel, kinetic sound installation
-Lyon, FR – Brussels, BE
-David Letellier and Lab[au]
www.designplaygrounds.com





▲ 2012
-Arum Shell
-Biennale di Venezia, IT
-Zaha Hadid Architects
www.robofold.com




▲ 2012
-Curved Folding, Metal Twins
-Bangalore, IN
-S. Chandra; S. Bhooshan; M. El-Sayed;
www.arcodet.blogspot.it




▲ 2012
-INVOLUTION
-Savannah, Georgia, US
-(LAB)normal, Larry O. Martin
www.arch2o.com

▲ 2012
-Rainbow Gateway
-Burnley, GB
-Tonkin Liu
www.tonkinliu.co.uk




▲ 2013
-Computational parabolic origami Shelter
-Komaba Museum, Tokio, JP
-Tomohiro Tachi
www.tsg.ne.jp




▲ 2013
-Rigid foldable generalized Miura
-Komaba Museum, Tokio, JP
-Tomohiro Tachi
www.tsg.ne.jp

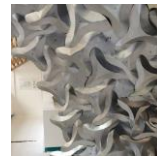




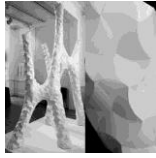
2014
 -Blumen Lumen
 -Black Rock City, US
 -Joerg Student - ideoLABS
www.labs.ideo.com



2014
 -One Fold
 -CA
 -Patkau Architects
www.straight.com



2015
 -Curved-Line Folding Workshop
 -School of Architecture, London, UK
 - Michael Weinstock, Axel Körner, Suryansh Chandra
axelkoerner.com/portfolio



2015
 -Computing Curved-Folded Tessellations through Straight Folding Approximation.
 -University of Stuttgart, DE.
 - Michael Weinstock, Axel Körner, Suryansh Chandra
www.researchgate.net



2016
 -Origami Pavilion.
 -Detmold University, DE.
 -Tal Friedman.
www.inhabitat.com



2016
 -"Surface to Form" pavillion.
 -University Innsbruck, AU.
 -Rupert Maleczek, et al.
www.maleczek.info/portfolio



2016
 -Arch(k)inetik workshop.
 -University of Stuttgart, DE.
 -Contemporary Architects Association Tehran, Axel Körner et al.
www.axelkoerner.com/portfolio

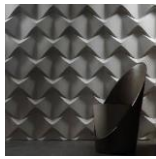


2017
 -Curved folded wooden assemblies.
 -Holzbau Saurer, Höfen, AU.
 -Rupert Maleczek, Gabriel Stern, et al.
<https://www.researchgate.net/publication/328899419>



2018
 -Curved-Folded Assemblies.
 -University of Innsbruck, AU.
 -Rupert Maleczek and Axel Körner
www.maleczek.info/portfolio

2.5. Goods and Furniture - Synoptic Tables



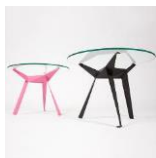
3D Surface
 -Caos
 -TRG, TRB
www.3dsurface.it



Petrucci Adrien
 -Paper cast teapot
 -Ceramic
www.pinterest.com



Alice Minkina
 -Chair AMi
 -Fabric and plywood
www.behance.net



Anthony Dickens & Tony Wilson
 -Origami table
 -Steel
www.anthonydickens.com



Ariel Zuckerman
 -Wood And Light Origami
 -Wood
www.yankodesign.com



ARTEMIDE, Issey Miyake
 -Mendori
 -Paper
www.artemide.com



Bell Phillips
 -Origami stairs
 -Stainless steel
www.dezeen.com



Ben Ryuki Miyagi
 -Elephant Seating
 -Felt
www.wearedesignbureau.com



Boaz Mendel
 -Loop Chair
 -Wood and metal
www.aadesignspace.blogspot.it



Brett Mellor
 -Facetation Butterfly Chair
 -Fabric and metal
www.behance.net



Brett Mellor
 -Flat Stanley Origami Chair
 -Wood, Canvas and Vinyl
www.behance.net



Brett Mellor
 -The Morgan Felt Folding Stool
 -Felt impregnated with resin
www.behance.net



-BUILT
-Origami Wine Tote
-Neoprene
www.builtny.com




-Cut and Fold by Andrea Kordos & Tony Round
-Aperture Pendant
-Metal and wood
www.cut-fold.com




-Cut and Fold by Andrea Kordos & Tony Round
-Origami Chair
-Metal and wood
www.cut-fold.com




-Daniel Milchtein Peltsverger
-Biombo Chair
-Wood
www.bookofjoe.com




-Daniel Schipper
-Green Green House
-Recyclable plastic
www.yankodesign.com




-DegreesOfFreedomCo by Brian Ignaut
-Loop table
-Wood
www.etsy.com




-DegreesOfFreedomCo by Brian Ignaut
-Legged wooden origami table
-Wood
www.instagram.com




DegreesOfFreedomCo by Brian Ignaut
Kinetic Ring Box
Wood
www.instagram.com




-DOMUS by Tobias Krafczyk
-Origami Intersections
-Paper
www.onlab.ch




-Donn Koh
-Origami for superheroes - pencil sharpener
-Stainless steel
www.yankodesign.com




-FiberStore
-Bubble
-Polypropylene
www.etsy.com




-FiberStore
-Pebble
-Paper
www.etsy.com




-FiberStore
-Poetry
-Paper
www.etsy.com




-FiberStore
-Ramekin
-Paper
www.etsy.com




-FiberStore
-Volant
-Paper
www.etsy.com




-Florian Kräutli
-Magnetic origami curtain
-Fabric, metal, magnets
www.kraeutli.com




-FLUX
-Flux Chair
-Plastic
www.fluxfurniture.com




-Foldschool
-Cardboard kid furniture
-Cardboard
www.foldschool.com




-FOSCARINI
-Diesel Rock Light
-ABS, Metal, nylon
www.foscarini.com




-Four-o-nine
-Pleat Diner chair
-Polyethylene
www.nienkamper.com




-Fox & Freeze
-Lounge Chair
-Felt
www.designboom.com




-Fredrik Färg
-The COAT Chair
-Felt
www.contemporist.com




-Gant Lights
-Concrete hanging lamp
-Concrete
www.etsy.com




-Gold Leaf Design Group
-Origami Paper Lamps
-Paper
www.goldleafdesigngroup.com






 -HOID
 -Pleat Box
 -Ceramic, glazed enamel, metal
www.marset.com





 -Ignatov Architects
 -News Coffee Table
 -Aluminium
www.interiorholic.com





 -Ilan Garibi
 -Tessellated origami mirrors
 -Aluminium
www.garibiorigami.com





 -Ilan Garibi
 -Tessellated origami Table Lamp
 -Paper and Wood
www.garibiorigami.com





 -Ilan Garibi
 -Tessellated origami tables
 -Wood
www.garibiorigami.com





 -INC Architecture & Design
 -Origami Stairs
 -Metal
www.designbuzz.it





 -Issey Miyake
 -Fukurou Lamp
 -Recycled polyester fibre fabric
www.artemide.com





 -Issey Miyake
 -Minomushi Terra Lamp
 -Recycled polyester fibre fabric
www.artemide.com





 -Issey Miyake
 -Mogura Lamp
 -Recycled polyester fibre fabric
www.artemide.com





 -Issey Miyake
 -Tatsuno-Otoshigo Lamp
 -Recycled polyester fibre fabric
www.artemide.com





 -James Slack
 -ORI
 -Cardboard
www.themag.it





 -Jan Sekula
 -Cardboard Playground
 -Cardboard
www.behance.net





 -Jiangmei Wu
 -Torus Folded Lamp
 -Recycled cotton paper
www.mocoloco.com





 -Joseph Joseph
 -Folding Colander
 -Plastic
www.josephjoseph.com





 -Jurmol Yao
 -Venom
 -Metal and carbon fibre
www.yankodesign.com





 -Kaj Franck
 -Origami Plate - K F 2
 -Ceramic
www.etsy.com





 -KARTON
 -Cardboard Furniture
 -Cardboard
www.kartongroup.com.au





 -KARTON
 -Twist Table
 -Cardboard
www.kartongroup.com.au





 -Keiji Ashizawa
 -Flat Pack Wall Magazine Holder
 -Steel
www.keijidesign.com





 -Kelly Lohr
 -Origami Chair
 -PETG thermoplastic polymer
www.behance.net





 -KNOLL
 -Washington Prism, Lounge chair
 -Urethane moulded foam, Baltic Birch plywood panels covered in plastic
www.knoll.com





 -Krings & Sebastian Mühlhäuser
 -Casulo
 -Cardboard
www.mein-casulo.de





 -Kyungeun Ko
 -Bentley tailormade
 -Aluminium
www.yankodesign.com





 -Lapalma, Shin Azumi
 -AP Foot stool
 -Wood
www.designboom.com





 -Le Klint
 -Pendant 150
 -Lampshade foil
www.leklint.com
  




 -Le Klint
 -Pendant 153
 -Plastic Foil
www.leklint.com
  




 -Le Klint
 -Pendant 169
 -Plastic Foil
www.leklint.com
  




 Le Klint
 Pendant 172
 Plastic Foil
www.leklint.com
  




 Le Klint
 Pendant 178
 Plastic Foil
www.leklint.com
  




 Le Klint
 Pendant 181
 Plastic Foil
www.leklint.com
  




 -Lim Ruiwen
 -Origami Shade
 -Fabric
www.yankodesign.com
  




 -Matsuoka furniture
 -Origami Chest
 -New Guinea Walnut
www.matsuokafurniture.com





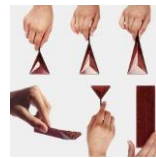
 -Max Hauser
 -Trifold
 -Anodised Aluminium
www.trifoldtable.com
  




 -McEwen Lighting Studio
 -Gear Ceiling Fixture
 -Satin Nickel
www.mcewenlighting.com
  



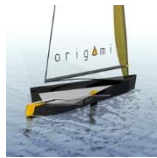

 Michael Sholk
 Foldable wooden Spoon
 Wood
www.yankodesign.com
  




 -Polygons Measuring Spoon
 -Rahul Agarwal
www.yankodesign.com
  




 -Kristina Wißling
 -Miura ori world map
 -Paper
www.flickr.com/photos/wissling_origami
  




 -Matteo Signorini
 -Origami Boat
www.yankodesign.com
  


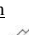




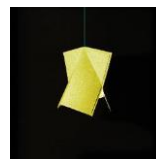

 -Max Frommled & Arno Mathies
 -Folding Boat
 -Plastic
www.maarno.com
  




 -Milk Design Limited
 -Origami Glow
 -Paper and wood
www.yankodesign.com
  




 -Moritz Menacher
 -Urban Origami Bike
 -Aluminium cut from a single sheet
www.5osa.com
  




 -NEO design studios
 -Vanity
 -Fabric
www.neo-studios.de
  




 -Novague
 -EDGE chair
 -Aluminium
www.novague.com
  




 -Patricia Urquiola
 -Antibody Chair
 -Reversible felt, wool fabric, stainless steel
www.kmpfurniture.com
  




 -Phil Cuttance
 -FACETURE lamps
 -Resin
www.philcuttance.com
 

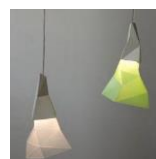



 -Phil Cuttance
 -FACETURE vases
 -Resin
www.philcuttance.com





 -Po Shun Leong
 -Cookie stool, Counter Stool, Po Chair
 -Wood
www.poshunleong.com
  




 -TO DO Product design
 -Papero lamp
 -ABS, polypropylene
www.behance.net
  




 -Rami Tareef
 -Foldigon, Outdoor Sofa
 -Wood and Textile
www.vurni.com/foldigon-coffee-table-sofa
   




 -Ran Amitai
 -Folded aluminium chair
 -Aluminium
www.designboom.com
  




 -Sebastian Burdon
 -Sawn Table
 -Aluminium and glass
www.pinterest.com





 -Semi Skimmed milk
 -Milk curved packaging
 -Cardboard
www.Pinterest.com
 






 -Shin Yamashita
 -Land Peel
www.shinple.com
  




 -Showroom Finland
 -Cardboard furniture
 -Cardboard
www.showroomfinland.fi
 




 -SLAMP
 -Bach
 -Opaflex
www.slamp.com
 




 -SLAMP
 -Chapeau
 -Metallized-Mirror
 Polycarbonate
www.slamp.com
 




 -SLAMP
 -Diamond
 -Opaflex
www.slamp.com
 







 -So Takahashi
 -Origami Chair
 -Steel
www.dezeen.com
 



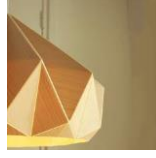

 -Soojin Kim
 -Origami Chair
 -Plastic and Velcro
www.yankodesign.com
 




 -Studio Ayaskan
 -GROWTH, an origami-like pot that grows with plant
 -Polypropylene
www.ayaskan.com
 



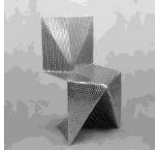

 -Studio Dror
 -Pick Chair
 -Wood and Metal
www.studiodror.com
 




 -Studio Snowpuppe
 -Chestnut wooden origami lamp
 -Birchwood veneer
www.studiosnowpuppe.nl
 




 -Taewon Hwang
 -Flat Pack Mouse
 -Polycarbonate, Silicone, Plastic
www.yankodesign.com
 




 -Tobias Labarque
 -Perforated aluminium folded chair
 -Aluminium
www.tobiaslabarque.com
 




 -Tobias Labarque
 -Perforated aluminium folded chair
 -Aluminium
www.tobiaslabarque.com
 




 -Tomohiro Tachi
 -Rigid foldable table
 -rigid panels with membrane hinges
www.tsg.ne.jp
 




 -Van Esch by Matthias Demacker
 -Origami Table
 -Aluminium
www.stylepark.com
 




 -Vondom by Karim Rashid
 -VERTEX Chair
 -recyclable plastic
www.vondom.com





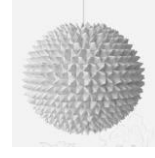
 -Uria Graver
 -CHAIR-IGAMI
 -Metal
www.yankodesign.com
 




 -Yuji Fujimura
 -ORIC, origami chair
 -Plastic
www.themag.it
 



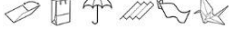





































































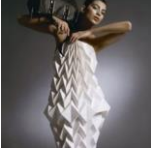











 -Zhang Zhoujie
 -Triangulation Series Furniture
 -Aluminium
www.zhangzhoujie.com
 

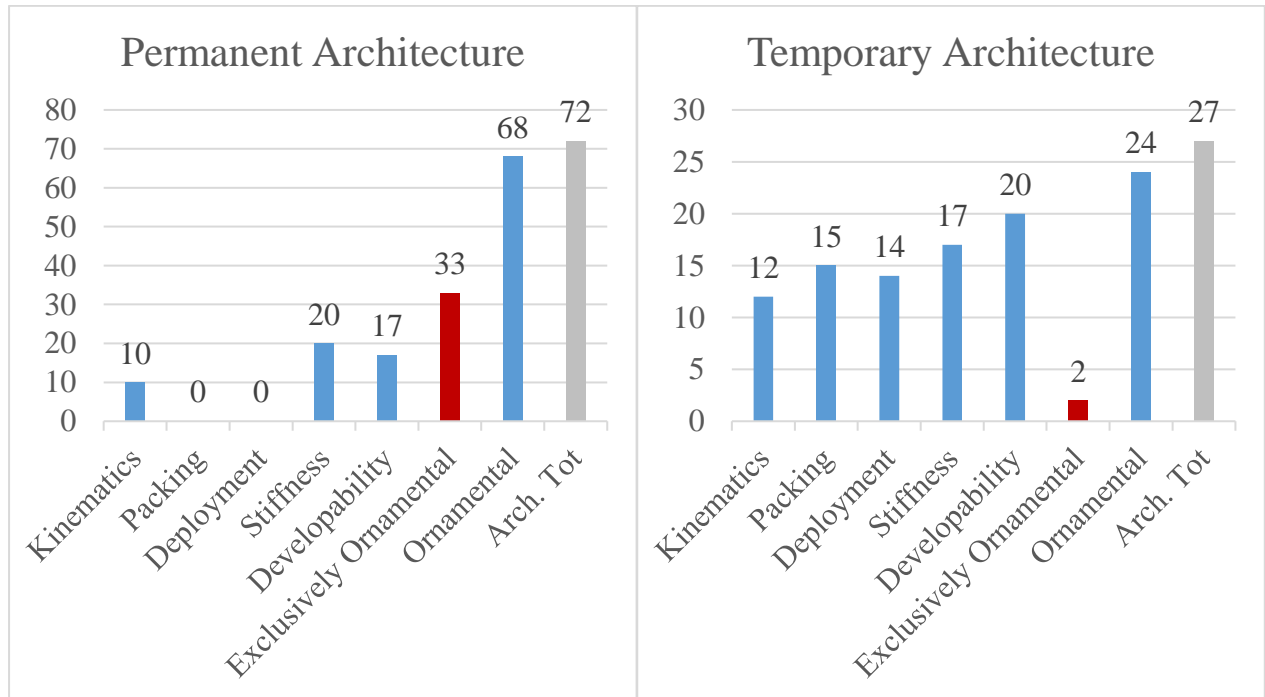



 -Zipper 8 Lighting
 -Large Dakota Pendant Light
 -Paper
www.amazon.com
 

2.6. Fashion and Clothing - Synoptic Tables

	<p> -EIN-TRITT -Catherine Meuter -Canvas and other materials www.virtualshoemuseum.com</p> 		<p> -Tridimensional Origami Phone -Chengyuan Wei -Cardboard www.yankodesign.com</p> 		<p> -Paper Bowtie -FiberStore -Paper www.etsy.com</p> 
	<p> -Melt -HOID -Cotton jersey, Iron on interface www.saatchiart.com</p> 		<p> -MUYBRIDGE PT.2 -HOID -Cotton jersey, Iron on interface www.saatchiart.com</p> 		<p> -NO 419 -HOID -Cotton jersey, Iron on interface www.saatchiart.com</p> 
	<p> -H+Bag -Hyo Jun Jeon -Paper www.yankodesign.com</p> 		<p> -Tessellated origami ring -Ilan Garibi -Gold www.garibiorigami.com</p> 		<p> -Tessellated origami necklace -Ilan Garibi -Gold www.garibiorigami.com</p> 
	<p> -Tessellated origami bracelet -Ilan Garibi -Metal and wood www.garibiorigami.com</p> 		<p> -Paper bags -Ilvy Jacobs -Paper www.ilvyjacobs.nl</p> 		<p> -Origami dresses -Jum Nakao -Paper www.jumnakano.com</p> 
	<p> -Sa Umbrella -Justin Nagelberg -Recyclable plastic polymers www.designboom.com</p> 		<p> -Folding Leather Stool -Louis Vuitton, Atelier Oi -Leather www.atelier-oi.ch</p> 		<p> -Collapsible Cycling Helmet -Mike Rose -Metal fabric and plastic www.yankodesign.com</p> 
	<p> -Folded plate shirt -MILIVOJEVIC MILOS -Cotton www.milivojevicmilos.com</p> 		<p> -Ecstatic Spaces collection -Tara Keens Douglas -Paper www.dezeen.com</p> 		<p> -Ecstatic Spaces collection -Tara Keens Douglas -Paper www.dezeen.com</p> 
	<p> -Flux Snowshoe -Eric Burnt www.core77.com</p> 		<p> -Jittala X bag -Issey Miyake www.finnishdesignshop.it</p> 		<p> -Silver-tone 'Prism' tote bag -Issey Miyake www.farfetch.com</p> 
	<p> -123 5. standard -Issey Miyake www.isseymiyake.com</p> 		<p> -Frame Pleats Bag -Issey Miyake www.isseymiyake.com</p> 		<p> -Luna Pleats -Issey Miyake www.isseymiyake.com</p> 
	<p> -Origami Fashion -Diana Gamboa www.abitiscultura.wordpress.com/2013/06/12/diana-gamboa/</p> 		<p> -Paper couture -Sylvia Lewandowska designdautore.blogspot.com</p> 		<p> -Nintai, Origami-Inspired ,Geometric Dresses -Mercedes Arocena and Lucia Benitez strictlypaper.com</p> 

2.7. Data Processing – Trend of Each Field

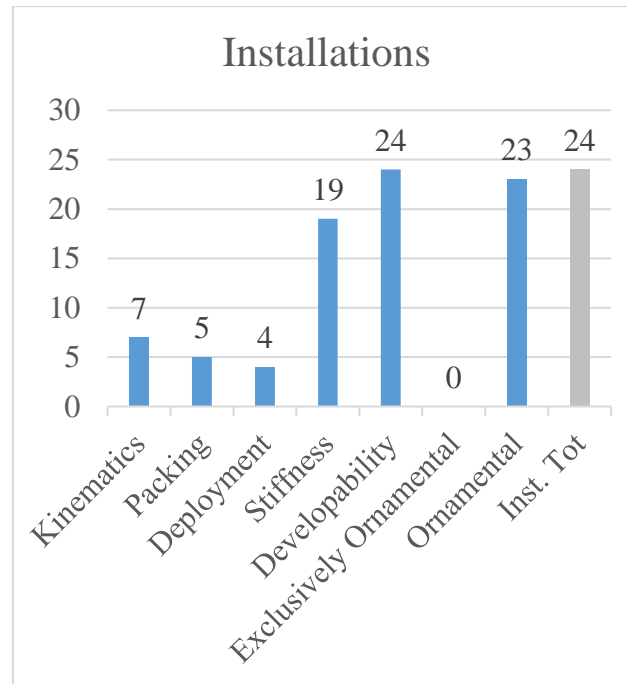


In the field of “Permanent Architecture”, it is evident that a major part of projects is inspired by origami only for ornamental reasons without any other functional purpose. The Tokyu Plaza, the Fuji television Wangan studio, the stage of the Cozzarelli price at the National Academy of Science and the Yokohama International Passenger Terminal are examples of this category. All these examples are clearly using folded surfaces only for ornamental purposes because, in this cases, the folding is neither contributing making the structure stiffer, nor to make the surface movable, nor to optimize the assembling or transportation.

When designing with origami, the designer often needs to control the shapes in a dynamic way, and not all architects are specialized in using advanced 3D-animation applications. In addition, static architecture cases are way more numerous than kinetic architecture ones, because they are less expensive and easier to maintain, but even if we analyse only the kinetic architecture field, the origami mechanisms are always simple and often copied from traditional well-known patterns. These numbers tell us that there is the desire of using the origami as a reference because of its beautiful appearance and useful functionalities, but due to the complexity of designing origami mechanisms at that scale, and due to the lack of tools which could simplify the process, the examples of buildings that are referenced to origami in a functional way are still rare.

Contrariwise, comparing “Permanent Architecture” to “Temporary Architecture”, we notice that kinematic and mechanical proprieties of origami are way more used as tools to improve the projects functionalities, and the projects inspired from origami exclusively for ornamental purposes are rarer. One interesting example of origami-inspired temporary architecture is the “Plate house” by Gattas and You (Gattas & You, 2016) who used origami techniques to design a self-supporting sandwich structure made by cardboard.

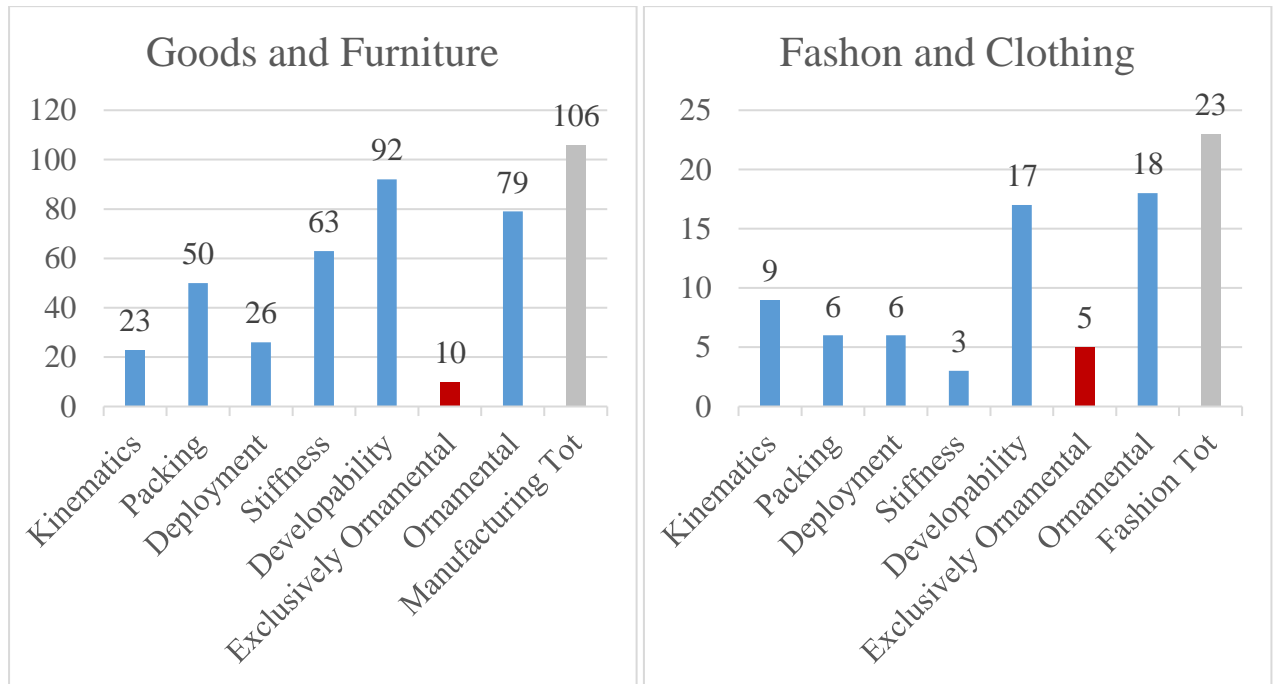
One of the reasons for this higher number of origami-inspired projects for functionality purposes, in the field of temporary architecture, is probably related to the scale of the objects. Smaller dimensions allow the designers to use the self-supporting properties of the materials, moreover, the developability is used a lot more because it can cut the production costs and time. Furthermore, the temporary architecture examples, by their nature, need to be moved, so the deployment and the packing characteristics become more relevant compared to the aesthetics. Nevertheless, the risk, highlighted earlier, of falling into the mere copy of traditional patterns while designing with origami is still an element strongly present also in this kind of projects. In fact, designers often search for solutions into existing patterns and standard constructions probably because of the lack of design tools or a lack in their knowledge and familiarity with origami constructions.



In the field of “Installations”, however, we can see increased efforts to find innovative solutions and patterns. For example, the Resonant chamber by RVTR (Thün, Velikov, Ripley, Sauvé, & McGee, 2012) is a virtuous example of applied origami, where the origami properties are used to make a morphing suspended ceiling capable of changing its shape according to the variable acoustic conditions of the space where it is installed into.

Other interesting examples are the “Computing Curved-Folded Tessellations through Straight Folding Approximation” (Chandra, Körner, et al., 2015) and the “Curved folding metal twins” installation by Chandra et al. (Chandra, Bhooshan, & El-Sayed, 2015), where they used curved folding as a tool to design nice looking curved stiff sculptures by folding a developable surface. In this case, the creases are not used to generate motion, but they are utilised to optimize the fabrication process and to increase the stiffness of the structure.

The same researchers (in collaboration with Zaha Hadid Architects) also designed the “Arum Shell” installation, exhibited at the “Biennale di Venezia” in 2012 (Bhooshan, 2016), which is a beautiful example of modular structure constructed with curved-folded developable metal plates folded with robotized mechanical arms at RoboFold company (Epps, n.d., 2014; Epps & Verma, 2013). These projects are usually academic works or experimentations made by groups of researchers and artists. Sometimes they have the only function of displaying design skills or advertise some architecture firm. Often the projects focus just on exploring the shape or on testing the properties of the material or the efficiency of a certain technology. In many cases, we have noticed that the prototyping phase proceeds in parallel with the creation of the generative algorithms and the analysis of the digital model. In this way, the correctness of the model can be tested through a comparison between the digital surface and the physical prototype.



Differently, from what happens in the field of “Permanent Architecture”, in the “Goods and Furniture” and “Fashion” fields, we found a higher percentage of projects that take advantage of origami design techniques, rather than projects that use origami exclusively for ornamental purposes. For example, the developability is a relevant point in both fields, not only for the possibility to produce an object from a single sheet of the same material but also to optimize the space consumption and the assembling time. The reason of this difference is probably due to the fact that in large-scale projects inspired by origami even if the folded surface is designed to be globally developable, it would require to be assembled instead of being cut and folded from one single sheet of the same material. Thus, the global developability does not really bring a real advantage in architectonic-scale origami. Furthermore, even if it would be found a way to produce and fold a large-scale sheet of the same material (which is already a difficult task), the material should be flexible enough to be foldable while being stiff enough to be self-supporting, which is not an easy target to reach for large-scale continuous surfaces.

2.8. Designing with Folded Surfaces - Critical Observations

According to the collected projects, and considering the analysed data, what we can observe is that it is more common to find small-scale projects rather than architectonic-scale projects that use origami as a reference for many different functional purposes and not only for ornamental purposes. Furthermore, in both the fields of manufacturing and architecture, we can find a multitude of designs that use well-known patterns taken from traditional origami designs, or from previous projects (e.g. the Yoshimura pattern, the Miura pattern, the water-bomb base pattern). There are many different reasons that may explain that. The first is probably due to the scale of the objects because using origami for large-scale projects involves the problem of thickness, and it becomes harder to fold a large-scale surface from a single sheet of the same material. Furthermore, in big-size projects, the typical continuous surfaces proper of origami designs introduces new issues about the mechanical resistance of the joints or about the shape and the dimensions of the hinges that could possibly replace the creases. Moreover, origami mechanisms may have moving parts which are harder, more expensive and more time-consuming to design and maintain compared to static projects. Lastly, small-size designs can be prototyped by using directly the physical models instead of passing through digital simulations. Contrariwise, for large-scale projects the accuracy needed is much higher, thus the digital models of the folded surfaces are necessary. This makes the workflow harder because to be able to simulate digitally the folding animation of origami, the designer must deal with the kinematics of the specific mechanism that he is trying to design. This requires a deep understanding of the origami theories. Furthermore, the moving parts influence the design process from earlier stages.



Figure 11: an example of a design process of a traditional static chair.

For example, if we want to design a traditional static chair the design process would be similar to the one schematized into Figure 11. The design process would usually follow a linear sequence of steps starting from the idea, up to the final object, passing through the sketch, the technical drawing (2D drawings and 3D model) and the prototype.

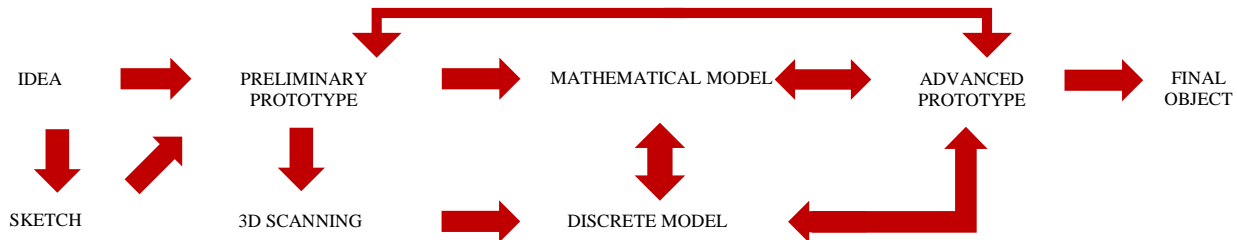


Figure 12: an example of a design process of an origami-inspired foldable chair.

If we compare this process with the one of a foldable chair, the design workflow would appear similar to the one illustrated in Figure 12. The sketch would have marginal importance because it would only contribute to the design of preliminary aesthetic aspects, which are not as crucial as the kinematics aspects. The preliminary conceiving phase would probably see the substitution of the sketch with a paper model which would already help the designer to reflect on some important aspects like the developability, the rigid-foldability, the blocking creases, and the DOF. The preliminary prototype, however, usually does not consider the thickness of the panels, which is something that it is usually postponed in a later step when a more accurate and rigid advanced prototype is built. However, the preliminary and advanced prototypes together are not sufficient to test every single aspect of the project, because the panels of which they are made may have a different elasticity compared to the one of the final object. Furthermore, the rigid-foldability and the DOF are difficult to verify only by using physical models, thus a digitalization of the prototype may help to make an accurate analysis of these aspects. The conversion of the physical prototype into a digital model may be achieved by 3D scanning the model¹⁴ or by constructing and animating it by following the mathematical rules that regulate its pattern which would return much more versatile results with much higher accuracy.

However, also the digital model has some limits. For example, it is hard to simulate accurately the folding motion considering thickness, friction, elasticity and deformations. Furthermore, it might be easy to run into self-intersected configurations which are possible in the digital model but not allowed in the real one. Thus, if not checked carefully, this may cause the final object to block at a certain point because of a non-perfect rigid-foldability or overlooked collisions and self-intersections. Thus, once verified the real behaviour of the advanced prototype, the designer may have to update and eventually implement the analysis of the mathematical model or the discrete model developed previously. Because of all these reasons, we can clearly see that the design process is much harder, and it is not a linear process anymore.

2.9. References - CHAPTER II

Bhooshan, S. (2016). Upgrading Computational Design. *Architectural Design*, 86(2), 44–53.
<https://doi.org/https://doi.org/10.1002/ad.2023>

Chandra, S., Bhooshan, S., & El-Sayed, M. (2015). Curve-Folding Polyhedra Skeletons through Smoothing. *Origami 6: I. Mathematics*, 231.

¹⁴ This solution is often used in curved-folding designs (Kilian et al., 2008)

Chandra, S., Körner, A., Koronaki, A., Spiteri, R., Amin, R., Kowli, S., & Weinstock, M. (2015). Computing curved-folded tessellations through straight-folding approximation. *Proceedings of the Symposium on Simulation for Architecture & Urban Design*, 152–159.

Epps, G. (n.d.). Robofold. Accessed February 14, 2016, from <http://www.robofold.com/>

Epps, G. (2014). Robofold and Robots.Io. *Architectural Design*, 84(3), 68–69. <https://doi.org/https://doi-org.ezproxy.unibo.it/10.1002/ad.1757>

Epps, G., & Verma, S. (2013). Curved Folding: Design to Fabrication process of RoboFold. *Proceedings of SMI/ISAMA2013 (Shape Modelling International): the Thirteenth Interdisciplinary Conference of the International Society of the Arts, Mathematics, and Architecture*, 75–83.

Gattas, J. M., & You, Z. (2016). Design and digital fabrication of folded sandwich structures. *Automation in Construction*, 63, 79–87. <https://doi.org/10.1016/j.autcon.2015.12.002>

Kilian, M., Flöry, S., Chen, Z., Mitra, N. J., Sheffer, A., & Pottmann, H. (2008). Curved folding. In *ACM Transactions on Graphics (TOG)* (Vol. 27, p. 75).

Thün, G., Velikov, K., Ripley, C., Sauvé, L., & McGee, W. (2012). Soundspheres: Resonant chamber. *Leonardo*, 45(4), 348–357. https://doi.org/10.1162/LEON_a_00409

3. CHAPTER III: Definitions and Theorems

In this chapter, we are going to define some focal topics raised by the origami constructions such as:

- Fold-angle
- Developability
- Rigid-foldability
- Degree of Freedom (DOF)
- Flat-foldability
- Non-flat-foldability.

In the following chapters of the thesis, we will refer widely to these terms and concepts. Thus, we clarify them in this section in advance, explaining carefully the mathematical or conceptual basis of every one of them.

3.1. Fold Angle

For “Fold angle” it is intended the dihedral angle between two consecutive faces divided by a crease at any moment of the folding motion. The dihedral angle is an angle between two planes in a third plane which is perpendicular to the intersection lines between the former two planes. To measure the fold angle, we can measure the actual angle between the two planes from surface to surface, or we can measure the angle between their normal vectors. In the former case, the fold angle of a flat-foldable origami with one single linear crease goes from 180° (unfolded flat configuration) to 0° (folded configuration) or from 180° to 360° depending on the mountain/valley assignment. In the latter, the fold angle goes from 0° (unfolded flat configuration) to $\pm 180^\circ$ (folded configuration). Usually, the scientific community favours the normal-to-normal measuring method.

3.1.1. Fold Angle Over Time - From Plot Analysis

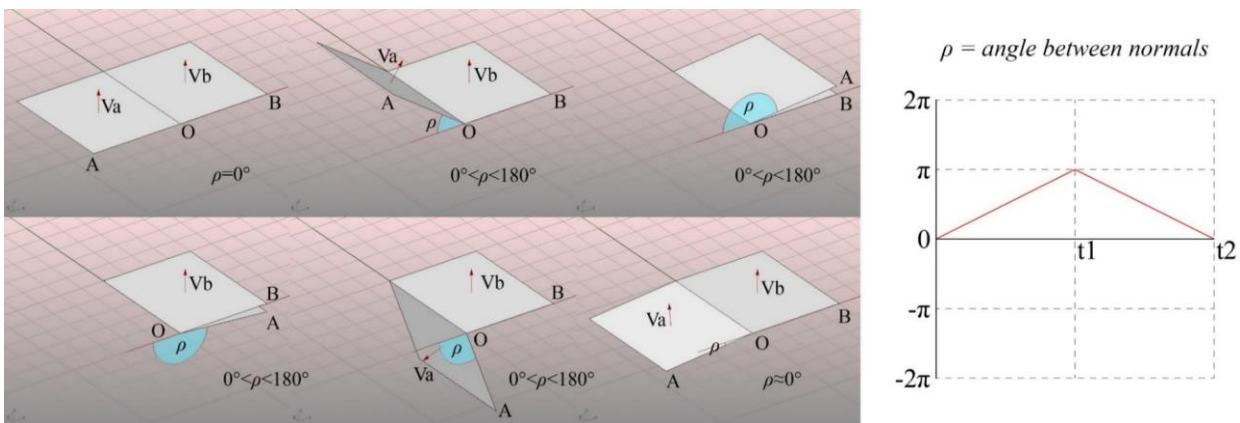


Figure 13: fold angle without folding verse information.

In Figure 13 you can see the plotted graph of the fold angle over time, however, it does not consider the sign of the crease or the verse of rotation of one or the other face. That happens because we asked the software to measure and return the angle between the normal vectors, and as a result, it plotted the smaller possible angle frame-by-frame. The two faces rotate around the crease, and at 180° they pass through each other and continue their motion until they reach the flat unfolded state again. After passing 180° the verse of the valley fold reverses instantly and it transforms to mountain, but in the graph, there is no evidence of that. We would have the same function shape if the two surfaces,

once reached 180°, would reverse their verse of rotation returning to the unfolded state without passing one through each other. Therefore, we need to add a piece of new information to define the fold angle.

We can, for example, multiply for -1 the angle value once the rotation angle is greater than 180°¹⁵. This is sufficient to define the mountain valley assignment. Mathematically it can be solved as follows. Consider a unit vector along the direction of the crease line, multiply it with the unitized cross product between the normal vectors of the two faces. This will return ±1 according to the verse of the crease in relation to the verse of the normal vectors of the surfaces. Multiplying this value with the angle between the normal vectors of the faces will return a signed angle according to the folding verse of the crease, as shown in Figure 14. The formula used to obtain the graph in the figure is the following:

$$\rho_s = \text{sign} (||V_b, V_a, V_o||) \cdot \rho. \tag{7}$$

Which, in the explicit form is:

$$\rho_s = \rho \cdot \frac{V_b \times V_a}{||V_b \times V_a||} \cdot V_o. \tag{8}$$

Where:

ρ_s is the signed angle between the normal vectors V_a and V_b according to the verse of the fold;

ρ is the angle between the normal vectors V_a and V_b ;

V_a is the normal vector to face A;

V_b is the normal vector to face B;

V_o is the vector along the direction of the fold.

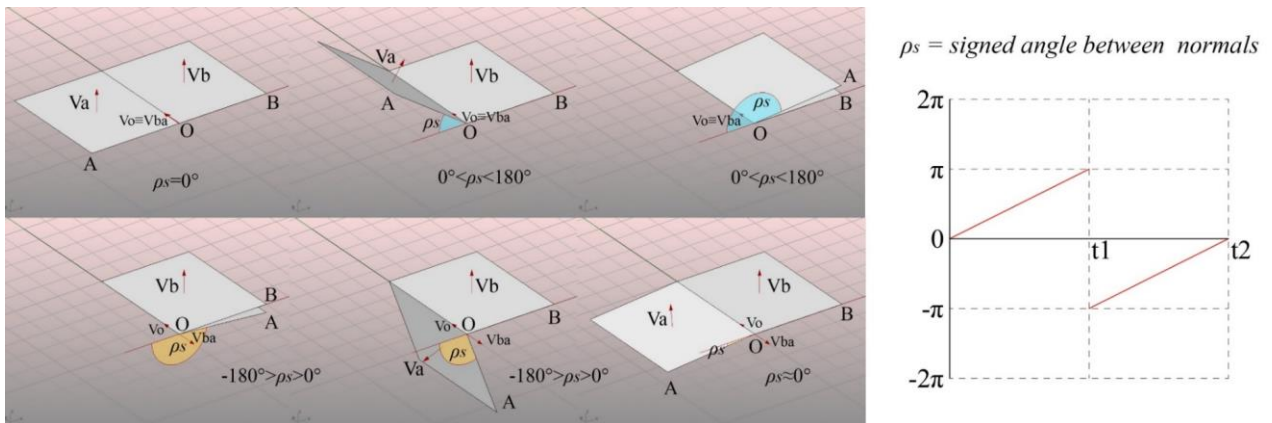


Figure 14: signed angle between normals.

As you can see the plotted function of the angle jumps from 180° to -180° at t_1 , which is what we were looking for because the jump corresponds to the instant flip of the verse of the fold at the moment of the self-intersection. In this case, the function is periodical, and every time it hit 0° it restarts equal to itself. Therefore, it gives us evidence about the mountain/valley assignment, but it does not keep track of the number of total rotations. Thus, if we want to also add that information, we need to implement the formula as follows:

$$\rho_t = \rho + 90^\circ - \left(90^\circ \cdot \frac{V_b \times V_a}{||V_b \times V_a||} \cdot V_o \right). \tag{9}$$

¹⁵ In grasshopper it can be simply done using a “Larger than” node and a “Multiplication” node.

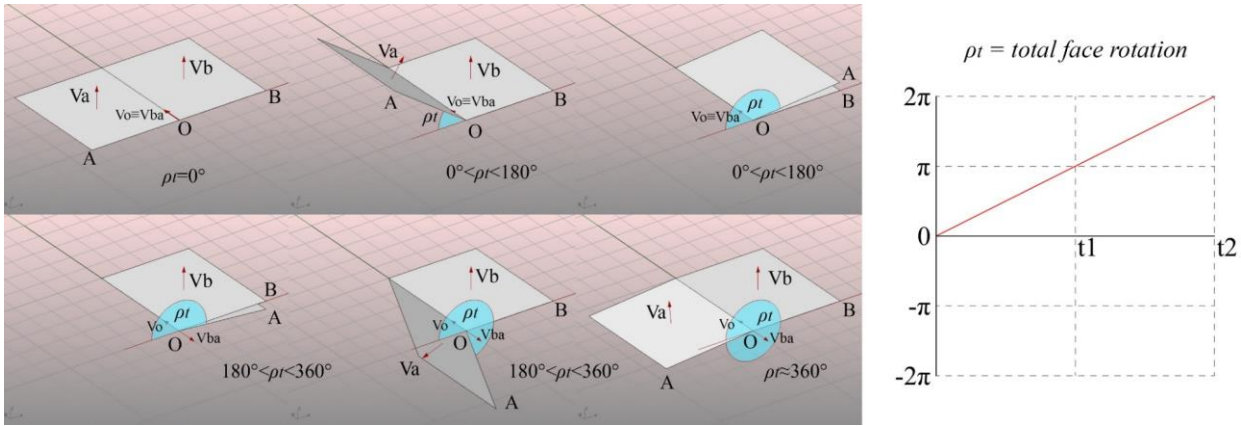


Figure 15: keeping track of the total rotation of the faces.

The graph shown in Figure 15 keeps track of the total reciprocal rotations of the faces A and B, and the fold changes verse when the function intersects the ordinates values multiples of 180° (π). To be able to keep track of rotations bigger than 360° (2π) though, the formula needs to be updated as follow:

$$\rho_t = 360^\circ \cdot n + \rho + 90^\circ - \left(90^\circ \cdot \frac{V_b \times V_a}{||V_b \times V_a||} \cdot V_o \right) \tag{10}$$

Where: *n* is the number of complete turns.

Now if we apply this method to measure the fold angles of every crease in a more complex pattern we would have something similar to the graph shown in Figure 16, which represents the plots of the fold angles over time of a degree-4 single vertex¹⁶.

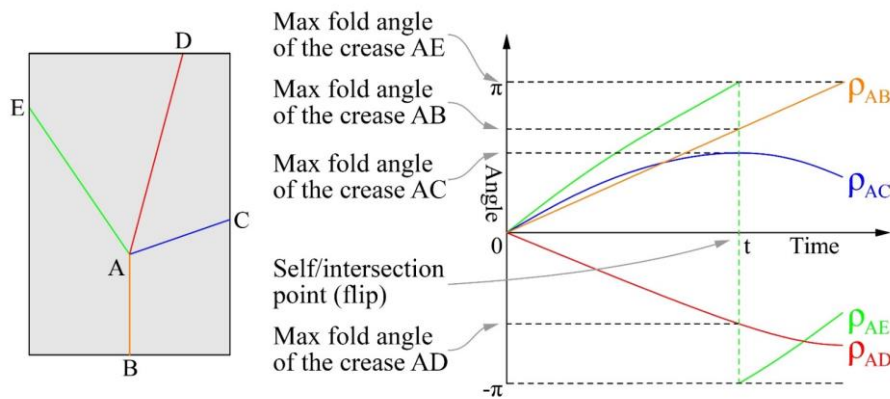


Figure 16: analysis of the fold angle speed for each fold in a degree-4 vertex CP (crease pattern).

The plot shown in figure follows the expression (8), therefore, when the function lies in the negative side of the Cartesian plane it means that the crease is mountain folded, contrariwise, when it lies in the positive side, the crease is valley folded. In Figure 16 the fold angle ρ_{AB} , which is the controller fold angle, has been animated with constant speed, therefore its function is the only one with a linear path, but it is not the one that hit 180° first. In fact, at the time *t* included in the Δt domain, one of the other folds flips and its function jumps from the positive space to the negative space of the Cartesian plane. The time *t* represents the moment when the vertex self-intersects and the verse of the fold AE (once the two faces adjacent to it passes through each other) instantly flips changing its mountain/valley assignment.

¹⁶ The degree-4 vertex is an internal vertex of a pattern with four creases converging into the same point. A comprehensive discussion about flat-foldable and non-flat-foldable degree-4 vertices will be carried out into section 3.5 and 3.6.

To find the values of the maximum fold angles for each crease, it is sufficient to intersect all the fold angle functions with the abscissa t and extrapolate the relative ordinate values. Furthermore, in the same way, it is possible to extrapolate all the fold angle values for each fold at any t .

3.2. Developability

The developability is the property of any surface to be unfolded or unrolled into a plane without distortions or cuts. Conversely, it is a non-planar surface which can be shaped by transforming a plane by folding, rolling. The developable surfaces are always ruled surfaces, but not every ruled surface is developable, for example, the hyperboloid is a ruled surface which is not developable (Migliari, 2009a). Ruled surfaces that are developable are for example cylinders or cones. A developable surface mathematically is a surface with zero Gaussian curvature, contrariwise non-developable surfaces have double curvature or non-zero Gaussian curvature. The Gaussian curvature in differential geometry is called K and represents the product of the principal curvatures K_1 and K_2 at a given point of the surface.

For example, a sphere has a Gaussian curvature equal to $1/r^2$ in every point of its surface. Contrariwise, a plane or a cylinder have Gaussian curvature equal to 0 everywhere. In these examples, the Gaussian curvature is equal in every point of the surfaces, but in general, it can be different from point to point, for example, a torus has negative Gaussian curvature in the inside and positive in the outside.

Because an origami is made by planar faces, we cannot use the Gaussian curvature to judge its developability. In origami, the developability of a given pattern is measured by summing all the sector angles between the creases at every vertex. If all the summations of all the sector angles at every vertex are equal to 360° the pattern is developable.

Traditional origami is always developable because it starts from a flat sheet of paper, but in the last few years some researchers started to study the possible applications of non-developable vertices into origami-like mechanisms, for example in the paper “Folding Mechanisms with Discriminate Extremal Configurations for Structural Purposes” Buffart et al. (Buffart et al., 2018) make some considerations about using non-developable non-flat-foldable vertices to design movable mechanisms with given extremal configurations. Also, Tachi proposed a method using degree-4 non-developable vertices to convert three-dimensional polyhedra (cut along some edges) into one-DOF mechanisms that can fold and unfold with a smooth motion without bifurcations (Tachi & Horiyama, 2018).

The vertices with the sector angles that sum up to an angle smaller than 360° can be configured into synclastic configurations (or pyramidal), The vertices with the sector angles that sum up to an angle bigger than 360° can be configured into anticlastic configurations (hyperbolic paraboloid, or saddle state). If they are degree-4, both the non-developable synclastic or anticlastic vertices have two extremal configurations that can be reached through a folding motion without bifurcations (because there is not any flat state), and the extremal configurations can be both flat-folded, or both non-flat-folded, or one flat-folded and one non-flat-folded. This characteristic increase greatly the design possibilities, but it is harder to design and fabricate than a developable vertex.

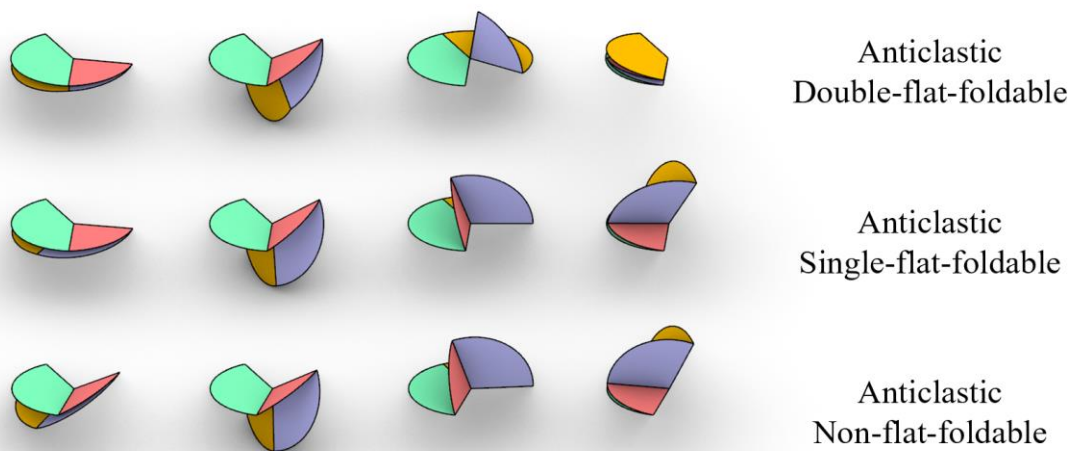


Figure 17: non-developable anticlastic degree-4 vertices – types.

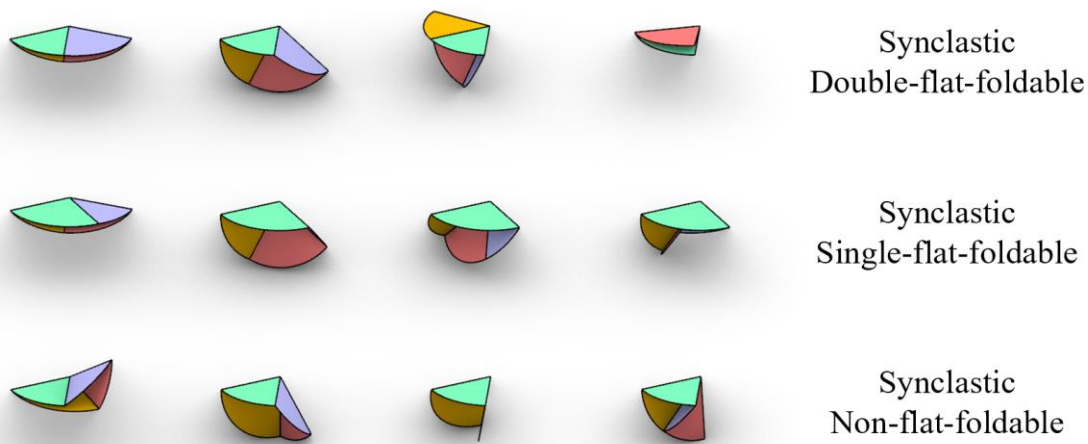


Figure 18: non-developable synclastic degree-4 vertices – types.

3.3. Degree of Freedom (DOF)

The “Degree of freedom” (DOF) of a system is the number of parameters that can vary independently. For example, a point in a plane has two degrees of freedom, which represent the possible translation axis or the coordinates which are needed to identify all the possible positions of the point. A non-infinitesimal object will have more than three degrees of freedom because it can also rotate in space. For example, a segment in three-dimensional space has six DOF, three for translations and three for rotations.

In rigid folding, the DOF usually represent the number of fold angles that can vary independently without bending, flexing or ripping the faces. The identification of the degree of freedom of folded surfaces is a problem which has not been generalized yet. Nevertheless, a rigid origami pattern can be compared to a rigid linkage, and there are many approaches that allow calculating the DOF of linkages. However, most of the times with symmetric and periodical patterns these methods give wrong results due to the occurrence of special conditions. For example, if we calculate the DOF of the Miura-ori¹⁷, without considering its symmetry conditions, it is apparently not foldable at all, but because of the symmetry conditions, the pattern still has 1 single DOF. In the Miura-ori case, as well as in all the cases with closed loops of faces, there are redundancies into the definition of the fold angles of each crease, which means that the same fold angle is constrained multiple times from different directions, but because of the symmetry conditions if the over-constrained angles are equal from all the directions then there are no inconsistencies and the mechanism can move anyway (Tachi, 2011a).

To calculate the DOF of a simple accordion it is sufficient to count all the creases, each one of them will increase the DOF by one. Thus, we can say that: if a pattern has some creases which do not converge to internal vertices, and there are no closed loops of faces, each new crease increases the global DOF by one. Another method to find the DOF of a pattern consists of counting the naked edges of the pattern and subtract 3 to that number, this approach works only with patterns with only triangular faces (e.g. Yoshimura pattern).

But why is the DOF analysis so important for the animation of origami geometries? In the Miura-ori case, it is well known that it is sufficient to constrain only one single fold angle to control the whole folding motion because folding two consecutive faces will propagate the motion to all the other faces in the pattern univocally¹⁸. This means that you need to change only one input fold angle, to control the folds of the entire surface, being able to shape the folded surface in all the possible available configurations. If we consider a straight accordion with only two non-intersecting linear folds, we need to control the two fold angles separately to be able to shape the folded surface in any possible

¹⁷ For an extensive description of the Miura-ori refer to section 4.7.4

¹⁸ The motion is univocal if the mountain/valley assignment is given, thus it may generate problems at flat state.

configuration. This means that each fold angle which can move independently from the others increases the DOF by one and requires one more controller input to configure the surface in all its possible configurations.

For accordions and symmetrical cases, it is relatively easy to foresee the number of necessary controller inputs by trial-and-error. However, in more complex patterns, it is harder. For this reason, it is important to analyse the DOF in advance. Unfortunately, there is not a general method to calculate the DOF yet. An easy approach to test the degree of freedom of any pattern is by building a rigid physical model, but it may be deceptive for wide patterns or when the material is not rigid enough. Another approach is by simulating the animation digitally through physics engines, for example using the software “Freeform origami” by Tachi or with Grasshopper and its plug-in Kangaroo Physics. This last solution is more reliable than the physical model, however, both methods give only qualitative results. They do not return automatically exactly the DOF of the pattern if it is more than one.

It must be said that special cases are often the most interesting cases for movable mechanisms, thus it would be important and interesting to study further this aspect of paper folding and develop a generalized method that does not necessarily need physical simulations and trial-and-error methods. One of the most interesting one-DOF origami mechanism known is the rigid-foldable degree-4 single vertex, a vertex where only four creases meet¹⁹.

3.4. Rigid-Foldability

An origami pattern is rigid-foldable when it can be folded and unfolded without bending, stretching or cutting the faces. This kind of origami structure is not like the paper origami, because the faces must be infinitely rigid. They are, instead, more related to the thick-origami²⁰, because in the real world the stiffness is strictly related to the area of the section.

Thus, the question now is how to judge if a pattern is rigid-foldable or not. There are some special cases where the rigid-foldability can be easily evaluated only by watching the distribution of the creases in the CP and their mountain/valley assignments. For example, in a developable degree-4 single vertex pattern, the rigid-foldability is guaranteed if and only if there are three creases with the same mountain/valley assignment spaced with sector angles smaller than 180° , plus one crease with the opposite sign (Abel et al., 2016).

Another example of a rigid-foldable, one-DOF pattern which is easily recognizable is a pattern composed by multiple degree-4 rigid-foldable vertices joined in a linear array (without making closed loops). Tachi refers to these patterns as a “ $2 \times n$ quadrangle array(s)”, and he says that they are always one-DOF rigid-foldable mechanisms, he also asserts that an “ $m \times n$ (where $m > 2$) quadrangle array... yields over-constrained static structure or a redundant one-DOF mechanism because fold angles are multiply defined” (Tachi, 2011a). Thus, how do we judge if whether an $m \times n$ quadrangle array is rigid-foldable or not?

Abel et al. give us a preliminary answer: “Rigid foldability has been represented using extrinsic parameters of the folded state, e.g., the existence of a set of fold angles satisfying compatibility conditions, or the existence of intermediate state” (Abel et al., 2016). With this statement, Abe et al. refer to two different methods to judge rigid-foldability of a pattern. The first approach refers to the method presented by Belcastro and Hull (Belcastro & Hull, 2002), where they evaluate the rigid-foldability by calculating the fold angle of a closed loop of creases, if the fold angles of the loop are all compatible, then the pattern is rigid-foldable. The second method reported by Abe et al. was stated by Tachi as follows (Tachi, 2010a): “If and only if BDFFPQ mesh, homeomorphic to a disk with more than one interior vertex, has one intermediate folded state, the surface is finitely rigid- foldable.”, which means that in an origami pattern if a flat-unfolded configuration and at least an intermediate folding configuration²¹ exist, then it is guaranteed that the faces during the whole motion do not deform.

We can try applying a qualitative approach based on this last assumption. However, to be able to test this condition qualitatively, we need to simulate the folding motion of the pattern, usually we do this operation with physical models or with digital simulators (like the software Freeform origami), but in both cases we do some errors related to the elasticity of the material or to the tolerance of the software. Thus, this kind of tests based on simulations may return positive results even if the pattern is not rigidly foldable for a small amount.

¹⁹ More about degree-4 vertices at sections 3.5, 3.6, 4.6, 4.7, 6.3.3.

²⁰ We will study further thick origami, and how to convert a zero-thickness origami into an origami with thick panels in section 6.1

²¹ The intermediate folding configuration must be free of deformations and cuts.

If we merge the two approaches in one, we can judge if a pattern is rigid-foldable precisely by calculating the fold angles of all the closed loops of a crease pattern in only one intermediate configuration, and if the compatibility is confirmed then the pattern is rigid-foldable.

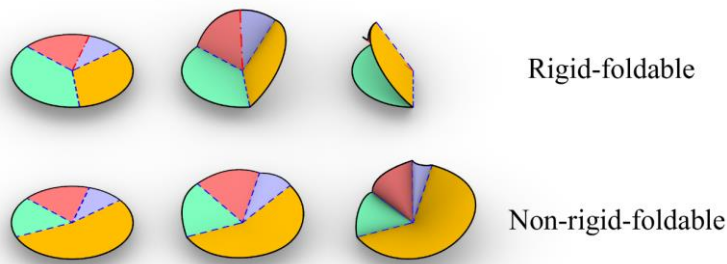


Figure 19: examples of a rigid-foldable and non-rigid-foldable degree-4 vertices.

3.4.1. Reciprocal Diagram to Judge the First-Order Rigid-Foldability

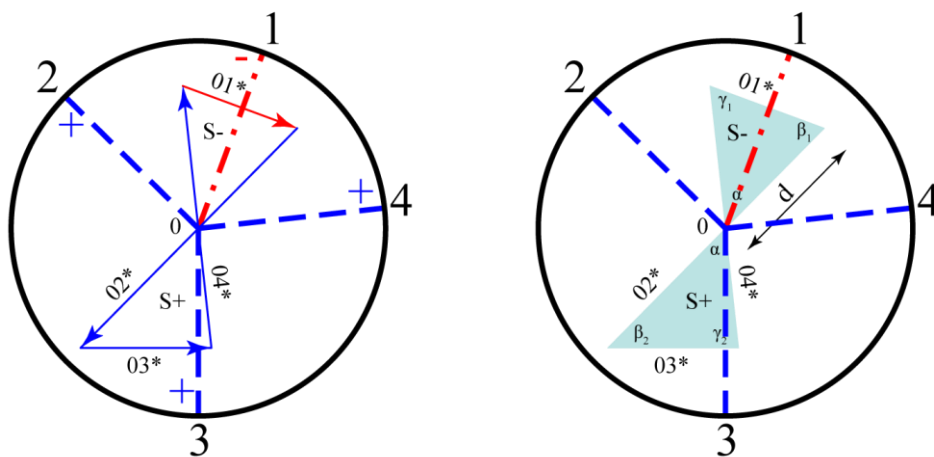


Figure 20: zero-area reciprocal diagram of a degree-4 single vertex pattern.

The reciprocal diagram is a well-known and powerful graphical tool for understanding and designing structural systems. It also has applications in the origami field, in which it has been introduced, for the first time, by D. A. Huffman in 1977 (Huffman, 1977). The reciprocal diagram is composed by straight segments perpendicular to each crease line in a CP, the perpendicular segments form a closed loop around the vertex, such that the direction of the perpendicular segment is $\pm 90^\circ$ relatively to the direction of the creases. The sign, and thus the verse of the vector, depends on the mountain/valley assignment of the folds. The area of the resulting self-intersecting polygon must be equal to zero, as shown in Figure 20.

The reciprocal diagram has been investigated more recently by Demaine et al. in the paper “Zero-Area Reciprocal Diagram of Origami”, where they assert that the reciprocal diagram can be used to investigate the first order approximation of rigid origami: “We can view a polyhedral lifting as the first-order approximation of rigid origami, i.e., an origami surface is composed of rigid panels and rotational hinges connecting them together. Hence, it seems proper to use the reciprocal diagram for the analysis of rigid foldability and the design of rigidly foldable structures. However, it turns out soon that the existence of reciprocal diagram alone is a poor tool to judge rigid foldability of origami. For example, a degree-3 vertex has a nontrivial reciprocal diagram, but there is no valid folding for this pattern” (Demaine et al., 2016).

According to what Demaine et al. assert the reciprocal diagram cannot be used to judge the rigid foldability in general, but it can be used as a tool to test the infinitesimal rigid-foldability which is the property of an infinitely rigid creased surface to behave like a movable mechanism when it is close to the unfolded state.

We will see later in section 3.5.3 an alternative use of the reciprocal diagram as a tool to animate a degree-4 flat-foldable vertex.

3.5. Flat-Foldability

The flat-foldability is the property of an origami pattern to be collapsible into a plane without cutting, stretching or adding new creases to the pattern. Almost all the traditional figurative origami are flat-foldable because the folding steps are performed flattening the model into a flat surface. Mathematically the flat foldability is described by simple rules that we are going to explain briefly in the next section.

3.5.1. Four Rules of Flat-Foldability - Kawasaki and Maekawa Conditions

The flat foldability of a crease pattern follows 4 simple rules²²:

- At any interior vertex, $M - V = \pm 2$: mountain and valley creases always differ by 2, 2 more or 2 less.
- 2 colourability: crease patterns can be coloured with just two colours without ever having the same colour meeting.
- Alternate angles around a vertex sum to a straight line: considering angles between creases around a vertex of the crease pattern, numbering the angles on a circle all the even numbers head up to a straight line, the same happens for the odd numbers.
- No self-intersection at overlaps: no matter how you stack folds and sheets, a sheet can never penetrate a fold

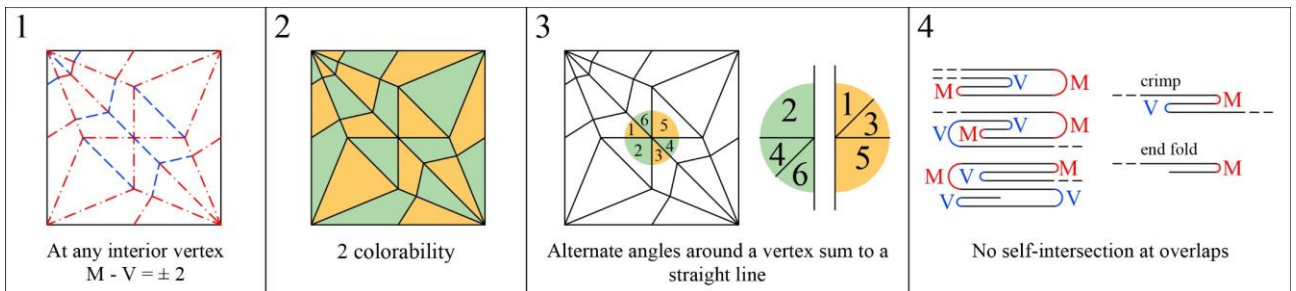


Figure 21: four rules of flat foldability.

These four simple rules are everything we need for judging a flat foldable origami. They are based on mathematical theorems discovered in the last four decades. The first rule is described mathematically by the Maekawa theorem.

Theorem 1: Maekawa-Justin (Hull, 2003a)

$$M - V = \pm 2. \tag{11}$$

Where: M and V are respectively the mountain and valley creases adjacent to a vertex in a flat origami CP.

It means that the mountain folds and the valley folds in a flat-folded single vertex pattern differ always by 2. The second and third rules are described by the Kawasaki theorem. It was discovered by Kawasaki in 1989, although was also discovered independently by Justin in the same year. It gives a criterion to determine if a single vertex crease pattern can be folded to form a flat figure. The theorem statement is the following:

Theorem 2: Kawasaki-Justin theorem (Demaine & O'Rourke, 2007; Hull, 2003a)

²² Which were briefly and easily explained by Robert Lang in his presentation at “TED talks” in 2008 (Lang, 2008)

A single-vertex crease pattern defined by angles $\theta_1 + \theta_2 + \dots + \theta_n = 360^\circ$ is flat foldable if and only if n is even and the sum of the odd angles (θ_{2i+1}) is equal to the sum of the even angles (θ_{2i}), or equivalently, either sum is equal to 180° :

$$\theta_1 + \theta_3 + \dots + \theta_{n-1} = \theta_2 + \theta_4 + \dots + \theta_n = 180^\circ. \tag{12}$$

It can also be written as follows:

$$\theta_1 - \theta_2 + \theta_3 - \dots - \theta_{2n} = 0. \tag{13}$$

The fact that the creases must be even implies that, for any flat-foldable crease pattern (even with multiple internal vertices), it is always possible to colour the regions between the creases with two colours, such that each crease separates two areas of different colours, this is always true for each side of the paper. Also, the fact that the sum of odd and even angles must be equal implies that either odds and evens angles sum to a straight line.

The Kawasaki theorem for developable flat-foldable vertices was generalized by Demaine in 2007 for non-developable pieces of paper as follows:

Theorem 3: Kawasaki-Justin-Demaine generalized for non-flat pieces of paper (Demaine & O'Rourke, 2007)

A single-vertex crease pattern defined by angles $\theta_1, \theta_2, \dots, \theta_n$ is flat foldable if and only if n is even and the alternating sum of the angles θ_i is equal to $0, 360^\circ$, or -360° :

$$\theta_1 - \theta_2 + \theta_3 - \theta_4 + \dots + \theta_{n-1} - \theta_n = \sum_{i=1}^n (-1)^i \theta_i \in \{0, 360^\circ, -360^\circ\}. \tag{14}$$

The theorem 2 (Kawasaki-Justin) is included in the theorem 3 (Kawasaki-Justin-Demaine) and can be only used when working with flat pieces of paper.

For what concerns the self-intersection rule the problem can be approached dividing the cases into two simple groups of crease patterns: a pattern with parallel creases, and a pattern with creases incident in a single vertex. The flat-foldability of the pattern depends on many factors: the order of mountain and valley creases, the distance or the angle between consecutive creases. For example, if the pattern is composed by all parallel folds with alternated verses, it is always foldable, but if there are consecutive folds with the same verse the foldability depends on the sequence of the verses of the folds, and on the distances between the folds. The same can be said for a case where the creases converge in a single vertex, but instead of the distances, we must consider the angles between them. For a much comprehensive explanation in mathematical terms and more bibliographic references refer to the extensive investigation made by Demaine, in his book "Geometric folding algorithms: linkages, origami, polyhedral" (Demaine & O'Rourke, 2007).

3.5.2. Flat-Foldable Degree-4 Single Vertex – Relations Between Fold Angles

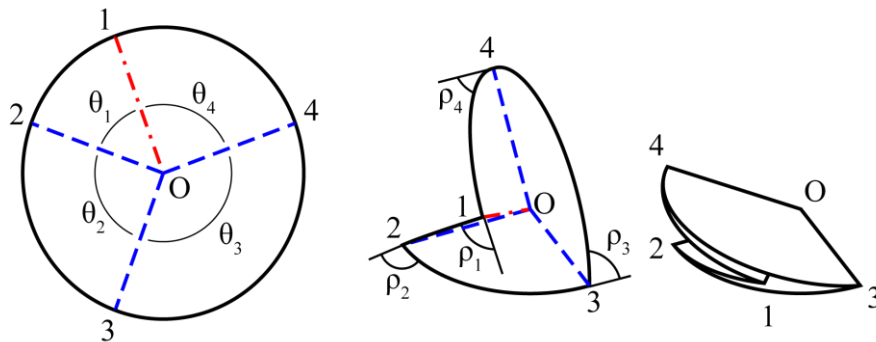


Figure 22: flat-foldable degree-4 vertex notation.

A particularly interesting flat-foldable pattern is the flat-foldable degree-4 single vertex. It is flat-foldable when it is characterized by a particular symmetry condition between opposite creases as shown in Figure 22. Because this particular pattern has only one-DOF every fold angle is univocally related to all the other fold angles. In this section, we are going to report the well-known formulations that relate the fold angles in a degree-4 vertex, and we are going to apply them to a folded surface with a Grasshopper's definition to test their correctness.

The relationship between the fold angles in a degree-4 vertex has been studied by many researchers such as David A. Huffman, Thomas C. Hull, Robert J. Lang and Tomohiro Tachi (Huffman, 1976; Hull, 2006; Lang, Magleby, & Howell, 2016; Tachi, 2009). In particular, Lang in his paper “Single Degree-of-Freedom Rigidly Foldable Cut Origami Flashers” asserts that the vertex is flat foldable if and only if:

$$\theta_1 + \theta_3 = \theta_2 + \theta_4 = \pi. \quad (15)$$

and for flat foldable vertices the major fold angles are equal:

$$\rho_2 = \rho_4. \quad (16)$$

and the minor fold angles are equal but with a different sign:

$$\rho_1 = -\rho_3. \quad (17)$$

Furthermore, he derives the known formulations of the fold angles of a flat-foldable degree-4 vertex proposing a particularly simple²³ expression that describes the relationship between adjacent fold angles as follows:

$$\frac{\tan\frac{1}{2}\rho_2}{\tan\frac{1}{2}\rho_1} = -\frac{\tan\frac{1}{2}\rho_2}{\tan\frac{1}{2}\rho_3} = \frac{\tan\frac{1}{2}\rho_4}{\tan\frac{1}{2}\rho_1} = -\frac{\tan\frac{1}{2}\rho_4}{\tan\frac{1}{2}\rho_3} = \frac{\sin\frac{1}{2}(\theta_1+\theta_2)}{\sin\frac{1}{2}(\theta_1-\theta_2)}. \quad (18)$$

This expression can be used to animate the pattern with Grasshopper by writing the following rearrangement of the expression (Expression 19) into the “Expression” component and using the result as the rotation value of the corresponding adjacent faces, as shown in Figure 23 (the full algorithm is also reported in Appendix A.1). The expression must be written in the following form, in order to be readable by the software:

$$2 * \text{Atan}(\sin((H1 + H2)/2)/(\sin((H1 - H2)/2)) * \tan(R1/2)) = R2. \quad (19)$$

Where:

Atan (...) is $\tan^{-1}(...)$

H1 is θ_1

H2 is θ_2

R1 is ρ_1

R2 is ρ_2

Whit this expression we calculate ρ_2 from ρ_1 , θ_1 and θ_2 , and because $\rho_3 = -\rho_1$ and $\rho_4 = \rho_2$ we already have all the four angles and we can animate all the faces of the degree-4 flat-foldable vertex²⁴.

²³ Its defined as “particularly simple” because it is much easier than the formulation for the non-flat-foldable degree-4 vertices that we show in 3.6.1.

²⁴ In section 4.6 we will see how to animate the same degree-4 vertex with synthetic method avoiding mathematical formulations.

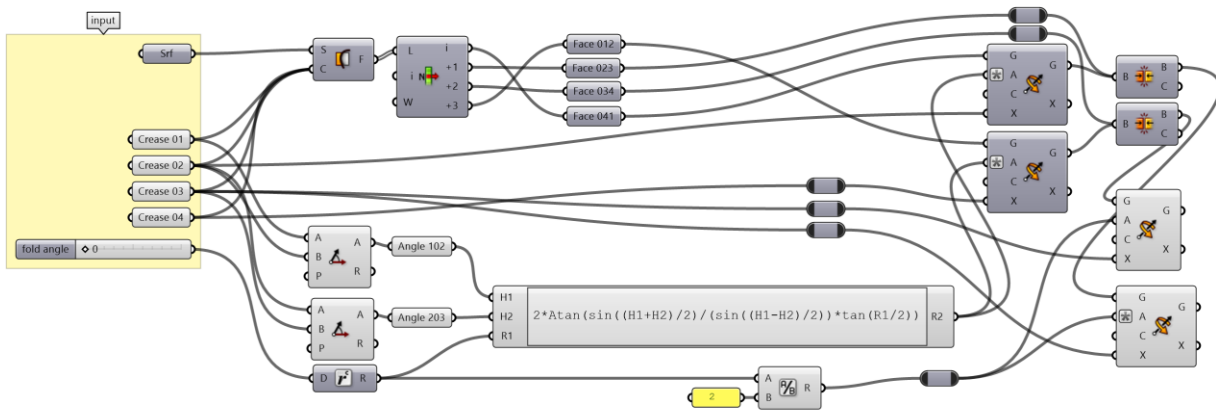


Figure 23: generative algorithm that animates a degree-4 flat-foldable vertex by calculating the fold angles with mathematical formulations.

3.5.3. Flat-Foldable Degree-4 Single Vertex – Reciprocal Diagram and Fold Angles

We anticipated in section 3.4.1 that the reciprocal diagram can also be used as a tool to identify the fold angles of a flat-foldable degree-4 vertex, this is possible because the lengths of the segments of the reciprocal diagram are strictly related to the sector angles, thus they have a relation to the expression (18).

The formulation (18) that relates consecutive angles can be rearranged in the following form:

$$\rho_i = 2 \tan^{-1}(k * \tan \frac{\rho_{i+1}}{2}). \tag{20}$$

Where k is:

$$k = \frac{\sin \frac{1}{2}(\theta_1 + \theta_2)}{\sin \frac{1}{2}(\theta_1 - \theta_2)}. \tag{21}$$

By experimental method, we discovered that the constant k , in a flat-foldable degree-4 vertex, can also be calculated by dividing the length of the longest segment with the length of the shortest segment of the reciprocal diagram as follows:

$$k = \frac{\max \text{ edge length}}{\min \text{ edge length}}. \tag{22}$$

To draw parametrically a reciprocal diagram, we need to identify the single crease with opposite sign and draw a vector with an angle equal to $+90^\circ$ relatively to that crease. We do the same thing with the other three creases but rotating the relative vectors by an angle of -90° . Then we draw a line along the direction of each vector, and we extend each one of them until they meet the relative adjacent two lines, like so we find 4 intersection points. We connect the 4 points with a polyline following the verse of the vectors, obtaining a self-intersecting closed loop of four edges shaped like a ribbon. The ribbon forms two triangular areas which need to be equalized to make a proper reciprocal diagram with zero-area. To equalize the areas, we translate one of the edges keeping it parallel to itself while extending the two adjacent edges of the ribbon until the two triangles have the same area. As shown in Figure 20, if we fix the position of the vectors 02^* , 03^* , 04^* we can find the position of 01^* by calculating d using the internal angles of the polygon as follows:

$$d = \sqrt{\frac{2S \sin \gamma_1}{\sin \alpha \sin \beta_1}}. \tag{23}$$

Once drawn the reciprocal diagram, we calculate k by measuring the maximum and minimum lengths of the edges²⁵. With k , obtained with parametrical method (as shown in the full generative algorithm shown in Figure 24 and Appendix A.2)., we can now calculate all the fold angles at any folded state in any flat-foldable degree-4 vertex.

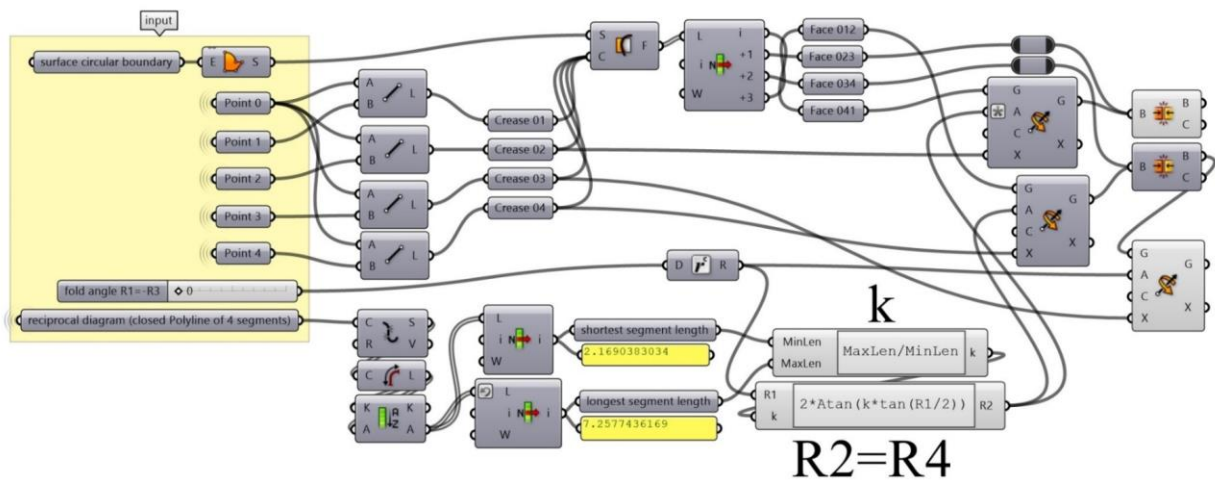


Figure 24: generative algorithm for the animation of a flat-foldable degree-4 vertex calculating k by using the reciprocal diagram.

3.5.4. Calculating k Through Reciprocal Diagram – Proved by Experimental Method

As stated in the previous section we proved by experimental method that the reciprocal diagram can be used to calculate the constant k needed in the equation 20 which allows to calculate all the fold angles of a flat-foldable degree-4 vertex. We proved it with the parametrical approach as follows.

Construct parametrically the reciprocal diagram of a given degree-4 vertex and calculate the constant k as explained in section 3.5.3. Choose one controller crease and fix its fold angle to a value between 0° and 180° . Calculate the fold angle of one of the adjacent creases applying the expression 20 using the constant k just calculated. Because the opposite fold angles in a degree-4 vertex are always equal we already have all the fold angles that we need to univocally define the position of each face of the degree-4 vertex. Now we rotate the faces around the adjacent creases to configure the flat pattern into the target folded configuration that matches the fold angle of the controller fold. If the angles are correct the faces will be configured into a closed loop of planar faces with no deformations in the faces.

Now, because the whole process is parametric, we can animate the folding and unfolding of the vertex by changing the input fold angle. By animating the vertex, we can prove that the faces always make a closed loop at any value of the controller fold angle. The preservation of the shape of the faces is guaranteed by construction, the preservation of the closed loop, instead, is verified by setting off the animation and testing the continuity between adjacent faces frame-by-frame. To prove that this approach works with every flat-foldable vertex we tested different flat-foldable degree-4 patterns at limit cases and at intermediate symmetric cases²⁶ as shown in Figure 25.

Of course, we can prove this also by the analytical method by relating the expression 20 with the construction of the reciprocal diagram by applying simple trigonometry rules and proportions between angles and lengths.

²⁵ In a flat-foldable degree-4 single vertex pattern the reciprocal diagram is always symmetric, thus there are two equal segments that are the longest and two equal segments that are the shortest, we just pick one of each pair of segments to calculate k .

²⁶ We avoided trivial cases like symmetry reflections of the patterns and flipped mountain/valley assignment.

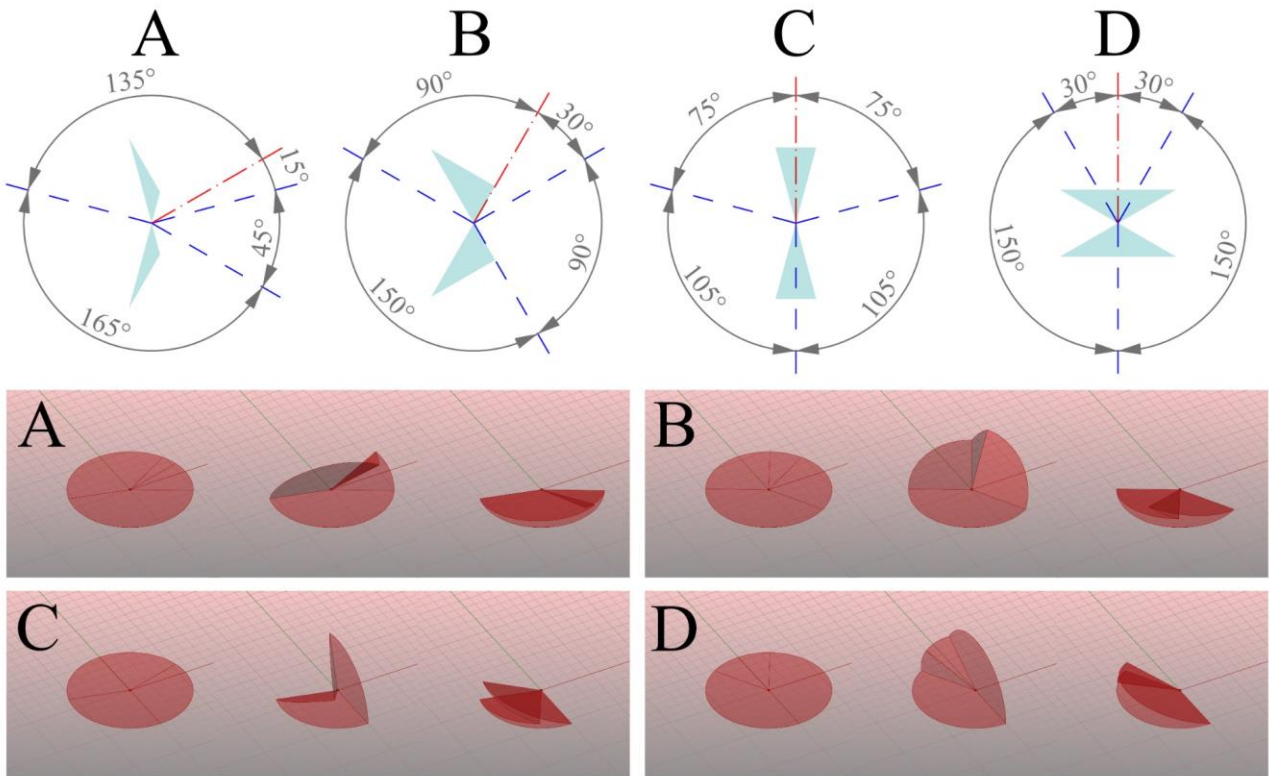


Figure 25: Examples of test cases of asymmetric and symmetric flat-foldable vertices animated by calculating the constant k by dividing the longest and shortest segment of the reciprocal diagram.

3.6. Non-Flat-Foldability²⁷

A non-flat-foldable pattern is a pattern that cannot be flat-collapsed into the plane without adding new creases. It is the counterpart of the flat-foldable pattern introduced in the previous section, and it has some interesting properties that may be used into a movable mechanism. One of the most useful property is that it blocks at a certain three-dimensional configuration. If the pattern has one-DOF the configuration is univocal (considering a given mountain/valley assignment) and this makes it very useful to design deployable or compactable objects. Two examples of self-blocking foldable mechanisms, designed using non-flat-foldable degree-4 vertices, are presented in section 6.3 and section 6.2 and they are a rigid-foldable chair and a rigid-foldable ladder.

The blocked configuration is often called “locked”, “arrested” (Buffart et al., 2017), or “binding” (Lang, 2018). We use “blocked” (Klett & Drechsler, 2011) because some of the terms already used may be interpreted as configurations where the movement is obstructed in both directions²⁸.

3.6.1. Non-Flat-Foldable Degree-4 Single Vertex - Huffman’s Formulations

Flat-foldable degree-4 vertices are special cases of generic degree-4 vertices. If we trace 4 creases that converge into a point with random angles, it is more probable to come up with a non-flat-foldable degree-4 vertex instead of a flat-foldable one. Thus, we can say that the major part of degree-4 vertices is non-flat-foldable. Furthermore, as we previously stated, non-flat-foldable vertices may be very useful for practical applications, for this reason, we want to

²⁷ Some parts of this sections are also published into the paper “*Designing Self-Blocking Systems with Non-Flat-Foldable Degree-4 Vertices*” (Foschi & Tachi, 2018) written by the author of this thesis and the co-supervisor Tomohiro Tachi. The paper has been presented at the 7-OSME (The 7th International Meeting on Origami in Science, Mathematics and Education). The meeting took place in Oxford between 5th and 7th September 2018.

²⁸ As an additional reference, we also want to mention that the block fold has been recently called “Blockfaltung” by Lang (Lang, 2018).

explain carefully how they work and how to treat them mathematically (in this section) and geometrically (in sections 4.6.2 and 4.6.3).

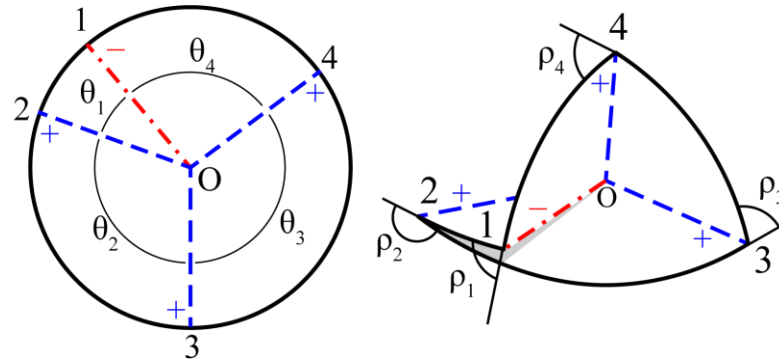


Figure 26: non-flat-foldable degree-4 single vertex notation.

Huffman in the paper “Curvature and Creases: A Primer on Paper” (Huffman, 1976) generalised the formulation, reported in section 3.5.2, for every degree-4 vertex. In fact, the formulations for flat-foldable degree-4 vertices are a simplification of the Huffman’s formulations which work both for flat and non-flat foldable vertices.

The following formulations relate ρ_4 to ρ_2 and ρ_3 to ρ_1 :

$$\frac{\sin^2 \frac{\rho_4}{2}}{\sin^2 \frac{\rho_2}{2}} = \frac{\sin \theta_2 \sin \theta_1}{\sin \theta_3 \sin \theta_4} \quad (24)$$

$$\frac{\sin^2 \frac{\rho_3}{2}}{\sin^2 \frac{\rho_1}{2}} = \frac{\sin \theta_4 \sin \theta_1}{\sin \theta_2 \sin \theta_3} \quad (25)$$

Huffman also associates ρ_2 to ρ_3 by a “very difficult”²⁹ derivation:

$$\left[1 \mp \frac{\sin \theta_3 \sin \theta_1}{\sin \theta_2 \sin \theta_4} \sqrt{\frac{1 - \frac{\sin \theta_2 \sin \theta_1}{\sin \theta_3 \sin \theta_4} \sin^2 \frac{\rho_2}{2}}{1 - \sin^2 \frac{\rho_2}{2}}} \right] \cdot \left[1 \pm \frac{\sin \theta_3 \sin \theta_1}{\sin \theta_2 \sin \theta_4} \sqrt{\frac{1 - \frac{\sin \theta_4 \sin \theta_1}{\sin \theta_2 \sin \theta_3} \sin^2 \frac{\rho_1}{2}}{1 - \sin^2 \frac{\rho_1}{2}}} \right] = \quad (26)$$

$$= 1 - \frac{\sin \theta_3 \sin \theta_1}{\sin \theta_2 \sin \theta_4}.$$

Rearranging these formulations in the forms $\rho_2, \rho_3 = f(\rho_1, \theta_1, \theta_2, \theta_3, \theta_4)$ and (once found ρ_2) $\rho_4 = f(\rho_2, \theta_1, \theta_2, \theta_3, \theta_4)$ we can find all the fold angles knowing only ρ_1 and the sector angles $\theta_1, \theta_2, \theta_3, \theta_4$.

Unfortunately, it is not trivial rearranging these functions, so we solved them with the help of mathematical software to calculate all the alternative forms and the possible solutions which could be more than one depending on the symmetry conditions.

For the rearranged forms, to be able to input them into Grasshopper, we used the original notation by Huffman even if it is not the standard notation of a degree-4 vertex, because it uses ASCII characters which are the only character that the “Expression” component in Grasshopper accepts, thus the factors change as follows:

$$\rho_1 = q, \rho_2 = n, \rho_3 = p, \rho_4 = m, \theta_1 = D, \theta_2 = C, \theta_3 = A, \theta_4 = B.$$

So, knowing n, A, B, C, D we can calculate q, p and m . For the purposes of this algorithm, we only consider interesting solutions³⁰. The variable q has two interesting solutions, one for each possible folding mode, variable p is related to q . For flat-foldable degree-4 vertices, the interesting solution is only one as well as the folding mode. The variable m has

²⁹ Huffman himself defines it as “very difficult”.

³⁰ We intend as “interesting solutions” the solutions which are not simple mirror reflections of the only 2 possible folding modes, that can be found simply changing the sign of the result of the interesting solutions.

$$\begin{aligned}
 & 1), 2) * \text{Pow}(\text{Sin}(C), -1) * \text{Pow}(\text{Sin}(D), 2) * \text{Pow}(1. * \text{Pow}(\text{Sin}(A), -1) * \text{Pow}(\text{Sin}(C), - \\
 & 1) * \text{Sin}(B) * \text{Sin}(D), 0.5) * \text{Pow}(\text{Pow}(1. * \text{Pow}(\text{Cos}(n/2.), -1), 2) - 1. * \text{Pow}(\text{Sin}(A), -1) * \text{Pow}(\text{Sin}(B), - \\
 & 1) * \text{Pow}(\text{Tan}(n/2.), 2) * \text{Sin}(C) * \text{Sin}(D), 0.5) * \text{Pow}(\text{Tan}(n/2.), 2) - 1. * \text{Pow}(1. * \text{Pow}(\text{Sin}(A), -1), 3) * \text{Pow}(\text{Sin}(B), - \\
 & 1) * \text{Pow}(\text{Sin}(D), 3) * \text{Pow}(\text{Tan}(n/2.), 4) + 1. * \text{Pow}(1. * \text{Pow}(\text{Sin}(A), -1), 3) * \text{Pow}(1. * \text{Pow}(\text{Sin}(C), - \\
 & 1), 2) * \text{Pow}(\text{Sin}(B), -1) * \text{Pow}(\text{Sin}(D), 5) * \text{Pow}(\text{Tan}(n/2.), 4) + 1. * \text{Pow}(1. * \text{Pow}(\text{Cos}(n/2.), - \\
 & 1), 4) * \text{Pow}(1. * \text{Pow}(\text{Sin}(C), -1), 4) * \text{Pow}(\text{Sin}(A), -1) * \text{Pow}(\text{Sin}(D), 3) * \text{Sin}(B) + \text{Pow}(1. * \text{Pow}(\text{Sin}(A), - \\
 & 1), 3) * \text{Pow}(1. * \text{Pow}(\text{Sin}(C), -1), 2) * \text{Pow}(\text{Sin}(D), 3) * \text{Pow}(\text{Tan}(n/2.), 2) * \text{Sin}(B) + 1. * \text{Pow}(\text{Sin}(A), - \\
 & 1) * \text{Pow}(\text{Sin}(B), -1) * \text{Pow}(\text{Tan}(n/2.), 2) * \text{Sin}(D) + 2. * \text{Pow}(\text{Sin}(A), -1) * \text{Pow}(\text{Sin}(B), -1) * \text{Pow}(1. * \text{Pow}(\text{Sin}(A), - \\
 & 1) * \text{Pow}(\text{Sin}(C), -1) * \text{Sin}(B) * \text{Sin}(D), 0.5) * \text{Pow}(\text{Pow}(1. * \text{Pow}(\text{Cos}(n/2.), -1), 2) - 1. * \text{Pow}(\text{Sin}(A), - \\
 & 1) * \text{Pow}(\text{Sin}(B), -1) * \text{Pow}(\text{Tan}(n/2.), 2) * \text{Sin}(C) * \text{Sin}(D), 0.5) * \text{Pow}(\text{Tan}(n/2.), 2) * \text{Sin}(D) + \\
 & 1. * \text{Pow}(1. * \text{Pow}(\text{Sin}(C), -1), 2) * \text{Pow}(\text{Sin}(B), -1) * \text{Sin}(A) * \text{Sin}(D) + 4. * \text{Pow}(1. * \text{Pow}(\text{Cos}(n/2.), - \\
 & 1), 2) * \text{Pow}(\text{Pow}(\text{Sin}(C), -1), 2) * \text{Pow}(\text{Sin}(A), -1) * \text{Sin}(B) * \text{Sin}(D) - 1. * \text{Pow}(1. * \text{Pow}(\text{Sin}(C), -1), 2) * \text{Pow}(\text{Sin}(A), - \\
 & 1) * \text{Sin}(B) * \text{Sin}(D) - 1. * \text{Pow}(1. * \text{Pow}(\text{Cos}(n/2.), -1), 4) * \text{Pow}(1. * \text{Pow}(\text{Sin}(C), -1), 2) * \text{Pow}(\text{Sin}(A), - \\
 & 1) * \text{Sin}(B) * \text{Sin}(D) + 2. * \text{Pow}(1. * \text{Pow}(\text{Cos}(n/2.), -1), 2) * \text{Pow}(\text{Pow}(\text{Sin}(C), -1), 2) * \text{Pow}(\text{Sin}(A), - \\
 & 1) * \text{Pow}(1. * \text{Pow}(\text{Sin}(A), -1) * \text{Pow}(\text{Sin}(C), -1) * \text{Sin}(B) * \text{Sin}(D), 0.5) * \text{Pow}(\text{Pow}(1. * \text{Pow}(\text{Cos}(n/2.), -1), 2) - \\
 & 1. * \text{Pow}(\text{Sin}(A), -1) * \text{Pow}(\text{Sin}(B), -1) * \text{Pow}(\text{Tan}(n/2.), 2) * \text{Sin}(C) * \text{Sin}(D), 0.5) * \text{Sin}(B) * \text{Sin}(D) - \\
 & 2. * \text{Pow}(1. * \text{Pow}(\text{Sin}(C), -1), 2) * \text{Pow}(\text{Sin}(A), -1) * \text{Pow}(1. * \text{Pow}(\text{Sin}(A), -1) * \text{Pow}(\text{Sin}(C), - \\
 & 1) * \text{Sin}(B) * \text{Sin}(D), 0.5) * \text{Pow}(\text{Pow}(1. * \text{Pow}(\text{Cos}(n/2.), -1), 2) - 1. * \text{Pow}(\text{Sin}(A), -1) * \text{Pow}(\text{Sin}(B), - \\
 & 1) * \text{Pow}(\text{Tan}(n/2.), 2) * \text{Sin}(C) * \text{Sin}(D), 0.5) * \text{Sin}(B) * \text{Sin}(D), -0.5))
 \end{aligned}$$

Fold angle p is in function of q, A, B, C, D .

$$2 * \text{Asin}(\text{Pow}(\text{Pow}(\text{Sin}(q/2), 2) * \text{Sin}(A) * \text{Sin}(D)) / (\text{Sin}(C) * \text{Sin}(B)), 0.5))$$

Fold angle m in function of n, A, B, C, D .

$$2 * \text{Asin}(\text{Pow}(\text{Pow}(\text{Sin}(n/2), 2) * \text{Sin}(C) * \text{Sin}(D)) / (\text{Sin}(A) * \text{Sin}(B)), 0.5))$$

These textual solutions have been generated using the software Mathematica by Wolfram research (WolframResearch, n.d.). Obviously they could have been simplified with subfunctions or they could have been written in a slimmer manner using alternative forms, but we decided to leave them as they have been returned by Mathematica because this is what the application returns as a first calculation step, which might convince a nonprofessional user to judge it as too complex to handle, making him/her giving up at this stage.

This kind of intimidating steps is less likely to happen while approaching the same problem with the geometrical constructive approach, that we are going to present in sections 4.6.2 and 4.6.3.

This case study is a clear example of the greater complexity of the algebraic approach compared to the graphical constructive approach.

3.6.2. The Blocking Crease

The blocking crease is the first crease that hit 180° in a CP. In a degree-4 non-flat-foldable single vertex the blocking crease is always one, but they can be more than one in a CP with multiple vertices or multiple degrees of freedom. The identification of the blocking crease is important for animating the folding and unfolding of a one-DOF pattern because if it is used as the controller crease and the domain of its fold angle is limited between 0° and 180° it prevents the pattern to self-intersect.

To identify the blocking crease before folding the pattern we could use the well-known Huffman formulations that would allow us to find the maximum fold angles of every crease, but because those formulations are valid at any time t , they are unnecessarily complex for finding only the fold angles at blocked state.

Thus, in the following sections, we present a simplified method using spherical trigonometry and triangular inequalities on the sphere, that will allow us to identify the crease that blocks first from the unfolded pattern, in a degree-4 single vertex, analysing exclusively the blocked state.

Adding this procedure at the beginning of the algorithms explained in 4.6.3 or 3.6.1 would solve the problem of the identification of the crease that blocks first before folding anything. This would allow us to choose the optimal controller crease from early stages of the animation process. Before explaining this new approach, we need to recall some concepts of the kinematics of a degree-4 vertex.

3.6.3. Understanding the Kinematics of a Non-Flat-Foldable Developable Degree-4 Vertex

A non-flat-foldable degree-4 developable vertex is a vertex with four incident creases forming a convex angle to adjacent ones, which does not satisfy Kawasaki's condition, i.e., the alternating sum of angles does not sum to 0° . The fold angle $\rho \in [-180^\circ, 180^\circ]$ is the angle between the normal vectors of adjacent faces. The sector angle $0 < \theta < 180^\circ$ is the angle between adjacent creases. First, we briefly characterize the kinematics of a non-flat-foldable degree-4 vertex.

In the following statements, it is assumed that the faces can pass through each other, and any state with two coplanar faces is called a “blocked state”.

- A non-flat-foldable degree-4 vertex forms a one-DOF mechanism with no bifurcations in its fold angle function except at the completely unfolded states.
- At the unfolded states, at most two folding modes intersect. The mountain/valley assignment of each folding mode always has three creases with the same signs forming a “Y” shape (convex angle to each other) and one crease with opposite sign (Abel et al., 2016). For non-flat-foldable degree-4 vertices, exactly two creases can be the oppositely signed crease, one for each folding mode.
- In either mode, only one single crease folds flat first, and it blocks the movement when self-intersections are avoided. Hence, the state is called the “first blocked state”.
- Ignoring self-intersection, if the folding motion continues, the faces can pass through each other and the single vertex pattern will reach another configuration where two different faces are coplanar, thus we call it the “second blocked state”.
- The signs flip after the self-intersection, and the second blocked state is equivalent to the first blocked state of the other folding mode (refer to Figure 27).

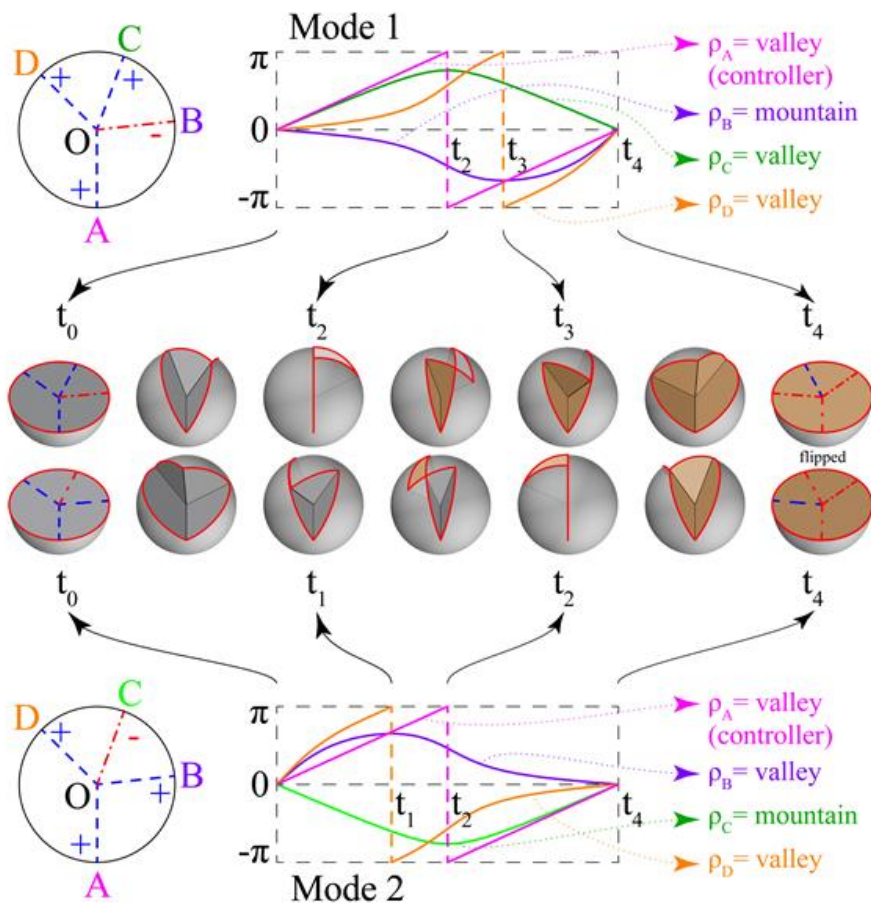


Figure 27: folding animation snapshots, and fold angle plots of a given degree-4 vertex (the folding mode one has the same kinematics as mode two played backwards with mirrored mountain valley assignment). Notice that the unfolded state in t_4 is flipped (upside-down compared to the flat-folded state in t_0).

Figure 27 shows the fold angles variation over time when ρ_A is the controller crease represented as a linear function of time. The fold angle functions of the other creases depend on the controller crease because it is a one-DOF mechanism. Focus on folding mode two. The folded state reaches the first blocked state at t_1 when the ρ_D function jumps from $+180^\circ$ (π) to -180° ($-\pi$). The jump happens because after that point, the faces pass through each other and the sign of the crease flips (passing from valley to mountain in this case). In t_2 , the folded surface reaches the second blocking configuration when ρ_A jumps from $+180^\circ$ to -180° . While two creases A and D rotate 360° , the other creases

B and C rotate to some amount smaller than 180° and go back to O . Function ρ_B reaches its maximum at t_1 , and ρ_C reaches its minimum at t_2 . At O and t_4 , all the fold angles go to 0 at the same time, because at O and t_4 the vertex is completely unfolded.

Because of the two creases ρ_A and ρ_D flipped their signs, when the pattern again reaches the flat state (at t_4), the mountain/valley assignment has changed to that of mode one except that all the signs are flipped. Thus, folding mode 1 is given by the backward play of folding mode two with mirrored mountain/valley assignment.

3.6.4. First Blocking Crease in a Developable Degree-4 Vertex

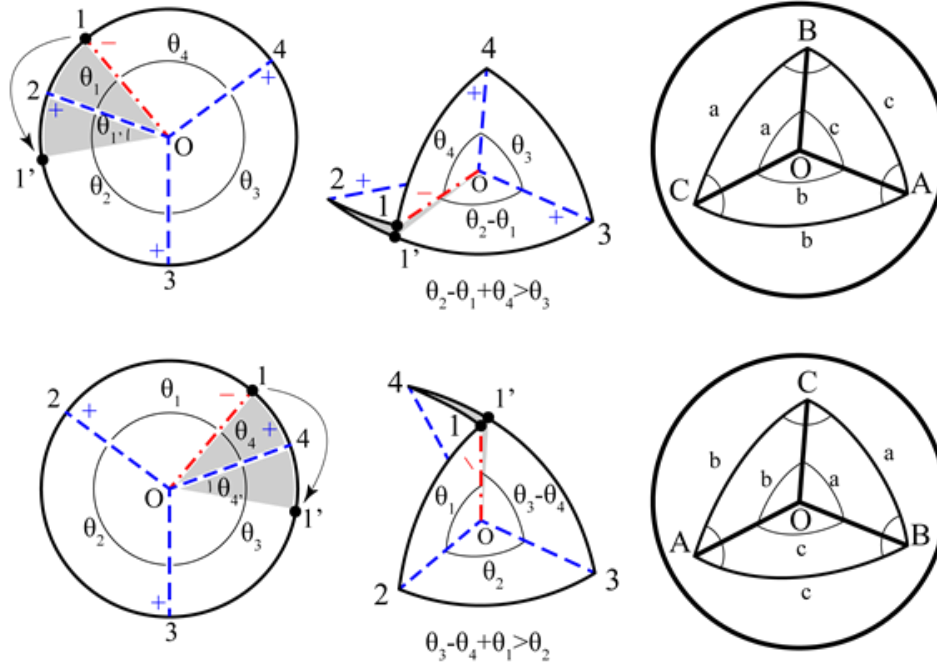


Figure 28: only two possible blocked cases in a generic degree-4 vertex (in the upper one the blocking crease is O_2 ; in the bottom one the blocking crease is O_4).

The following considerations prove that in a developable non-flat-foldable degree-4 single vertex pattern there are only two possible creases that can be the candidate creases among which there is only one that hit 180° first.

- Focus on the first blocking state. The mountain/valley assignment must guarantee rigid foldability from the unfolded state, so there must be three creases with the same sign and one crease with opposite sign (Abel et al., 2016). Assume that they are three valleys and one mountain, without loss of generality.
- In the blocked state, only one crease is flat-folded in non-flat-foldable cases. This is true because if at least two creases are flat at the same time, then all four creases are coplanar in this configuration, and the pattern would be flat-foldable.
- Refer to Figure 28. Consider the first blocked state. Because only one crease is fully folded, a three-faced pyramid ($OABC$) is formed. Two edges of the pyramid (\overline{OA} and \overline{OB}) are formed by faces adjacent in the unfolded state, and one edge (\overline{OC}) is formed by two faces non-adjacent in the unfolded state but touching in the folded state. The former two edges have the same mountain/valley assignment, which is valley, and the other edge (\overline{OC}) is made by two creases of opposite signs ($\overline{O_1}$ and $\overline{O_2}$ or $\overline{O_1}$ and $\overline{O_4}$), one of which folds flat.
- The turn angle at C is positive (valley) because ABC is a spherical triangle, but this should be equal to the summation of fold angles of the two creases forming \overline{OC} . This means that the crease hitting 180° (the one with bigger absolute value) is positive (valley). So, the crease that hits 180° first must be subsequent or precedent to the crease with opposite sign. This limits the solutions to two possible candidate flat-folded creases ($\overline{O_2}$ or $\overline{O_4}$).

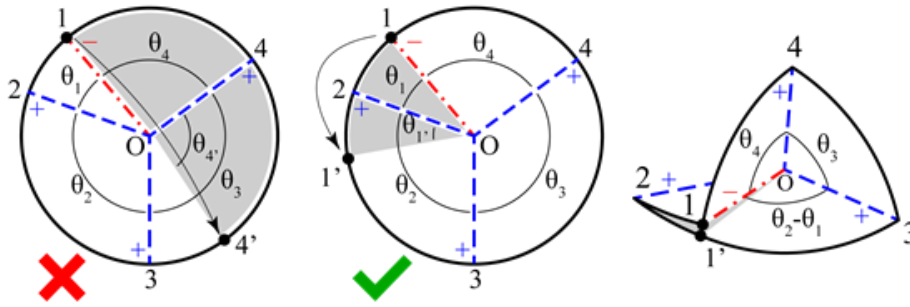


Figure 29: testing which crease blocks the movement first, among the two possible candidates.

Consider having an unfolded pattern where the crease that blocks the movement is still unknown (Figure 29). Considering the previous assumptions, it is known that the crease that hits 180° first is always one of the two valley creases adjacent to the single mountain crease. The following formulations are aimed to test which of the two identified candidate creases is the actual one that hits 180° first, without the need of folding the pattern. Spherical trigonometry and triangular inequality on a sphere are used. The pyramid can be considered as a spherical triangle on a unit sphere. Triangular inequality on a sphere is given by:

$$+b > c \text{ and } b + c > a \text{ and } c + a > b. \tag{27}$$

Because:

$$a, b, c < 180^\circ. \tag{28}$$

The mountain crease is called 1, and the valley creases are called 2, 3, and 4 counterclockwise. Considering the previous assumptions, the flat-folded crease is in general either 2 or 4. If crease 2 folds flat first, then creases 3 and 4 form edges \overline{OA} and \overline{OB} . Therefore, $a = \theta_4$, $b = \theta_2 - \theta_1$, $c = \theta_3$, and this should satisfy $\theta_2 + \theta_4 > \theta_1 + \theta_3$. If crease 4 folds flat first, then creases 2 and 3 form edges \overline{OA} and \overline{OB} . Therefore $a = \theta_3 - \theta_4$, $b = \theta_1$, $c = \theta_2$, and thus it should satisfy $\theta_2 + \theta_4 < \theta_1 + \theta_3$. Conversely, judging from the given set of angles, the following tests can be used:

$$\text{If: } \theta_2 + \theta_4 > \theta_1 + \theta_3 \text{ then } \overline{O2} \text{ folds flat first.} \tag{29}$$

$$\text{If: } \theta_2 + \theta_4 < \theta_1 + \theta_3 \text{ then } \overline{O4} \text{ folds flat first.} \tag{30}$$

$$\text{If: } \theta_2 + \theta_4 = \theta_1 + \theta_3 \text{ the degree-4 vertex is flat-foldable (limit case).} \tag{31}$$

Thus, if we want to use the crease that blocks first as controller crease into a Grasshopper definition, we can insert one of these very easy inequations into the “Expression” component of grasshopper, setting as input the sector angles, and with a “Key/Value search” component we can substitute to the “False” or “True” result the index of the crease $\overline{O2}$ or $\overline{O4}$ as shown in Figure 30 (or Appendix A.4). This index will afterwards be used to select the crease that will be the first axis of rotation and we will set the domain of the rotation angle of its adjacent faces from 0° to 180° .

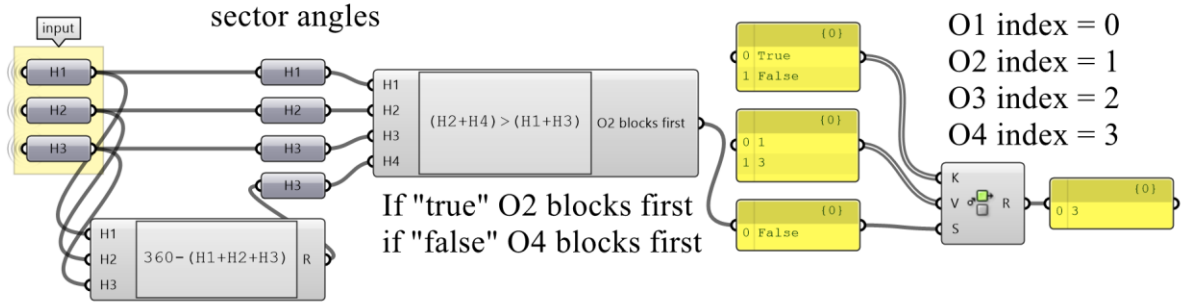


Figure 30: identification of the index of the crease that blocks first.

3.6.5. Other Fold Angles at Blocked State – With the Spherical Law of Cosine

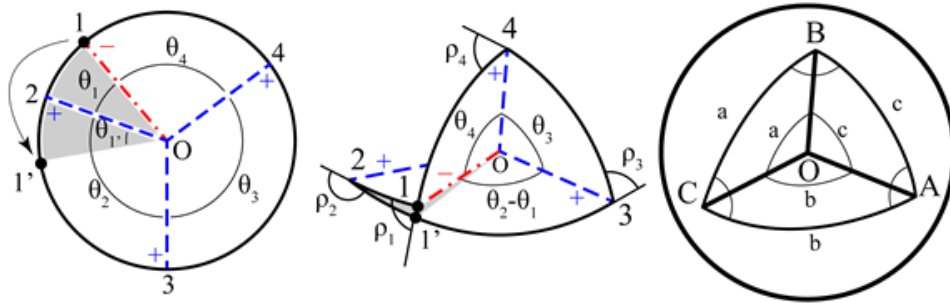


Figure 31: spherical trigonometry standard notation compared with the degree-4 vertex notation when O2 blocks first.

Once the crease that blocks the movement is identified, its fold angle is equal to 180° at the blocked state. The next question is how to calculate the fold angles of the other creases at the blocked state. Refer to Figure 31. Assume that the blocking crease is $\overline{O2}$. (For cases where the blocking crease is $\overline{O4}$, the notation is a mirror reflection). Then, by the cosine rule of spherical trigonometry,

$$\cos A = \frac{\cos a - \cos b \cos c}{\sin b \sin c} \tag{32}$$

Applying this to the fold angles in the degree-4 vertex we will get:

$$\rho_1 = -\cos^{-1} \frac{\cos \theta_3 - \cos(\theta_2 - \theta_1) \cos \theta_4}{\sin(\theta_2 - \theta_1) \sin \theta_4} \tag{33}$$

$$\rho_2 = 180^\circ \tag{34}$$

$$\rho_3 = 180^\circ - \cos^{-1} \frac{\cos \theta_4 - \cos \theta_3 \cos(\theta_2 - \theta_1)}{\sin \theta_3 \sin(\theta_2 - \theta_1)} \tag{35}$$

$$\rho_4 = 180^\circ - \cos^{-1} \frac{\cos(\theta_2 - \theta_1) - \cos \theta_4 \cos \theta_3}{\sin \theta_4 \sin \theta_3} \tag{36}$$

These expressions to calculate the fold angles are valid only at the blocked state. We can use this approach to design patterns of developable foldable three-dimensional structures with specific fold angles as shown in section 6.2.2.

3.7. Conclusions – Relation Between Origami Functionality and Real Applications

Some of these definitions highlight possible connections with the functionality of the origami when applied to real projects. For example, designing considering developability may be a way to reduce the cutouts and scraps from the production, or it may be a way to produce assembling-free objects reducing the production costs and eventually the assembling time and issues. Furthermore, the rigid-foldability is strictly related to the fabrication with rigid panels and stiff materials, also the non-flat-foldability is related to patterns that block at a certain non-planar configuration thus realizing something with folded rigid panels will open new possibilities in the creation of mechanisms that self-block at a certain three-dimensional configuration or that can use blocking folds to increase the structural stiffness and stability. The study of the DOF could be useful to design deployable systems, for example designing a one-DOF mechanism helps preventing unexpected behaviour, it would also prevent the mechanisms to jam because of bifurcations in its folding and unfolding, it would decrease the amount of the necessary actuators and motors to move the mechanism. Lastly, designing considering flat-foldability may be an efficient way to design objects that have to be stored in a small space for transportation or stoking. All these relations are clearly reflected in the projects that we collected and analysed in CHAPTER II.

3.8. References – CHAPTER III

- Abel, Z., Cantarella, J., Demaine, E. D., Eppstein, D., Hull, T. C., Ku, J. S., Lang, R. J., Tachi, T. (2016). Rigid Origami Vertices: Conditions and Forcing Sets. *Journal of Computational Geometry*, 7(1), 171–184. <https://doi.org/10.20382/jocg.v7i1a9>
- Belcastro, S. M., & Hull, T. C. (2002). Modelling the folding of paper into three dimensions using affine transformations. *Linear Algebra and Its Applications*, 348(1–3), 273–282. [https://doi.org/10.1016/S0024-3795\(01\)00608-5](https://doi.org/10.1016/S0024-3795(01)00608-5)
- Buffart, H., Hoffmann, S., Paris, J., Siebrecht, J., Corves, B., & Trautz, M. (2017). Non-flat folding mechanisms for structural purposes. *Proceedings of IASS Annual Symposia*, 2017(13), 1-8.
- Buffart, H., Hoffmann, S., Paris, J., Weigel, C., Siebrecht, J., Corves, B., & Trautz, M. (2018). Folding Mechanisms with Discriminate Extremal Configurations for Structural Purposes. *Origami 7: Engineering 1*, 685–697.
- Demaine, E. D., & O'Rourke, J. (2007). *Geometric folding algorithms: linkages, origami, polyhedra*. New York: Cambridge University Press.
- Demaine, E. D., Demaine, M. L., Huffman, D. A., Hull, T. C., Koschitz, D., & Tachi, T. (2016). Zero-Area Reciprocal Diagram of Origami. *Proceedings of IASS Annual Symposia*, 2016(13), 1-10.
- Foschi, R., & Tachi, T. (2018). Designing Self-Blocking Systems with Non-Flat-Foldable Degree-4 Vertices. *Origami 7: Engineering 1*, 795–809.
- Huffman, D. A. (1976). Curvature and Creases: A Primer on Paper. *IEEE Transactions on Computers*, C-25(10), 1010–1019. <https://doi.org/10.1109/TC.1976.1674542>
- Huffman, D. A. (1977). Surface curvature and applications of the dual representation. *Workshop on Computer Vision Systems*, 213–222
- Hull, T. C. (2003a). Counting mountain/valley assignments for flat folds. *Ars Combinatoria*, 67, 175–187.
- Hull, T. C. (2006). *Project origami*. New York: A K Peters/CRC Press.
- Klett, Y., & Drechsler, K. (2011). Designing technical tessellations. *Origami 5: Fifth International Meeting of Origami Science, Mathematics, and Education*, 5, 305–322.

- Lang, R. J. (2008). The math and magic of origami. *TED talk*. ted.com. Accessed June 21, 2018, from https://www.ted.com/talks/robert_lang_folds_way_new_origami#t-156890
- Lang, R. J. (2018). *Twists, Tilings and Tessellations. Mathematical methods for Geometric Origami*. (First ed.). Boca Raton, FL, USA: K Peters/CRC Press.
- Lang, R. J., Magleby, S. P., & Howell, L. L. (2016). Single Degree-of-Freedom Rigidly Foldable Cut Origami Flashers. *Journal of Mechanisms and Robotics*, 8(3), 31005–31015. <https://doi.org/10.1115/1.4032102>
- Migliari, R. (2009a). *Geometria Descrittiva - metodi e costruzioni (Vol. 1)*. Novara: Città Studi edizioni.
- Tachi, T. (2009). Generalization of rigid foldable quadrilateral mesh origami. *Journal of the International Association for Shell and Spatial Structures*, 50(October), 2287–2294.
- Tachi, T. (2010a). Freeform rigid-foldable structure using bidirectionally flat-foldable planar quadrilateral mesh. *Advances in Architectural Geometry 2010*, 87–102. https://doi.org/10.1007/978-3-7091-0309-8_6
- Tachi, T. (2011a). One-DOF rigid foldable structures from space curves. *Proceedings of the IABSE-IASS Symposium*, 20–23.
- Tachi, T., & Horiyama, T. (2018). 1-DOF Pattern to Fold into Multiple Polyhedra. In *7th International Meeting on Origami in Science, Mathematics and Education (7OSME)*.
- WolframResearch. (n.d.). Mathematica. Accessed January 10, 2019, from <http://www.wolfram.com/mathematica-home-edition/>.

4. CHAPTER IV: Constructive Methods for Solving the Kinematics of Origami

4.1. Families of Folded Surfaces

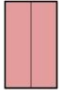
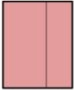
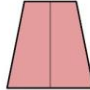
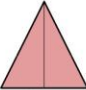
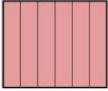

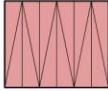
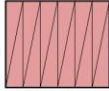
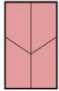
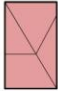
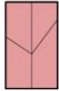
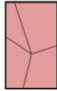

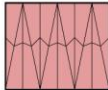
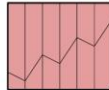
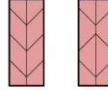

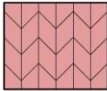
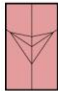



Single linear crease	 Single linear crease between rectangular faces	 Single linear crease between asymmetric rectangular faces	 Single linear crease between trapezoidal faces	 Single linear crease between triangular faces	
Multiple non-intersecting linear creases	 Straight accordion	 Accordion with converging creases	 Triangulated accordion with alternated diagonals	 Triangulated accordion with parallel diagonal	
Degree-4 single vertex	 Single symmetrical reverse fold	 Single simmetrical reverse fold on triangular faces	 Single asymmetrical reverse fold	 Generic degree-4 vertex	
Chain of degree-4 vertices	 Flat-foldable reverse fold on a straight accordion	 Reverse fold on a triangulated accordion	 Non-flat-foldable reverse fold on a straight accordion	 Multiple reverse folds on a single straight fold	 Discretized curve fold
Multiple degree-4 vertices	 Miura-ori	 Sink fold on a single degree-4 vertex	 Multiple discretized curve folds		
Multiple degree>4 vertices	 waterbomb base pattern/ magic ball pattern	 yoshimura pattern			

Figure 32: families of folded surfaces that we studied in this section.

In the book “Architettura delle superfici piegate” Casale et al. assert that the infinite variety of configurations that can be obtained folding a planar surface can be divided into three groups: “Chaotic”, “Shape-oriented”, “Structured”.

In the “Chaotic” family, the surface is crossed by a dense mesh of irregular creases. Once collapsed, the surface can be configured in various three-dimensional irrational shapes, this behaviour is hard to control and to foresee. Furthermore, in architecture, there is no reason to try to analyse it from a kinematic point of view. “If we take a sheet of paper and we crumple it strongly with our hands, we can force it to assume infinite different configurations, opening it and stretching it properly. The more is dense the starting crease pattern, the more the surface will be capable to adapt to specific configurations. Apart from the obvious difficulty in determining the relationship between the initial subdivision and the final shape, it is equally difficult and meaningless searching for the geometrical relationship between the parts participating in this kind of spatial configuration.” (Casale et al., 2013).

In the “Shape-oriented” family, the plane is divided into a multitude of different polygons, placed side by side to generate a pattern that must assume a specific spatial configuration. Figurative traditional origami and packaging can be categorized in this group. Some of the projects, among the ones that we selected in section 2, which could be added to this category are, for example, the “Origami pavilion” by Tal Friedman, the “Common Ground” by Zaha Hadid Architects (Bhooshan, 2016), the “Folding Table” by Tachi or the “Curved Folding Metal Twins” by Chandra, Bhooshan, El Sayed, et. al. (Bhooshan, 2015; Chandra, Bhooshan, et al., 2015).

The “Structured” family is defined by groups of equal tiles. The surface can be configured into a lot of different shapes, using a little number of different tiles, this characteristic makes this family of folded surfaces easier to animate and to design. The well-known solar panel by Koryo Miura (Miura, 1985), the self-deployable cardiac stent by Kuribayashi et al. (Kuribayashi et al., 2006), or the “Resonant Chamber” by RVTR (Thün et al., 2012), are related to this family of surfaces. In general, the tessellations and the corrugations from traditional origami, are perfect examples of this family of folded surfaces. In this thesis, we will focus only on the “Shape-oriented” and “structured” families. The structured folded surfaces are easy to design because they are characterized by groups of equal faces, also the variety of shapes that they can assume is limited, thus the algorithms will be more focused on the animation of the surfaces instead of being focused on the final folded shape. The “Structured” family will be explored in this chapter (CHAPTER IV). The “Shape-oriented” family will be addressed in CHAPTER V and VI.

To study the “Structured” family, we divided it into six sub-classes of patterns which will be presented following a growing complexity criterion. The sub-classes synthetized in Figure 32 are patterns with: a single linear crease, multiple non-intersecting linear creases, a single degree-4 internal vertex, a chain of degree-4 vertices, multiple internal degree-4 vertices and multiple degree>4 vertices.

4.2. Operative Tools

All the crease patterns proposed will be created and animated with a constructive synthetic approach applied with a parametric three-dimensional modeller, Grasshopper³¹ (Rutten, n.d.), a node based parametric modeller integrated into Rhinoceros 6 by McNeel associates (McNeel, n.d.). Because of that, for clarity sake, sometimes we will refer to specific components of Grasshopper or Rhino. Nevertheless, we will try to put the reader in the condition to reproduce the same constructions also with different parametric modellers explaining the processes and describing the algorithms step by step.

4.3. Analogy with Computer Programming and Terminology Clarification

4.3.1. Clustering and Nesting

In computer programming, a widespread practice that helps to keep the code simple and clear is to divide the code into clusters and save them for future uses. This type of approach is very common in object-oriented-programming (OOP), where these clusters of code are called objects and classes. This approach is useful when scripting because it allows the programmer to keep the code short and clear and more importantly to find the errors faster because there is no need to test the previously tested clusters of code. Furthermore, it helps to keep the script easily readable, transmissible and editable.

To make digital three-dimensional parametric animated folded surfaces, it can be followed a similar approach, starting from elementary cases grouped in families, up to harder ones by referring to already solved simpler problems adding variables and components to them. The algorithms will be presented with a growing complexity criterion, starting from patterns with one or more single non-intersecting linear creases, followed by patterns with one or more internal degree-4 vertices and patterns with vertices with a degree greater than 4. For this reason, the first cases may appear trivial, but they are the necessary building blocks for the following algorithms of higher complexity.

³¹ In version Rhinoceros 5 or previous versions, Grasshopper was an external standalone plugin (Rutten, n.d.). In Rhino 6 or newer Grasshopper became a built-in tool.

The operation of grouping some nodes inside a single new component is called “nesting”, we will refer to these nested nodes as “clusters” as they are called in Grasshopper. Furthermore, we will refer to a small part of a folded surface as a “molecule”, because we consider it as a group of “atoms” (creases and faces) that can be joined to make bigger patterns or “macro-molecules”³².

4.3.2. Definition of “Algorithm”

We consider the “Algorithm” as a process or set of rules that we need to follow to reach an expected result. Another interesting definition of “Algorithm” is the one given by Kostas Terzidis in his book “Algorithmic architecture”: *“An algorithm is a computational procedure for addressing a problem in a finite number of steps. It involves deduction induction, abstraction, generalization, and structured logic, it is the systematic extraction of logical principles and the development of a generic solution plan. Algorithmic strategies utilize the search for repetitive patterns, universal principles, interchangeable modules, and inductive links... An algorithm may be compared to the steps in a recipe; the steps of gathering the ingredients, preparing them, combining them, cooking, and serving are algorithmic steps in the preparation of food... Theoretically, an algorithm is the abstraction of a process and serves as a sequential pattern that leads towards the accomplishment of a desired task.”* (Terzidis, 2006).

In computational modelling, the word “Algorithm” is often used to refer to the parametric generative procedures.

4.4. Single Linear Crease

We start the study of the animation of the folded surfaces with the most elementary crease pattern, which is composed of one single linear crease. This kind of fold has been called by Casale et al. “First fold” (Casale et al., 2013). A rectangular piece of paper can be folded in half along its middle line generating two rectangular equal faces, or it can be folded along any other line, dividing the piece of paper into trapezoidal, parallelogrammatical, or triangular faces. Even if the fold line is only one, there are many possible ways to animate the folding of a single creased piece of paper. For example, we can simply rotate the faces around the crease, or we can intersect the paths of the vertices or the edges of the faces and use the intersections as geometric references. Furthermore, we can anchor different parts of the piece of paper to the construction plane, for example, we can make the crease lifting from the construction plane while constraining the opposite edges to slide on the plane. Or we can anchor a face, the crease, or an edge to the construction plane rotating the unconstrained elements out of plane. We can even use a reference curve or a curved surface as a rail on which the edges would slide. We will explore many different methods and we will apply them on patterns with a single crease line before approaching more complex cases.

4.4.1. Single Linear Crease Between Equal Rectangular Faces, Two Edges Slide on Construction Plane – Intersecting Circles

This method uses intersecting circles as geometric references to find all the possible configurations. The circles represent the paths of the vertices opposed to the crease when the adjacent faces rotate around it. This approach works only if the starting rectangular surface is folded in half generating equal rectangular faces. We perform a symmetrical motion of the two faces making the opposite edges sliding on the construction plane of the same amount while lifting the crease from the plane. The following method refers to Figure 33.

³² In many origami design methods, we find the word “molecule” to define a part of a pattern composed by many different folds, in particular in the book “Origami design secrets” by Robert J. Lang (Lang, 2011) we can find a comprehensive explanation of a design method based on the stitching of different molecules.

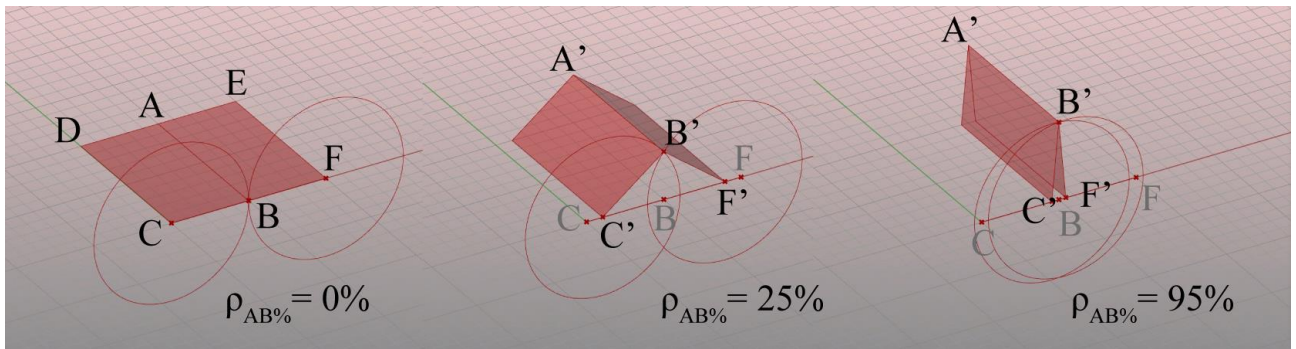


Figure 33: single linear crease between rectangular faces with intersecting circles. The input slider controls the distance from C to B and from F to B.

Draw two rectangular surfaces, then draw the crease AB, and the edges BC and BF³³, we will use these geometries as inputs of the Grasshopper's definition. Now, reparametrize the domain of the curves BC and BF between 0 and 1³⁴. Match the parameter 1 of each curve with the point B and the parameters 0 with points C and F. On an input slider (that we call "Folding percentage") set a value between 0.00 and 1.00 and extract a point on both BC and BF curve at that parameter and call those points C' and F'. Draw two circles on C' and F'. The circle radii are equal to the length of the edges BC and BF³⁵. The circles are drawn on a plane perpendicular to the crease AB³⁶. If we move the cursor of the slider, we will see the circles moving along the edges BC and BF. At this point, intersect the circles getting two points, and select the upper one or the lower one³⁷. This last operation allows us to switch between mountain and valley folding. We call B' the chosen intersection of the circles. Lastly, draw a polyline passing through C', B', and F' and extrude it along AB. In this way, we construct the rectangular faces and we can see them folding and unfolding by moving the cursor of the folding-percentage slider. The 0.00 and the 1.00 values³⁸ on the slider represent the unfolded state (0%) and the completely folded state (100%). We can notice that with this method the edges DC and EF slide on the construction plane and the crease AB leaves the plane moving along the Z axis. The full algorithm with the used nodes is shown in Figure 34 (and Appendix B.1).

³³ We could also have started from a single rectangular surface extracting the edges and the crease by splitting and exploding it, but we decided to start drawing the single elements directly into the rhino workspace and using them directly as inputs of the grasshopper's definition to keep the process easier.

³⁴ In Grasshopper we can reparametrize a curve between 0 and 1 just by right clicking on the input of the following node and clicking on reparametrize.

³⁵ In this case the radii are equal because we considered having two equal rectangular faces.

³⁶ We can do that because we considered having rectangular faces, thus the edges of the rectangles are already perpendicular to the crease.

³⁷ In grasshopper we can use the "Boolean toggle" component or the "Value List" component to make the selection.

³⁸ We could also use integer values, but adding decimals makes the animation more fluid.

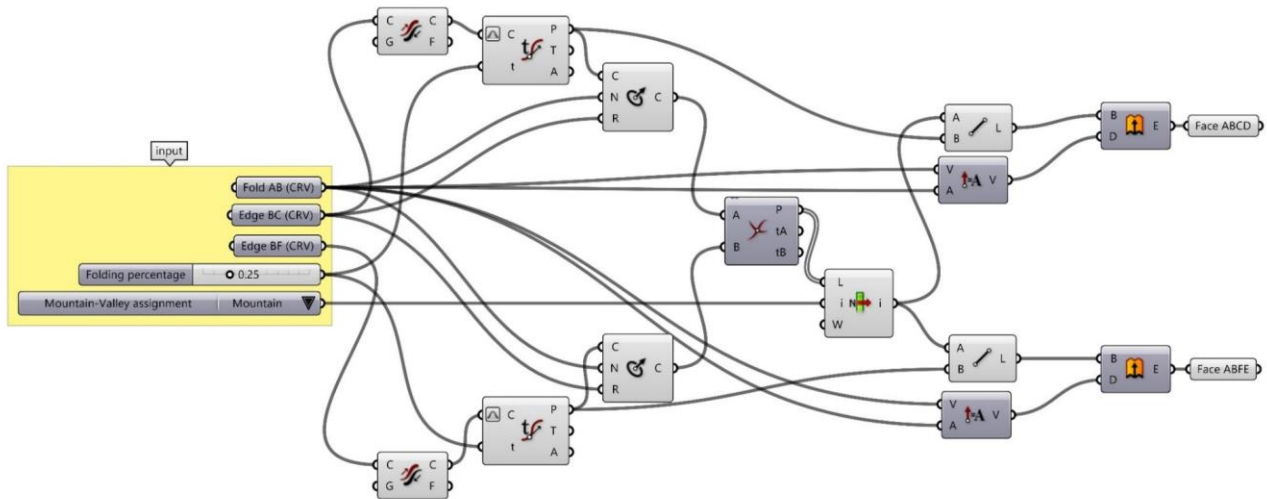


Figure 34: generative algorithm for the single linear crease between equal rectangular faces with intersecting circles.

4.4.2. Single Linear Crease Between Asymmetric Rectangular Faces, Two Edges Slide on Construction Plane – Intersecting Circles

In the previous example, we solved the kinematics of a rectangular surface creased exactly in half. But what if we move the crease a bit toward one side or the other? We can use intersecting circles to identify the position of the crease as we did in the last example. However, if we want to constrain the opposite edges (CD and EF) to slide on the construction plane, we cannot consider a vertical symmetry. So, the algorithm works as follows.

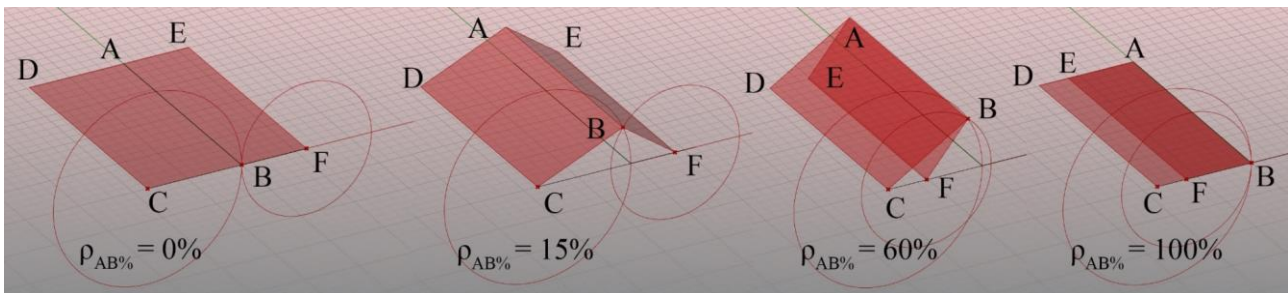


Figure 35: single linear crease between asymmetric rectangular faces animated with intersecting circles, making the edges EF sliding on the construction plane.

First, draw the edges CB and BF and draw the crease AB. Set a slider between 0.00 and 1.00 and remap the output value to a domain between 0 and the length of the segment BF. Multiply this value by two and use the result to move the point F along the segment CF. Like so the point F will never be farther than its original distance from point B. Now, draw two circles on C and the moving point F with radii respectively equal to the initial edges CB and FB. Move the point F together with its relative circle and intersect the two circles. Select one intersection point and draw a polyline passing through the points CBF as we did in the previous algorithm. Extrude the polyline to generate the folded surface. The full generative algorithm is shown in Appendix B.2.

4.4.3. Single Linear Crease Between Rectangular Faces, Crease on Construction Plane – Varying Fold Angle

In this section, we show a different approach. Now we use the fold angle as a variable parameter instead of moving and intersecting two circles on the construction plane. This method is conceptually easier to understand but it gives a different result. Compared to the method with intersecting circles, the method with fold angle returns a fold animation of the surface where the crease stays on the construction plane and the edges leave the plane along an arch of circumference centred in B. Furthermore, we use an angular input instead of a percentage value.

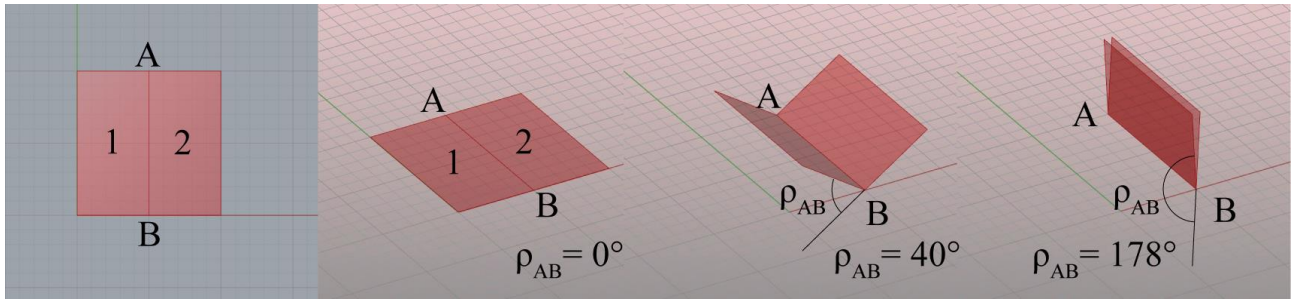


Figure 36: single linear crease between rectangular faces with the fold angle as a variable input.

The algorithm is developed as follows. Refer to Figure 36. Draw two rectangular faces and the crease AB. After that, rotate both faces around the crease AB, face 1 clockwise, and face 2 counterclockwise. To match the input angle to the exact angle between the normal vectors of the two faces, it is necessary to divide it by two before plugging it into the corresponding “Rotate axis”³⁹ components. This step is necessary because we plugged the same angle into both the “Rotate axis” nodes to have vertical symmetry. Contrariwise if we would have rotated only one face keeping the other on the plane, we would not have needed to halve the angle.

To animate the folding process of the surface it is sufficient to move the angle slider which has as boundaries 0° and +180°. We could also set the domain boundaries from -180° to +180° so that the crease assignment would flip from valley to mountain once passed the flat state. Nevertheless, if we choose bigger absolute values to limit the domain, the surface would self-intersect after passed 180°. Figure 37 (and Appendix B.3) shows the complete generative algorithm.

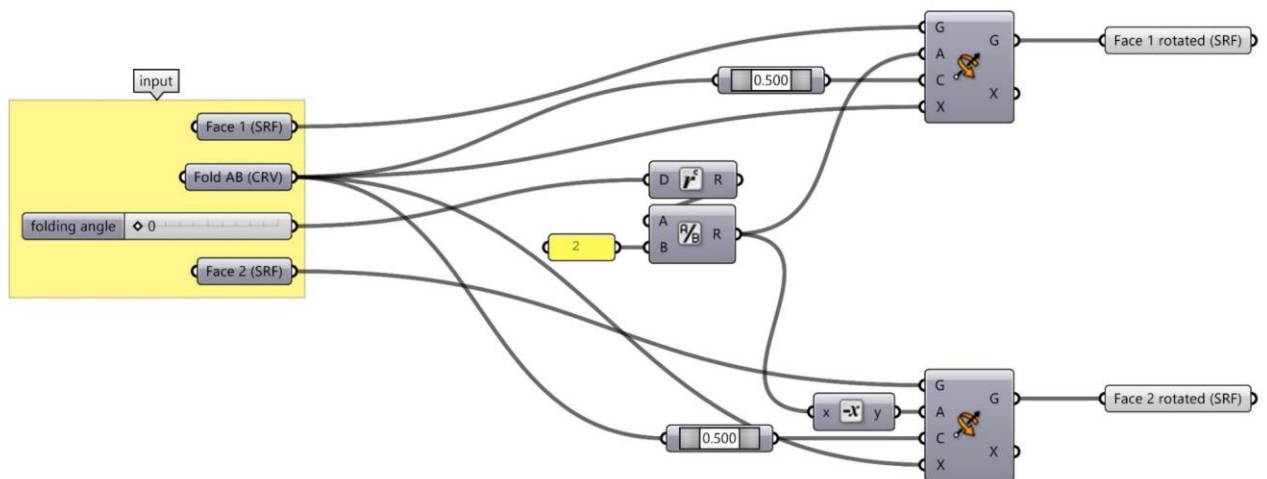


Figure 37: generative algorithm for single linear crease between equal rectangular faces with fold angle input.

4.4.4. Single Linear Crease Between Triangular Faces, Crease on Construction Plane – Varying Fold Angle

The single linear crease between triangular faces (Figure 38) is conceptually no different from the single linear crease between rectangular faces (Figure 36) explained in section 4.4.3, because we rotate the two faces around the fold line on the construction plane as we did in the previous case. However, we decided to present also this case because we used a little different method to generate faces. Furthermore, this algorithm will be part of a more advanced algorithm later. In particular, we used the “Extrude Point” node instead of the “Extrude” node. The “Extrude Point” node creates a triangular face starting from a segment and a point which is a faster solution to re-create the faces in this case. As in the case of the single linear crease between rectangular faces, we considered vertical symmetry, and we divided the input angle by two

³⁹ “Rotate 3D” component can be used as alternative.

to make the slider value matching exactly the angle between the normal vectors of the two faces. In Figure 39 (and Appendix B.4) it is shown the full generative algorithm.

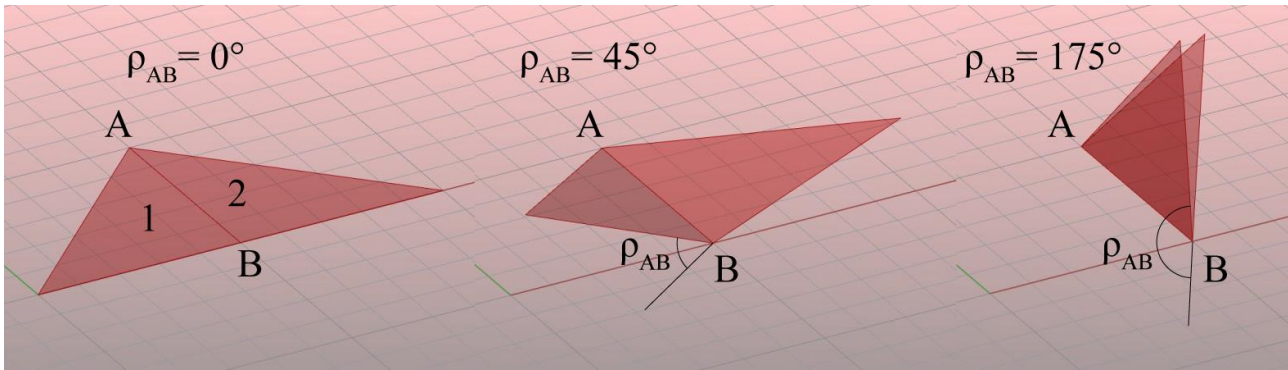


Figure 38: single linear crease between triangular faces animated by varying the fold angle.

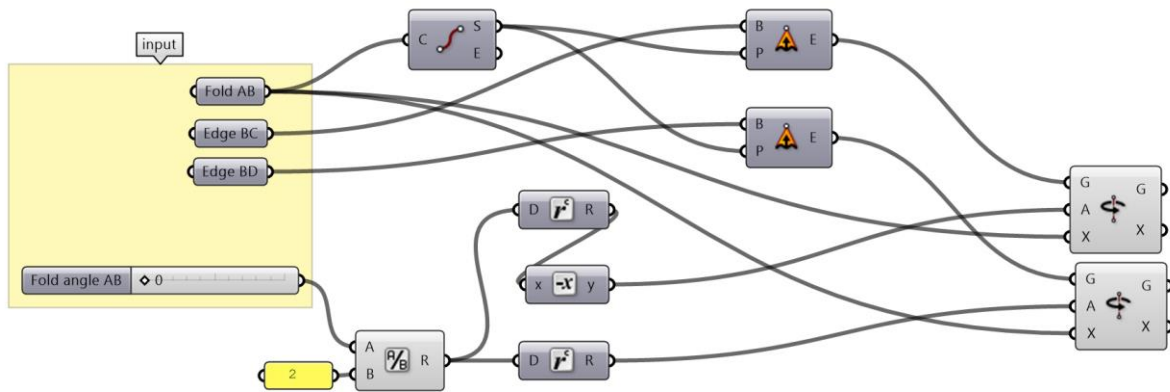


Figure 39: generative algorithm for the single linear crease on triangular faces animated with fold angle AB.

4.4.5. Single Linear Crease Between Triangular Faces, Two Edges Slide on Construction Plane – Intersecting Circles

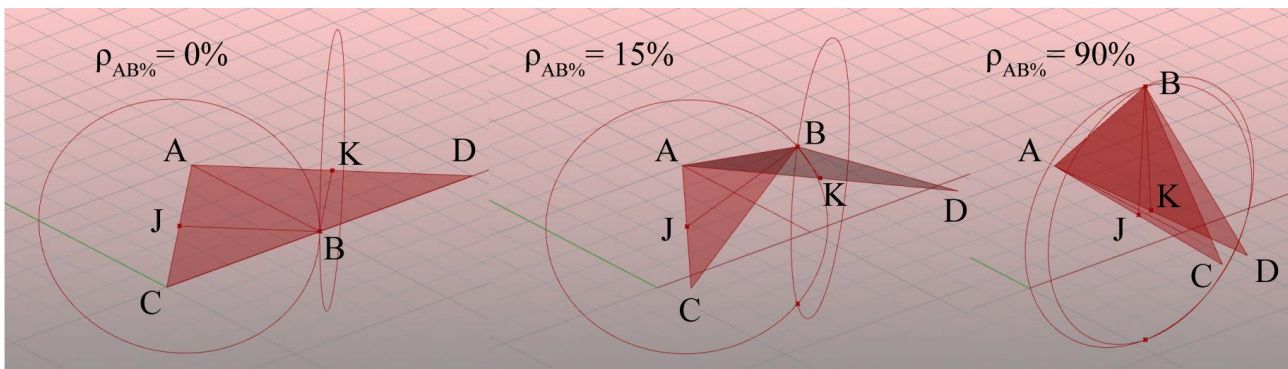


Figure 40: single linear crease between triangular faces with intersecting circles, the outer edges slide on the construction plane.

In this case, we use again intersecting circles to find the only two possible positions of the crease while constraining the edges AC and AD to slide on the construction plane. However, this time the circles are drawn on different planes because the crease and the outer edges are not parallel anymore.

The algorithm works as follows. Draw the crease AB, the edges AC and AD. Measure the absolute value of the angle between AC and AD (we will use this value in a moment). Project the point B on the edges AC and AD finding the

relative points J and K. Draw the two planes passing through the points J and K and perpendicular respectively to AC and AD. Draw one circle on each plane with centres respectively on J and K and radii equal to JB and KB. Set one input slider with a domain that goes from 0.00 to 1.00 and remap the output value to a domain that goes from 0.00 to the angle between AC and AD just measured. Rotate the edges AC and AD around the point A (on the construction plane) of half of the remapped value and rotate with them the relative circles centred on J and K. Find the intersection points between the two circles and chose one of them. That point is now the new position of B. Draw a polyline passing from the moved points CBD and extrude it toward point A. Like so we generated the two triangular faces that we can animate by moving the slider from 0.00 to 1.00. In most of the definitions that use intersecting circles, at the limit cases, the circles perfectly overlap (when the surface is 100% folded in this case), this causes the “Curve | Curve” node (which solves intersection events between two input curves) to return a “null” value. To solve this problem, we can both extend the generative algorithm with an “if” statement that triggers only when the problematic configuration occurs, or it can be simply limited the domain of the input slider to stop a bit earlier of the critical values (99,999% in this case). This last method is the one we used in the generative algorithm shown in Figure 41 (and Appendix B.5).

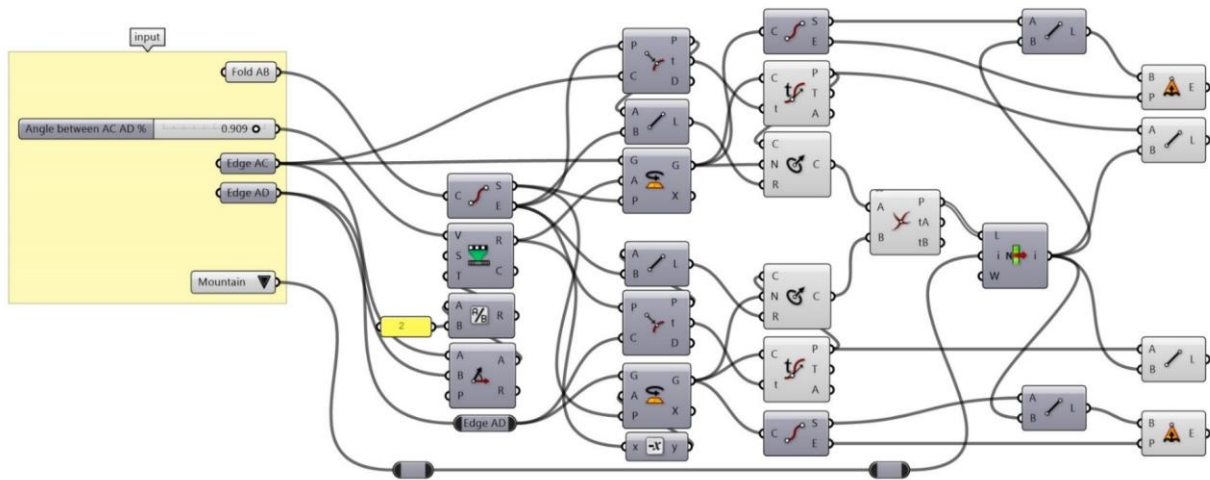


Figure 41: generative algorithm for the single linear crease between triangular faces with intersecting circles, the outer edges slide on the construction plane.

4.4.6. Single Linear Crease Between Trapezoidal Faces, Two Edges Slide on the Construction Plane – Intersecting Circles

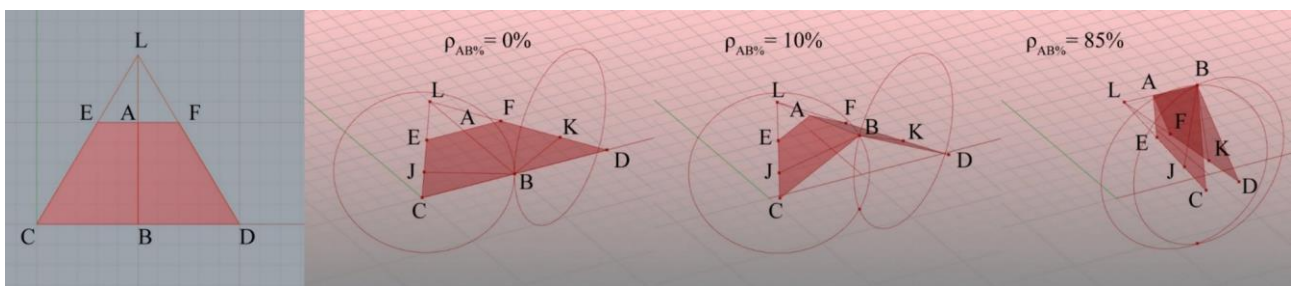


Figure 42: single linear crease between trapezoidal faces, built and animated with intersecting circles.

The method to build and animate two trapezoidal faces with outer edges and crease converging to a point, while constraining the edges EC and FD to slide on the construction plane, is analogous to the triangular faces case shown in section 4.4.5. The trapezoidal faces can be asymmetric, but the edges EC and FD and the crease AB must converge to the same point L so that we can use the same approach used for the triangular faces, because the trapezoid faces would be simply a slice of two triangular faces.

In general, if we have two trapezoid faces that do not have the outer edges and the crease converging to the same point, we would not be able to force the edges EC and FD to slide on the same plane (while rigid-folding the surface) because the edges would belong to the same plane only at completely unfolded configuration.

Contrariwise if we do not want to keep the outer edges CE and DF on the same plane, we can apply the method that uses the fold angle as the only variable input, as shown in section 4.4.3 and 4.4.4. In that way, any combination of trapezoidal faces would work.

The algorithm that we used to animate the surface shown in Figure 42 has the same structure of the algorithm presented in section 4.4.5 with some additional nodes that cut the triangular faces into two trapezoidal faces. Refer to Figure 43 (and Appendix B.6) for the full algorithm.

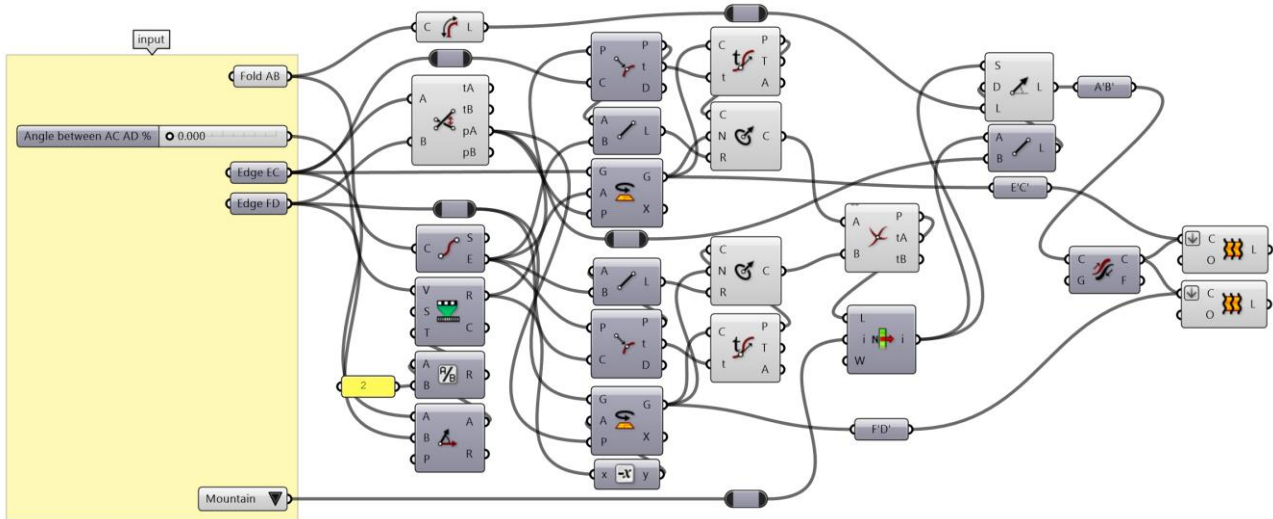


Figure 43: generative algorithm for the folding animation of two trapezoidal faces with outer edges and crease converging into the same point. The outer edges are constrained to slide on the construction plane.

4.5. Patterns with Multiple (Non-Intersecting) Linear Creases

If we fold a piece of paper with two non-intersecting creases, we obtain a crease pattern with two DOF. Adding another non-intersecting crease, the DOF will increase to 3, and so on. Thus, an ideal parametric generative algorithm should have an input controller parameter for every DOF. This approach would guarantee the maximum shaping freedom, and the surface could be conformed to every possible configuration. When the creases are a small number this is feasible, but when the pattern has a high number of creases, even if having a controller for each fold would be the most versatile solution, working with it would rapidly become cumbersome. However, we can forcefully limit the number of controllers to make it more manageable. For example, we can force all the creases to fold of the same amount at the same time, by using as inputs the same fold angle for every crease. Or if we want a more versatile behaviour, we can make the surface sliding along a linear or a curved rail. We can also set a mathematical rule to control automatically the propagation of the fold angle non-linearly.

What is important to keep in mind is that using a smaller number of input parameters compared to the number of DOF would reduce the available configurations into which the pattern could be shaped. Furthermore, if we want to fabricate a pattern with more than one DOF where several creases must move at the same time of a precise amount, we must add an actuator for each one of those creases, even if in our algorithm we used the same input angle. In this section we propose some examples starting from the straight accordion, up to the triangulated accordion, animated with specific fold angles applied to groups of creases, or constraining the creases to slide on a curved and linear rails.

4.5.1. Straight Accordion – Array of “Single Linear Crease Between Rectangular Faces” Molecules

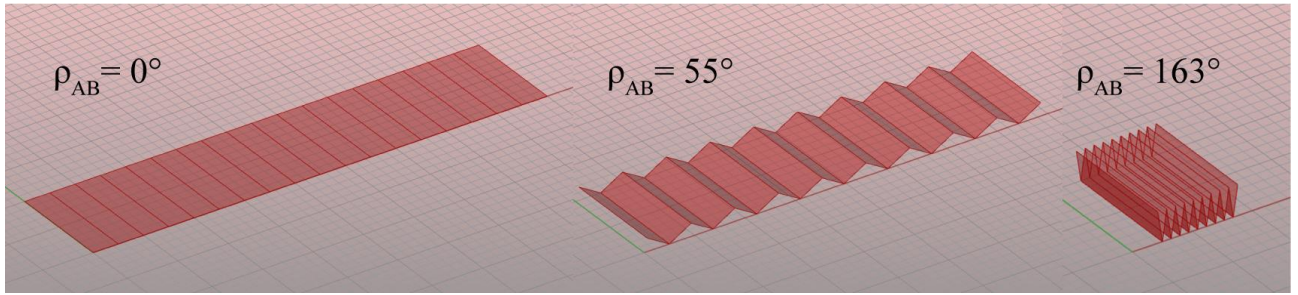


Figure 44: straight accordion joining rectangular molecules animated with fold angles.

In section 4.4.1 we have shown how to make a base generative algorithm to animate a surface folded into two equal rectangular faces. Now, that we have the base molecule, it is easy to make a sequence of parallel linear creases. To do that, we join multiple base molecules linearly. The new generative algorithm starts with the clustered algorithm shown in Figure 37. Then extract the bounding box of the base molecule finding its dimensions along X, Y, and Z axes. After that, use the X dimension as the input of the “Linear array” node which uses it to space the consecutive copies of an amount equal to the animated base molecule width. In this way, the distance is related to the fold angle, that reaches its maximum at the completely unfolded state and its minimum at its completely folded state. The full generative algorithm is shown in Figure 45 (and Appendix B.7). This algorithm returns an animated straight accordion where all the fold angles are equal and fold at the same time with constant propagation, but, as we said this does not cover all the possible configurations of a straight accordion, because its DOF is higher than the number of the controller inputs used. Thus, to increase the animation freedom in the next section we will show how to make the accordion sliding on a linear and a curved rail.

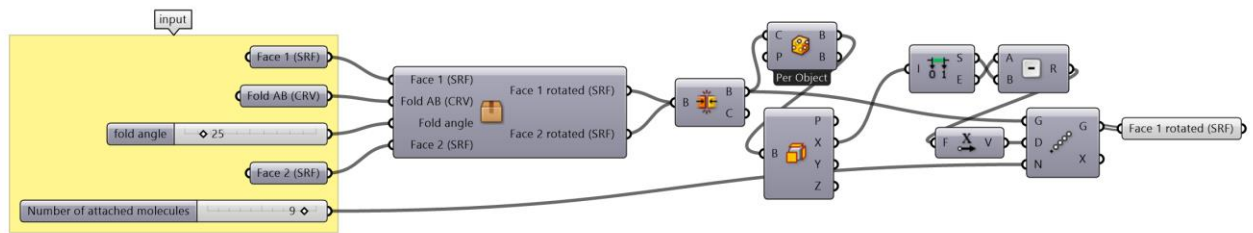


Figure 45: generative algorithm for the straight accordion joining 9 molecules with a single linear crease. Inside the initial cluster node, there is the generative algorithm shown in Figure 37.

4.5.2. Straight Accordion Sliding on a Rail – Intersecting Circles

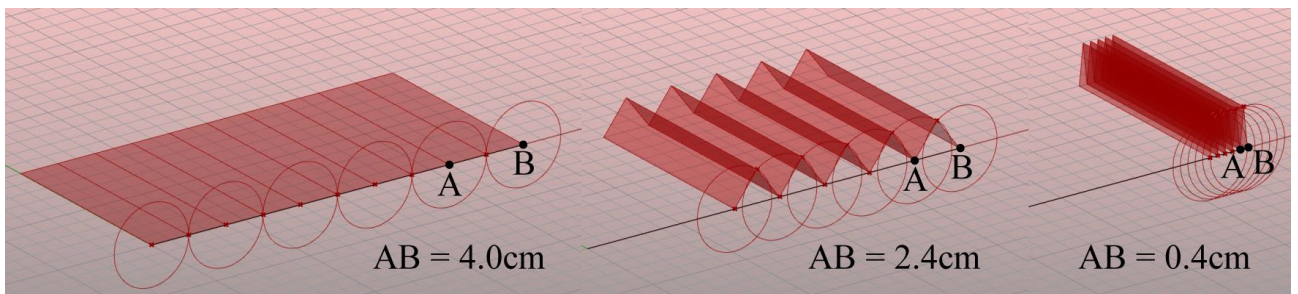


Figure 46: straight accordion, uniform motion on a linear rail.

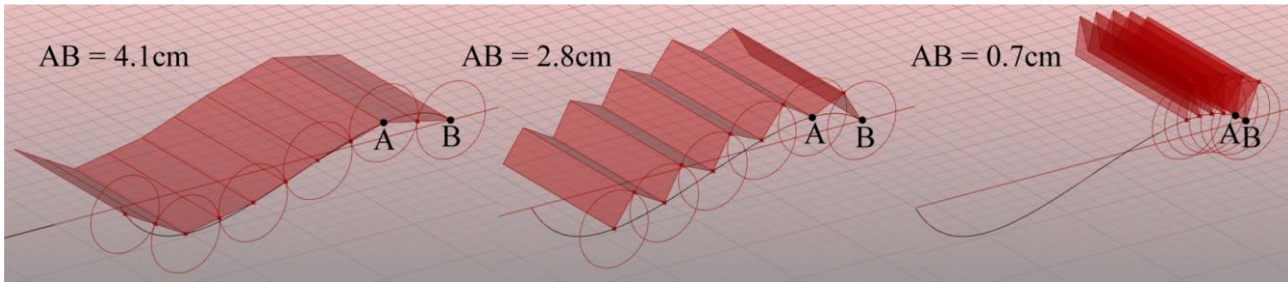


Figure 47: straight accordion, folding and unfolding along a curved path.

In Figure 46 it is synthesized the construction of a straight accordion made with intersecting circles. This approach gives a similar result to the one shown in Figure 44, but it is much more versatile, because the molecules are not equal copies, thus they can be conformed not only to a linear segment but also to a curved path as shown in Figure 47.

The generative process is similar to the one explained in section 4.4.1, but it starts with a curved rail. This curve (it can also be a straight line) is divided in “n” parts (5 in this case), which represent the number of mountain folds (or valley). Between adjacent points, there must be the same linear distance. To achieve this result, we used Grasshopper’s “DivDist” node. On each point we draw a circle, the construction plane of the circle is perpendicular to the creases, and their radii are equal to half the initial distance between two consecutive points on the curve⁴⁰. Then, all the points are moved uniformly along the curve to make all the circles intersecting. The intersection points are filtered and used to build and animate the surface with the same approach used in section 4.4.1. The full definition is shown in Figure 48 and Figure 49 (and Appendix B.8).

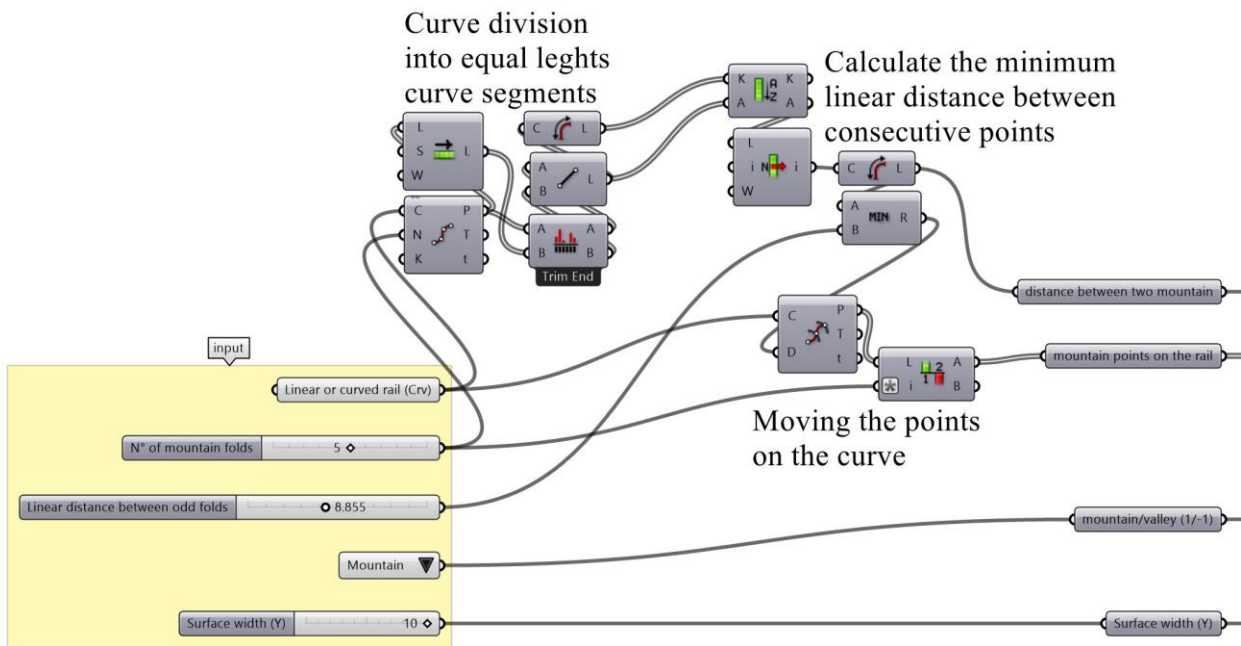


Figure 48: generative algorithm to animate a straight accordion on a linear or curved rail - Part 1.

⁴⁰ As input for the radii of the circles, it is important to use the distance between the points on the curve before moving them, because otherwise the circles would change their radii and they would never intersect.

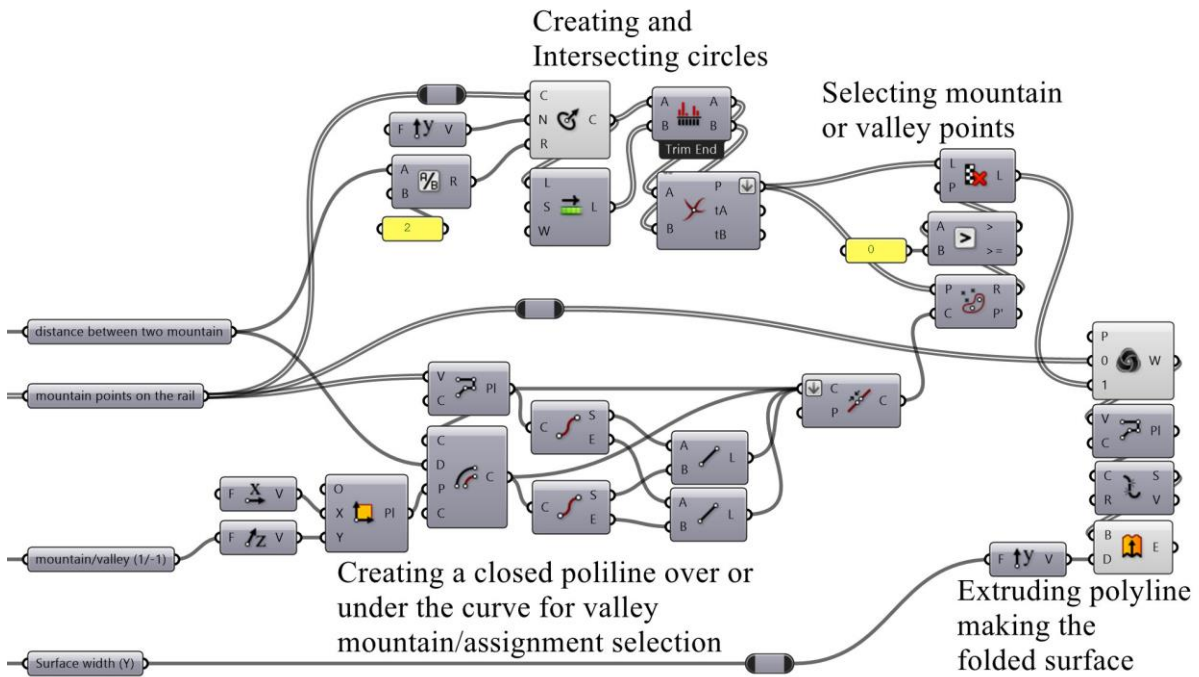


Figure 49: generative algorithm to animate a straight accordion on a linear or curved rail - Part 2.

4.5.3. Straight Accordion on a Rail with Non-Uniform Fold Angle Distribution – Intersecting Circles and “Graph Mapper”

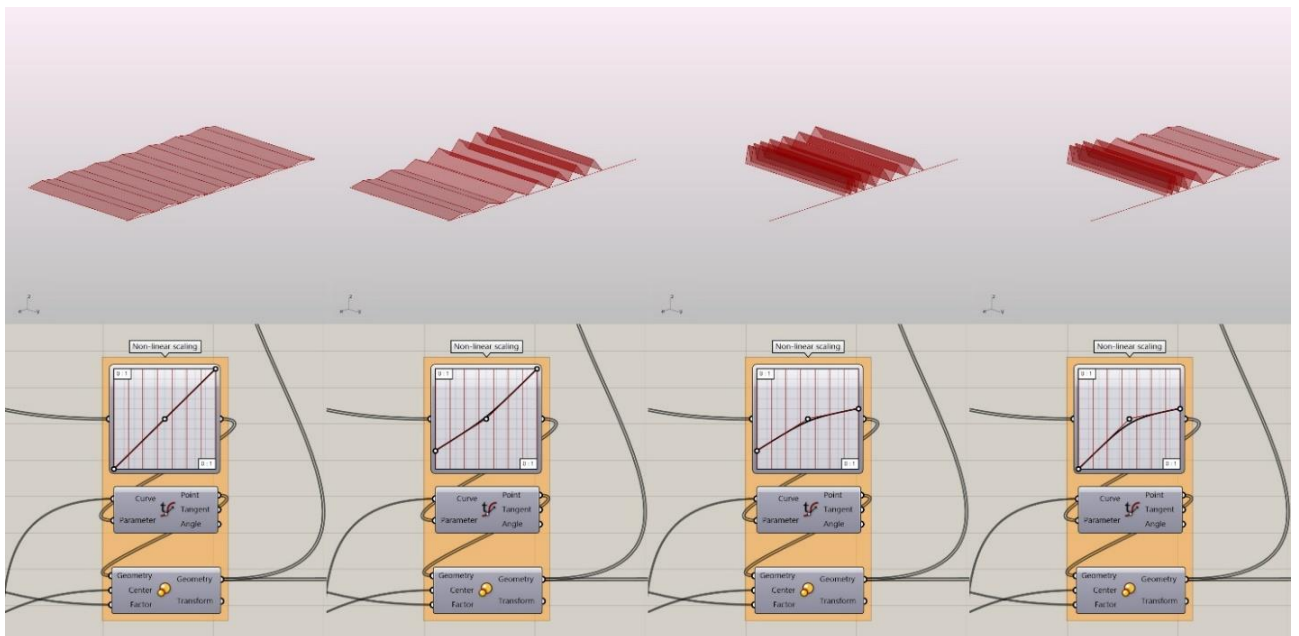


Figure 50: straight accordion animation with non-uniform fold angle distribution on a linear rail.

To increase even more the shaping freedom without increase too much the number of controller inputs we can remap non-uniformly the fold angles on each fold without necessarily controlling them one by one. We can do that with the “Graph Mapper” component, this component remaps the values of a list according to a chosen mathematical function. In this example, we used a Bezier function. We set as the input of the graph mapper the parameters of each point along the curve so that we can remap and use them as new parameters that define the new position of each point along the curve. When the Bezier is a linear function all the points stay at the original position, when we move the Bezier control points the surface starts folding non-uniformly because the points on the curve are no more uniformly spaced. In this way, we

can partially fold some section of the surface leaving completely unfolded other sections as shown in Figure 50. It must be pointed out that with this approach to get correct behaviours, we must know which shape of the remapping function are usable and which are not, with some particular shape of the Bezier curve, the points, when remapped, may be too far one from the other and the surface would lose its developability or behave in an unpredictable way. To avoid this kind of inconveniences it is suggested to use a Bezier curve and to move one control point at a time checking in real time if the surface does not stretch or self-intersect as shown in Figure 50. The full definition for the animation of a straight accordion with non-uniform fold angle distribution is shown in Appendix B.9.

4.5.4. Accordion on Two Circular Rails – Intersecting Circles

The accordion on two circular rails has a behaviour similar to the straight accordion on a linear or a curved rail, but the unfolded pattern has the creases converging into a point rather than being parallel to each other, thus the faces are trapezoids instead of rectangles. The approach used here starts from multiple adjacent “Single linear crease between trapezoidal faces” molecules constructed following the same approach used in section 4.4.6. An accordion with parallel creases can be conformed only into a cylindrical surface. Contrariwise, the accordion with all the creases converging into a point can be conformed into a cone. An example of the conical motion is shown in Figure 51.

The animated surface is obtained from a generative algorithm that takes as inputs two concentric circles used as rails, and an integer numeric slider which defines the number of folds that are distributed at equal distances along the two circles. The circles can be coplanar, or they can belong to two different parallel planes. The circles are divided into a given number of parts, the points so obtained are remapped to make them slide along the circular paths, similarly to what done in section 4.5.2. To do so, the domain of each circle is reparametrized between 0.00 and 1.00, then the parameter of the curve where each point is located is extracted. Afterwards, all the parameters are remapped to a new domain smaller than 1, and they are redistributed again on the circles. Moving continuously the top boundary of the domain between 1.00 and 0.00 will make the point slide on the circle. The point located on the start of the circular path will remain fixed. The other points, when remapped, will tend to compress getting closer to the initial point sliding along the reference curve. On each odd point, we draw a circle that at the completely unfolded state is tangent to the adjacent circles drawn centred on the adjacent odd points. When the points slide on the rails, they get closer and every circle intersect the adjacent ones in two points. Only one of two intersecting points is chosen for each pair of adjacent circles (the upper or the bottom one). Choosing one or the other intersection will flip the mountain /valley assignment of the surface and will make it fold inside or outside the reference cone defined by the two starting circular rails. Once selected all the intersections all the points are connected to make a zig-zag line that alternates the intersection points and the odd points on the circles. Lastly, the two zig-zag lines are plugged into a “Loft” component which generates a surface between each segment of the upper zig-zag line with the correspondent aligned segment of the zig-zag line constructed on the bottom circle⁴¹. To animate the surface, it is sufficient to move the top boundary of the remapped domain with a slider with a range that goes from 0.00 to 1.00. When the top boundary of the remapped domain is 0.5 the surface is exactly halfway to be completely folded, so the slider that controls that number can be considered as a percentage of the folding motion. The full generative algorithm for the accordion on two circular rails with intersecting circles is shown in Appendix B.10.

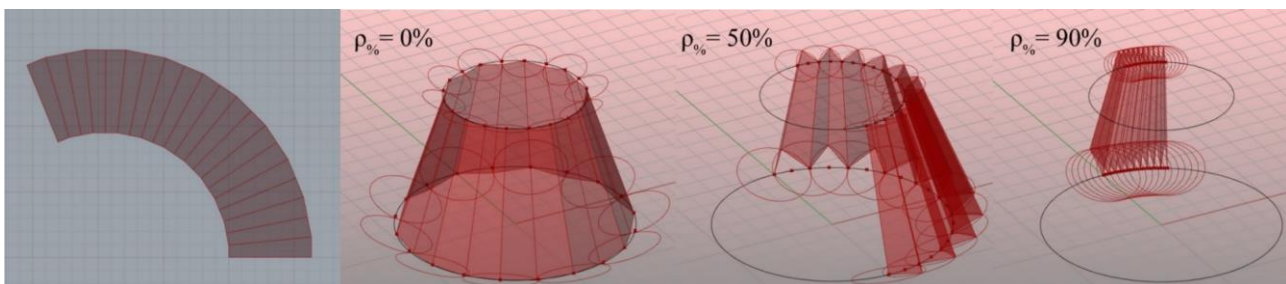


Figure 51: radial accordion sliding on two non-coplanar circular rails.

⁴¹ In general, we need to be careful when using a loft command to generate an animation of a folded surface, because if the two polylines used as input sections of the loft are not precisely drawn it may give wrong results. However, in this case all the relative edges of each polyline are parallel at every folded state, this is true because the upper circle is simply a scaled down version of the bottom circle, thus the relative mated segments always have the same direction and the resulting face would be planar.

4.5.5. Triangulated Accordion – Joining Multiple “Single Linear Crease Between Triangular Faces” Molecules

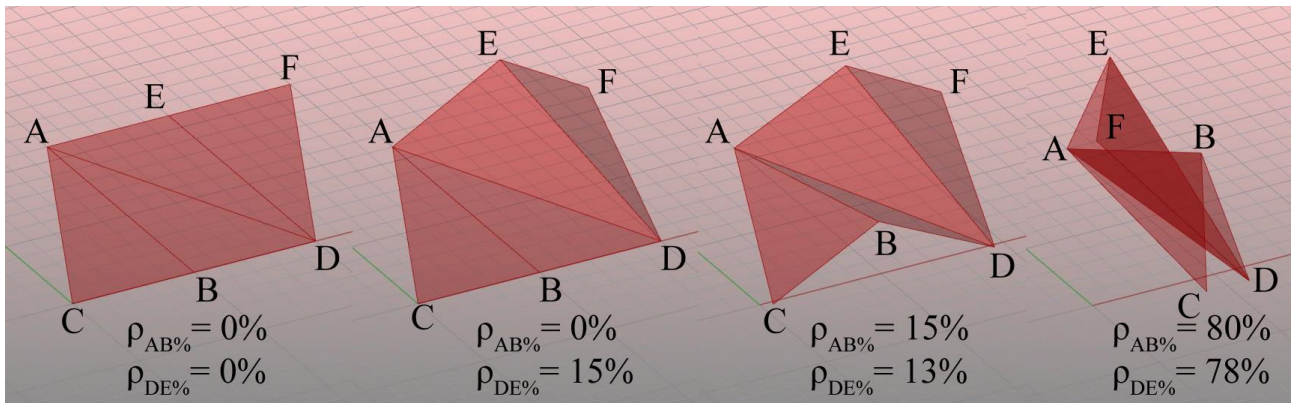


Figure 52: two equal molecules joined that can fold independently making a macro-molecule composed of 4 faces.

A triangulated accordion is an accordion where all the faces are triangular, and the mountain valley assignment is alternated. Thus, the linear folds are not parallel anymore and they touch on the perimeter of the paper. To model and animate it we can join many “Single linear crease between triangular faces” molecules (explained in section 4.4.5). We can both use as input a single slider that controls the fold angles of all the molecules at once, or we can use one input slider for each newly attached molecule. The former approach returns a less versatile result in terms of shaping freedom. In this section, we propose a method where two different sliders are used to control separately the folding of all the odd and even triangular molecules. In this way, the formers can be folded independently from the latter molecules and this approach allows to configure the folded surface into a fan, as shown in Figure 55. Figure 53 shows the full generative algorithm to join 2 molecules of 2 triangular faces. The clustered nodes contain the algorithm proposed in section 4.4.5. The two molecules can be folded independently by moving the sliders that control the folding amount of each one of them. The algorithm is developed as follows (refer to Figure 52 for notation). We refer to the vertices of the first molecule as A_1, B_1, C_1, D_1 , and the vertices of the copied molecule as A_2, B_2, C_2, D_2 . Copy the first molecule and move it⁴² along the A_1D_1 edge matching the vertex A_2 of the copied molecule with the vertex D_1 of the first molecule, then rotate the copied molecule around the vertex D_1 of the first molecule to match the vertex D_2 of the second molecule with the vertex A_1 of the first molecule. Now the two molecules are joined, and they can be controlled with different input sliders. Now the vertices D_1 and A_2 become D , the vertices A_1 and D_2 become A , the vertices C_1 and B_1 become C and B , and the vertices C_2 and B_2 become F and E .

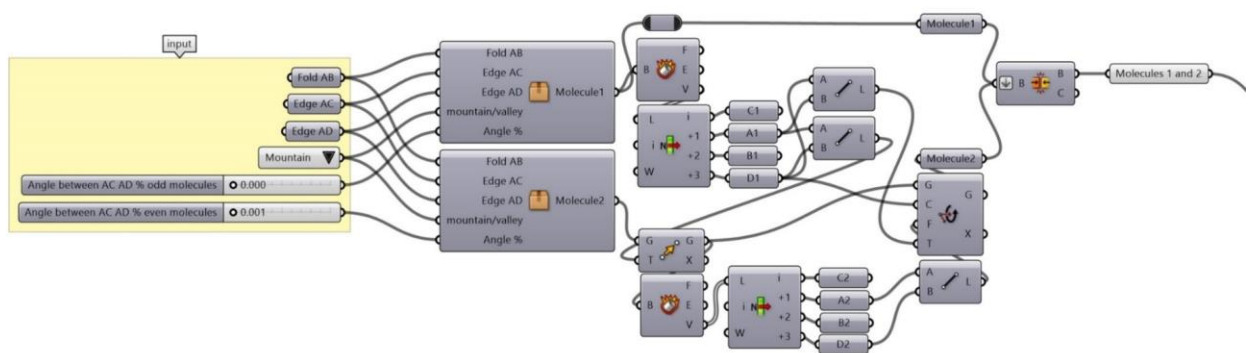


Figure 53: joining 2 equal molecules controlled by 2 different fold angle (%) sliders.

⁴² In Grasshopper the move and copy transformations are made with the same node (“Move”), because the geometry generated from the previous nodes never disappear. To perform a simple move operation the input geometry must be turned off, to perform a move and copy operation both geometries must be kept visible.

The new macro-molecule (with vertices ABCDEF) is made by 2 smaller molecules of two faces each. We can now mate as many macromolecules as we want to make a chain of them where the odd ones fold together independently from the even ones as shown in Figure 55. Grasshopper, unfortunately, does not allow looping or recursive definitions, so each molecule must be copied manually as many times as needed. A more elegant alternative can be achieved using a plug-in called Anemone⁴³. Anemone implements Grasshopper with 2 new nodes that perform loops. The “Loop Start” that needs as input one or more variables (in our case the animated macro-molecule of 4 faces) and the “Loop End” that records the data from each cycle and resend the resultant data to the “Loop Start” component. The number of cycles can be set attaching an integer number as an input into the “Loop Start” node. In-between the two nodes there must be connected the definition that needs to be repeated. In our case the copy and rotation of the macro-molecule (A_{i+1} and C_{i+1} must be matched with D_i and F_i). The loop definition (that follows the definition shown in Figure 53) is shown in Figure 54 (the full generative algorithm is reported in Appendix B.11). It must be pointed out that in the solution that uses Anemone, the animation has a flickering problem. Every time that the cursor of the slider that animates the surface moves, the surface disappears for an instant because the loop definition needs to update. For a flicker-free animation, the copy and paste method (with no loops) is suggested.

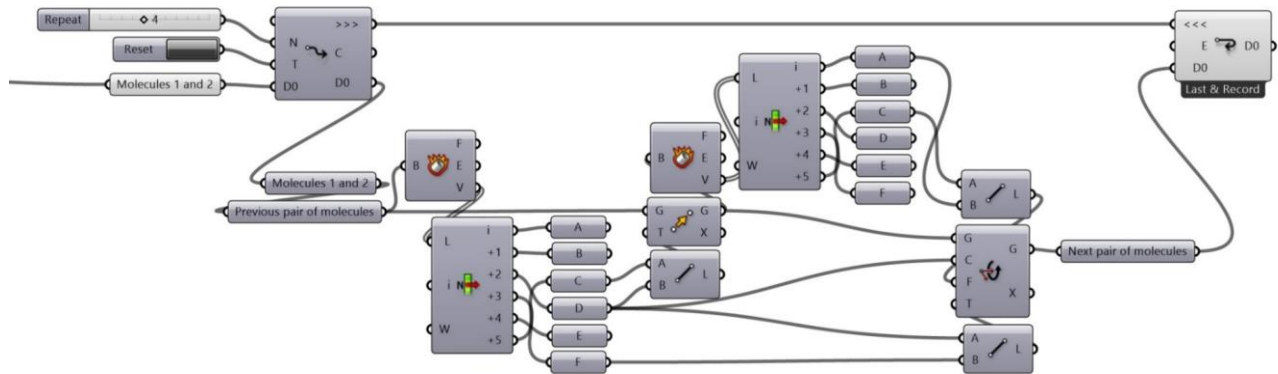


Figure 54: Looping generative algorithm that repeats the cycle 4 times. The definition that is cycled copies and rotates the macro-molecule 4 times starting every time from the newly created macro-molecule. The two upper nodes, with two arrows in their icons, are from Anemone plug-in for Grasshopper.

The cases in Figure 55 and Figure 56 are particular cases where all the faces are equal, but with a different the orientation of the diagonals, thus the kinematics of the surface changes. They both can be folded starting from straight accordions creased along the diagonal of each face. A faster and easier approach to triangulate and animate a straight accordion is by reflecting a straight accordion with respect to a plane that cuts all the faces along their diagonals⁴⁴ as shown in Figure 57. However, this method is limited in terms of possible configurations compared to the one explained above, because in this method we use only one single slider to control all the folds at once.

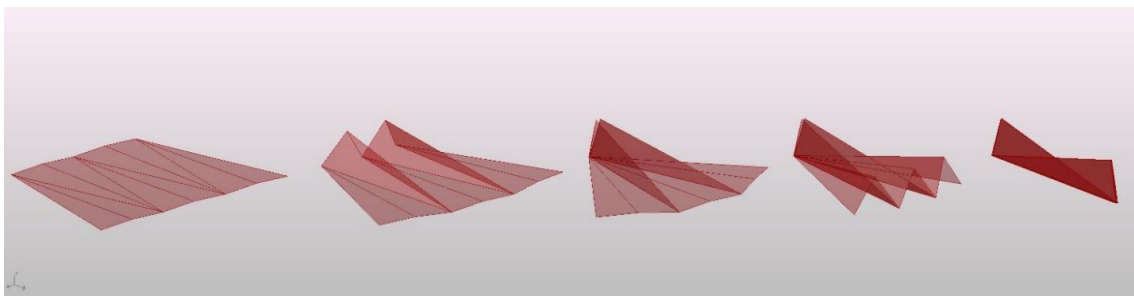


Figure 55: triangulated accordion, alternated diagonals, non-uniform motion.

⁴³ <http://www.food4rhino.com/app/anemone>

⁴⁴ The accordion must have a uniform fold angle distribution and all the faces must be equal to each other to be able to have all the alternated vertices on the same plane so that we can reflect the accordion obtaining equal triangular faces.

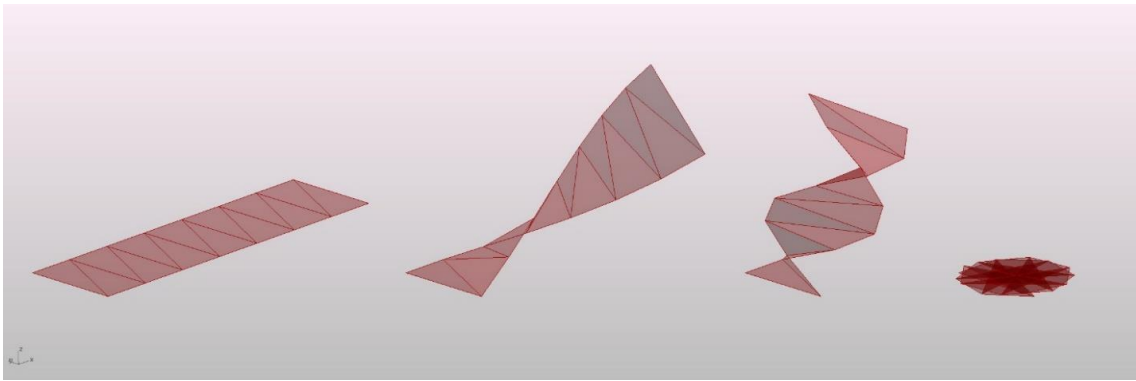


Figure 56: triangulated accordion, parallel diagonals, uniform motion.

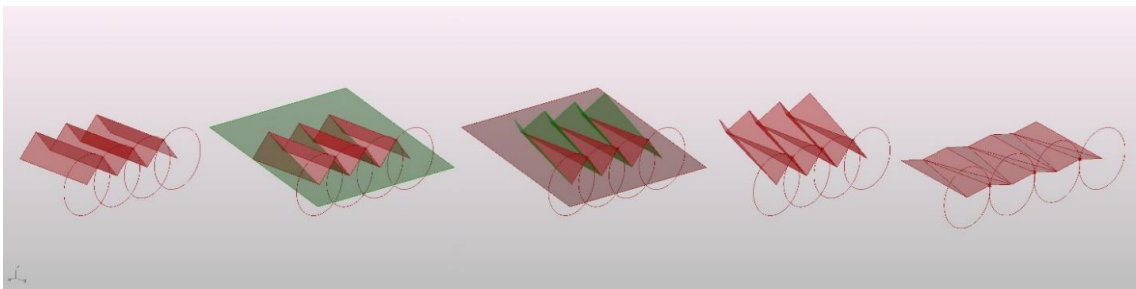


Figure 57: triangulated accordion obtained by reflecting the straight accordion, uniform motion.

4.6. Single Degree-4 Vertex⁴⁵

Now that we explored the animation of patterns with multiple linear non-intersecting creases, according to the increasing complexity criterion, we investigate patterns with a single internal vertex. The simplest rigid-foldable pattern with only one internal vertex is the degree-4 vertex as demonstrated by Abel Z. et al. in the paper “Rigid Origami Vertices: Conditions and Forcing Sets” (Abel et al., 2016). They also proved that any degree-4 vertex must have one and only one crease with the opposite verse with respect of the other three to be rigidly foldable. Also, they asserted that “A *single-vertex crease pattern* (C, μ) can be continuously parameterized in a family of rigid origami folds if and only if (C, μ) contains a *bird’s foot*.” This means that in a degree-4 vertex there must be a “Y” shaped family of three folds to be rigid-foldable.

As the reader can see, the problem increased rapidly in complexity. The patterns with more non-intersecting creases studied previously, only involved animation problems related to the increasing DOF and controller inputs. Contrariwise, now we cannot focus only on the animation of the pattern, but also with the correct pattern design. Furthermore, in patterns with internal vertices, the fold angle of each crease may be influenced by the adjacent creases. In fact, the degree-4 single vertex as we saw in section 3.5.2 is a one-DOF mechanism (Tachi, 2011a), thus, to animate it, we do not need to deal with an increasing number of controller inputs.

⁴⁵ The reader may find confusing the fact that in this section we used a different notation compared to the one used in sections 3.5.2, 3.5.3, 3.6.1, although in the generative algorithms there are already a lot of nodes containing integer numbers, thus for the sake of clarity the use of number to indicate points it is not suggested. Furthermore, we used a rectangular perimeter instead of a disc perimeter because some of the algorithms that generates a single vertex will be used as building blocks to generate more complex patterns where the rectangular shape is preferable.

4.6.1. Symmetric Reverse Fold – Reflecting a Single Linear Crease

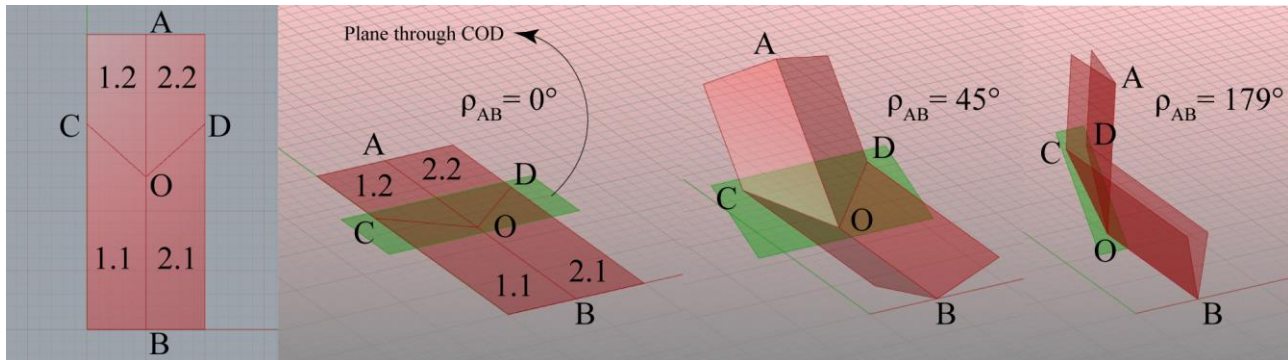


Figure 58: symmetric reverse fold on a single linear fold molecule by reflection with respect of the plane passing through COD points.

The easiest way to make and animate a degree-4 vertex is by reflecting a “single linear fold” molecule. This kind of approach, based on reflection, has been extensively used also for curve folded designs by Mitani et al. (Mitani & Igarashi, 2011). This type of fold in traditional origami is called “Reverse fold”. The “Reverse fold” can be performed reflecting any completely flat-folded or partially folded surface with respects of a reflection plane⁴⁶. Casale et al. call it “Second fold” and they define it as a valley or mountain zig-zag crease⁴⁷ running in a transversal direction relative to a set of linear folds which they call “First folds” (Casale et al., 2013). This kind of terminology (first and second folds) focuses the attention on the order of the steps of the folding process, contrariwise, the traditional terminology (reverse fold) focuses the attention on the nature of the fold itself. When the first creases intersect the second creases, the verse of the first creases flips changing from valley to mountain or vice-versa. The reverse fold can generate flat-foldable or non-flat-foldable patterns depending on the angle of the reflection plane and the configuration of the set of first creases. Performing a reverse fold to a pattern with “ n ” non-intersecting creases will change its DOF from “ n ” to one. For example, if we add to a straight accordion with five linear creases, a transversal reverse zig-zag crease intersecting all the linear creases, the DOF changes from 5 to 1.

In section 4.4 we learned how to solve the kinematics of patterns with a single linear crease, starting from those algorithms we can easily construct a symmetric reverse fold by reflection. The method used here is based on splitting the original poly-surfaces and reflect it with respects of an angled plane⁴⁸.

Refer to Figure 58. First, draw on the two given faces (face 1 and face 2) two symmetrical segments, OC and OD, with respects of the single given linear crease AB. Because OC and OD are symmetric, the pattern is flat-foldable. Copy the transformation of each face (simple rotation around an axis) and apply it to the relative segments OC and OD so that they will move together with their relative faces⁴⁹. After that, construct a plane passing through the animated segments (OC, OD) and split and mirror the faces with respect of the plane. Now, to animate the vertex just change the fold angle value continuously. The full generative algorithm is shown in Figure 59 (and Appendix B.12).

⁴⁶ We used the same technique to make the triangulated accordion in the previous section (4.5.5). The triangulated accordion is a limit cases of a reverse fold.

⁴⁷ The segments making the polygonal chain which is the second fold in the unfolded pattern, must be not aligned along a single line. This is a limit case that has a different kinematics.

⁴⁸ This method works on faces of any shape (e.g. triangle, rectangle, trapezoids) and orientation as far as they share a single linear crease.

⁴⁹ The “Transform” component of Grasshopper copies the rotation of the faces 1 and 2 and apply it on each one of the two new segments (OC, OD), so that the segments move together with their reference faces.

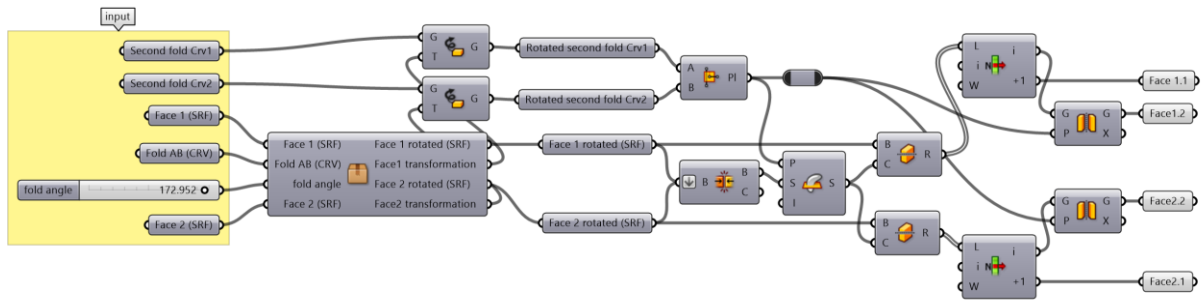


Figure 59: symmetric reverse fold on a single linear fold molecule by reflection, generative algorithm. The initial cluster contains the algorithm explained in 4.4.2.

4.6.2. Asymmetric Reverse Fold – Reflection and Collision Detection

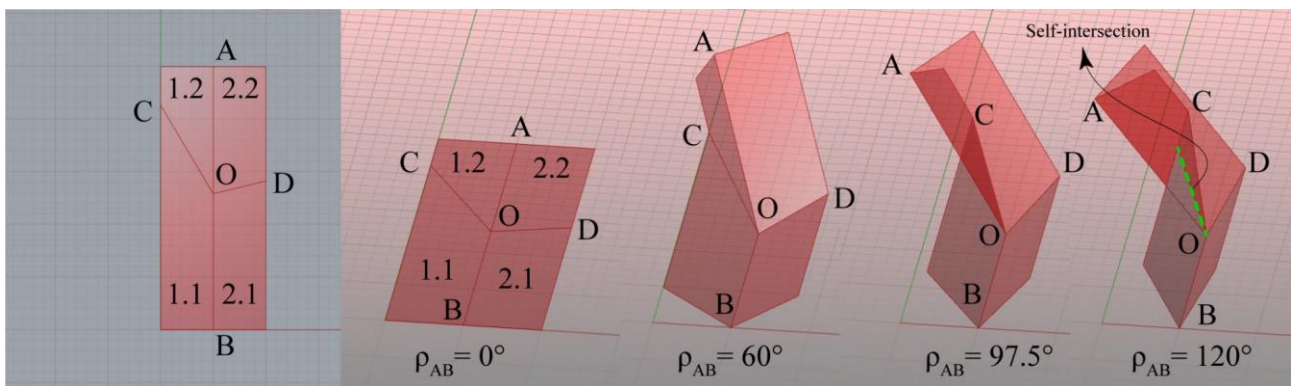


Figure 60: asymmetric reverse fold animated with the reflection method when ρ_{AB} is equal to 97.5° the folded surface blocks because poc hits 180° . After that point, if we continue folding the surface will self-intersect. The intersection between the faces 1.1 and 2.2 is highlighted in green.

The construction method for the asymmetric reverse fold is analogous to the method explained in the previous section (4.6.1). However, if we do not limit the domain of the controller fold angle properly, the surface will self-intersect after passed the blocking configuration as shown in Figure 60. Thus, if we want to know which angles make the vertex self-intersecting, we can apply the following method.

First, explode the input 4 faces 1.1, 1.2, 2.1, 2.2 (not animated), and count how many collisions there are between the unfolded faces⁵⁰ (with the “Collisions Many|Many” component). Then, perform the reverse fold as explained 4.6.1. Partially fold the vertex and test the collisions again. Compare the collisions at flat state with the collisions at folded state. If the collisions increased the algorithm will return “True”, if they remain unvaried it will return “False”. When we change the fold angle value ρ_{AB} if it is “True”, then we passed the blocking point, or we are exactly on the blocking point.

Now if we want to synthetically and automatically extract the maximum value that we can assign to ρ_{AB} without self-intersecting the vertex, we can apply the following method. Move slowly the cursor of the slider ρ_{AB} from 0% to 100%⁵¹, and record frame by frame (with a “Data recorder” component), in two separate parallel lists, the values of ρ_{AB} and the relative Boolean values⁵² resultant from the test of the collisions. Now compare the two lists and erase all the angular values that correspond to “True” (with a “Cull pattern” component). Sort the angles from the smallest to the largest and choose the largest one. In this way, we just found an approximation of the blocking angle. The accuracy of the maximum angle value is proportional to the number of frames between the flat and the folded state. The full definition is shown in Figure 61 (and Appendix B.13).

⁵⁰ The number of collisions will be greater than 0 also at non-self-intersecting configurations because the adjacent faces are touching.

⁵¹ You can also automatize this operation by animating the cursor of the slider by right clicking on it.

⁵² The Boolean values are “True” and “False” or respectively “1” or 0”.

We can also use the maximum fold angle found to limit the domain of the ρ_{OB} value by inputting the calculated maximum ρ_{OB} and the fold angle slider into the same “Minimum” component as shown in Figure 62. In this way, even if we set a fold angle greater than the maximum ρ_{OB} , the output value will stop at the maximum ρ_{OB} .

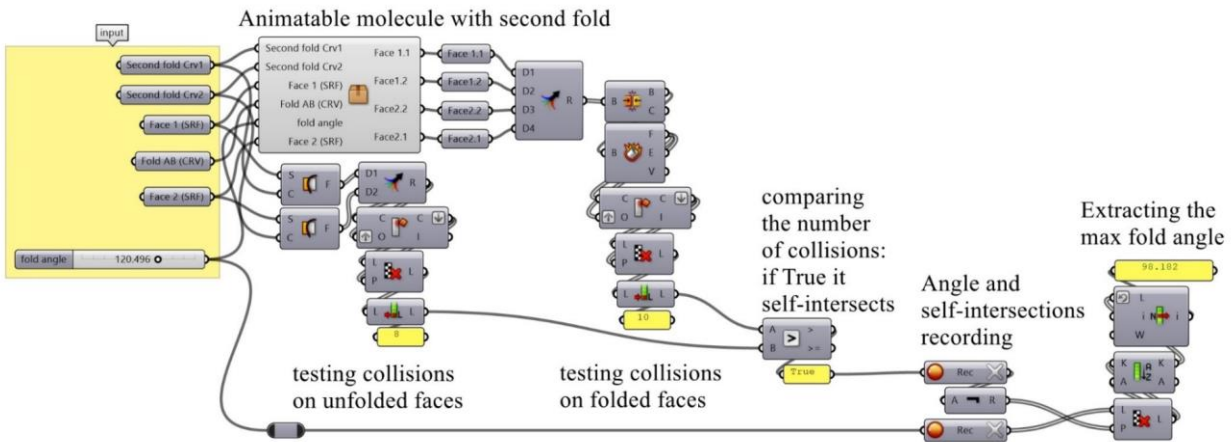


Figure 61: the generative algorithm for the identification of the maximum fold angle, testing the animated surface for collisions; the maximum fold angle is generated within a given tolerance, thus it is an approximation; the cluster contains the definition shown in Figure 59.

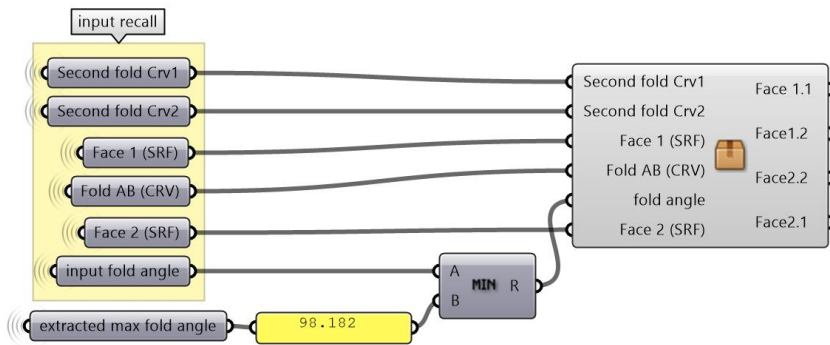


Figure 62: re-animating the second fold molecule avoiding self-intersections, the extracted max fold angle node is the result of the algorithm in Figure 61.

4.6.3. Generic Degree-4 Vertex – Intersecting Cones

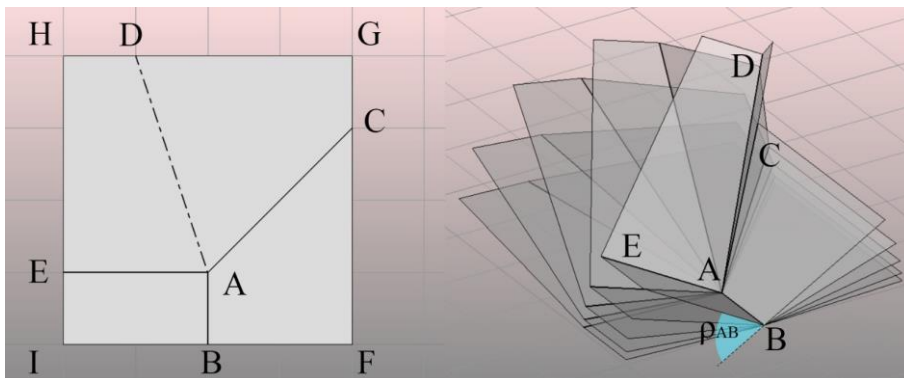


Figure 63: animation of a degree-4 single vertex CP.

The reflection method shown in the previous sections is an easy approach, but it does not solve all the possible degree-4 vertices. It can be used only to animate vertices where the opposite mountain and valley creases are colinear. The

vertex shown in Figure 63, for example, cannot be solved with the reflection method. In this section, we propose a different approach to animate any rigid-foldable degree-4 vertex.

The algorithm is visualized in Figure 64 and Figure 65 and it works as follows. Draw 4 adjacent faces ABFC, ACGD, ADHE and AEIB as shown in Figure 63⁵³. Revolve the crease AD using as axis the fold AE generating a cone with apex in A. Similarly revolve the AD fold around the axis AC⁵⁴. Rotate the faces ABFC and ACGD around the crease AB clockwise, and the faces AEIB and ADHE around the same axis of the same amount but counterclockwise. Doing so the vertex D will split in D' and D'' and the two cones intersect generating 2 segments, meeting into the apex of the cones⁵⁵. These two segments represent the possible positions of the AD fold so that rotating the faces ACGD and ADHE to that point their AD edge would perfectly match. Choose the intersection line AK' which matches the mountain valley assignment of the given pattern⁵⁶. Rotate AD''HE around AE to mate D'' with K'. Do the same thing with the face ACGD' rotating it around the AC axis mating D' with K'. The algorithm is finished.

Now, if we change the value of ρ_{AB} we will be able to animate the surface. If the pattern is non-flat-foldable, and if the controller fold AB is not the fold that hit 180° first, the model will self-intersect during motion, we can solve it by testing the collisions as shown in the previous section (4.6.2). The full definition is reported in Appendix B.14.

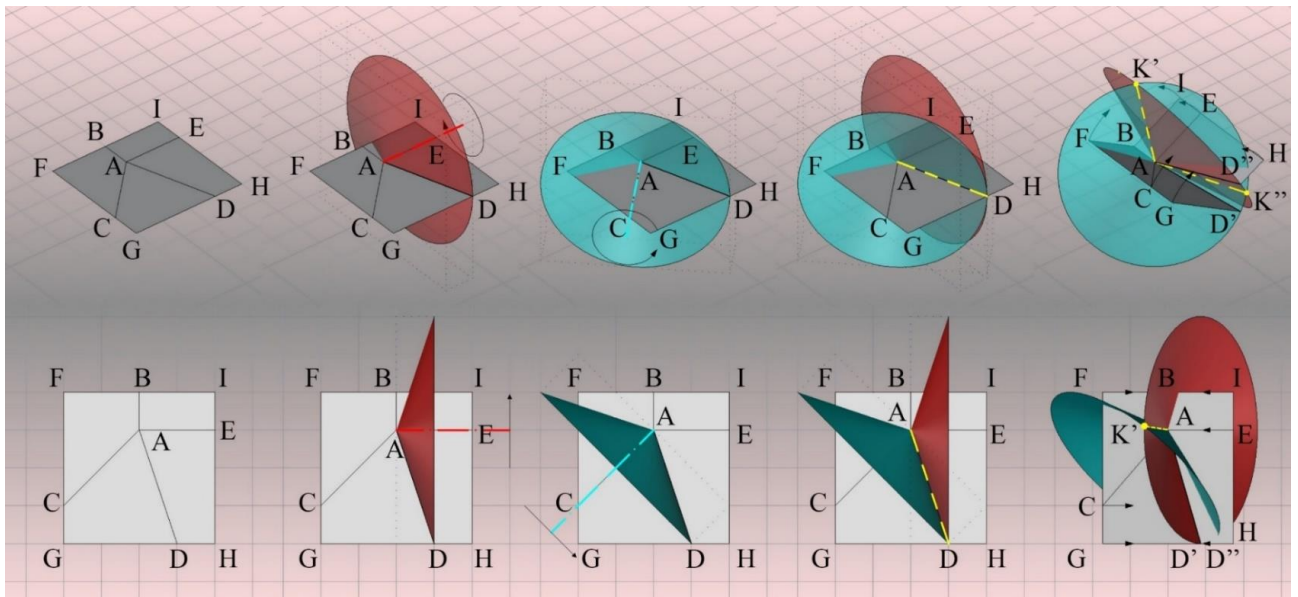


Figure 64: three-dimensional modelling and animation of a generic degree-4 single vertex with intersecting cones - Part 1.

⁵³ The faces must be drawn considering the rigid-foldability conditions of a degree-4 vertex presented in section 3.4.

⁵⁴ When the model is unfolded the intersection between the two cones is a single line, which corresponds to the crease AD, this obviously means that it exists only one flat unfolded state.

⁵⁵ If we intersect two cones that share the same apex in Rhinoceros and Grasshopper, instead of returning two lines, it does not return any line. This is a known bug that when this thesis has been written was not fixed yet. Thus, to generate this algorithm we had to use a workaround looking for the intersection points of the two circular bases of the cones and connecting them to the apex of the cones to generate the two segments AK' and AK''. The bug has been fixed in Rhino 6.

⁵⁶ Choosing the other intersection line will flip the mountain/valley assignment of some creases of the pattern.

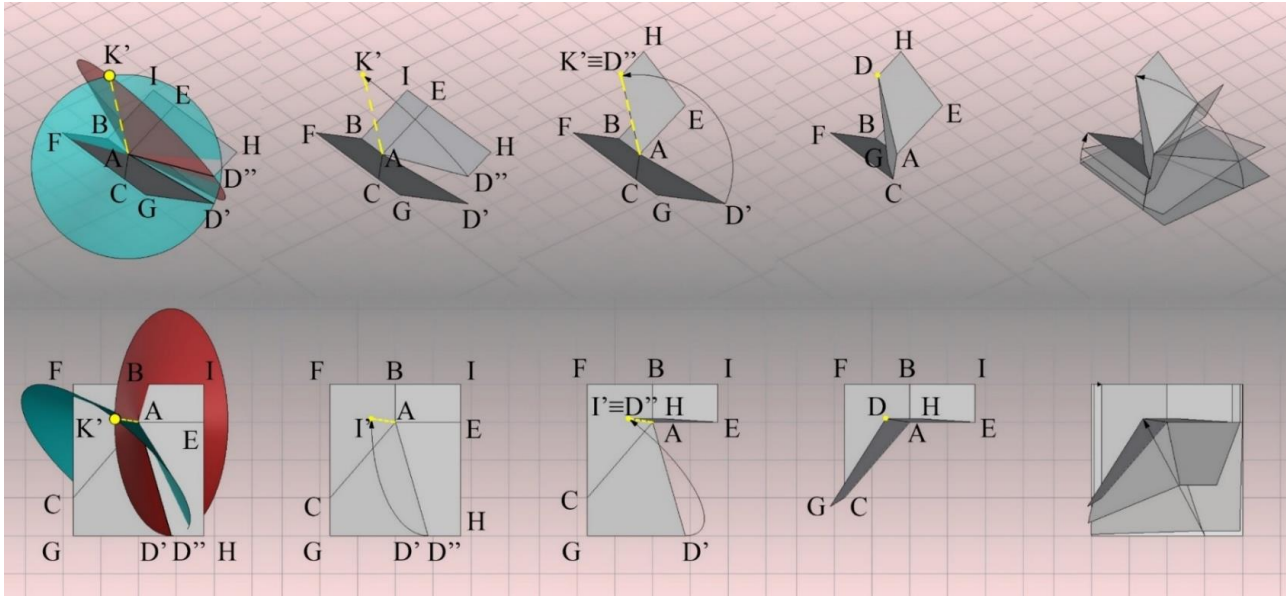


Figure 65: three-dimensional modelling and animation of a generic degree-4 single vertex with intersecting cones - Part 2.

4.7. Multiple Degree-4 Vertices

In section 3.3 we introduced some concepts about the DOF, and in section 3.5 and 3.6 we explained the kinematics of degree-4 vertices. As we said, patterns with multiple degree-4 vertices may not be rigid-foldable if some symmetry conditions do not occur. However, it is not always easy to recognize those patterns. Furthermore, testing the compatibility of every fold angle in every closed loop of faces may be a very time consuming and cumbersome operation. Thus, in this section, we will start solving the kinematics of easy symmetric well-known patterns with multiple degree-4 vertices that are known to be rigid-foldable.

4.7.1. Joining “Symmetric Reverse Fold” Molecules – Critical Observations About Global Rigid-Flat-Foldability

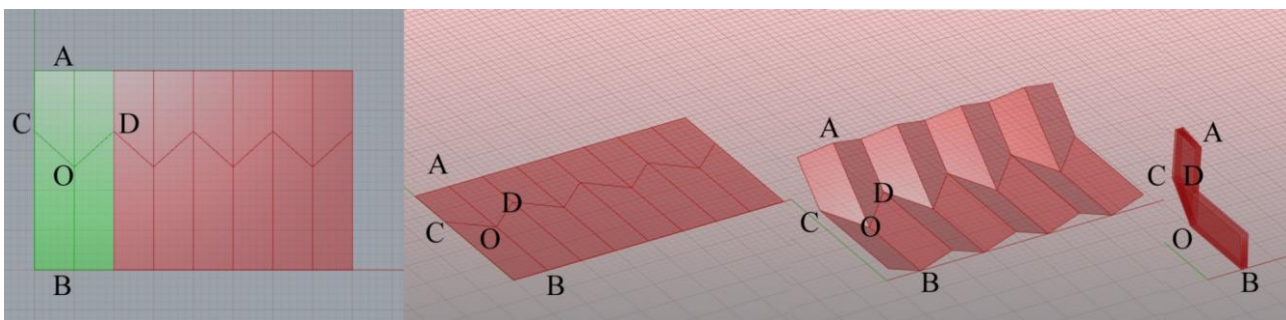


Figure 66: reverse fold on straight accordion, joining “symmetric reverse fold” molecules.

A straight accordion without reverse folds has more than one DOF. If we add one reverse fold to the same accordion, as shown in Figure 66, its DOF will decrease to one. Furthermore, if every segment of the reverse fold is symmetric with respect to the adjacent linear first folds, the pattern is also flat-foldable.

To animate a flat-foldable straight accordion with a single reverse fold, we can reflect a straight accordion with respects of a reflection plane following the same approach explained in section 4.6.1, or we can perform a linear array of a “symmetric reverse fold” molecule following the same approach that we proposed in section 4.5.1 (the definition using this approach is shown in Figure 68 and Appendix B.15).

If we want to use the former approach (the “reflection of a straight accordion” method), we need to pay attention to the fact that the straight accordion must be animated using the same fold angle for every crease, so that we can reflect

the first two consecutive animated faces of the accordion as shown in 4.6.1 and using the same animated plane to reflect all the other faces.

If we want to apply the second method (the linear array of “symmetric reverse fold” molecules), we can follow two main approaches: we can join the molecules side-by-side or along their linear first folds. If they are mated side by side we will have a pattern with one long single zig-zag shaped reverse fold as shown in Figure 66, if we mate them along their linear first fold we will have a surface with more V-shaped reverse folds and one single first fold, as shown in Figure 67. A pattern with more than one reverse fold can be shaped in different ways depending on the orientation of the molecules and the angle of the reverse folds.

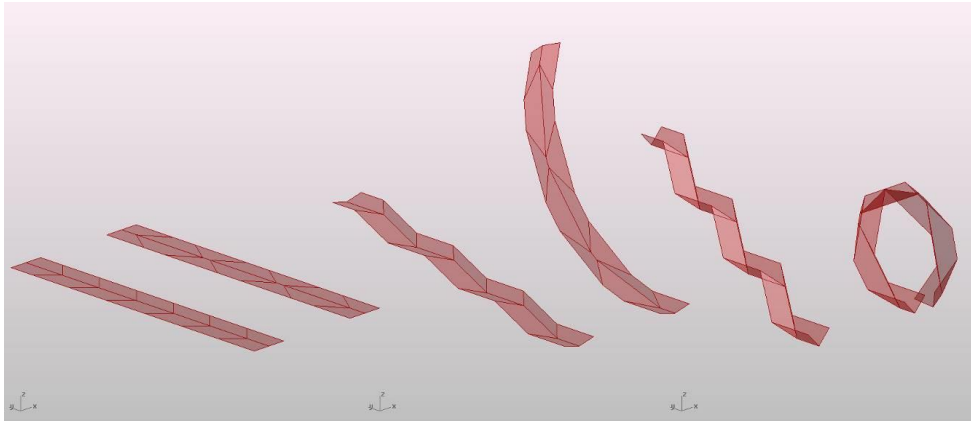


Figure 67: different behaviour during the collapsing, depending on the direction of the second folds.

If we join more than one “symmetric reverse fold” molecule along their linear first crease with alternated orientation, we would risk of ending up having self-collisions between the ending molecules at the opposite sides of the pattern, and it would be impossible to complete the folding motion without self-intersecting or flexing the faces, as shown in Figure 69. This means that it is not sufficient to attach rigid-flat-foldable molecules to have a guaranteed globally rigid-foldable pattern. Furthermore, if we attach side by side two molecules with symmetric second folds but different angles, we obtain a globally non-fat foldable pattern because the new internal vertex (resulting from the attaching of the two molecules) does not respect the Kawasaki’s condition, as shown in Figure 70. The problem of global rigid-flat-foldability avoiding stretches and self-intersections, for a generic pattern, is proven to be at least NP-hard (Akitaya et al., 2016), thus simulating the folding motion, for now, is one of the most reliable methods to test if a pattern is rigid-flat-foldable or not.

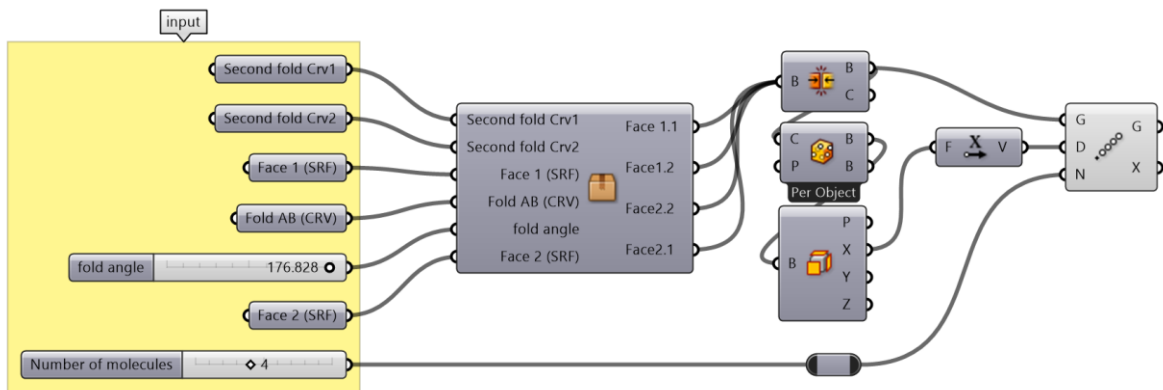


Figure 68: generative algorithm for the symmetric reverse fold on a straight accordion, joining “symmetric reverse fold” molecules, the cluster on the right contains the generative algorithm explained in section 4.6.1.

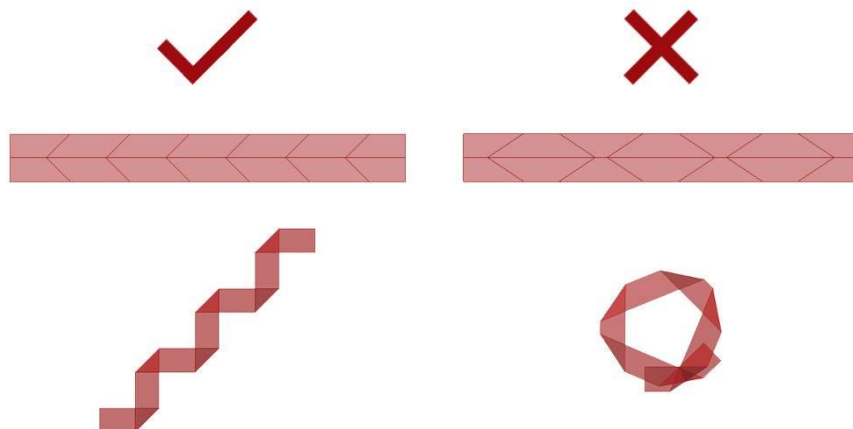


Figure 69: possible and impossible rigid flat-foldability due to self-intersections, even if the Kawasaki theorem is verified in every internal vertex.

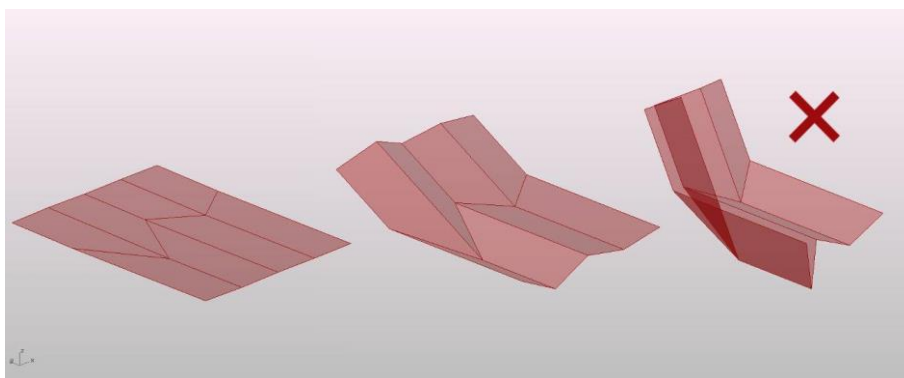


Figure 70: stitching two different symmetric flat foldable molecules side by side generates a globally non-flat-foldable pattern.

4.7.2. Joining “Asymmetric Reverse Fold” Molecules

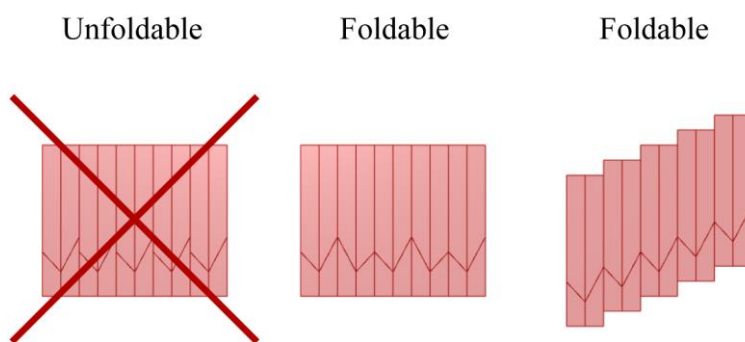


Figure 71: joining asymmetric molecules, the first case on the left is unfoldable, the second and third cases are non-flat-foldable.

In section 4.7.1 we placed side by side a series of “Symmetric reverse fold” molecules making a reverse-folded flat-foldable accordion. With the “Asymmetric reverse fold”, the result will be non-flat-foldable, but the procedure is similar. However, the molecules must be mated matching the endpoints of the reverse fold instead of aligning their outer perimeter. Alternatively, to match the endpoints of the reverse fold and also the outer perimeter of adjacent molecules, we can mirror the even or odd molecules as shown in Figure 71. Alternatively, instead of mating equal molecules side-by-side we can reflect a straight accordion with an angled plane as we do in the following algorithm.

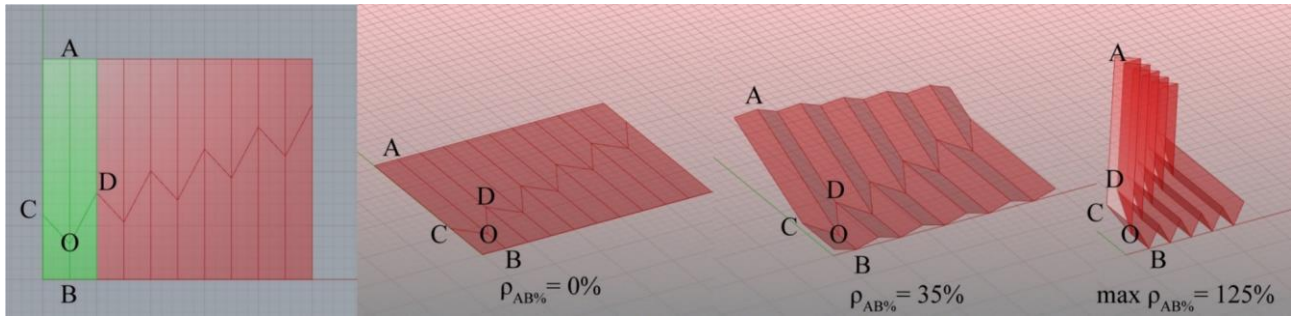


Figure 72: animation of an asymmetric reverse fold on a straight accordion, with the reflection of a straight accordion with respects of a mirror plane constructed on CO and DO.

Refer to Figure 72. First, animate the straight accordion as explained in 4.5.1. Then, draw two asymmetric creases OC and OD on the first two faces. Reverse fold the first two faces of the accordion following the method explained in section 4.6.1 and 4.6.2. After that, slice the whole accordion with the same plane and reflect it consistently with the first two faces. The full generative algorithm is shown in Figure 73 and Appendix B.16. To keep the structure of the nodes simple and clear we animated the surface with self-intersections. However, if there is the need to stop the animation at the blocked state, we can apply the collision detection method explained in 4.6.2.

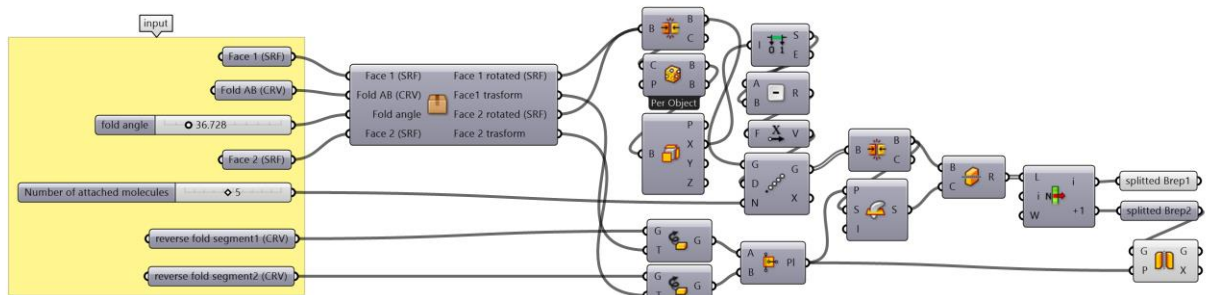


Figure 73: generative algorithm to animate a straight accordion with an asymmetric reverse fold the cluster on the right contains the algorithm explained in section 4.4.2.

4.7.3. Reverse Fold on Triangulated Accordion – Joining “Symmetric Reverse Fold” Molecules

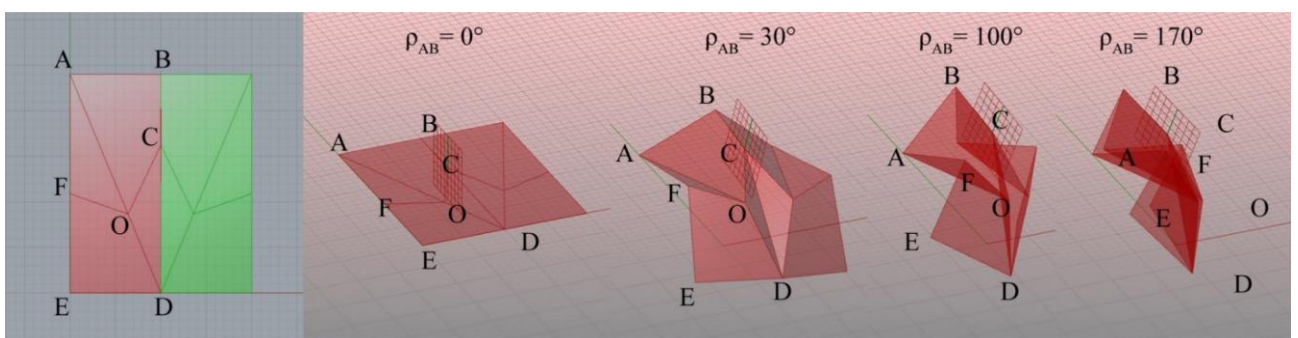


Figure 74: reverse fold on a triangulated accordion - construction and animation of the macro-molecule.

The reverse fold on a triangulated accordion is comparable to the reverse fold on a straight accordion, but in the starting rectangular molecule, the first fold is drawn along the diagonal AD instead of along the symmetry vertical axis of the rectangle. The algorithm works as follows.

Refer to Figure 74. Animate the faces AED and ABD by rotating them around the crease-line AD symmetrically. Draw the creases FO and CO to be symmetrical with respects of the crease AD. Once drawn the two creases apply the reflection method to perform a reverse fold as shown in section 4.6.1. Now draw a plane passing from B, C and D and use it as a

reflection plane to mirror the first molecule⁵⁷. We now obtained a symmetrical macro-molecule with 8 faces, which we are going to copy and paste one after another, as shown in Figure 75, using a looping definition. We use a looping definition because the macro-molecules need to be rotated other than translated to match perfectly the following molecule edges, thus we cannot use a simple translational array as we did in the previous section. The looping definition is shown in Figure 77 and it consists into matching the two planes constructed on the points A, F and E and the plane passing from their respective reflected points A', F' and E'.

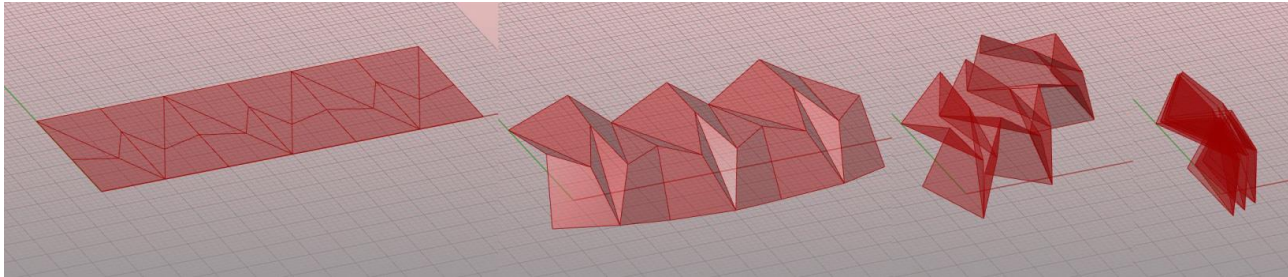


Figure 75: joined macro-molecules to make a longer triangulated accordion with the reverse fold.

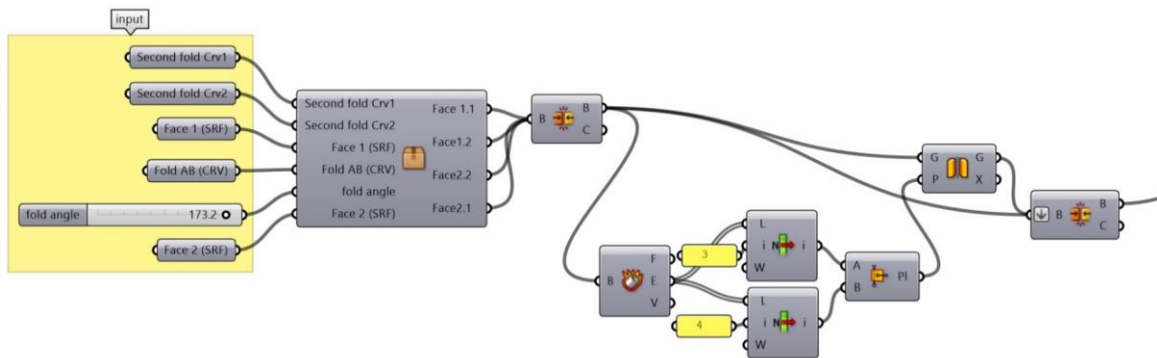


Figure 76: generative algorithm for a reverse-folded triangulated accordion – Part 1.

Even in this case, it is not easy to foresee if the surface will self-intersect just by watching its CP. It is much easier to judge it by animating the surface. In fact, not every configuration of the reverse-fold gives rigid folding motions from start to finish. For example, in Figure 78 we can see two examples of flat-foldable reverse folded triangulated accordions with different behaviours. Both can be folded in-plane, but in the second case, the surface can fold flat and rigidly, without colliding or self-intersecting. Contrariwise in the first case, the surface is rigid-foldable only for a certain amount, and once reached a specific fold angle it starts self-intersecting. Thus, to be able to reach the flat configuration continuing the folding motion without self-intersecting the surface, it would be necessary to flex the faces or slide a bit the fold-lines (as it would happen into a real model made by paper). In Figure 79 we can see an example of a paper model that apparently can be folded rigidly, but the digital simulation proves the opposite. This misalignment between the two models is caused by the fact that the paper is flexible, and the digital model is not. Furthermore, in the paper model the creases try to self-correct shifting from the original position for a small amount so that the initial pattern would slightly change and in some cases, it would be barely perceptible.

⁵⁷ At the unfolded state the plane is not univocally defined because B, C, D are colinear and we can construct an infinite star of planes passing from the same three aligned points. Thus, if we want to keep the reflected faces on the same plane of the two reference faces at the unfolded state, we may need to force it to be perpendicular to the construction plane. However as soon as they are animated the plane will be univocally defined because B, C, D will be no more colinear.

Testing the rigid foldability is very important especially if we want to use the pattern for real applications made by rigid patterns, because using a pattern that is not perfectly rigid-foldable may cause serious problems over the short or the long term. For example, if the faces are very rigid and connected with hinges, but the used pattern is not perfectly rigid-foldable (even for a small amount as in Figure 79), given that we are able to fold it forcefully exploiting the elasticity of the material, every time the mechanism is folded and unfolded, it would be subject to stresses and deformations caused by the colliding faces and that may cause faster deterioration of the joints.

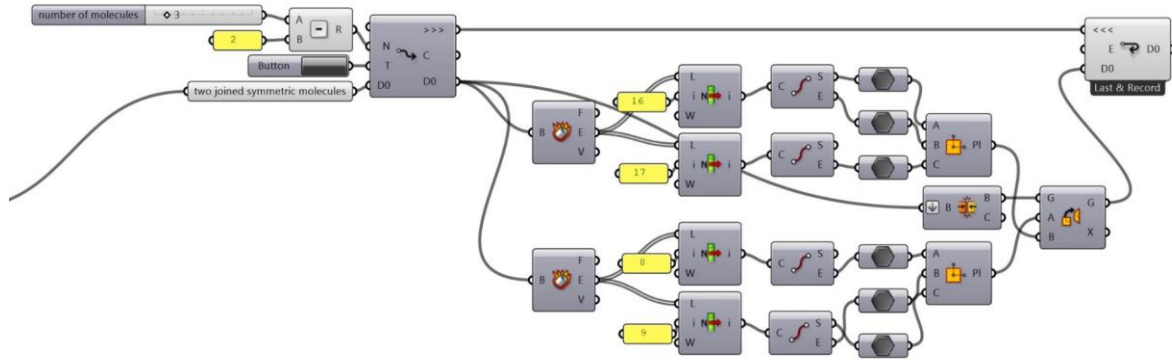


Figure 77: generative algorithm for a reverse-folded triangulated accordion – Part 2.

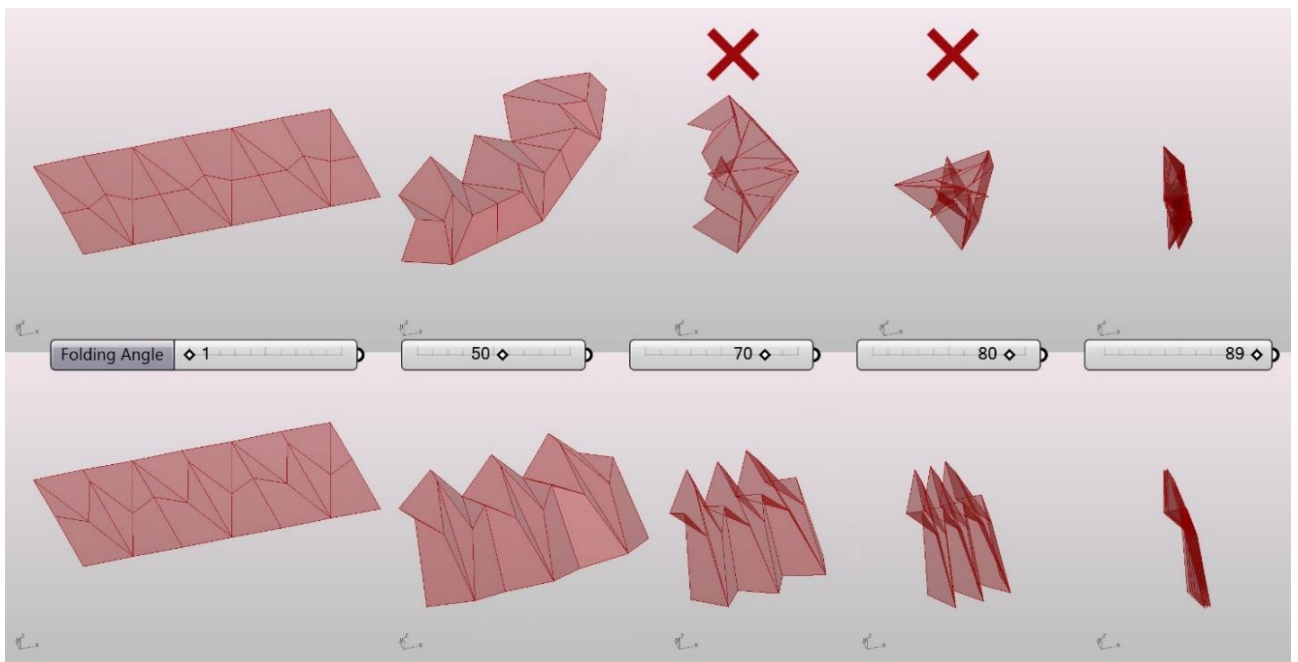


Figure 78: non-flat-rigid-foldability and rigid-flat-foldability of the triangulated accordion, varying the angle of the reverse fold.

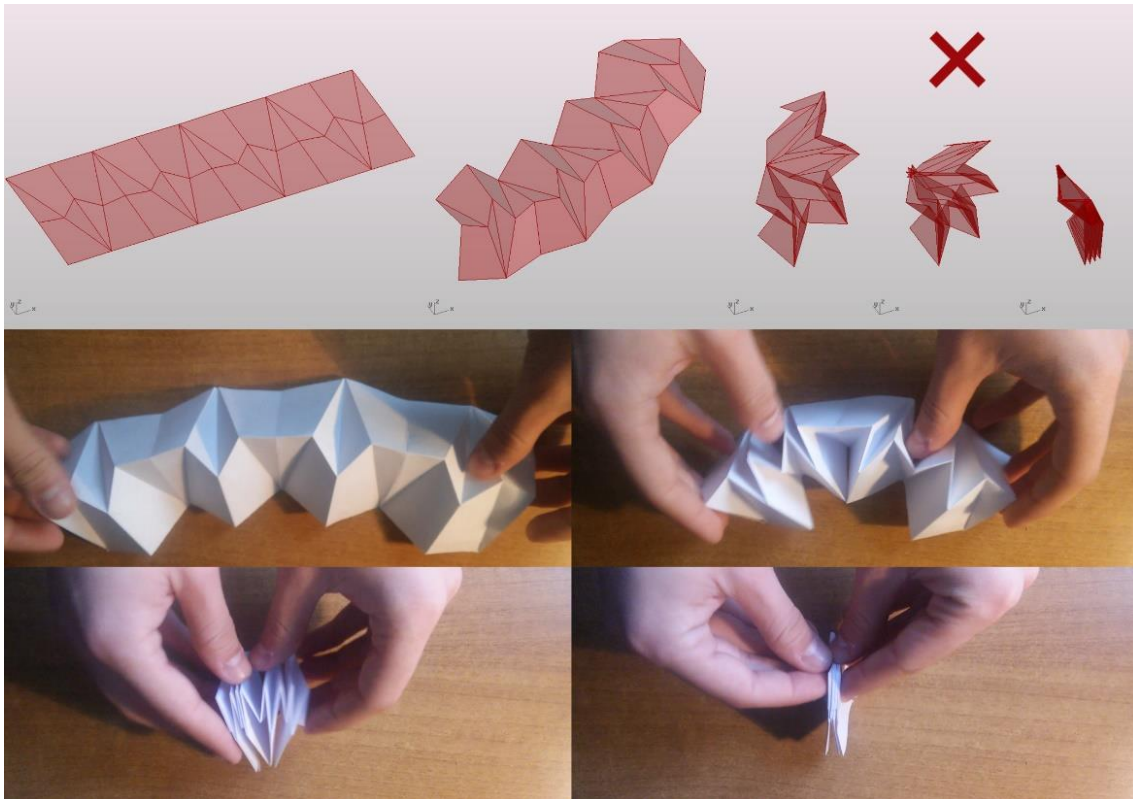


Figure 79: apparent incongruence between the digital and physical models; the faces of the former self-intersect, the faces of the latter remain apparently planar.

4.7.4. The Miura Pattern – Planar Rectangular Array of “Symmetric Reverse Fold” Molecules – Intersecting Circle with Plane of Symmetry



Figure 80: Miura pattern.

The Miura pattern, or Miura-ori, is probably the most famous and most used corrugations of all times, it has been studied and used for actual applications in several fields. Its diffusion is due to the fact that it is a one-DOF mechanism and it has a particular property of expanding and contracting with negative Poisson's ratio. The Japanese engineer Koryo Miura, in the mid-80s, studied this pattern, which derives from the uniform compression buckling pattern of a thin plate (Miura, 1997), to create a solar panel deploying system. This system was revolutionary because the solar panel so folded was able to unfold univocally with minimal fold actuators and without the help of the human interaction (Miura, 1985), for this reason, it has been renamed with his name. However, according to what recently stated by Hellmuth Stachel, the Miura ori might already have been known before: “However, already before K. Miura, this technique was known; according to a personal communication with Gy. Darvas, it was kept as a military secret in Russia in the thirties of the last century. There are many applications of Miura-ori.” (Stachel, 2015).

The Miura-ori pattern is composed of equal parallelogram faces, this guarantees that the surface has an in-plane expansion and contraction. Recent studies developed methods to modify the traditional pattern but preserving the rigid foldability, in order to give to the surface different spatial configuration (Tachi 2010b; Tachi 2009).

The traditional Miura pattern can be divided into elemental equal molecules composed by four adjacent faces and it can be digitally modelled and animated by reflecting many times a straight accordion, or by joining many equal molecules of four equal parallelogram faces. In this section, we are going to follow the second approach.

We can use the method explained in section 4.6.1 to animate the molecules, but the faces must be all equal and with a parallelogram perimeter before applying a rectangular array. However, we highlighted that this method generates problems in the flat-folded configuration because when the two segments of the reverse fold converge into one (at flat-folded state) the reflection plane would be no more univocally identified. Thus, the algorithm at that limit case could behave in an unexpected way. In the same section we solved this problem limiting the domain of the controller fold angle, however, in this section we want to propose an alternative method to solve the problem at the limit configurations without limiting the domain or using cumbersome “if statements”.

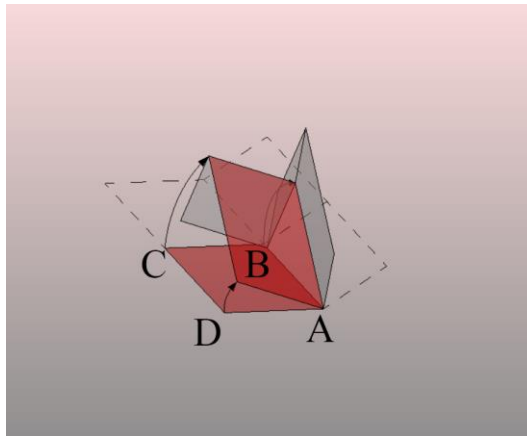


Figure 81: single Miura-ori face used to model the symmetrical molecule of the Miura-ori.

In Figure 81 it is represented one single Miura molecule. We can further simplify the problem focusing only on one single face (ABCD), because the faces are all equal, thus any other face is a simple translation or reflection of the same reference face. To be able to obtain an XY in-plane expansion of the Miura-ori during folding we want the segment AD to stay on the XY plane and the segment AB on the YZ plane.

The algorithm for the construction of the parametric animatable Miura-ori works as shown in Figure 82. Define a construction plane XY. Define point A in the origin of the plane, copy and move that point along X and Y to define other 3 points: B, C and D to form a rectangle. Move the points C and D along Y to shear the rectangle to get a rhomboid. Connect three sliders to these nodes to be able to control the width the length, and the amount of shear of the rectangle⁵⁸. Rotate clockwise ABCD around the Z-axis passing from A. Set the angular domain between the segment AD and the Y-axis. The rotation angle will be remapped in 0-100 domain to be controlled with a slider that we call “Collapsing (%)”. Draw a circle on the plane perpendicular to AD passing from B. Intersect the circle with the plane YZ obtaining 2 points, one over the XY plane (I’) and one under the XY plane (I’'). Select the upper point⁵⁹. Rotate the polygon ABCD around the AD axis to match B to I’. Mirror ABCD along YZ plane and mirror the two polygons together along XY plane. Then, translate the last two polygons along AB. The Miura molecule is finished. To make a wider Miura-ori pattern just copy and move this molecule as many times as you need along the direction X and Y. To animate the collapsing of the Miura-ori just move the Collapsing% slider, and to change the initial Miura pattern proportions, move the sliders connected to the “Width (cm)”, “Length (cm)” and “Shear (cm)” inputs. With this method, the circle has always one or at most two intersection points with the plane, so that the limit cases are univocally defined, and the algorithm never returns

⁵⁸ Instead of drawing each point parametrically we could have set as input directly the parallelogram face extracting the needed points. Nevertheless, with this method we are constructing a completely parametrical symmetric Miura-ori which is more versatile.

⁵⁹ If selected the bottom point, mountain and valley assignments would be reversed. The “value list” component can be used to select I’ or I’'' and change the verse of the folds anytime: set Mountain = 0 and Valley = 1 and use these values as searching indices in the list containing I’ and I’''.

unexpected behaviours. This approach works only for modular symmetric flat-foldable Miura-ori. The full generative algorithm is reported in Appendix B.18.

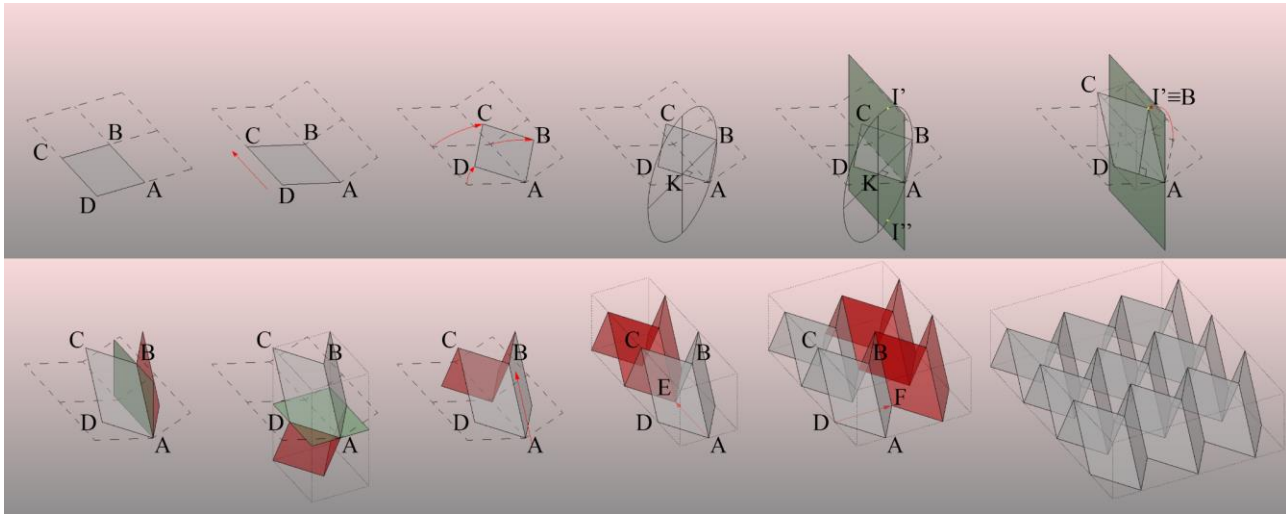


Figure 82: Miura-ori constructions and animation.

4.7.5. The sink fold – Reflecting the tip of a degree-4 vertex

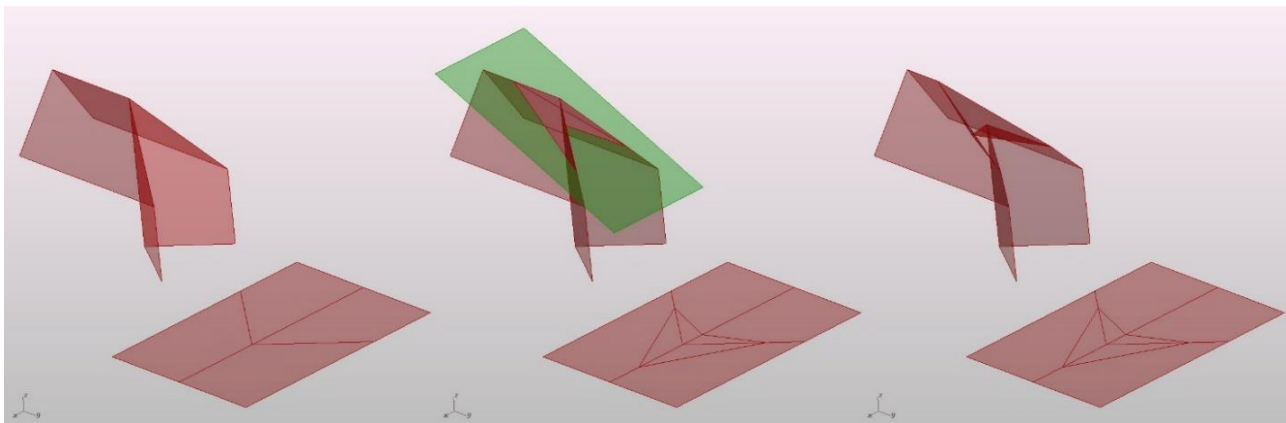


Figure 83: sink fold obtained by reflection.

Another known pattern with multiple degree-4 vertices is the sink fold. It consists into a closed loop of creases around a single vertex. Consecutive edges of the loop are symmetrical with respects of the crease that they touch. In particular we are going to sink fold a degree-4 vertex. The sink fold is a traditional fold that pushes a folded vertex inside the model using the reflection method. There are two types of sink folds in traditional origami, the closed sink and the open sink. The former does not fold rigidly, thus we will only consider the open sink in this section. The sink fold is called by Casale (et. al.) “*third fold*”. They define it as the fold that articulates the structure in the points where the direction of the configuration changes, thus in concomitance with the intersection between what they call “*second fold*” and “*first fold*”. They assert that this fold changes the formal quality of the surface and changes its structural characteristics, because adding ribs to the structure affects its static behaviour, but it does not change the DOF or the global behaviour of the previous pattern during motion, it only changes the local geometry (Casale et al., 2013). Nevertheless, sometimes the global rigid-flat-foldability could be compromised, depending on the configuration of the sink fold.

To make a sink fold with paper in the traditional way it is sufficient to fold a piece of paper making a single flat-folded vertex, at this point fold and unfold its tip marking a new crease through multiple layers of paper. Once unfolded the whole pattern we see a closed loop of new creases around the vertex which have to be marked as a mountain. Lastly, we reverse all the creases inside the loop of new creases and fold again the vertex pushing the tip inside the model.

In digital reconstruction, we can perform the same action using a reflection plane. However, even if we start from a flat-foldable degree-4 vertex, not every reflection plane guarantees a flat-rigid-foldable sink-folded pattern, because once pushed the tip of the vertex inside the model if the plane has not a specific orientation, it could cause collisions

during folding. The following exemplification will help us understanding how the angle of the reflection plane may affect the rigid-flat-foldability of the pattern.

In the example shown in Figure 84, we perform a sink fold on a molecule with a single symmetric reverse fold constructed with the method proposed in section 4.6.1 and reflected with respect of a plane. To prevent the pattern with sink fold to be no more rigid-flat-foldable the angle between the reverse-folded linear crease and the sink fold plane must be bigger than 0° and smaller than 90° . In general, an easy way to construct a sink folded degree-4 vertex preserving the same kinematic of the original pattern without sink fold⁶⁰ is to fold the pattern all the way to reach its blocking configuration, at this point reflect the tip of the degree-4 vertex with respect of the chosen reflection plane. The reflection plane must be angled making sure that self-intersections are avoided. If there are no self-intersections at the blocked state (or flat-folded state), then the kinematics of the mechanism is preserved, and the surface will not intersect during the whole motion.

Another issue that it needs to be considered when making a digital simulation of a sink fold, is that the reflection plane must intersect all the creases of the vertex inside the boundaries of the surface because, differently, it would generate a pair of new reverse folds instead of a sink fold (Figure 85).

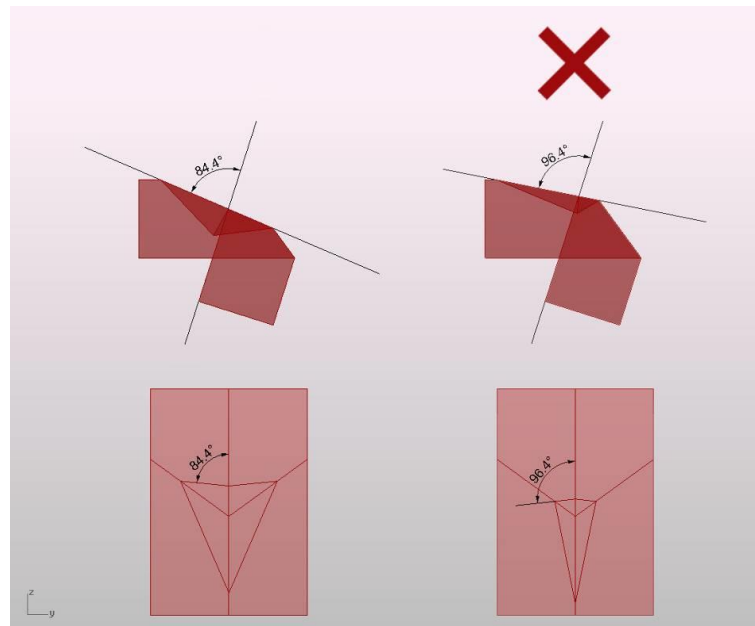


Figure 84: rigid-flat-foldability condition for the sink fold on reverse folded degree-4 vertex.

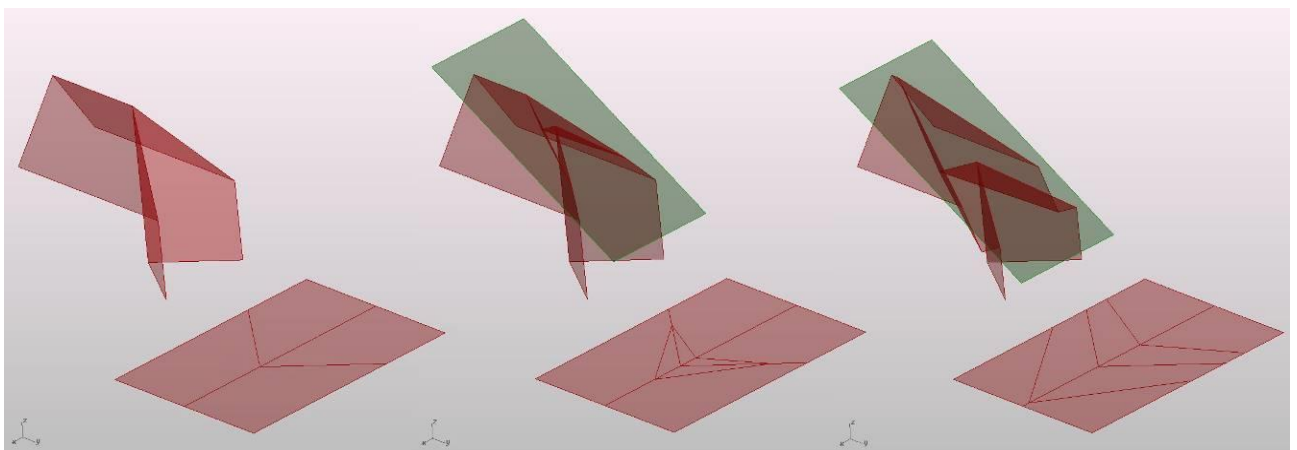


Figure 85: sink fold that degenerates into two simple reverse folds. This happens when the reflection plane does not intersect all the creases of the initial degree-4 vertex.

⁶⁰ Thus, preserving also its rigid-foldability.

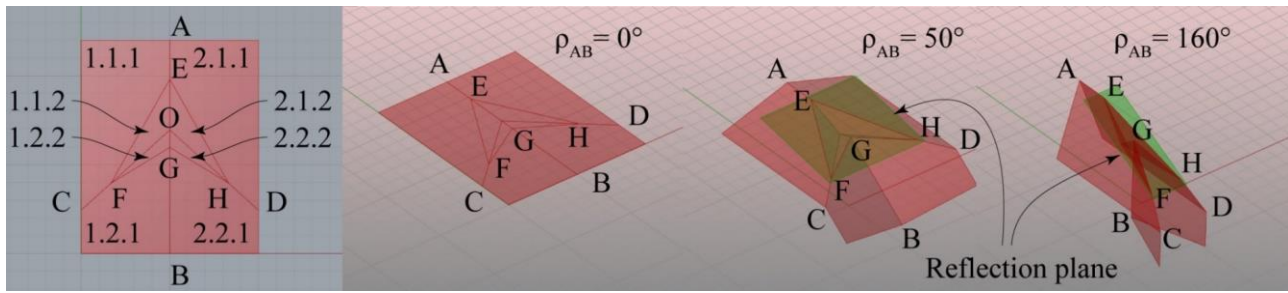


Figure 86: sink fold by reflecting a reverse folded molecule explained in 4.6.1.

To animate a pattern with sink fold we start from the reverse fold molecule and we reflect the tip of the degree-4 vertex. Refer to Figure 86 for the notation. First, start from a flat-foldable degree-4 vertex pattern, then add to that pattern some new creases that form a closed loop around the single vertex. The segments of the newly drawn loop of creases must be symmetric with respects of the creases that they touch⁶¹. Then use the same definition shown in 4.6.1 to animate the molecule with “symmetric reverse fold”. After this, move and rotate two of the segments of the sink fold drawn on the plane by copying and re-applying the rotations and translations of the relative faces to which they belong⁶². In this case, we copy the transformations of the faces 1.1 and 2.1 of the original reverse fold molecule to the new segments EF and EH. Draw a plane passing through EF and EH segments and use it to split the surface. The folded surface is now split into two independent poly-surfaces which are called in Grasshopper B-reps⁶³ they are split along the EFGH planar polygon. Pick the upper or the lower B-rep and reflect it with respects of the same plane. Lastly, we can animate the surface with the sink fold by moving the cursor of the slider that controls the fold angle. With this approach, the kinematics of the original starting molecule without sink fold is preserved. The generative algorithm is shown in Figure 87 (and Appendix B.19) and the initial cluster contains the algorithm explained in 4.6.1.

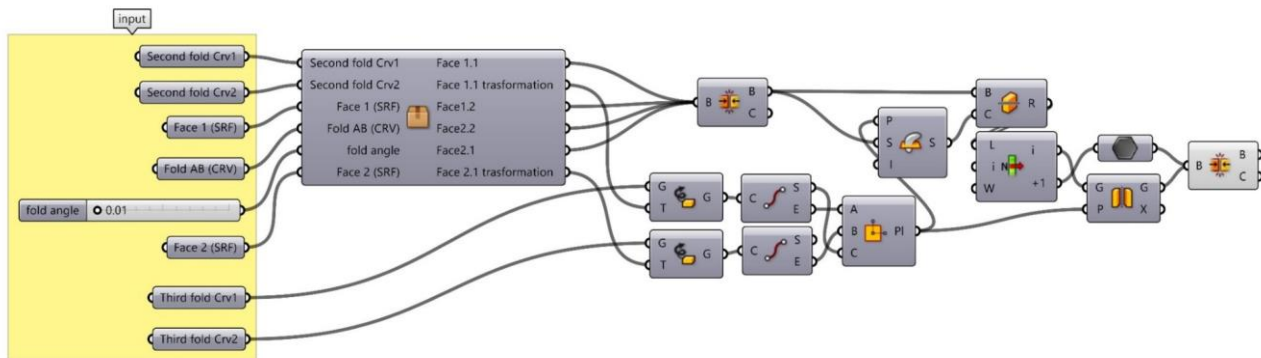


Figure 87: generative algorithm of the sink fold molecule animated with reflection with respect of a plane passing from at least two segments of the sink fold, the cluster node contains the algorithm explained in section 4.6.1.

4.8. Patterns with Single or Multiple Degree>4 Vertices

So far, all the patterns with internal vertices that we studied were made only by degree-4 vertices, and they had only one-DOF and for this reason, we were able to animate them with only one single controller crease that propagated its motion to all the other creases univocally. But how can we animate all the other patterns with vertices with a degree greater than four and with a DOF greater than one?

⁶¹ In our algorithm we draw only the creases EC and ED. FG and HD are extracted automatically from successive steps of the algorithm.

⁶² We do not need to re orient also the other two segments of the sink fold because we need only two to define the reflection plane.

⁶³ B-reps stands for “Boundary representation”, it is a representation method widespread in CAD software where the surfaces are limited by geometric entities like boundaries and edges. In Grasshopper any surface or polysurfaces is called B-rep.

The possibilities are several, and the complexity of the problem increases drastically. At the present moment, the approach which is mostly used by the scientific community to animate a generic origami pattern is based on physical simulations that iteratively distribute the errors on every face and crease, preserving its developability and rigidity of the faces according to a certain tolerance. The software Freeform Origami by Tachi (Tachi, 2010b) works with this principle, as well as the web-based application Origami Simulator by Amanda Ghassaei (Ghassaei, n.d.). These simulators try to fold the crease pattern all at once. To do so, the surface is stretched and displaced during motion and it temporarily loses its developability for a small amount. These deformations are due to forces exerted by mountain and valley creases. Because there are forces involved, we often refer to this kind of simulations as physical simulations.

Even if some applications that fold almost any origami pattern exist, they are hard to include into a professional designing pipeline, due to the reasons we highlighted in section 1.5.3. Furthermore, integrating the simulation into the original design context would open new possibilities about the interaction with the context and other parts of the project that are not necessarily origami-related.

Fortunately, even if Grasshopper does not have built-in components for physical simulations, a plug-in called Kangaroo physics (Piker, n.d.) scripted by Daniel Piker will allow us to work with such type of simulations into Grasshopper without the necessity of scripting our own custom components. Kangaroo Physics is a “*live physics engine for interactive simulation, form-finding, optimization and constraint solving*”. This plugin implements in Grasshopper a set of new tools that facilitate working with (e.g.) forces, meshes, point clouds, and interconnected points. It also implements a wide set of “Goal nodes” which constrain some properties of the input geometry during the simulation, and a “Kangaroo Solver” which animates a given geometry according to the forces and constraints set by the goal nodes. Once set off the simulation, the solver generates a set of motion vectors for each goal node plugged into the “GoalObjects” input. The move vectors are applied to each particle they act on (e.g. the vertices of a mesh, the endpoints of some segments, the origin points of a group of solids), and the solver iteratively minimises the total sum of the weighted squares of all the move distances. With this method all the constraints have a certain amount of error inversely proportional to the strength we set for each of them, thus the error is distributed non-uniformly to all the constraints.

The formulation that the Kangaroo solver uses to calculate the position P of each point is the following:

$$P_{i,new} = P_{i,cur} + \frac{\sum_{j=1}^n \omega_j \cdot G_j}{\sum_{j=1}^n \omega_j} \quad (37)$$

Where: i refers to the particle index, n is the number of goals acting on that particle, ω is the weighting and G is the moving vector for goal j (Brandt-Olsen, 2016).

For example, we can set the strength of the nodes that constrains the preservation of the developability of the original pattern to a very high value, and we can set the strength of the node that constrains the fold angle of each crease to a certain given fold angle with a lower strength. Like so even if the real fold angles of each crease may be different from the one that we set while preserving the invariance of the shape and planarity of the faces as much as possible.

This approach is similar to the one used by Tachi and Ghassaei in their applications, it is fast and efficient to calculate because it performs the folding of each fold all at once, but it stretches and deforms a bit the surface during motion. The same approach could solve all the cases shown in the previous sections faster, but with lower accuracy, thus it can be considered an alternative method but with different aims and needs.

4.8.1. Degree>4 Vertices – Physical Simulation

The aim of the algorithm presented in this section is to simulate the folding animation of an origami pattern with one or more degree-4 vertices or vertices with a degree greater than four, and a DOF greater than one, with a given mountain/valley assignment. To help the designer controlling the animated surface we implement the possibility of anchoring some points and sliding some other points on a given plane. Furthermore, for vertices with a DOF greater than one it will be possible to set a different fold angle for each crease or group of creases. The first part of the algorithm is focused on identifying the creases which are mountain, valley or unassigned, the second part is focused on setting some constraints that will be inputted into the “Kangaroo Solver” component. As a result, we will obtain the real-time folding simulation of the given pattern.

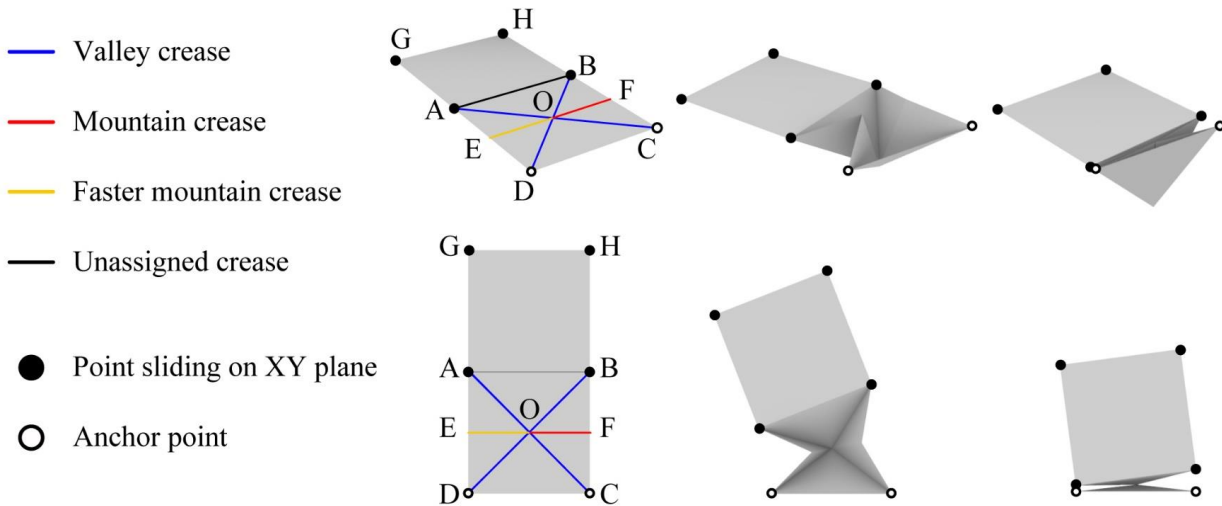


Figure 88: an example of a degree > 4 vertex, animated with physical simulation, applying different fold angles to the creases, in this way the animation is asymmetric even if the pattern is symmetric.

In Figure 88 we show an exemplification pattern with a generic degree-6 vertex with a DOF greater than one. The crease AB is left unassigned, the creases AO, BO, CO, DO are set to be folded with a positive given fold angle, the same angle, but negative, is assigned to FO. EO is a mountain crease as FO but its fold angle is set to be the double of the other crease angles. In this way, we experiment asymmetric folding motions on symmetric patterns.

The steps of the algorithm are the following. First, set the inputs of the definition: a planar surface which can be compared to the piece of paper that we are going to fold, and a set of straight lines arranged on the surface which are going to form the CP⁶⁴. Now divide the creases into two lists: mountain and valley⁶⁵. Then slice the surface along the creases so that each face of the crease pattern is a separate piece. Join all the surfaces into a single poly-surfaces (B-rep) and convert it into a simple mesh⁶⁶. Now, compare the position of each input valley crease and mountain crease to the position of each edge of the mesh and divide them in two separate lists. To do so, use the “Closest Points” component comparing the mid-point of each mesh edge to the mid-point of each crease line. Extract for each mountain or valley edge of the mesh the two adjacent mesh faces. As a result of these steps, we obtained two branched lists⁶⁷. Each branch represents the mesh edge index and it contains a list made of two elements which are the two indices of the two adjacent faces. To do this last step more easily we used the Sandbox plugin for Grasshopper (Schwinn, n.d.) which analyses the input mesh topology and returns for each edge the list of adjacent faces automatically. Lastly, triangulate the mesh, because if the faces are all triangular it is sufficient to constrain the length of each edge to be able to preserve the developability of the surface.

Now we have all we need to set up the Kangaroo goal nodes. The goal nodes that we are going to use are: “CoPlanar”, “Length(line)”, “Anchor”, “OnPlane”, “NoFoldThrough”, “Hinge”, “Show” and “Grab”. The “CoPlanar” and “Length(line)” nodes are used to constrain the surface to remain developable and rigid. These two components are sufficient to guarantee and preserve the rigid-foldability of the surface because the “Length(line)” takes as input the edges of the triangulated mesh so that the developability is preserved, and the “CoPlanar” node takes as input the edges of each face of the mesh before the triangulation, so that the original faces will try to remain planar preserving the rigidity of the faces. Then we use the “Anchor” and “OnPlane” goal nodes to lock the surface in one place or to constrain the expansion and contraction of the surface along one particular plane so we prevent the surface to navigate the three-dimensional space uncontrollably while folding. Specifically, the “Anchor” node tries to keep a group of points on a

⁶⁴ If we draw the lines randomly, the pattern could be unfoldable, thus we suggest starting to test the algorithm with known patterns.

⁶⁵ To facilitate this operation, divide the mountain creases and the valley creases in two different layers. Furthermore, split all the creases into separate segments.

⁶⁶ We convert the polysurfaces into a mesh because Kangaroo does not accept as input a polysurfaces or a nurbs surfaces.

⁶⁷ They are called branched because they are organized into a tree structure that have more than one level of hierarchy, practically they are lists of lists.

given location⁶⁸, and the “OnPlane” node tries to keep a group of points on a given plane⁶⁹. The “OnPlane” node is different from the “CoPlanar” node, because the “OnPlane” node tries to keep the points on a given plane, if no plane is set as input it considers the XY plane as target attractor plane, the “CoPlanar” node instead, tries to keep the points on a plane (recomputed for each iteration) that is the interpolation of the input point cloud. The “NoFoldThrough” and “Hinge” nodes are the components responsible of the folding motion, the former prevents the surface to intersect once the adjacent faces reach their maximum fold angle, the latter takes two triangular faces as input and rotates them around the common edge of a certain given angle. We need two different “Hinge” nodes to perform mountain and valley folds, we multiply to -1 the angle that is inputted into the mountain “Hinge” node.

We said that only triangular faces can be processed by the “Hinge” node but also patterns with polygonal faces can be animated. It is sufficient to split their faces into triangles before plugging them into the “Hinge” node. However, we need to add an additional “Coplanar” constraint to keep the triangular faces that belong to the same polygonal face on the same plane because otherwise, the pattern would fold as if we added new unassigned creases. The higher the strength of this constraint is, the stiffer the faces are; and if we want the surface to behave more elastically, we can simply decrease the strength of this constraint.

To make some creases folding faster or slower than other as shown in Figure 88 we need a third “Hinge” node which is going to take as input the same angle multiplied or divided by a certain number (in this case we multiplied it by two). There is no limit to the number of “Hinge” nodes that can be used. We potentially could add one hinge node for every crease, setting a different fold angle for every one of them. In this way, we would increase the shaping freedom at the expenses of easier operability. In the example shown in the figure, we added only one additional “Hinge” node as an exemplification.

Lastly, we use the “Show” node to set the geometry that we want to see during the simulation, and the “Grab” node to add the possibility to interact with the surface in real time into the Rhino viewport by grabbing the vertices with the mouse pointer. This node is useful to help the designers judging the DOF of the surface or helping the surface to fold properly if it gets stuck for any reason. The generative algorithm is shown in Appendix B.20. This algorithm can be used to simulate, potentially, the folding animation of any foldable pattern, even one-DOF patterns. This versatility makes this approach very effective.

4.8.2. Testing the Algorithm with Different Patterns

In the last section, we asserted that the folding animation based on physical simulation is very efficient and versatile. Once built the generative algorithm, the simulation is easy to set up because we only need to draw the CP and divide the creases into groups: mountain, valley and unassigned (and faster mountain and valley if needed). In this section we show some tests we did on well-known traditional patterns, to prove its efficiency and versatility. In Figure 89 and Figure 90 we simulated the folding of the traditional “magic ball” and “Yoshimura” patterns, both patterns have more than one DOF, thus we tested them with uniform and non-uniform fold-angle distribution. As the reader can see, the surface can be folded symmetrically or asymmetrically just by changing the fold angle speed of some designated creases.

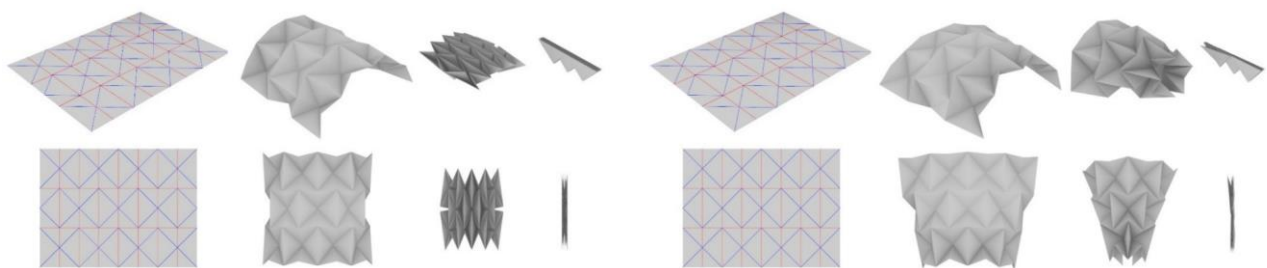


Figure 89: folding physical simulation of a traditional “magic ball” origami pattern, with uniform and non-uniform fold angle distribution.

⁶⁸ We fix only the vertices of one single face on the original location. Fixing the vertices of many faces could prevent the surface to fold and unfold properly.

⁶⁹ It is important to constrain only the vertices that we know that they are capable of staying on the same plane while folding, otherwise we could prevent the surface to fold and unfold properly.

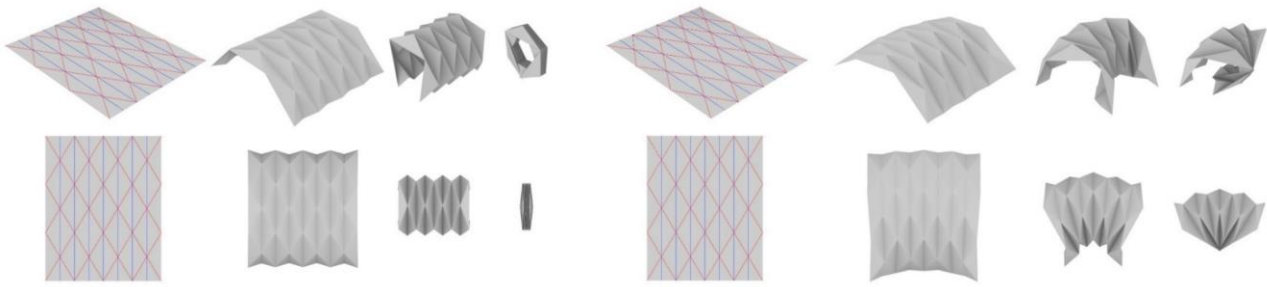


Figure 90: folding physical simulation of a traditional "Yoshimura" origami pattern, with uniform and non-uniform fold angle distribution.

We verified the preservation of the developability of the pattern during and after the simulation, and we compared the area of the surface and the unfolded pattern before and after the animation, and as expected it loses the developability only for a small amount during motion. Nevertheless, once reached the equilibrium state, the global error is minimal, and, in most scenarios, it would be already acceptable. However, we can minimize the developability and rigidity errors even more, by increasing the strengths of the "CoPlanar" and "Length(line)" nodes by a great amount. Nevertheless, if we increase the strengths of these two nodes too much the animation would slow down drastically because the forces applied by the "Hinge" nodes would be overwhelmed by the forces applied by the "CoPlanar" and "Length(line)" components. Thus, to minimize the developability and rigidity errors without slowing down the animation too much, we can balance the strength of the various goal nodes during the simulation, and once reached the desired configuration, we can make the strengths of the goal nodes equal to zero all at once except for the strength of the "CoPlanar" and "Length(line)" nodes. In this way, the forces applied on the surface disappear except for the forces responsible of preserving the developability and the rigidity properties, so that the surface self-adjusts finding a new equilibrium configuration which is almost equal to the previous equilibrium configuration, but with minimal geometry errors.

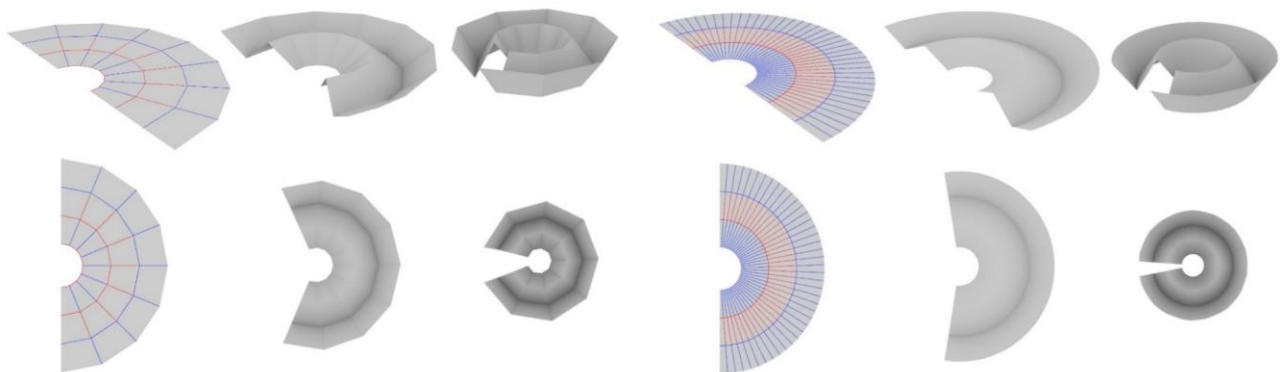


Figure 91: folding simulation of two discretized curve creases (with a different discretization degree) with physical simulation.

In Figure 91 it is shown the simulation of a pattern with two discretized curved creases. The patterns on the left and on the right start from the same two curve creases but with different discretization degrees. The ruling of the curved surface has mountain or valley assignments, in this way the folding animation is more stable, nevertheless it could also be left unassigned and they would assume a mountain or valley assignment automatically from the adjacent creases with an assigned verse. This example approximates a curve crease because with discretization all the vertices are degree-4, thus the surface has only one-DOF. Nevertheless, in the real world, the curved creases can be performed only on flexible materials and they are usually made without deciding the ruling in advance, thus the ruling can change over time and the DOF would be more than one. This case is an easy special case that uses two concentric arcs of circumference as curved creases, thus the ruling match the direction of the radii of the circles, however for more complex curved creases the calculation of the ruling that is necessary to connect the curves while preserving the rigid foldability of the discretized pattern may not be as easy to calculate as in this case. There are some interesting studies about this problem

(Bhooshan et al., 2015; Demaine et al., 2015, 2018; Dias, Dudte, Mahadevan, & Santangelo, 2012; Kilian et al., 2008; Tachi, 2013; Tachi & Epps, 2011) but there is not a generalized theory yet.⁷⁰

4.8.3. Limits of the Algorithm and Known Problems – Pop-Up and Pop-Down

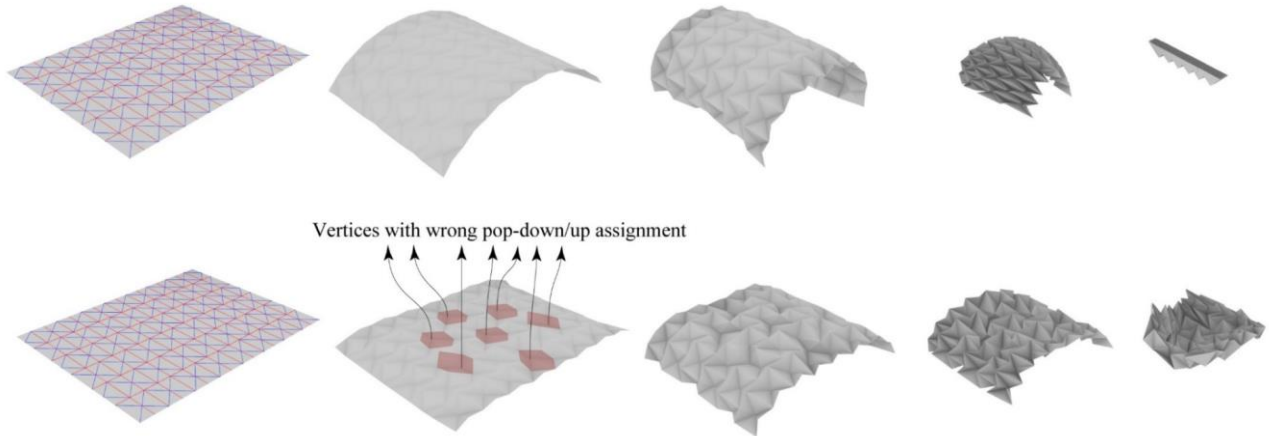


Figure 92: self-folding animation of a wide “magic ball” pattern, without and with the pop-up assignment problem.

Unfortunately, the physical simulation is not always reliable, the reason of that is that folding all the creases at the same time may cause some defects and problems on some vertices, it happens especially when there are a big number of creases in the pattern. We can try to tweak the strength values of the goal nodes or move the slider that animates the folding very slowly or grabbing the surface directly from the Rhinoceros viewport⁷¹ trying to correct the defects while they occur, and most of the times these tricks work, but sometimes the simulation still fail for a known problem which sometimes occurs in self-foldable origami. This problem is caused by the fact that most of the origami vertices can be folded in two different ways without changing the mountain/valley assignment. These two possible configurations are known as “pop-up” and “pop-down” states (Tachi & Hull, 2016). Some origami single vertex patterns can be folded pushing the central vertex upward or downward without changing their mountain/valley assignment, and the bifurcation of the motion happens at the completely unfolded state. Thus, when we try folding a pattern just by constraining the mountain valley assignment there are equal chances to get a pop-up or pop-down result if no other forces are applied. Furthermore, in patterns with a big number of vertices, because the physical simulation for its nature displace the vertices for a small amount while distributing the errors, it makes the surface behaving as a flexible surface, thus some vertices could take the path of the “pop-up” state and some other of the “pop-down” state even if they are not compatible, blocking the folding of the surface as shown in Figure 92.

To solve the problem, we can use many different methods, for the “magic ball” pattern shown in figure it was sufficient to slow down the animation of a big amount giving the necessary time to the Kangaroo solver to distribute the error to all the faces and to let the surface self-adjusting before passing the point of no-return where some vertices take the wrong pop-up/down assignment. Other methods could use attractor forces that may help the vertices to move in the correct direction from the first instant, or we could decrease the stiffness of the edges making the pattern more willing to self-correct exploiting the flexibility of the faces. Anyway, this kind of solutions has to be evaluated and tested case by case.

This kind of defects does not happen only in digital simulations, but also in the real world if the surface is flexible enough. The implications of these defects on real folded materials has been extensively studied by Silverberg et al. who consider a Miura-ori defected pattern as a case study to make some considerations about the design of reprogrammable mechanical metamaterials (Silverberg et al., 2014).

⁷⁰ An interesting tool to study curve folding is the “Origami Simulator” by Amanda Ghassaei (that we mentioned in Section 1.5.3). This application allows to simulate the folding and unfolding of complex curve folded patterns even with imperfect ruling, however it must be pointed out that fixing a ruling in curve folding is always an approximation and it limits the possible configurations in which a curved folded pattern could be configured, thus it is preferable to precisely design the ruling according to specific rules to achieve particular results.

⁷¹ We can drag the geometry during the simulation only if we add a “Grab” node to the goal nodes of Kangaroo.

4.9. References – CHAPTER IV

- Abel, Z., Cantarella, J., Demaine, E. D., Eppstein, D., Hull, T. C., Ku, J. S., Lang, R. J., & Tachi, T. (2016). Rigid Origami Vertices: Conditions and Forcing Sets. *Journal of Computational Geometry*, 7(1), 171–184. <https://doi.org/10.20382/jocg.v7i1a9>
- Akitaya, H. A., Cheung, K. C., Demaine, E. D., Horiyama, T., Hull, T. C., Ku, J. S., & Tachi, T. (2016). Box Pleating is Hard. *Discrete and Computational Geometry and Graphs*, 9943, 167–179.
- Bhooshan, S. (2015). *Interactive Design of Curved-Crease-Folding*. University of Bath.
- Bhooshan, S. (2016). Upgrading Computational Design. *Architectural Design*, 86(2), 44–53. <https://doi.org/https://doi.org/10.1002/ad.2023>
- Bhooshan, S., Bhooshan, V., El-Sayed, M., Chandra, S., Richens, P., & Shepherd, P. (2015). Applying dynamic relaxation techniques to form-find and manufacture curve-crease folded panels. *Simulation*, 91(9), 773–786. <https://doi.org/10.1177/0037549715599849>
- Brandt-Olsen, C. S. (2016). *Calibrated Modelling of Form-active Structures*. The Technical University of Denmark.
- Casale, A., Valenti, G. M., & Calvano, M. (2013). *Architettura delle superfici piegate: le geometrie che muovono gli origami*. Roma: Edizioni K.
- Chandra, S., Bhooshan, S., & El-Sayed, M. (2015). Curve-Folding Polyhedra Skeletons through Smoothing. *Origami 6: I. Mathematics*, 231.
- Demaine, E. D., Demaine, M. L., Huffman, D. A., Koschitz, D., & Tachi, T. (2015). Characterization of curved creases and rulings: design and analysis of lens tessellations. *Origami 6*, 209–230.
- Demaine, E. D., Demaine, M. L., Huffman, D. A., Koschitz, D., & Tachi, T. (2018). Conic crease patterns with reflecting rule lines. *Origami 7: Mathematics*, 573–589.
- Dias, M. A., Dudte, L. H., Mahadevan, L., & Santangelo, C. D. (2012). Geometric mechanics of curved crease origami. *Physical Review Letters*, 109(11), 114–301. <https://doi.org/10.1103/PhysRevLett.109.114301>
- Ghassaei, A. (n.d.). Origami Simulator. Accessed July 31, 2018, from <http://apps.amandaghassaei.com/OrigamiSimulator/>
- Kilian, M., Flöry, S., Chen, Z., Mitra, N. J., Sheffer, A., & Pottmann, H. (2008). Curved folding. *ACM Transactions on Graphics (TOG)*, 27(3), 75.
- Kuribayashi, K., Tsuchiya, K., You, Z., Tomus, D., Umemoto, M., Ito, T., & Sasaki, M. (2006). Self-deployable origami stent grafts as a biomedical application of Ni-rich TiNi shape memory alloy foil. *Materials Science and Engineering A*, 419(1–2), 131–137. <https://doi.org/10.1016/j.msea.2005.12.016>
- Lang, R. J. (2011). *Origami design secrets: mathematical methods for an ancient art, second edition*. Boca Raton, FL, USA: CRC Press.
- McNeel (n.d.). Rhinoceros. Accessed August 20, 2010, from <https://www.rhino3d.com/>
- Mitani, J., & Igarashi, T. (2011). Interactive Design of Planar Curved Folding by Reflection. *Pacific Conference on Computer Graphics and Applications - Short Papers*, 77–81. <https://doi.org/10.2312>
- Miura, K. (1985). Method of Packaging and Deployment of Large Membranes in Space. *The Institute of Space and Astronautical Science report No 618*. Sagamihara, Japan.

- Miura, K. (1997). Fold - its physical and mathematical principles. *Proceedings of the Second International Meeting of Origami Science and Scientific Origami*, 41–50.
- Piker, D. (n.d.). Kangaroo Physics. Accessed June 27, 2018, from <https://www.food4rhino.com/app/kangaroo-physics>
- Rutten, D. (n.d.). Grasshopper official page. Accessed July 31, 2018, from <http://www.grasshopper3d.com/>
- Schwinn, T. (n.d.). Sandbox Topology. Accessed June 27, 2018, from <https://www.food4rhino.com/app/sandbox-topology>
- Silverberg, J. L., Evans, A. A., McLeod, L., Hayward, R. C., Hull, T., Santangelo, C. D., & Cohen, I. (2014). Using origami design principles to fold reprogrammable mechanical metamaterials. *Science*, 345(6197), 647–650. <https://doi.org/10.1126/science.1252876>
- Stachel, H. (2015). Flexible Polyhedral Surfaces with Two Flat Poses. *Symmetry*, 7(2), 774–787. <https://doi.org/10.3390/sym7020774>
- Tachi, T. (2009). Generalization of rigid foldable quadrilateral mesh origami. *Journal of the International Association for Shell and Spatial Structures*, 50(October), 2287–2294.
- Tachi, T. (2010b). Freeform variations of origami. *Journal for Geometry and Graphics*, 14(2), 203–215.
- Tachi, T. (2011a). One-DOF rigid foldable structures from space curves. *Proceedings of the IABSE-IASS Symposium*, 20–23.
- Tachi, T. (2013). Composite rigid-foldable curved origami structure. *1st International Conference on Transformable Architecture*, 18–20.
- Tachi, T., & Epps, G. (2011). Designing One-DOF Mechanisms for Architecture by Rationalizing Curved Folding. *Proceedings of the International Symposium on Algorithmic Design for Architecture and Urban Design*.
- Tachi, T., & Hull, T. C. (2016). Self-foldability of Rigid Origami. *Journal of Mechanisms and Robotics*, 9(2). <https://doi.org/10.1115/1.4035558>
- Terzidis, K. (2006). *Algorithmic architecture*. Amsterdam [etc.]: Routledge.
- Thün, G., Velikov, K., Ripley, C., Sauv e, L., & McGee, W. (2012). Soundspheres: Resonant chamber. *Leonardo*, 45(4), 348–357. https://doi.org/10.1162/LEON_a_00409

5. CHAPTER V: Pattern Design from a Given Shape

Given Shape

Designing an origami-inspired object does not always require solving its kinematics and digitally simulate the folding and unfolding of the surface. Animating the surface is useful for example for rigid-foldable kinetic mechanisms. However, movable mechanisms, even if they are one of the most important targets of applied origami, are not the only cases that may benefit from origami properties. For example, for a paper lampshade, or a cardboard box, we do not necessarily need to simulate the folding and unfolding of the pattern, but we may want to manipulate the three-dimensional object in space while preserving its developability. Thus, in this part of the thesis, we present some case studies that exemplify the design of objects or buildings inspired by already existing projects, through the use of specific algorithms developed with Grasshopper (Rutten, n.d.; Tedeschi, 2014) that are aimed to achieve a three-dimensional folded configuration that is developable. Thus, instead of starting from the unfolded pattern, we start from reference geometries in space (e.g. curves, surfaces, meshes) that we consider as attractors, guides or rails, and we build the folded geometry on them while following strict rules that guarantee the developability of the CP. These case studies are mainly focused on the construction of the generative algorithms, and they do not solve all the issues that may arise from fabrication. We will focus on the fabrication problems in CHAPTER VI.

5.1. Lampshade – Vertices Extrusion and Reflection



Figure 93: Le Klint lamp n° 306, the versatile lamp.

Imagine having an old lamp by Le Klint like the one shown in Figure 93 (Le Klint, n.d.), that is missing its original shade, and we want to renew it by making a different shade that fits perfectly the old structure. Because we already have a reference structure, we cannot use any accordion-shaped piece of paper because with a high probability it would not perfectly fit on it. For example, we cannot use a straight accordion, because, as we saw in section 4.5.2 it is conformable into cones⁷². We could instead use the method explained in section 4.5.4 to design an accordion with converging creases that would fit perfectly on a cone. However, that solution leaves no room for creativity, thus, because the design possibilities are endless, in this section we propose a more versatile procedure that allows us to manipulate the folded shape constraining it to the two circular rails while preserving its developability. We start generating a triangulated accordion between the two rails, and to make it more appealing we reflect the bottom points with respects of specifically placed reflection planes, and we deform and manipulate the global shape to make it asymmetric.

⁷² If we don't consider elastic deformation of the faces.

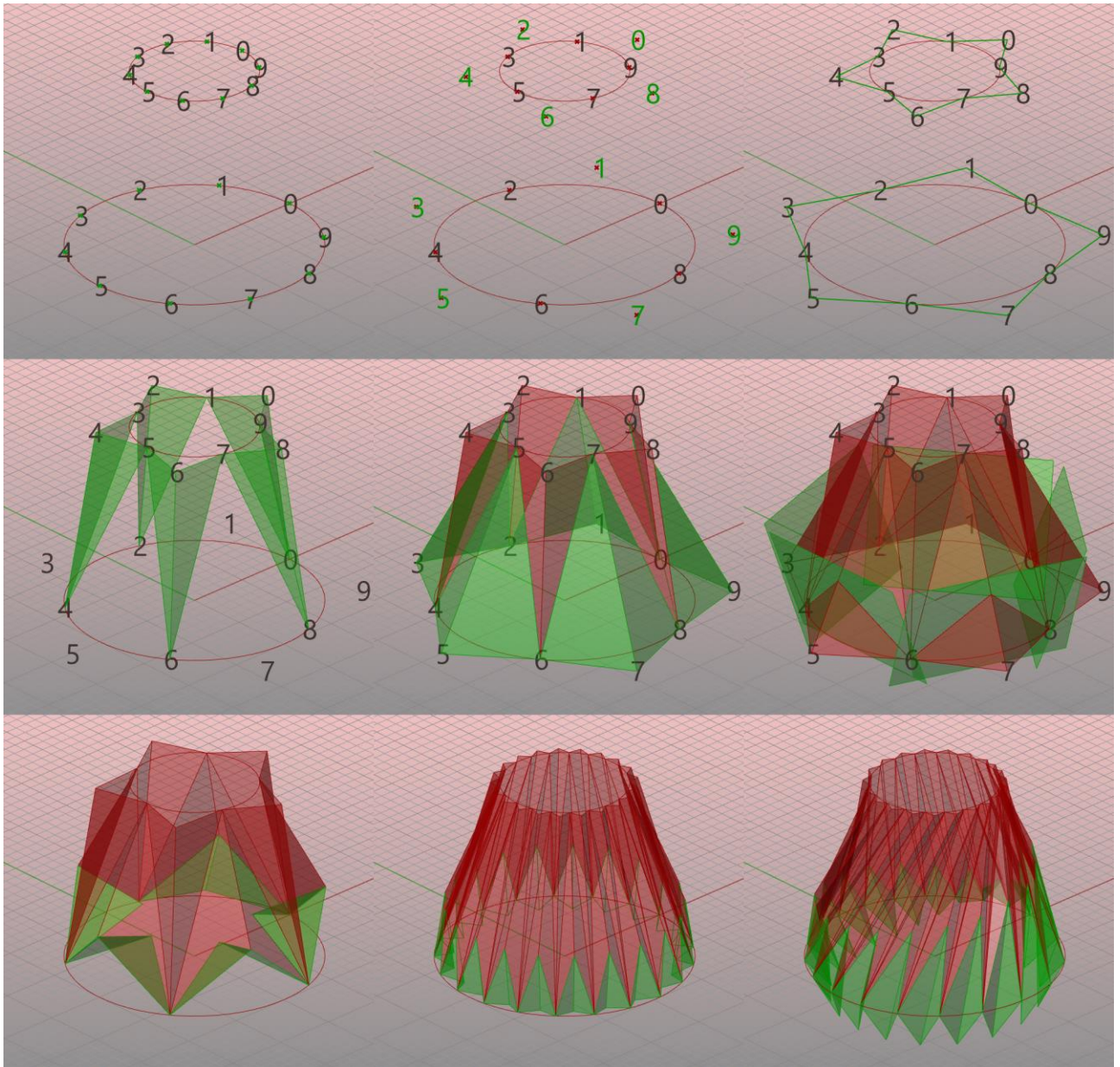


Figure 94: folded lamp shade algorithm, steps.

Refer to Figure 94. First, draw two concentric circles on the same plane, then move on the Z axis one of the two circles⁷³. Draw an equal number of equally spaced points on the two circles. Take the even points of the upper circle and move them away from the circle along the radii directions. Do the same thing with the odd points of the bottom circle. Connect the points of the upper circle to make a zig-zag-shaped closed polyline. Do the same thing with the bottom points. Select the two segments adjacent to each even point of the upper polyline and extrude them to the relative even point of the bottom polyline making triangular faces. Do the same thing with the bottom polyline but using the odd points. With this method, we constructed a “ $1 \times n$ ” chain of triangular faces that is guaranteed to be a developable surface because the triangles are always planar. Thus, starting from this developable surface, to push even further the research of an appealing shape, we reflect the bottom points inside with planes passing from pairs of even points and a third point, not on the horizontal plane. Now the algorithm is ready, and we can play with the inputs to explore different shapes. We can add more faces, or change the angle of the reflection planes, or even rotate independently the upper and bottom circles to get a twisted look⁷⁴. It is also possible to add variation to the design by adding “Graph Mappers” nodes as shown in section

⁷³ The radii are given, and they are equal the radii of the circles of the reference structure

⁷⁴ Be careful to not twist it too much, it may causes self-intersections.

4.5.3 to distribute non-uniformly distances, lengths and angles. In the example shown in Figure 95 we reported two examples of possible shapes that can be obtained with this approach. The full definition is shown in Appendix C.1.

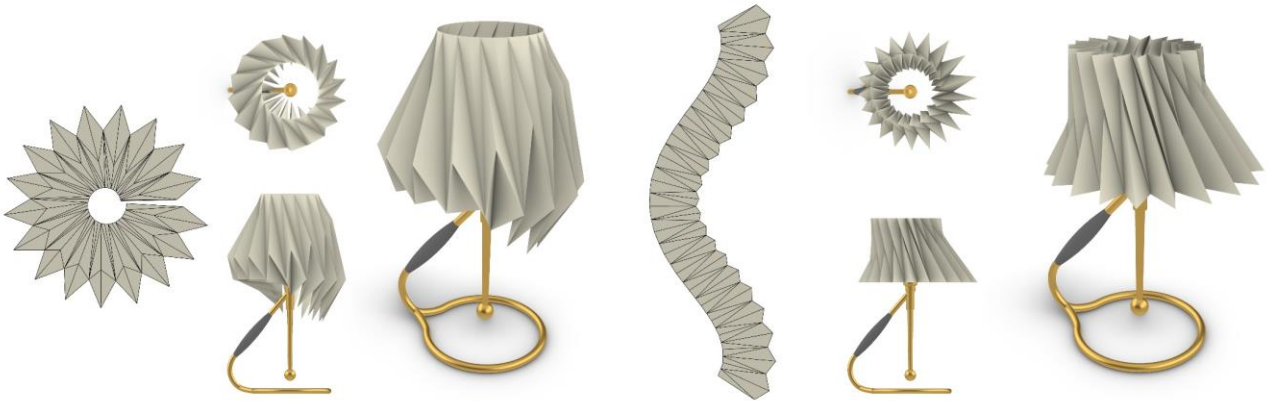


Figure 95: two possible solutions of lampshades for the same support structure, achieved with the same algorithm.

The last thing to do to be able to fabricate this lamp cover is to develop on a plane the folded surface and check if there are no overlapping parts on the unfolded pattern. If some parts are overlapping, we can either split the pattern into different parts and assemble them later, or we can change a bit the design, for example lowering the number of points or shortening the moving distances of the points, to be able to get a CP which does not overlap.

5.2. Folded Facade – Vertices Extrusion from Reference Curved Rails



Figure 96: Biomedical Research Center by Vaillo & Irigaray Architects.

The same technique used for the lampshade can be used to design any other geometry that uses triangulated accordions placed on support rails, like the façade of the Biomedical Research Center by Vaillo & Irigaray Architects (Figure 96). In this section we show a variation of the project by Vaillo and Irigaray, using curved support rails instead of straight ones. In this case, the property of being developable is probably not crucial for construction purposes due to the bigger dimensions, but it may be useful for decreasing the waste and trims from the production phase. The algorithm has the same structure of the algorithm shown in section 5.1, but we add variation by drawing additional reference curve rails instead of using “Graph Mapper” nodes.

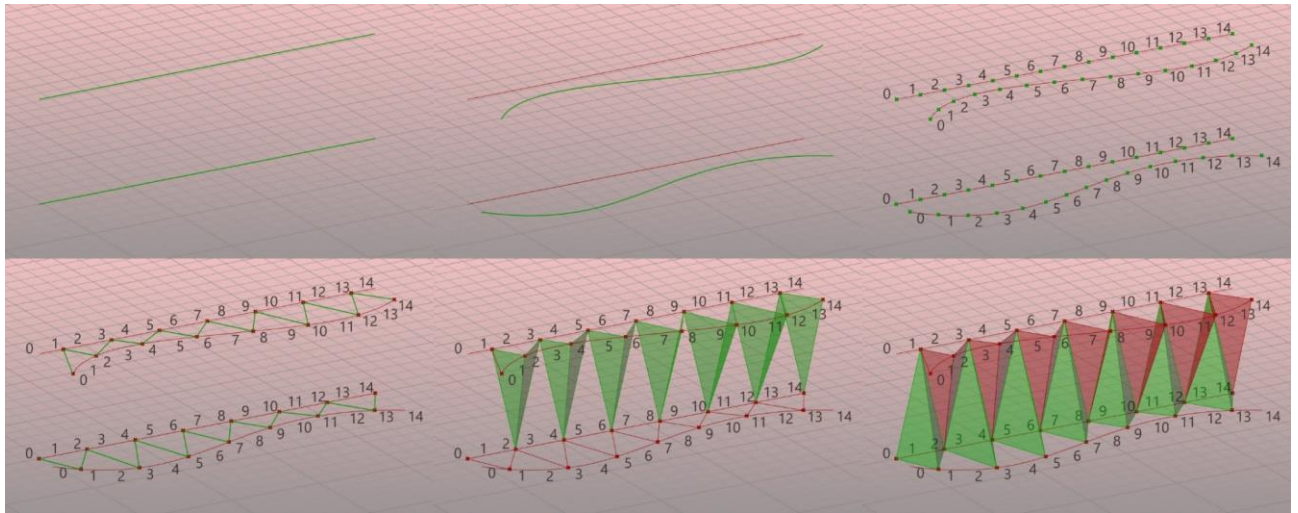


Figure 97: folded triangulated façade algorithm, steps.

Refer to Figure 97. Draw one straight line, copy it and move it along the Z axis. Draw two freeform curves close to the straight lines. Divide the curves into an equal number of pieces. Connect the even points of the bottom freeform curve with the odd points of the relative closest straight line. Do the same thing with the upper points but with inverted even/odd assignment. Explode the upper polyline in independent segments and split the list of segments into sub-lists with two elements each. Extrude each pair of segments to the relative closest even point of the bottom straight line. Do the same thing with the bottom segments. As well as the algorithm shown in 5.1, this algorithm generates a developable “1 × n” chain of triangular faces. The developability is guaranteed by the fact that the triangles are always planar and there are not internal vertices in the CP. The full generative algorithm is shown in Appendix C.2. In Figure 98 it is shown a possible application where many folded patches are anchored to a generic building façade.

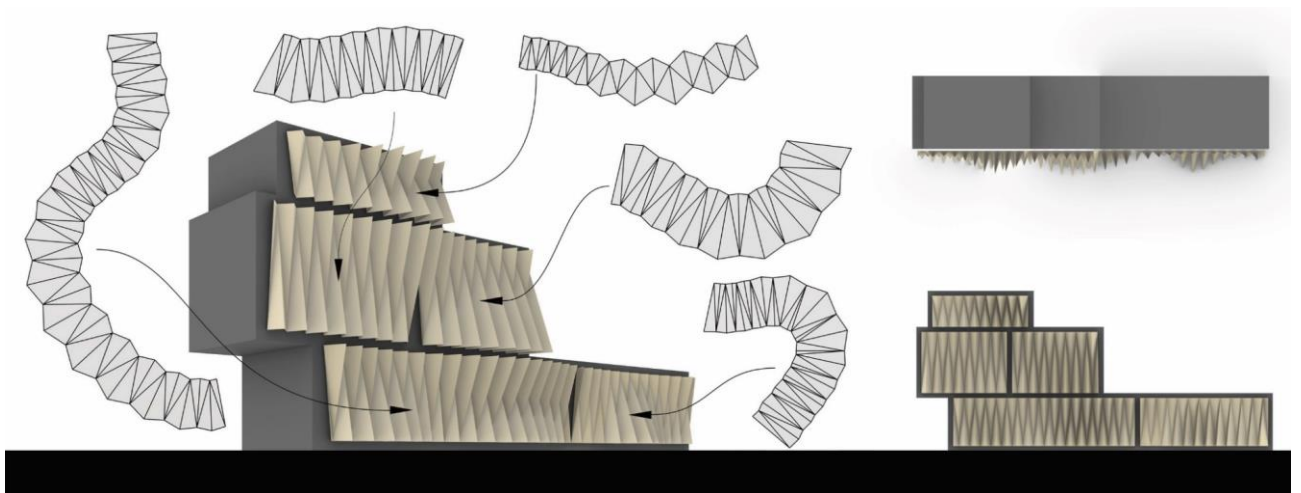


Figure 98: an example of a foldable facade shaped like a triangulated accordion on curved rails.

5.3. Building Envelope – Reflection of a Creased Developable Surface



Figure 99: temporary chapel for the Deaconesses of St-Loup, Localarchitecture + Danilo Mondada.

The project by Localarchitecture and Danilo Mondada of the temporary chapel for the Deaconesses in Saint-Loup is one beautiful example of architecture designed with origami rules. In this case, it has been used the reflection method⁷⁵ (Mitani & Igarashi, 2011) as a tool for the shape-finding phase (Buri & Weinand, 2008). In this case, from a structural point of view, the developability property may even have a negative impact because being developable entails the fact that it may tend to slide until it lies on a plane, which is not desirable for a structure that must be self-supporting. However, with properly designed anchor points this factor may have no relevance at all. Nevertheless, developability may play an important role in the manufacturing process. For example, for a wood and hinges structure, the panels might be assembled on the ground and lifted up all at once in a single motion limiting the need of scaffoldings and cranes; or if built in concrete, the panels may be pre-casted in situ, placing them one next to each other, without empty spaces between them, with minimal shuttering, minimal soil occupation, and minimal costs of transportation.

In this section we explore an approach to design this inspiring and versatile shape proposed by Buri and Weinand, starting from a polyline path and a section profile.

Refer to Figure 100. Draw a polyline with the first point on 0 on the XZ plane (this will be the path). Draw a polyline with the first point on 0 on the XY plane (this will be the profile). Build the first reflection plane on the first kink point of the path, its normal vector is directed like the bisector of the angle between the first two segments of the path. Now project the profile points to the reflection plane along the direction of the first segment of the path, and draw a new polyline passing through them. Now perform a straight loft with the first profile and the projected profile as sections. The first section of the folded surface is built, and it is an accordion with parallel creases. To build the restart sections we need to repeat this process on all the other segments of the path. To do so, we need to exclude the first segment of the path and switch the original profile with the new projected profile and apply the same algorithm over and over until all the segments of the path are processed. To perform this kind of looping definitions in grasshopper, we need to use the Anemone plug-in that we already introduced in section 4.5.5.

The algorithm explained above fails when it reaches the last segment because there is not a subsequent segment to calculate the bisector, thus, to solve this problem, when only one segment remains, the projection plane can either be set as the plane perpendicular to the last segment or as the XY plane⁷⁶. We solved the selection of the correct plane only for the last segment as follows. Every time the algorithm repeats, it erases the first segment of the path, when only one segment remains it returns “True”. “True” in Grasshopper can also be interpreted as a 1, and False as a 0, 1 and 0 are also the indices of the list containing the two planes, if the algorithm returns “True” use the XY plane, if it is “False” build the plane perpendicular to the bisector of two consecutive segments. The full algorithm is shown in Appendix C.3.

⁷⁵ We have shown an example of application of the reflection method in 4.6.1

⁷⁶ In this case we chose the latter solution, where the projection plane is set to be the XY plane, so that the folded surface will lay on a planar surface.

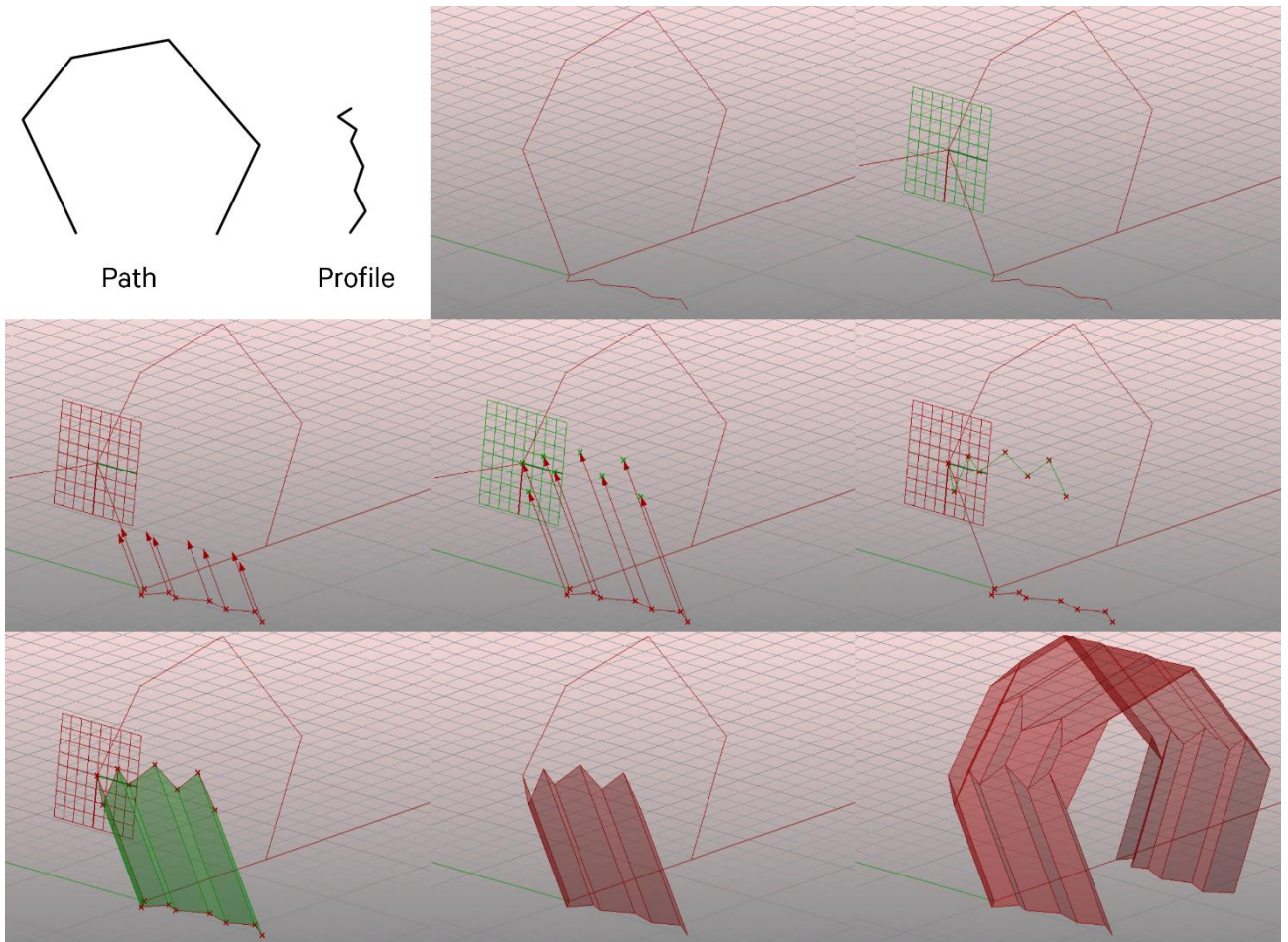


Figure 100: folded roof by reflection, steps of the algorithm.

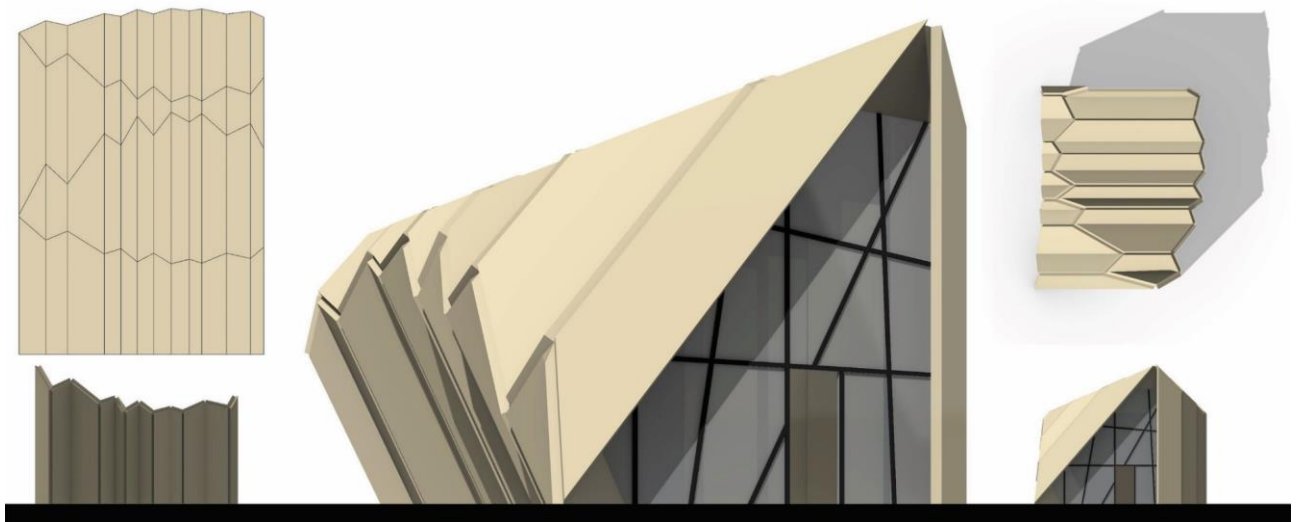


Figure 101: building envelope example shaped like a reflected accordion.⁷⁷

⁷⁷ In this figure we also thickened the folded surface, the method is quite straight forward in this case because there are no folds that hit 180°. Thus, we simply extruded the faces to the outside and we tapered the panels in correspondence of the valley creases, with an angle equal to half the fold angle of that specific crease. For an in-depth study about the thickening of origami, refer to section 6.1.

5.4. Curve-Folded Table

5.4.1. Reflection of a Developable Curved Surface



Figure 102: rigid foldable table by Tomohiro Tachi.

The reflection method shown in section 5.3 is not only valid to make reverse folds starting from folded surfaces with linear creases, but it can also be used to reverse fold generic developable ruled surfaces (Mitani & Igarashi, 2011) generating curved creases. For example, we can use the reflection method to design a curved folded table similar to the one designed by Tachi (shown in Figure 102) applying the method shown in Figure 103.

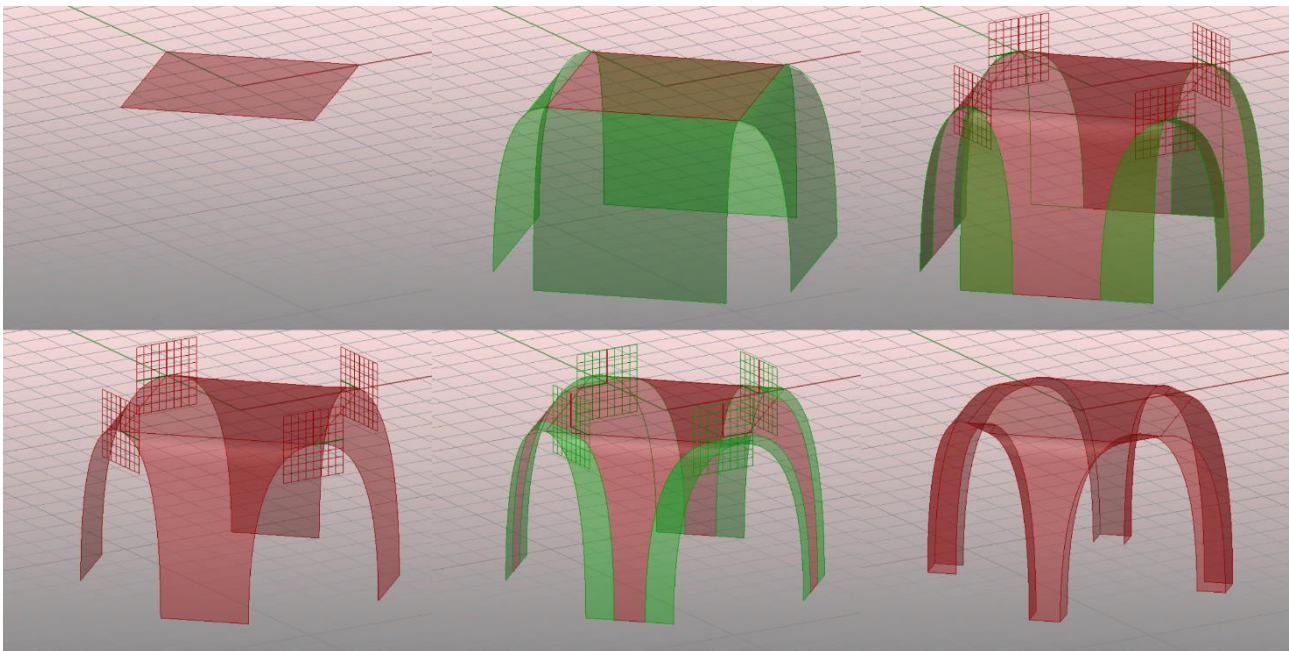


Figure 103: curve-folded table algorithm, steps.

The method works as follows. Draw a planar horizontal polygon (a square in this case). Extrude the edges along curved paths tangent to the surface⁷⁸. Draw vertical planes with origins coincident to the vertices of the polygon and rotate them around their relative Z axes to make them intersect both the adjacent surfaces (the planes are perpendicular to the relative angle bisector in this case). Split the poly-surface and erase the outer split as shown in the figure. Move the planes along their local Z-axis to make them intersect the horizontal polygon and the four curved legs. Then, split

⁷⁸ To easily draw a curved extrusion path that is tangent to the horizontal surface it is sufficient to draw a curve placing the first two or more control points on the horizontal plane.

the polysurface again with the planes paying attention to not intersect the curved sections. Mirror the outer splits with respect of the relative splitting plane, so that we obtained a developable surface with curved creases. As we show in Figure 104, we can achieve different results by changing the number of sides, the shape of the initial polygon or the orientation of the reflection planes. The full definition is shown in Appendix C.4.

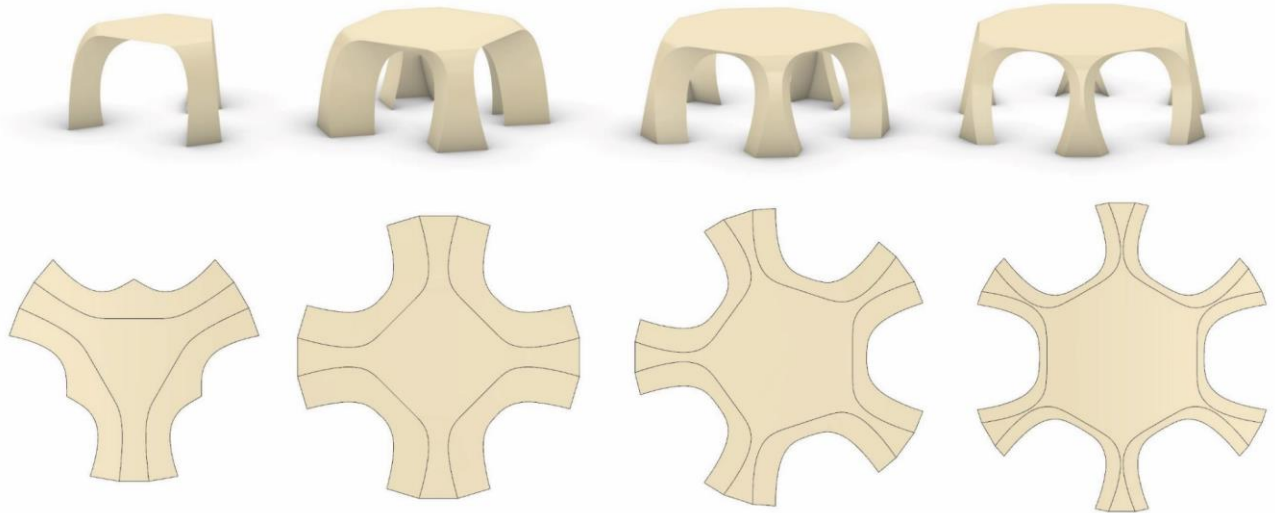


Figure 104: curve-folded table variations and unrolled CPs.

5.4.2. Discretization of the Curved Crease

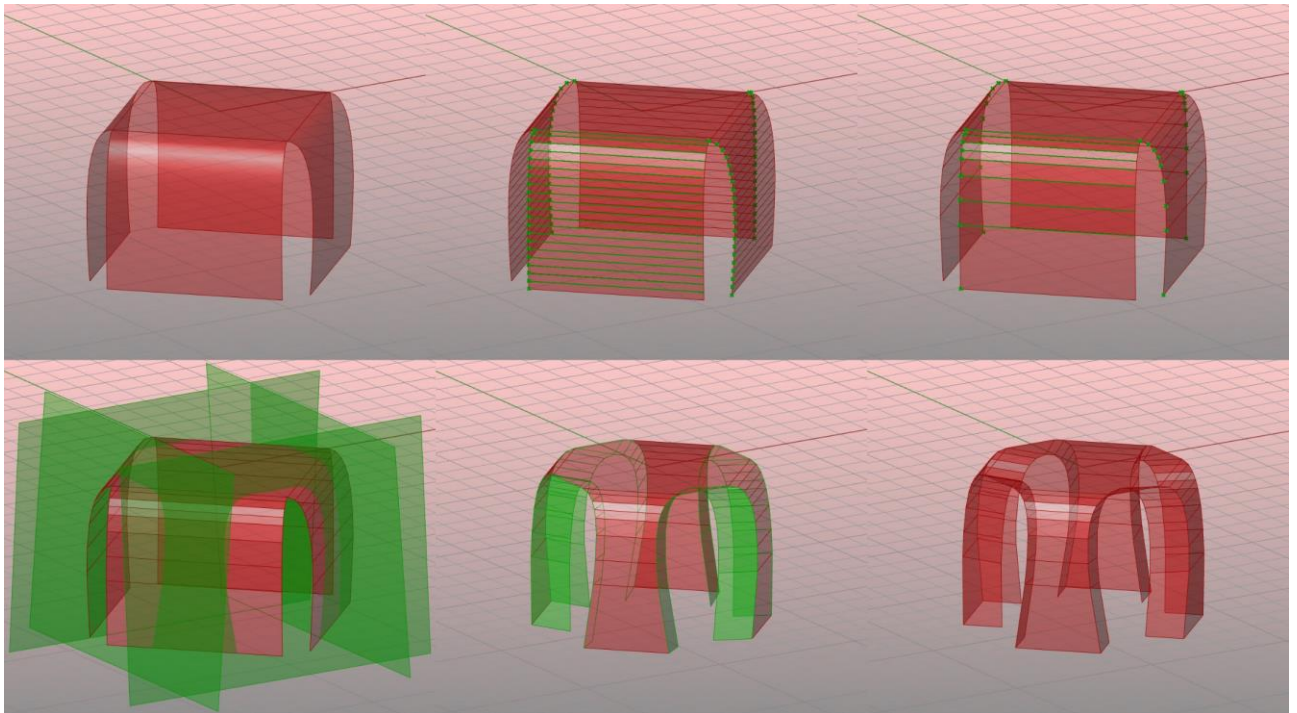


Figure 105: discretization of a curve-folded table.

The pattern that we obtained could already be used as a cutting template to be fed to a CNC machine that would return a pre-creased thin sheet of metal ready to be folded. However, folded metal has a limited number of folding cycles, thus, to make a kinetic deployable table this might not be the optimal solution. An alternative solution, more suitable for making moving mechanisms, might be the discretization of the curved surface into planar quadrangular faces. In general, the discretization of a curved folded surface into planar faces is not an easy problem to solve. However, it becomes very easy if we generate the curve fold by reflecting a developable cylinder or cone. This is because in general, in a developable surface, two consecutive linear generatrices do not always lie on the same plane unless they are infinitesimally spaced.

Cylinders and cones however are special cases where all the consecutive generatrices lie on the same plane regardless of the distance between them. This means that we can simply convert the curved surfaces that we already used in the previous algorithm into a discretized polysurface where all the faces are planar and quadrangular, and we can reflect it with the same planes of reflection. We started from the same algorithm presented in the last section and we implemented it as follows.

Refer to Figure 105. Draw a developable polysurface shaped like a table as we did in section 5.4.1. Extract the lateral boundary curve of each leg and divide it into a certain number of parts. We want to add more points where the curvature is high. There are many approaches to solve this problem, because we do not need to have a perfect relation between the position of points and the curvature, we can use the following workaround. Create a very dense polyline that approximate the curve and reduce it with the “Reduce polyline” component⁷⁹. After that extrude the polyline to generate a polysurface that approximates the initial curved surface. The polysurface so generated is a developable surface made by planar rectangular faces, thus we can use the reflection method as we did in the previous section. In figure 106 we show the correct unfolding of the discretized pattern

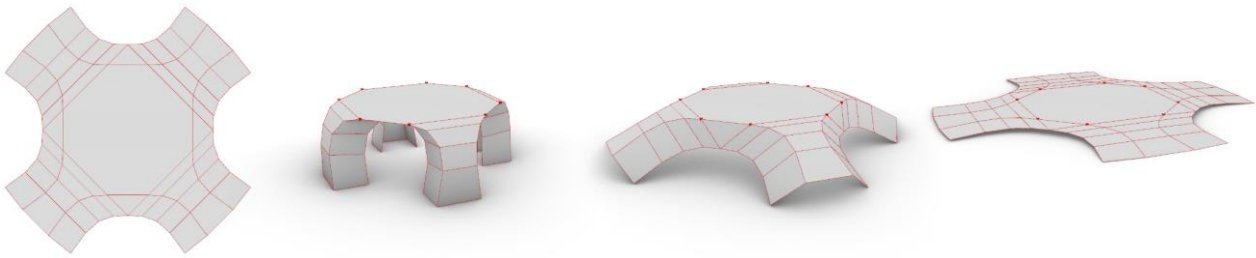


Figure 106: unfolding of the discretized curve-folded table, which is only made by planar quadrangular faces.

5.5. Conformable Corrugated Suspended Ceiling⁸⁰



Figure 107: Tessel by David Letellier and Lab[au] on the left, and Resonant chamber by RVTR on the right.

The installations “Tessel” by David Letellier and Lab[au] and “Resonant chamber” by RVTR, are two perfect examples of sculptures in form of suspended ceilings that make use of a folded corrugated surface as a tool to create interesting shapes and movements. Both installations are kinetic sculptures that change their shape interacting with the perception of sound in a certain space. The first one, “Tessel”, is programmed to react to the sound and “dancing” with it. The aim of this sculpture is “...combining influences that question the link between geometry, movement and chaos, thus continuing the quest for beauty in the synesthetic perception of sound and spatial phenomena.” (Letellier, 2010). Perceptively it creates a beautiful visual and acoustic effect that is similar to the behaviour of an almost living creature.

⁷⁹ This component compare the angles between the segments adjacent to each point and according to a certain tolerance keeps or erase the point.

⁸⁰ This section is excerpts from the paper “Conformation of a flexible Miura pattern on a double curvature surface” written by the author of this thesis. The paper has been presented at the AFGS 2017 (the 11th Asian forum On Graphic Science). The meeting took place in Tokyo between 6th and 10th August 2017. The paper is part of the results of the research carried out during the PhD course (Foschi, 2017).

The second project, “Resonant chamber”, has a more sophisticated behaviour and connects a beautiful geometric and enigmatic appearance to the practical need of acoustic optimization. It also combines the principles of rigid origami and dynamic, spatial, material and electro-acoustic technologies (Furuto, 2012). The intention of this project is creating a continuous surface that changes automatically according to the sound conditions to influence its perception in the environment where it is placed, one of the possible application fields pointed out by the designers is a theatre or any other place with a variable audience, where the acoustic conditions are very important and they may vary in relation to the distribution and number of the spectators.

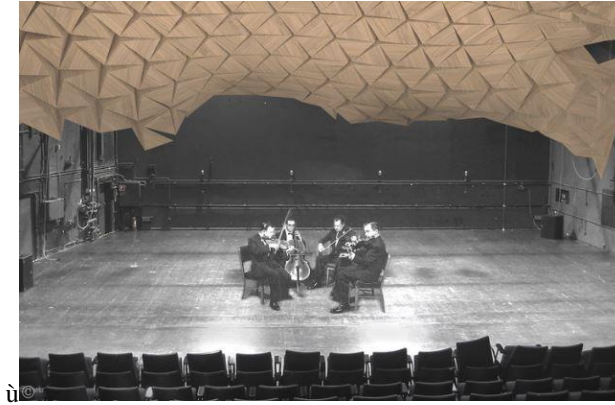


Figure 108: Resonant chamber, example of a possible use (source: www.arch2o.com).

Some of the most obvious challenges that the designers of these sculpture had to face were how to control the motion of these surfaces; and how to hang them with an optimized number of cables. First of all, they have chosen patterns with more than one single DOF, to be able to increase the shaping possibilities, then they connected motors to the hinges, or they used retractile cables to be able to change the shape of the surface dynamically. In this section we are going to explore this type of concept through parametric design, to be able to conform the shape as a given reference surface and to optimize the number of necessary cables to keep the shape in position once hanged.

5.5.1. Conformation of a Rigid Creased Surface to a Curved Surface

First of all, we focus on the shaping of the corrugation. The aim of the following method is to change the shape of a given creased rigid surface conforming it to a given curved surface without changing the pattern. To do so we are going to use Kangaroo Physics (Piker, n.d.), the plug-in for Grasshopper we already introduced in 4.8, where it has been used to animate the folding and unfolding of degree > 4 CPs. Contrary to what we did in 4.8, this time we are not going to set mountain/valley assignment, because we are more concerned about the global shape of the corrugation.

First of all, draw a planar surface. Then, draw the creases, split the surface with them, generating a polysurface, and convert the polysurface into a mesh. In this case, we draw the creases to generate only triangular faces. Draw a reference curved surface in the proximity of the original surface with similar proportions, this surface will be the attractor surface. Now we need to set up the Kangaroo nodes as shown in Figure 110 in order to move the mesh vertices to the attractor surface along the lines that connects the vertices and their relative closest point on the surface and at the same time preserving the developability of the mesh. To do so, we add a “Length(Line)” and an “OnMesh” goal nodes and connect them to the Kangaroo solver. The “Length(Line)” node constrains the length of the edges of the mesh, and the “OnMesh” node will try to bring the mesh vertices on the surface. Because the Kangaroo solver, once set off, tries to minimize the errors of the goal nodes by weighing them with the strength input of each node, we need to set the strength of the “Length(Line)” node much higher than the strength of the “OnMesh” node in order to prioritize the preservation of the developability of the surface more than the minimization of the distances between attracted points and surface. Like so, when the simulation starts, the mesh vertices start moving toward the surface while keeping their relative distance, thus keeping the faces of the surface rigid. By changing the attractor surface, the corrugation updates its shape trying to conform as better as possible to the new configuration.

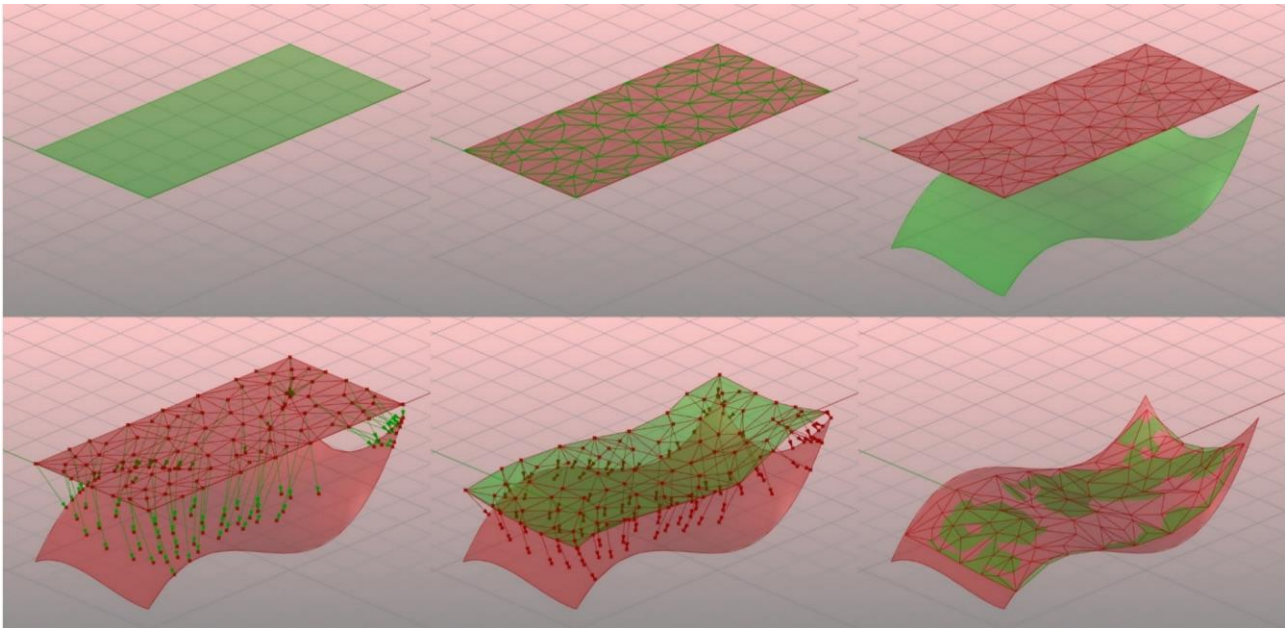


Figure 109: conformation of a corrugation to curved surfaces without changing the CP.

In this case study, we used only triangular faces as in the “Tessel” reference, but what if we wanted to use a CP with quadrangular faces? We know that degree-4 vertices may generate patterns with only one-DOF. Thus, first of all, we need to test if the DOF of the CP is one or more. This is important because if it is one, the surface will not be able to be conformed to a freeform surface, thus a one-DOF pattern would not be suitable for this kind of applications. If it is more than one and we want to keep the quadrangular faces planar we need to add a “CoPlanar” node⁸¹ setting as input every vertex relative to each face of the mesh so that the faces will remain planar. Also, we will need to triangulate the mesh before setting it as input for the “Length(Line)” node, as shown in Appendix C.5.1. Constraining the diagonals lengths and keeping the boundaries of the quadrangular faces planar we guarantee the preservation of the developability and rigidity of the faces.

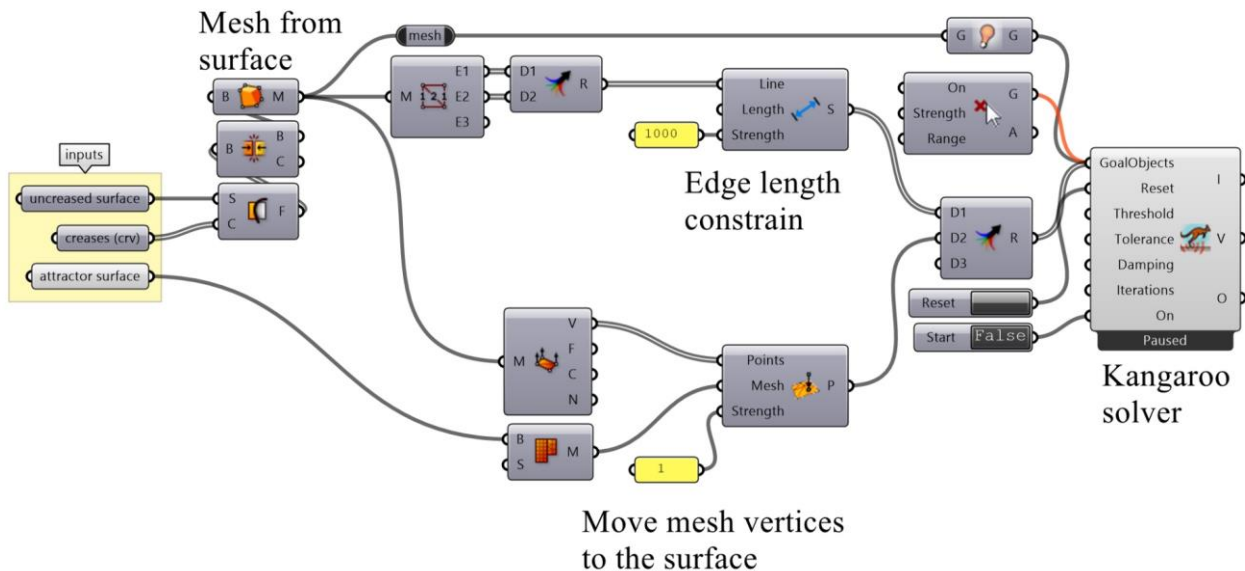


Figure 110: generative algorithm of the conformation of a corrugation to a curved surface using Kangaroo.

⁸¹ The “CoPlanar” node must have a high strength as the “Length(Line)” node.

5.5.2. Conformation of a Flexible Miura-Ori to a Curved Surface

Not only an unfolded pre-creased pattern can be conformed to curved surfaces, but also semi-pre-folded patterns. With semi-pre-folded pattern, however, we cannot make all the vertices of the mesh being attracted from the surface, because otherwise, the corrugation would flatten out completely, losing the mountain/valley assignment, trying to conform as best as it can to the curved surface. In the case of the Miura-ori, shown in Figure 111, the vertices that are attracted from the surface are all the bottom vertices. Furthermore, the Miura-ori is a pattern with one single DOF, thus we had to triangulate all the faces to increase the DOF allowing non-uniform out-of-plane deformations of the global shape. We treated the diagonals as loose hinges as all the other creases. However, we can also simulate a flexible behaviour of the Miura-ori by adding a rotational stiffness to the faces adjacent to the diagonals. We can do that by adding a “Hinge” node that tries to keep the dihedral angles between the triangles divided by the diagonal equal to 180° . Thus, the quadrangular faces would have a more or less flexible behaviour according to the “Strength” value set to be very high for a stiffer behaviour, or low for a more flexible behaviour. We also added a “SphereCollide” node among the goal nodes, to avoid collisions between faces. See the complete generative algorithm in Appendix C.5.2.

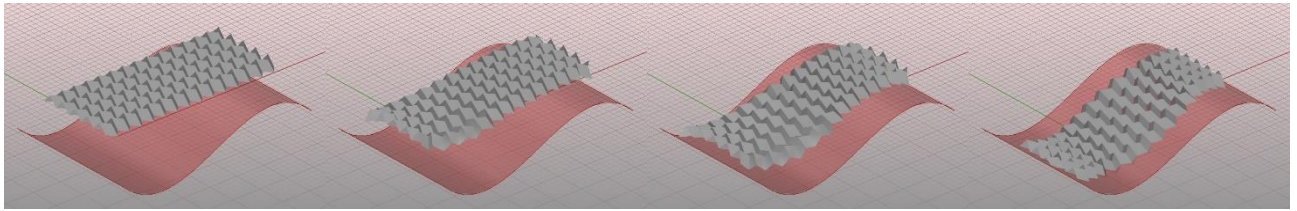


Figure 111: conformation simulation keyframes.

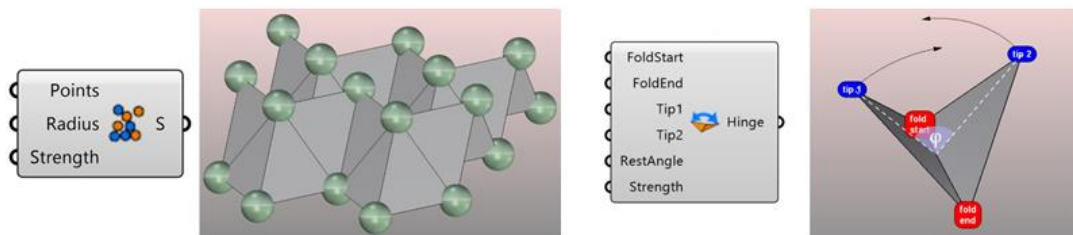


Figure 112: “SphereCollide” node that avoids collisions between mesh faces; and “Hinge” used to control the flexibility of the Miura-ori.

Most of the origami pattern cannot be conformed to any curved surface. The accuracy of the conformation depends on the pattern itself or from its scale in relation to the local curvature of the attractor surface. For example, in Figure 113 the triangulated Miura-ori pattern is conformed to the same cylindrical surface with different results according to the different orientation of the pattern in relation to the surface. In the first case, the Miura ori conforms better than in the second case. The average distance between the attracted points and the surface in the former is approximately ten times smaller than the one in the latter. The average distance between the attracted points and the surface is an important factor that contributes evaluating the quality of the conformation, but most of the times not every section of the corrugation conforms equally to the surface, so how can we visualize better the error distribution?

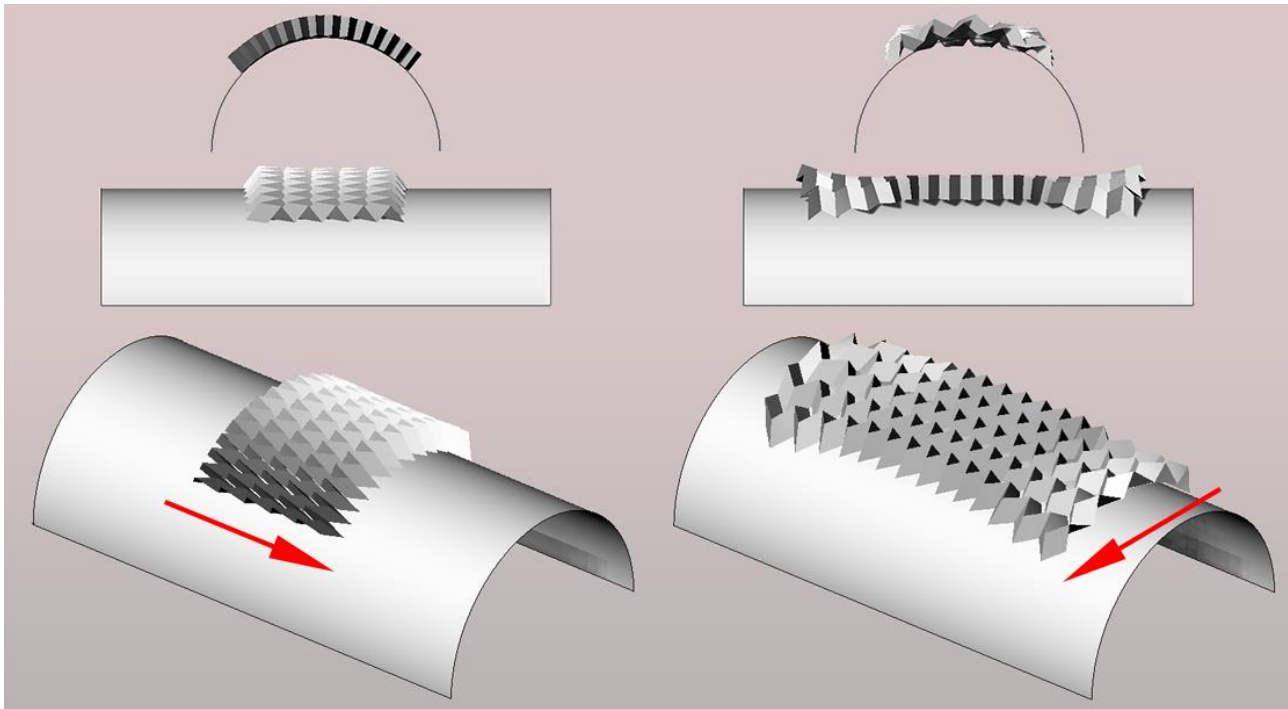


Figure 113: different results due to the different orientation of the pattern compared to the attractor surface.

To visualize better the error distribution we applied a gradient texture map on the surface coloured in grey scale that colours with black the areas of the surface close to the projection of the most distant points from the negative side of the surface, with white the areas close to the projection of the most distant points from the positive side of the surface and with grey the areas close to the projections of the most accurate points, as shown in Figure 115. In Figure 114 it is shown the generative algorithm to colour a surface with Grasshopper on the left, and the histogram of the error distribution of the configuration shown in Figure 115 on the right.

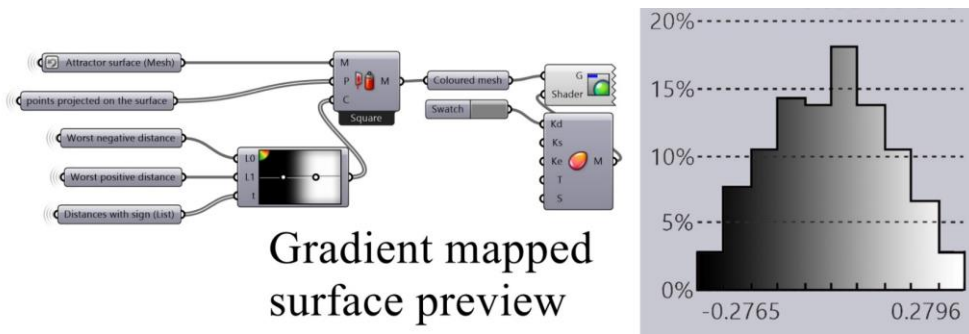


Figure 114: gradient error map, generative algorithm, and the histogram of the error distribution.

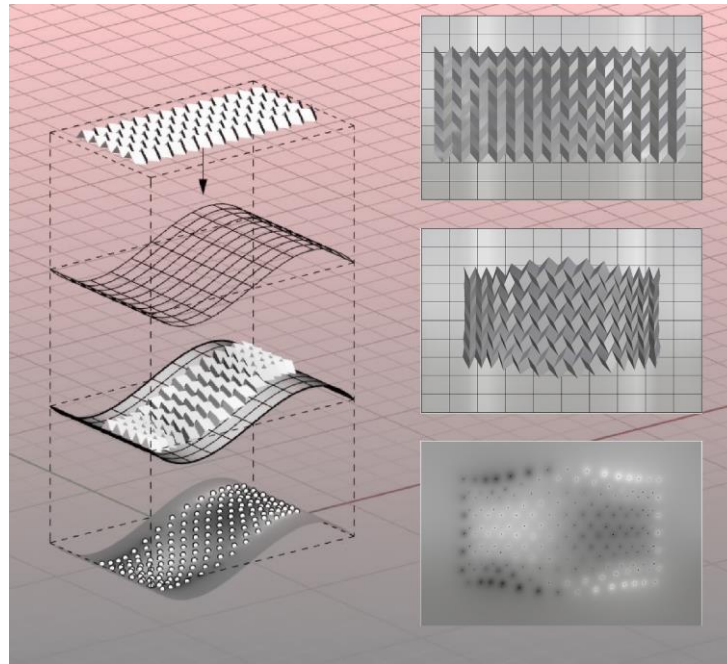


Figure 115: gradient error map on a single curvature curved surface. Axonometric and top view.

5.5.3. Optimization of Supporting Cables and Anchor Points

The most trivial way of hanging a corrugated surface while keeping its shape perfectly is by anchoring all the vertices of the mesh, attaching them to wires with specific lengths. The lengths are given by the distances of the vertices themselves and their relative projected points on the ceiling. Because the force of gravity pulls the vertices vertically, they try to move downward, but because all the loads are absorbed entirely by the wires, the system is balanced and there is no residual movement. However, for complex tessellations and corrugations hanging hundreds of vertices may be not optimal in the real world. However, most of the corrugations built with loose hinges are impossible to hang with fewer cables than vertices, while keeping perfectly their shape, thus we need to choose either if anchoring all vertices, or if partially lose the initial shape. This is true for corrugations with faces built for example with wood attached with hinges, but it is not necessarily true for corrugations folded for example with cardboard. Usually, a continuous material creased does not have a loose behaviour, because the creases still have some sort of stiffness, thus we can exploit that stiffness to lower the number of anchor points while preserving their global shape. Furthermore, some corrugations have a lower number of DOF and they behave more rigidly than others. Therefore, we need to analyse case by case to be able to find the optimal solution. In the digital world is very hard to make a physically accurate simulation of a creased sheet made by a continuous material, because in the real world a crease correspond to a plastic deformation, thus the stresses and the internal forces are hard to foreseen and to replicate precisely digitally, because they may be not homogeneous according to how much strength we used while creasing or how many times we folded and unfolded that specific crease. Thus, for those cases where we need to hang a corrugation made by a folded sheet of continuous material, once tested if the conformation is possible with that pattern on a specific curved surface, it is preferred to realize the prototype of the surface with the same material at a similar scale and make tests in the real world. For those cases with loose hinges, however, we can simulate their behaviour more easily.

In this section, we are going to test some specific set of anchor points on a conformed Miura-ori by adding the force of gravity to our digital environment⁸². The algorithm that we used to add the wires and to test the equilibrium of the system with the force of gravity is shown in Appendix C.5.3 and it works as follows.

First, set up the standard nodes of Kangaroo as shown in previous sections. Among the standard goal nodes used to preserve the developability of the corrugation, add another “Length(Line)” node for the wires with a lower strength compared to the “Length(Line)” node used for the Miura-ori edges. Then, add a “Load” node which pulls the assigned vertices along an assigned vector (we assigned a vector directed as the Z-axis with an amplitude of -1, and we set as input

⁸² The results we found are specific for this case study, we may have different solutions for other corrugations or other conformation of the same corrugations.

all the vertices of the Miura-ori). Then project all the Miura-ori vertices to a virtual planar ceiling, placed above the conformed Miura-ori, and anchor those points in place adding an “Anchor” goal node.

By setting off the Kangaroo solver now, we would not see any change into the system, because all the vertices are anchored, and all the forces are balanced, thus we need first to decrease the number of wires to see some changes. Decrease the number of wires by culling some vertices among the list of vertices that are projected to the ceiling plane, while doing that try to find a set of vertices that, once attached to the wires and hanged, preserves the global shape of the corrugation without making it collapse. After tested many sets of vertices, we found out that anchoring the first ring of vertices of the Miura-ori is not sufficient to keep the global shape, however, anchoring the second ring of vertices is sufficient to find an equilibrium state which is very close to the initial configuration as shown in Figure 116. In the figure we set the Miura-ori to have loose hinges, in fact even if the global shape is preserved while anchoring the second ring of vertices, the outer vertices sometimes collapse, it is particularly evident for the vertices of the outer left border. In the algorithm in Appendix C.5.3, we show how to anchor both the first and the second rings of vertices to enhance the stability of the system even with completely loose hinges.

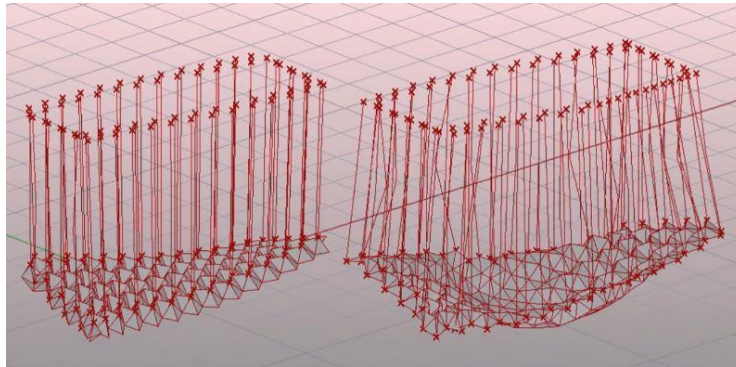


Figure 116: gravity simulations comparison of a conformed Miura-ori with different patterns of anchored vertices. On the left we anchored the upper ring of external vertices and the system is in an equilibrium state, on the right we anchored the bottom ring of external vertices and the system collapse.

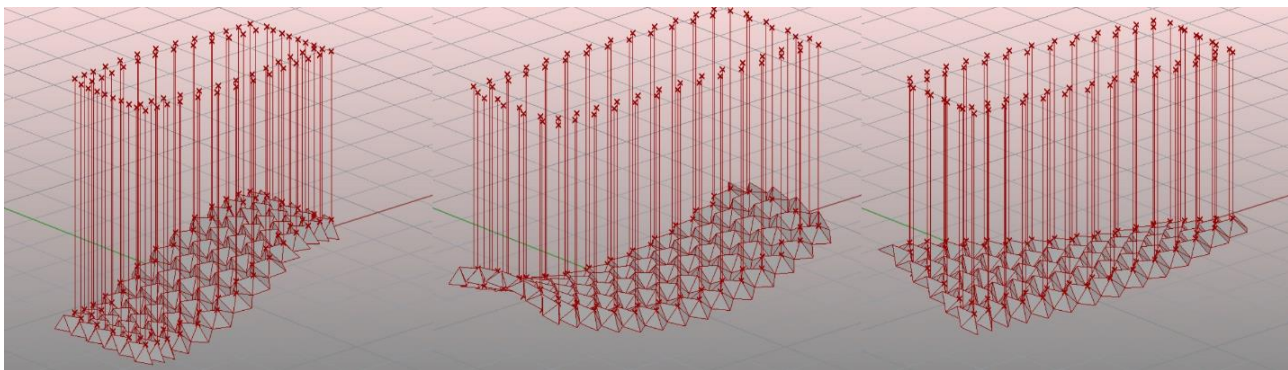


Figure 117: anchoring the second ring of vertices to find an equilibrium state once applied the force of gravity.

In Figure 117 contrariwise we added a little bit of reciprocal rotational stiffness to the faces adjacent to the diagonals, simulating a behaviour qualitatively similar to a flexible Miura-ori folded with paper, and as you can see only by anchoring the second ring of vertices the global shape is almost perfectly preserved in all the cases we tested.

Because we added some reciprocal rotational stiffness to the faces simulating a behaviour similar to a sheet of paper, anchoring the second ring of vertices entirely is probably an over-kill. Thus, the next question is how can we find a more optimized solution without necessarily guessing a better set of anchored vertices? To optimize even more the vertices without guessing, we propose a method that compares the lengths of the wires before and after applying gravity, so that we can identify the wires that are completely or almost completely unloaded and exclude them. Because the lengths of the cables are constrained with a “Line(length)” node also known as “spring” node, they behave exactly like springs. This means that they obey the relationship:

$$F = kx . \quad (38)$$

Where F is the Force, k is the stiffness and x is the extension (or Δ length). Thus, Δ length and tension are proportional. Therefore, we can use the length variation to apply a colour to the wires and visualize qualitatively the tension applied to each cable using the standard gradient map for tensions that goes from green to yellow to red as shown in Figure 118.

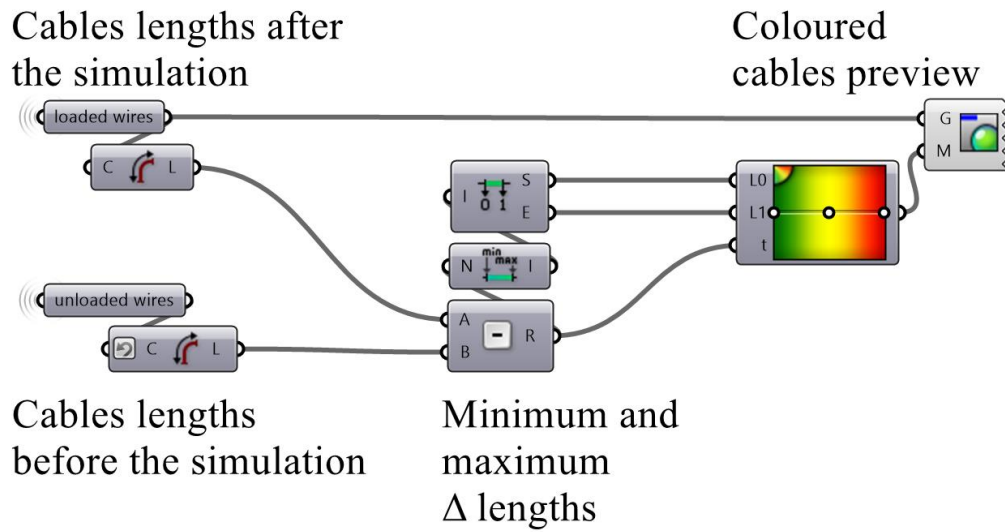


Figure 118: generative algorithm for colouring cables from green to red according to their load and deformation.

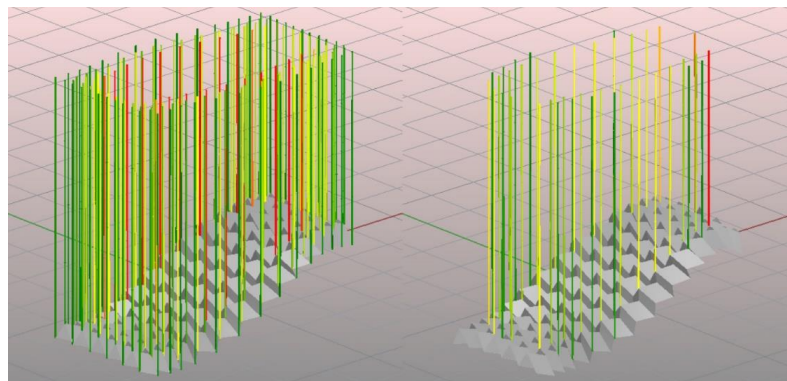


Figure 119: optimization of the cables through tension analysis.

After erasing unloaded (or almost unloaded) wires we can run the simulation again and check if the corrugation keeps its shape as shown in and Figure 119. If we try to apply this method before erasing some cables by guessing we would not have found any unloaded cable, thus it may not work properly. Furthermore, in some corrugations even erasing a single wire would change its shape greatly, thus every case must be analysed specifically.

5.5.4. Changing shape to the Surface - Adjusting Cables Lengths

In section 5.5.1 and 5.5.2 we show how to conform a creased surface to a curved reference surface and in section 5.5.3 we show how to hang it with wires. In this section, we are going to propose a reversed approach, that starts from a hanged un-conformed surface that we conform changing the lengths of the cables.

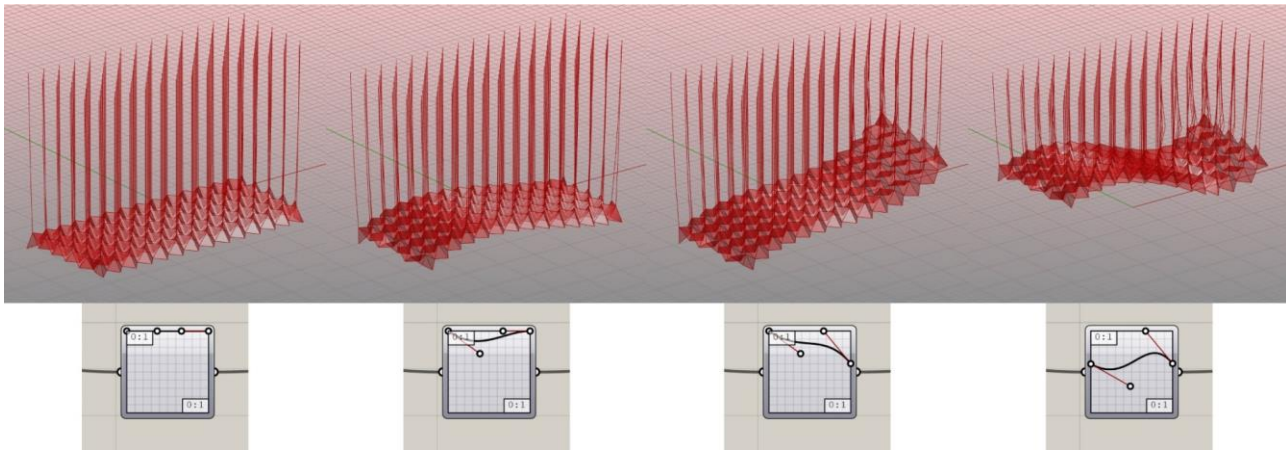


Figure 120: moving the surface changing cables lengths using a “Graph Mapper” node.

In Figure 120 we show how a semi-pre-creased Miura-ori can be shaped by using the “Graph Mapper” node. The full generative algorithm can be consulted in Appendix C.5.4 and it works as follows.

Import the semi-pre-creased Miura-ori as a mesh. Extract all the vertices of the mesh, sort the list of vertices according to their z position and select all the upper vertices. Project the vertices on a plane placed above the corrugation. Connect with a line the upper vertices and their relative projection. Rescale the lines using as base points the relative projected points. To rescale the wires gradually and following the shape of a function, use a “Graph Mapper” node. Then set up the Kangaroo nodes like explained in section 5.5.3 adding “Anchor”, “Load” and “Length(Line)” goal nodes attached to the Kangaroo “Bouncy Solver”. Before setting off the simulation set a Bezier function in the “Graph Mapper” and move all the control points on the top to make it shaped like a constant function $y=1$ so that the wires as the simulation begins are non-scaled. After setting off the simulation change the function shape in the “Graph Mapper” moving the control points of the Bezier curve. As the points are moved, the wire length changes and the corrugation while being pulled down by the force of gravity and pulled up by the cables, finds a new equilibrium state changing its shape according to the cables lengths.

5.6. References – CHAPTER V

Buri, H., & Weinand, Y. (2008). ORIGAMI-folded plate structures, architecture. *10th World Conference on Timber Engineering*, 2–5.

Foschi, R. (2017). Conformation of a Flexible Miura Pattern on a Double Curvature Surface. *Proceedings of the 11th Asian Forum on Graphic Science AFGS2017, (USB)*, 1–10.

Furuto, A. (2012). Resonant Chamber / rvtr. Accessed December 29, 2018 from <https://www.archdaily.com/227233/resonant-chamber-rvtr>

Le Klint, P. V. J. (n.d.). The story of LE KLINT. Accessed July 19, 2018, from <https://www.leklint.com/en-GB/About-LE-KLINT/History.aspx>

Letellier, D. (2010). Tessel. Accessed November 29, 2018, from <https://www.davidletellier.net/TESEL>

Mitani, J., & Igarashi, T. (2011). Interactive Design of Planar Curved Folding by Reflection. *Pacific Conference on Computer Graphics and Applications - Short Papers*, 77–81. <https://doi.org/10.2312>

Piker, D. (n.d.). Kangaroo Physics. Accessed June 27, 2018, from <https://www.food4rhino.com/app/kangaroo-physics>

Rutten, D. (n.d.). Grasshopper official page. Accessed July 31, 2018, from <http://www.grasshopper3d.com/>

Tedeschi, A. (2014). *AAD Algorithms-Aided Design. Parametric Strategies Using Grasshopper* (First edit.). Brienza (PO): Le Penseur Publisher.

6. CHAPTER VI: Fabrication-Aimed Designs

The case studies that we presented so far were all focused on the creation of patterns aiming to achieve a specific movement or aiming to a specific shape, but we always visualized and studied them through zero-thickness conceptual models. However, in the manufacturing and architecture fields, we may need to produce rigid-foldable mechanisms, or folded structures able to resist to certain loads. Rigid-folding and structural properties are strictly related to the stiffness of the material used, and as a matter of fact, the stiffness of any material is strictly related to its elasticity and to the area of its section (thus to its thickness). Thus, in this section we will study the origami-like mechanisms from another point of view, considering thickness, bending, forces, gravity, stability. In this chapter, we are going to present two case studies: a foldable ladder and a deployable chair. Both projects are originally designed, and we present them from start to finish focusing especially on the fabrication issues and on the possible solutions.

6.1. Known Origami Thickening Methods – State of the Art⁸³

A zero-thickness surface is a good approximation to model an origami-like geometry folded with paper. However, in manufacturing, architecture and engineering, is often necessary to use thick panels to enhance stiffness and rigidity of the folded mechanism. Most of the times the designers start modelling using zero-thickness surfaces, focusing only on the kinematics of the mechanism, but when they get to the prototyping phase, they cannot disregard the thickness. Thus, the problem that they face, is finding a way to add thickness to the zero-thickness surface without losing the original kinematics, preserving the DOF and avoiding self-intersections or collisions between the panels that would stop the folding motion. Many solutions have been already studied, proposed and used by many researchers. The most relevant known techniques are:

- “Offset panels” (Edmondson, Lang, Morgan, Magleby, & Howell, 2015; Lang, Tolman, Crampton, Magleby, & Howell, 2018)
- “Hinge shifting”, also known as “Axis shifting” (Chen, Peng, & You, 2015; Lang et al., 2018; Tachi, 2011b)
- “Tapered panels” (Tachi, 2011b)
- “Constant thickness attached panels” (Tachi, 2011b)
- “Membrane hinges” (Lang et al., 2018; Zirbel et al., 2013)
- “Rolling contacts” or “SORCE technique” (Lang et al. Patent No. US 2017/0219007 A1, 2017; Lang, Nelson, Magleby, & Howell, 2017; Lang et al., 2018)
- “Strained joint” (Lang et al., 2018; Pehrson, Magleby, Lang, & Howell, 2016)
- “Double hinge” (Ku & Demaine, 2016; Lang et al., 2018)
- “Symmetric Miura-ori vertex by shifted hinges and carved panels” (Hoberman, Patent No. 4780344, 1988; Lang, Tolman, Crampton, Magleby, & Howell, 2018; Tachi, 2011b)
- “Slidable Hinges” (Lang et al., 2018; Tachi, 2011b; Trautz & Kunstler, 2009)
- “Double line” (Hull & Tachi, 2017)

⁸³ The study of the thickening methods presented in this chapter was in a large part referenced to the paper “A Review of Thickness-Accommodation Techniques in Origami-Inspired Engineering” by Lang et al. (Lang et al., 2018) and “Considering Manufacturing in the Design of Thick-Panel Origami Mechanisms” by Crampton (Crampton, 2017); we extended the study of these methods and we commented them case by case.

6.1.1. Offset Panels

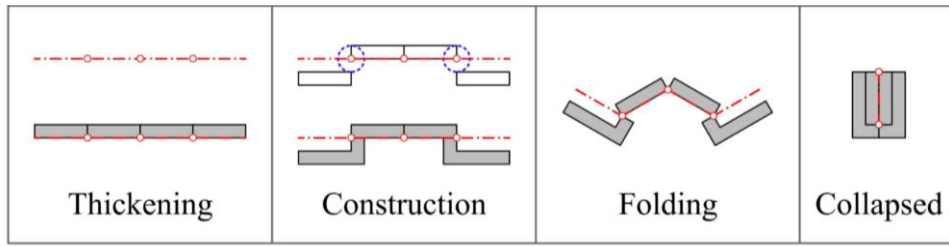


Figure 121: "Offset panels" method.

The "Offset panels" method, theorised by Edmondson et al. (Edmondson et al., 2015), is a versatile method that works with both flat-foldable and non-flat-foldable vertices. It allows the overlap of multiple layers, but it must be necessarily assembled, and the unfolded configuration does not lie on a plane. Furthermore, self-collisions are very common, and they must be checked carefully during the design phase. To avoid self-collisions, it may be necessary to carve out or cuts some parts from the faces, thus the mechanism may present holes which is not optimal for applications that require material continuity. Refer to section 6.2.3 for an example of this technique applied to a deployable ladder.

6.1.2. Hinge Shifting

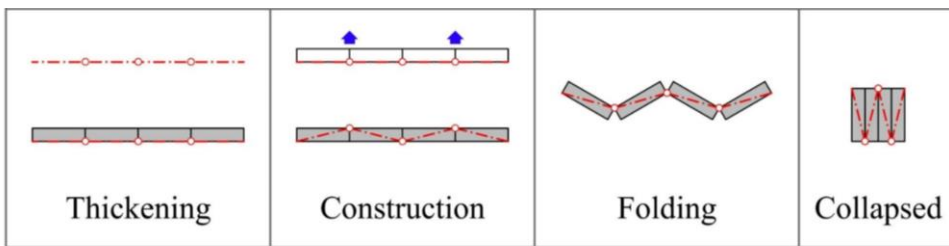


Figure 122: "Hinge shifting" technique.

The "Hinge shifting" is one of the oldest known techniques for thickening origami, and it is cited by Lang et al. and Tachi in their reviews on thickening methods (Lang et al., 2018; Tachi, 2011b), and extensively studied by Chen et al. (Chen et al., 2015). This technique is easy to apply for a single linear crease, and it consists into moving the hinge on the valley side of the fold after thickened the panel. It may seem easy at a first glance, but it becomes trickier when it is used to solve patterns with internal vertices. Furthermore, the panels often need to be carved in some areas or fabricated with different thicknesses to be able to reach the perfectly flat-folded state. The dihedral angles between the adjacent faces are preserved, but because the hinges are shifted, the relative translations are not preserved, thus some holes generate in correspondence of the internal vertices when we start folding, and the DOF may change because we moved the creases out of plane.

6.1.3. Tapered Panels

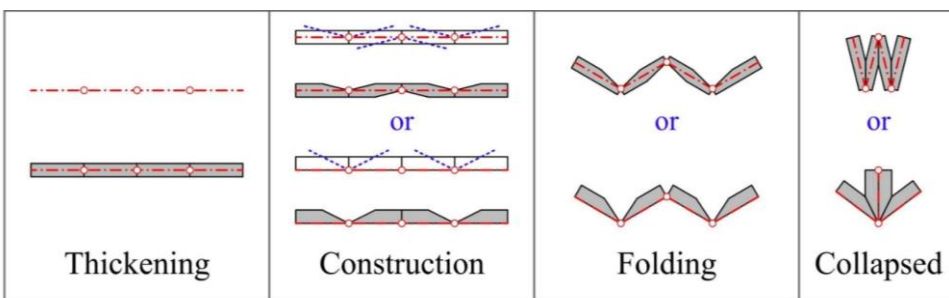


Figure 123: "Tapered panels" method.

The “Tapered panels” method proposed by Tachi (Tachi, 2011b), is one of the best methods to preserve the original kinematics⁸⁴ of the zero-thickness model, because it is easy to design and it preserves the position of the hinges, thus the thickened surface lies flat on a plane when unfolded. Furthermore, this method preserves the continuity of the material without generating holes. It can be built by marking or carving the crease lines⁸⁵ from a single panel of the same material. However, there are some major cons such as the fact that it is not possible to overlap more than two faces and the fact that the blocking creases cannot reach their maximum fold angle. The maximum collapsing amount can be regulated by changing the tapering angles of the panels, the smaller the tapering angles are, the smaller the collapsing amount is; the bigger the tapering angles are, the greater the collapsing amount is, and the thinner the panels become.

6.1.4. Constant Thickness Attached Panels

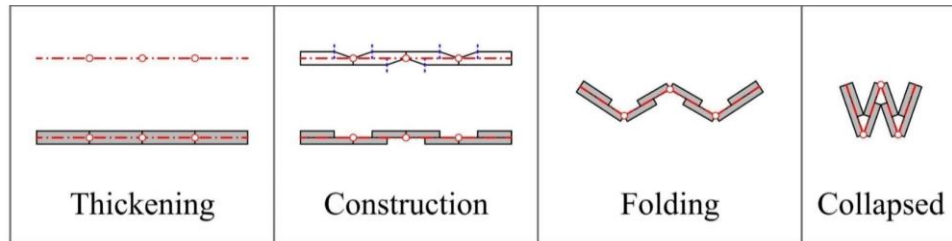


Figure 124: "Constant thickness attached panels" method.

The “Constant thickness attached panels” is a direct consequence of the “Tapered panels” method demonstrated by Tachi (Tachi, 2011b). It consists into substituting each tapered panel by glueing together two non-tapered panels with a constant thickness equal to half the thickness of the substituted tapered panel. This is possible only when the top and bottom faces of the tapered panel overlap for a significant amount. The mechanism so configured can be produced, by sandwiching a strong fabric or film between the two shifted panels (not by folding or carving a single panel). This method is easier to fabricate by hand rather than the tapered panel method. That is why is often used for prototyping. However, it suffers the same problems of the “Tapered panels” technique, about the limited fold angle. Furthermore, the mechanism at the folded state tends to work like a lever which tries to pull apart the film and the attached panels, thus the durability is strongly dependent on the film and glue quality.

6.1.5. Membrane Hinges

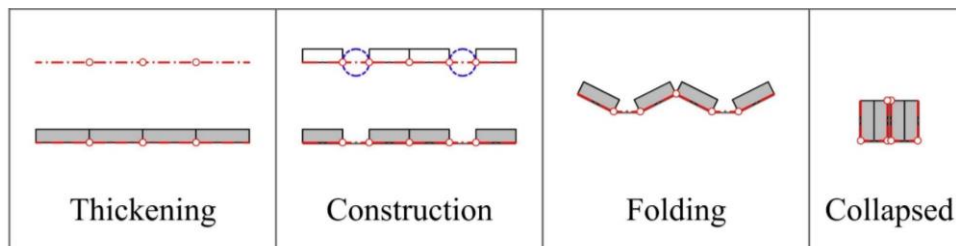


Figure 125: "Membrane hinges" method.

The “Membrane hinges” technique explored by Zirbel et al. (Zirbel et al., 2013) is easier to assemble and apply compared to other thickening techniques. However, once applied, the structure becomes floppy, because the faces are glued to a flexible membrane leaving a little space in correspondence of the valley (or mountain) creases equal to double the thickness⁸⁶ of the panels, which makes the hinges loose and flexible. This technique has been proposed for structures that have to move in zero-gravity, where the stiffness is not as crucial as in other circumstances.

⁸⁴ Both relative rotations and translations of adjacent faces.

⁸⁵ With a specific tapering angle, which is equal to half the relative fold angle at the chosen partially-folded configuration.

⁸⁶ Or even more than twice the thickness for cases where there are multiple overlapping layers.

6.1.6. Rolling Contact or “SOURCE” Technique

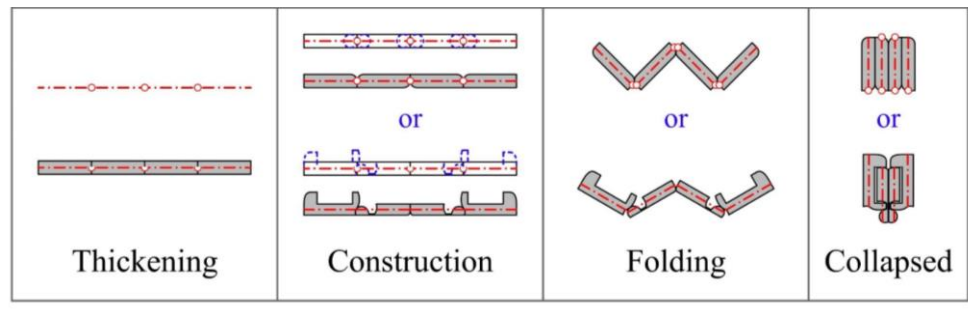


Figure 126: "Rolling contact" or "SOURCE" technique.

The “Rolling contacts” method, also known as “SORCE technique” has been demonstrated and patented by Lang et al. (Lang et al., Patent No. US 2017/0219007 A1, 2017). It is a method inspired by Jacob’s ladder toy, and similar mechanisms have been used in spinal implants, robot fingers and prosthetic knee joints. Lang et al. in the paper “Thickness-Accommodation Techniques in Origami-Inspired Engineering,” assert that “A notable aspect of the SORCE technique is that it marries a fully flat unfolded state... with a folded state incorporating arbitrary offsets between panels; furthermore, the DOF of the mechanism exactly reproduces the DOF of the zero-thickness model.” (Lang et al., 2018).

However, like other thickening techniques, also this method has some cons such as the fact that flexible membranes are used to keep together the rolling contact hinges, thus the elasticity of the membranes may increase the unexpected deformations of the theoretical model. Furthermore, this kind of mechanisms must be assembled, and their robustness is strictly related to the assembling quality. Relating to this problem Lang also asserts that “While conceptually simple to implement, modelling flexible membrane hinges is considerably more complicated than mechanisms with discrete hinges. Also, the curvature and convexity of the rolling contact surfaces and the tolerances must be considered during design to ensure robust joints.” (Lang et al., 2018)

6.1.7. Strained Joint

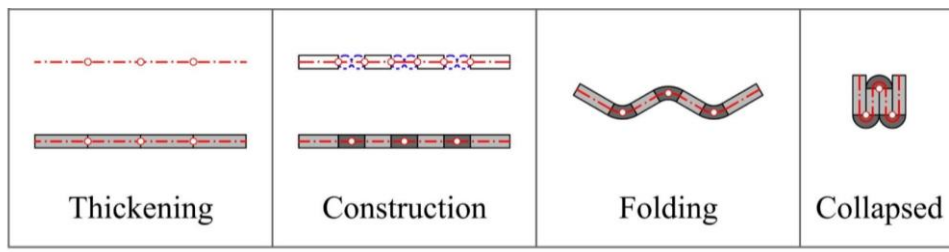


Figure 127: "Strained joint" Technique.

The “Strained joint” technique, is a method demonstrated by Pehrson et.al (Pehrson et al., 2016).

Lang et al. in the paper “A Review of Thickness-Accommodation Techniques in Origami-Inspired Engineering” assert that “The strained joint technique for accommodating thickness... is related to the membrane technique. Instead of using a thin membrane, the thick material itself acts as an effective membrane, i.e., one in which the “fold” is distributed across a region, rather than being a discrete revolute joint. In this case, the panel material itself is dissected so as to be flexible along desired hinge lines” (Lang et al., 2018). The main con of this method is that we need to use different materials to realize a mechanism with strain-able joints while having rigid panels, which makes the fabrication harder than other methods that uses one single material. Instead of mixing different materials with different elasticity, there is a monolithic alternative that makes use of particular cuts in correspondence of the creases area. The system consists of dissecting the panels isolating some linked bars that can be flexed and twisted which makes the connections behaving like flexible joints. The larger the holes and the thinner the bars are , the more flexible will be the joint. However, if we chose to apply the dissection technique, we must use a flexible enough material, otherwise, the joints would break after a few folding cycles. This means that, to be able to have flexible hinges also the faces would be a little bit flexible, thus the rigid-motion would not be perfect.

6.1.8. Double Hinge

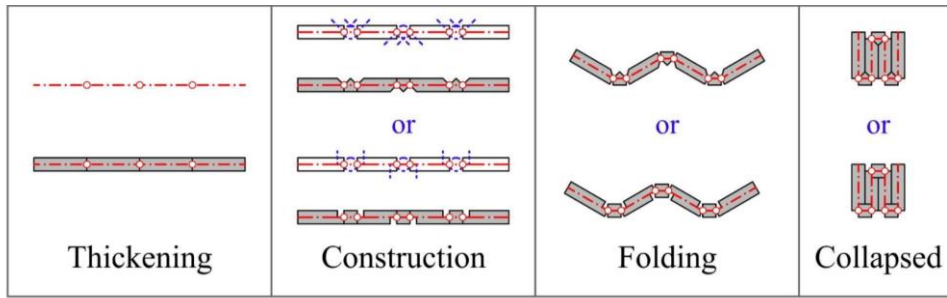


Figure 128: "double hinge" method.

The “Double hinge” method explored by Ku et al. (Ku & Demaine, 2016), is a method studied to thicken flat foldable patterns by doubling all the creases similarly to what happens in thick cardboard boxes. They proved that a double hinged solution for flat-foldable patterns with a single-vertex always exists, but the problem of thickening a flat-foldable pattern with multiple-vertices is still open. The main con of this method is that it needs holes to solve the internal vertices.

6.1.9. Symmetric Miura-Ori Vertex by Shifted Hinges and Carved Panels

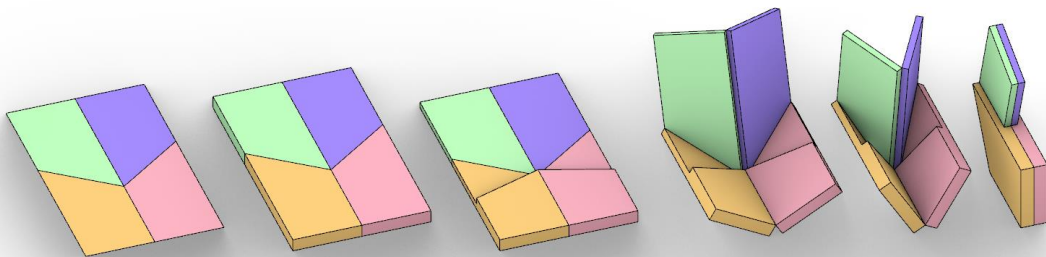


Figure 129: "Symmetric Miura-ori vertex by shifted hinges and carved panels" method.

The method patented by Hoberman in 1988 (Hoberman, Patent No. 4780344, 1988) was cited by Tachi as a thickening method in “Rigid-Foldable Thick Origami” (Tachi, 2011b). It is a special application of the “Hinge shifting” method as explained by Lang et al. (Lang et al., 2018). A limit of this method is that only symmetric Miura-like degree-4 vertices (bird’s foot vertices) can be thus accommodated.

6.1.10. Slidable Hinges

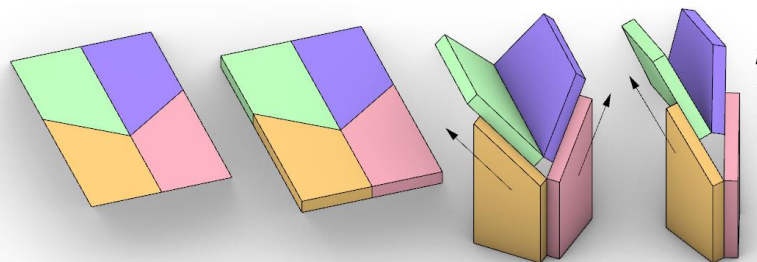


Figure 130: "Slidable hinges" method.

The “Slidable hinges” method has been studied for the first time by Trautz and Kunstler (Trautz & Kunstler, 2009) on degree-4 vertices and it consists in sliding the faces longitudinally in relation to the adjacent faces along the common crease lines while folding the pattern. The more the panels slide, the more the collapsing amount increases. The main cons of this method are that it cannot be built with material continuity, it does not reach the completely collapsed state, it generates holes during folding, and the technology to realize slidable hinges is very likely more complex and more subject to friction than traditional hinges.

6.1.11. Double Line

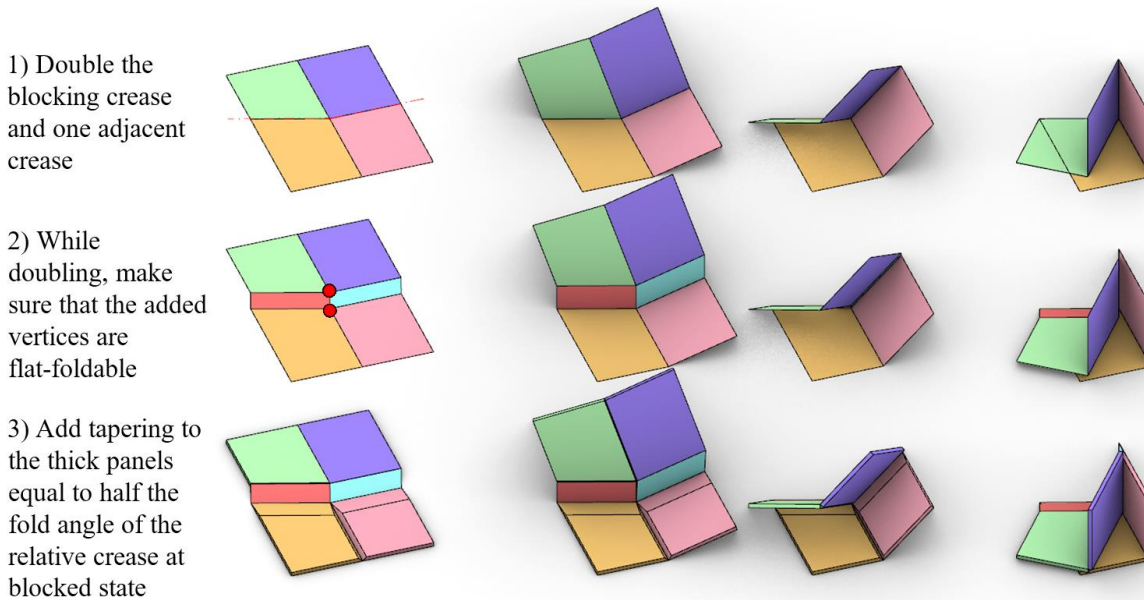


Figure 131: "Double line" technique.

The last method we review here is the “Double line” method proposed by Hull and Tachi (Hull & Tachi, 2017). This method is probably the most versatile even if it is probably harder to apply than most of the other methods. The “Double line” method consists in splitting some critical creases⁸⁷ into two parallel creases⁸⁸, like in the “double hinge” method proposed by Ku (Ku & Demaine, 2016), but with additional creased structures at the vertex. The additional creased structure at the vertex is a set of new flat-foldable vertices that solves the intersection of the doubled creases and the other non-doubled creases that converged in the same vertex. The new vertices are connected with a single polyline (which generates an additional planar face if it forms a closed loop). Once doubled those creases the faces can be thickened and tapered following the same approach used in the “Tapered panels” method. Doubling the correct creases allows to space the touching faces while keeping their relative orientation during motion, creating room for thickening the faces. The main pros of this method are that it can be produced by a monolithic single panel. The crease lines can be marked by carving or stamping as it happens in the “Tapered panels” method, but with lower tapering angles, which is better to preserve the thickness and stiffness of the panels. The collapsing amount is not limited, and the relative rotation of adjacent faces is preserved. Also, all the mountain and valley creases can be marked from the same side of the panel with half-cuts if they are mountain and triangular-groves if they are valley. Traditional CNC machines or hot-stamping machines can be used to mark the creases and there is no need to build specifically designed machines helping to decrease the production costs. Furthermore, without any assembling phase, the product is ready to use. For all these reasons, this method is very suitable for industrial production. The main cons of this method are that it is harder to apply than most of the other methods we reviewed, and it preserves the kinematics of the mechanism only for what concerns

⁸⁷ The creases that needs to be doubled are, mainly, the creases that block and some incident creases. In flat-foldable patterns all the creases are doubled.

⁸⁸ They call those creases “double lines”.

the reciprocal rotation of the faces, not the translation. Furthermore, because every internal vertex split into multiple degree-4 flat-foldable vertices the DOF of the pattern may change to one. However, even if the translations are not preserved, no holes appear during motion, because the structure at the vertex of the split line has its own rigid cinematic that preserve material continuity. Lastly, because doubling the lines spaces the faces, to be able to achieve a result with the same dimensions of the original non-doubled model, the original faces must be resized and rearranged case by case after doubling the critical creases. In the following case studies, we tested different thickening method, but we ended up always using the “Double line” method by Tachi and Hull because, for our purposes, it was more efficient than other techniques.

6.2. Case Study - One-DOF, Developable, Non-Flat Rigid-Foldable Ladder⁸⁹

The first case study we propose is a one-DOF, developable, rigid non-flat-foldable ladder. This design is an exemplification of a one-DOF thick structure with multiple blocking degree-4 vertices. The structure self-blocks (or self-arrests) when the blocking creases reach the maximum fold-angle of 180°. The main issues raised during the design phase were: making a one-DOF rigid foldable mechanism that self-blocks at a ladder-shaped configuration; dimensioning the steps correctly while preserving the developability of the ladder; thicken the panels without losing the original kinematics and making it self-supporting and self-balanced.

All these issues will be discussed further in the next sections, but what we want to highlight is that all these points influenced the design of the chair from the early design phase, thus even if we will present the design process as a linear sequence of steps for clarity's sake, the reader should keep in mind that most of the stages of the process were developed in parallel, and they were redesigned and discussed several times before reaching the final product.

6.2.1. Preliminary Paper Prototype and Digitalization

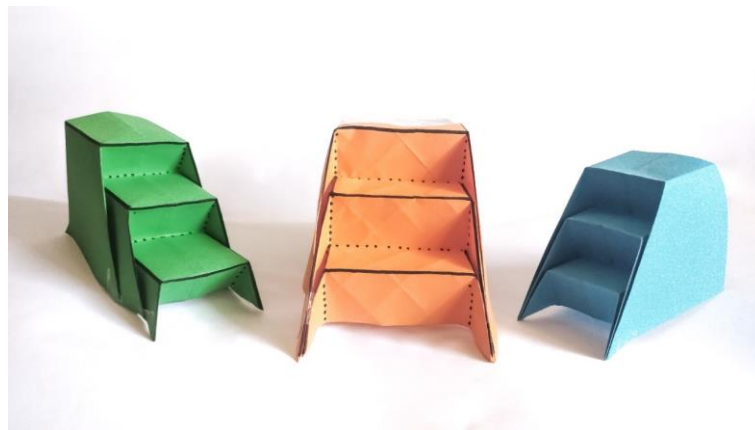


Figure 132: study models of the ladder made with printer paper.

One of the first steps when designing something that follows origami rules is almost always the folding of the paper prototype. It helps to materialize the idea and testing if it works as imagined. Also, it helps to make small changes to the initial pattern because, as long as the paper does not rip, the developability of the paper is preserved and guaranteed. This preliminary phase is crucial, and it helps the designer understanding fast how the global shape would look. However, because the paper model is flexible, it may mislead the understating of some formal or kinetic aspects, especially for what concerns the rigid foldability and the identification of the blocking configuration. Thus, is highly suggested as from now,

⁸⁹ The ladder design is also published into the paper “Designing Self-Blocking Systems with Non-Flat-Foldable Degree-4 Vertices” written by the author of this thesis and Tomohiro Tachi, presented at the 7OSME (The 7th International Meeting on Origami in Science, Mathematics and Education). The meeting took place in Oxford between 5th and 7th September 2018. The paper is part of the results of the research carried out during the period abroad encouraged by the PhD course (Foschi & Tachi, 2018).

converting the paper model into a much more accurate digital model. The preliminary digital model is not only useful to verify the rigid foldability and to make the first considerations about the shaping and folding motion, but it is the basic requirement for later accurate proportioning, and it is the fundamental starting point for the thickening phase.

The three models shown in Figure 132 are a selection of three among the multitude of paper study models that we folded before moving to the digitalization phase. The concept of the ladder came from the grafting of a Miura-ori pattern as shown in Figure 133. Similar patterns are used in the aerospace industry for making ultra-light sandwich panels (Klett & Drechsler, 2011), here we use a little portion of it for a completely different purpose. The preliminary digitalized prototype of the ladder was designed by trial-and-error method. Because the model is very simple, it is possible to get sufficiently accurate results using only reference points and simple graphical constructions. By trial-and-error method we tried to give a first rough shaping to the ladder. We angled the rises of the steps to make it steeper while keeping the treads long enough to fit a foot, and we dimensioned the steps to make the external corners aligned to the same oblique crease generated from the exceeding paper of the highest step as shown in Figure 134.

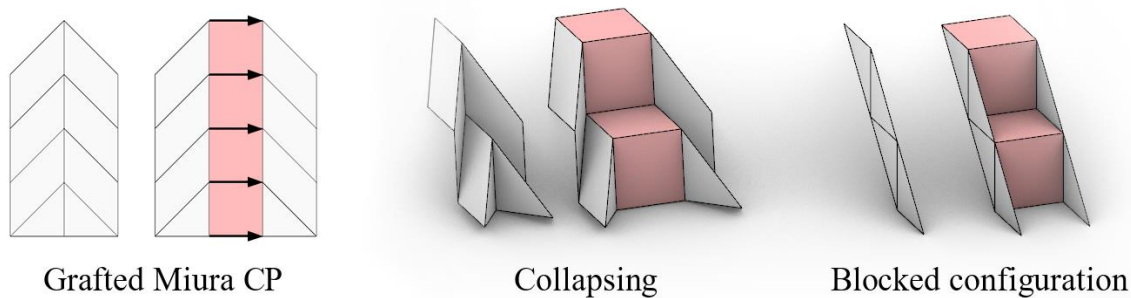


Figure 133: ladder concept by grafting a chain of three Miura-like vertices.

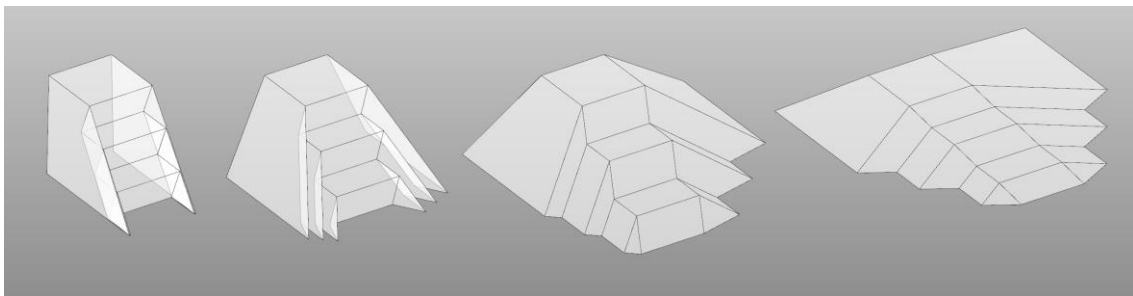


Figure 134: the unfolding of the preliminary digitalized model of the ladder with angled rises.

6.2.2. Fine-Tuning the Dimensions of the Ladder with Trigonometry

Because the model is very simple, it is possible to get sufficiently accurate results by applying the trial-and-error method, only using reference points and simple graphical constructions. Although, to enhance even more the accuracy and to have total control on the shape and proportions of the model, we propose below a method based on simple mathematical formulations that allow the designer to get the wanted blocked state with fixed proportions without even needing to fold the CP. This method is a more accurate alternative of the trial-and-error method, but it may return similar results.

We start fixing some parameters⁹⁰ according to the desired shape, refer to Figure 135:

- The angle ρ_4 between each riser and tread of each step is fixed ($\rho_4 = 80^\circ$).
- Each riser and tread must be rectangular ($\theta_4 = \theta_3 = 90^\circ$).

⁹⁰ We could choose any other value. Here we chose a height and a depth of 30 cm for every step, because the ladder was supposed to be a steep 3-step generic indoor portable ladder design.

- The risers and the treads lengths (l) must be equal (to have the ribs $\overline{O2}$ and $\overline{65}$ aligned at blocked state).
- Each step height (h) is fixed (30 cm).

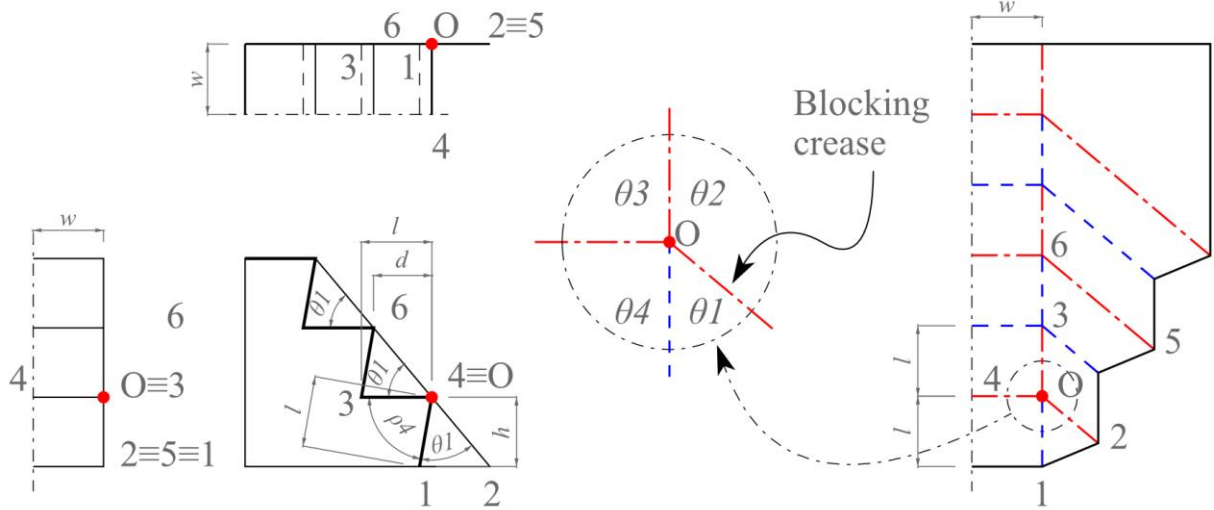


Figure 135: ladder design fixing some variables ($\theta_4 = \theta_3 = 90^\circ, \theta_2 = 180^\circ - \theta_1, h = 30\text{cm}, \rho_4 = 80^\circ$). θ_1 must be found.

Because the ladder has mirror symmetry, we can focus on one half of the pattern. The half pattern presents a chain of degree-4 vertices which is known to be a one-DOF mechanism (Tachi, 2011a). Also, because all the vertices have the same pattern, they all block at the same time. This allows us to focus only on one vertex (refer to vertex O in Figure 135). The creases $\overline{O1}$, $\overline{O3}$, and $\overline{O4}$ have fixed lengths and angles, thus the only crease that needs to be tuned is $\overline{O2}$, which is also the crease that blocks the degree-4 vertex. To find the $\overline{O2}$ direction, either θ_1 or θ_2 are needed. Because $\theta_1 + \theta_2 = 180^\circ$, we have $\theta_2 = 180^\circ - \theta_1$. So, finding θ_1 is all we need to solve the problem. The fixed parameters are the fold angle $\rho_4 = 80^\circ$, the angles $\theta_4 = \theta_3 = 90^\circ$, $\theta_2 = 180^\circ - \theta_1$, and $\theta_1 + \theta_2 + \theta_3 + \theta_4 = 360^\circ$. If we substitute these values into the equation 19 and rearranging it, we obtain the following simplified expression:

$$\theta_1 = \frac{180^\circ - \rho_4}{2}. \tag{39}$$

Once we know all the angles, we can calculate the riser and the tread length (l), fixing h and ρ_4 :

$$\overline{O1} = \overline{O3} = \overline{O4} = l = \frac{h}{\sin \rho_4} = \frac{30\text{ cm}}{\sin 80^\circ} = 30.46\text{ cm}. \tag{40}$$

$$\overline{O2} = 2(\overline{O1}) \cos \theta_1 = 2 \times 30.46\text{ cm} \times \cos 50^\circ = 39.16\text{ cm}. \tag{41}$$

It is also possible to calculate $\overline{O1}, \overline{O3}, \overline{O4} = l$ and ρ_4 fixing h and d using the Pythagorean theorem and trigonometry:

$$\overline{O1}, \overline{O3}, \overline{O4} = l = \frac{h^2 + d^2}{2d}. \tag{42}$$

$$\rho_4 = 90^\circ - \cos^{-1}\left(\frac{h}{l}\right). \tag{43}$$

6.2.3. Thickening – “Offset Panels” Method

Once defined the zero-thickness pattern we moved to the thickening phase. The first method we tested was the “Offset panels” method. The Figure 136 shows the steps that we followed to design the first thick version of the ladder. To be

able to offset the panels properly we folded and unfolded continuously the ladder, so we were able to visualize and measure better the correct offset distances and position of the vertical connections of the joints. This method is convenient because it allows the designer to animate the thickened surface (Figure 137) by matching the transformations of the original zero-thickness animated folded surface. This is possible because the kinematics of the faces is perfectly preserved after thickening⁹¹. However, due to the multiple overlapping layers, we had to cut numerous parts in correspondence of the hinges to avoid collisions, this problem caused the physical prototype to have much floppier behaviour than expected. Furthermore, the overlapping layers forced us to double the offset distance of the panel for every step, this caused the unfolded model to be too thick and not very useful for actual applications. For all these cons, we had to move to another thickening method.

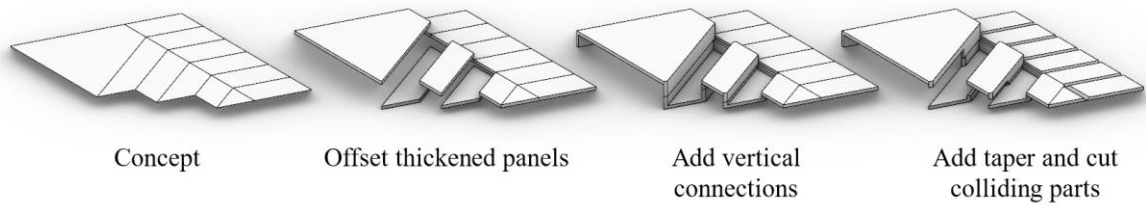


Figure 136: thicken the ladder with “Offset panels”.

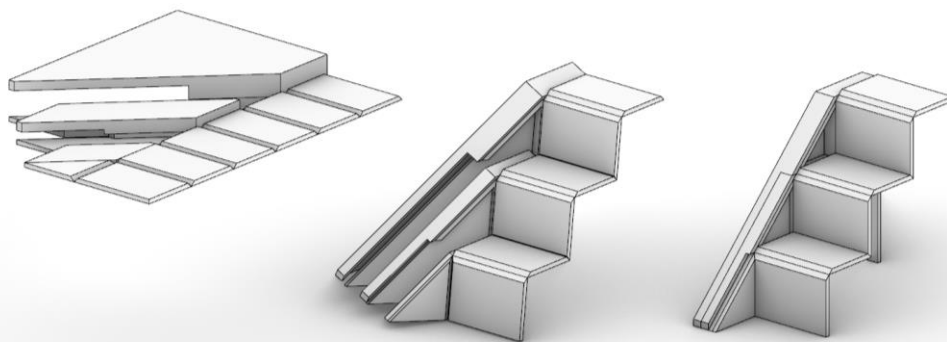


Figure 137: folding of the ladder thickened with “Offset panels” technique.

6.2.4. Thickening – “Tapered Panels” Method

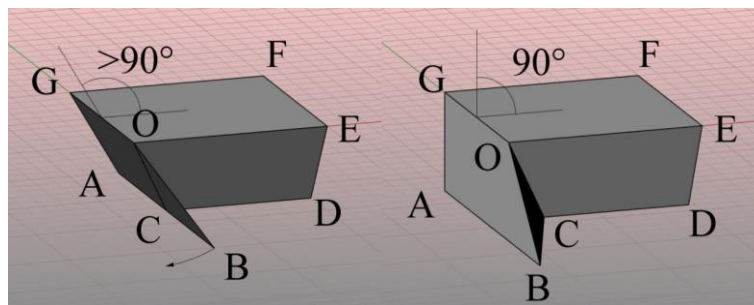


Figure 138: correcting the pattern to make the top and the side faces blocking at a fold angle greater than 90°.

The next thickening method we tested was the “Tapered panels” method. This method is convenient because it does not require to move the faces or the creases. The method consists into extruding the faces in one direction (perpendicular

⁹¹ Both rotation and translations of adjacent faces are preserved.

to the plane of the unfolded model) and taper the panels along the bisecting planes, relative to each pair of adjacent faces, at the blocked configuration. So far, everything appears easy and straightforward, however, at the blocked configuration, there are faces that touch, and because the bisecting plane of two touching faces lies into the same plane of the two faces themselves, we cannot add thickness to those faces at their maximum fold angle. So, we must stop folding before reaching the blocking configuration so that the faces are spaced of a certain amount allowing us to thicken and taper the faces without self-intersections or excessive tapering angles. Stopping the folding before reaching the blocking configuration, however, will prevent the model to reach the three-dimensional configuration that we designed in the first place. Thus, to be able to apply this thickening technique we must change a little bit the pattern to be able to reach the wanted three-dimensional configuration before reaching the blocked state. In Figure 138 you can see how we corrected the pattern of each vertex. With this new pattern, the face on the side reaches the vertical position before reaching the blocking configuration so that there is room to add a certain thickness between the faces ABOG and BCO. Then, we corrected the whole pattern according to the single-vertex test, and we folded it to reach the semi-folded configuration as shown in Figure 139. After that, we thickened the panels by extruding them along the direction of their normal vectors to the inside, and we tapered them slicing the extruded panels with the bisecting planes between each pair of adjacent faces as shown in Figure 140.

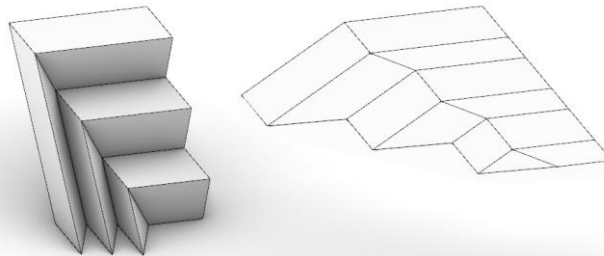


Figure 139: thickened ladder from the top, with tapered panels method.

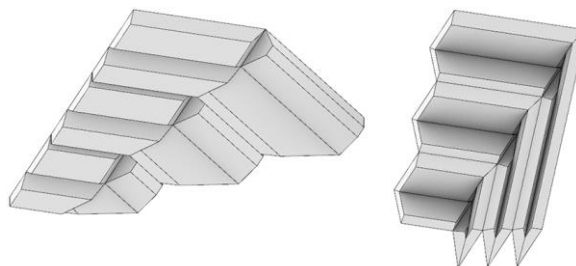


Figure 140: thickened ladder from the bottom, with tapered panels method.

This method is efficient and reliable; however, the adjacent panels are contacting only along the faces of the panels resultant from the tapering. Thus, the new blocked configuration is less stable than the previous blocked configuration because the contacting areas are smaller, and this may generate additional stresses on the hinges.

We may find a more stable blocked configuration by spacing for a smaller amount the blocking faces while keeping the same thickness of the panels, or by keeping the same semi-folded configuration and increasing the thickness. In both ways, after tapered the panels, the contacting area would be larger. However, such type of tapered panels is harder to fabricate, because traditional folding machines are not designed to taper the panel on such a wide area. It may be possible to fabricate the ladder with this thickening solution by tapering the panels one by one by CNC milling and glueing them onto a thin membrane or film, but because we wanted to limit the assembling, we decided to test a different thickening method.

6.2.5. Thickening – “Double Line” Method

The last thickening method we applied was the “Double line” method by Hull and Tachi. In the original approach that they propose, all the creases are doubled and the internal vertices resulting from the doubling process are forced to be always flat-foldable, in this way there is only one possible solution for any flat-foldable CP. However, the ladder is a non-flat-foldable special case, thus we discovered that there is no need to double all the creases to be able to add thickness while preserving the maximum fold angle. Furthermore, to increase the design freedom, we did not constrain the internal vertices to be flat-foldable.

The ladder has mirror symmetry and even if all the vertices have the same CPs, some of them have inverted mountain/valley assignments. Thus, there are only two types of degree-4 non-flat-foldable vertices. If we add thickness to the panels downwards, we can solve the vertices with the valley blocking fold simply applying the “Tapered panels” method, thus we focused only on the vertex with the mountain blocking fold as shown in Figure 141.

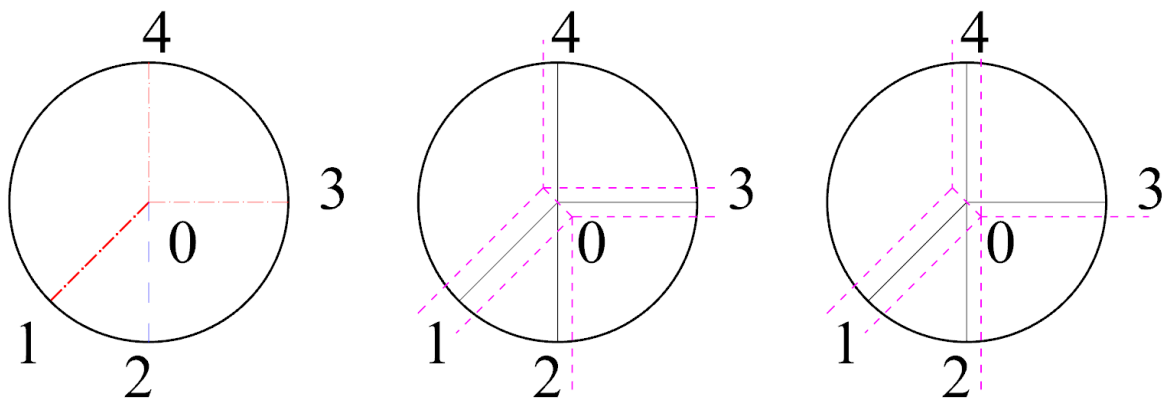


Figure 141: valid “Double line” solutions of a degree-4 vertex when the crease 01 is mountain and blocks.

We started doubling the mountain blocking crease, and after that, we solved the intersections with other existing creases by doubling only one of the other creases⁹². In Figure 141 we illustrated two possible solutions with two doubled creases. Nevertheless, the ladder has multiple vertices connected, thus the illustrated solution where the creases 01 and 04 are doubled, is not applicable, because to continue the pattern of the ladder we should attach the crease 04 to the crease 02 of the adjacent molecule, which are not compatible because they are respectively a doubled and non-doubled creases. Thus, the solution where the creases 01 and 03 are doubled is the only valid solution in this case. After we decided which were the creases that needed to be doubled and because we chose to not constrain the internal vertices to be flat-foldable, we had to choose the offset distance and the angle of the crease connecting the two new vertices. In Figure 142 two possible solutions are illustrated. The creases AJ and BK are parallel, and their offset distance is equal in both cases. What it is changing are the angles $\theta_{j,2}$ and $\theta_{k,2}$, that make in the first case two non-flat-foldable vertices, and in the second case two flat-foldable vertices. Changing the internal angles of the vertices changes the distance of the parallel faces AHJI and BCK at blocked state, thus the maximum allowed thickness of the panels also changes. The case with internal flat-foldable vertices is apparently more efficient because with the same offset we can get a result where there is more space between the faces AJHI and BCK, thus apparently, we can use thicker panels. However, the thickness of the face EFJK⁹³ is almost halved because of a higher tapering angle. Keeping tapering angles small makes the thickness more homogeneous, and thus also the loads are better distributed. Furthermore, with smaller tapering angles it is easier to be produced by CNC or folding machines. Moreover, in the first case the face EFJK is more perpendicular to the ground, thus it can transmit the load better to the bottom face.

Once designed the single vertex, we repeated the same structure to every equal vertex of the ladder. This method allowed us to preserve the relative rotations of the thick faces while keeping thin enough the unfolded configuration. However, the conversion from thin to thick model while keeping the same height and width of the steps was not trivial.

⁹² We call those creases “critical creases”, which are those creases that need to be doubled to be able to solve the internal vertices, but they are not necessarily blocking creases.

⁹³ Which is one of the most stressed during use because it is the element placed right under the step edge which tend to bend under the user weight.

After doubled the critical creases and solved all the internal vertices, we followed the process illustrated in Figure 143 to rectify the shape and dimension of the ladder matching the concept model dimensions.

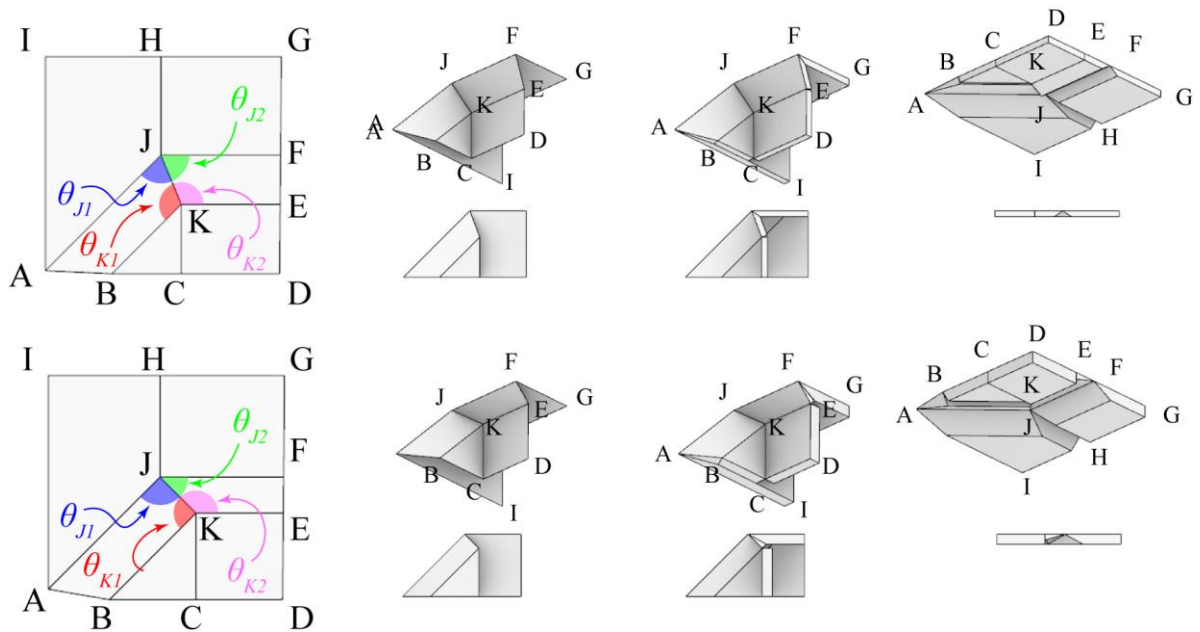


Figure 142: comparison of different internal vertices after doubling the internal critical crease in a single degree-4 corner.

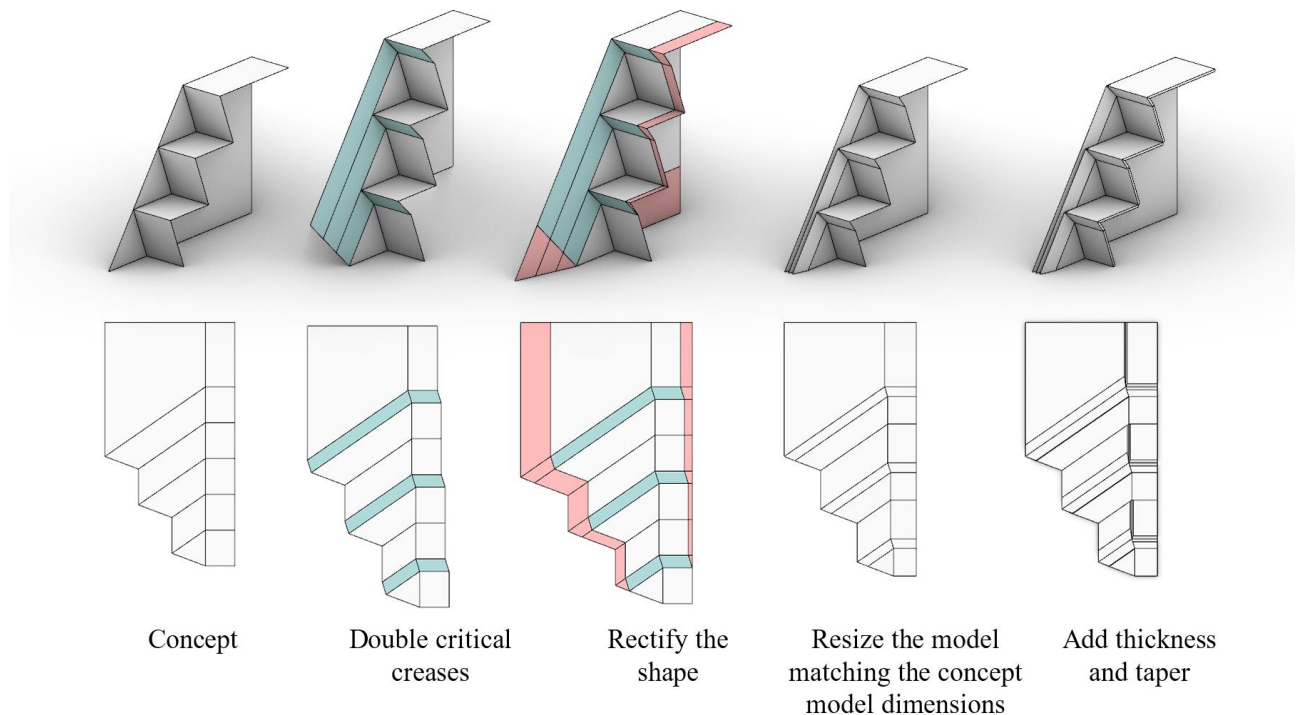


Figure 143: design process of the ladder, from the concept to the model with thick panels.

First, we identified the critical creases that we needed to double, and we added new strips of paper (light blue) to the surface following the angles defined previously on the single vertex. Then, because we expanded the surface and we added some creases, the final dimensions and overall shape at folded state changed a little bit, thus we rectified it by adding missing parts and resizing everything to match the concept prototype as much as possible. Lastly, we added the

thickness and we tapered the panels by bisecting the angles at folded configuration. As a final step before building the prototype, we simulated the folding and unfolding with thick panels. We checked and corrected possible problems like self-intersections, colliding panels, missing tapers, missing parts etc.

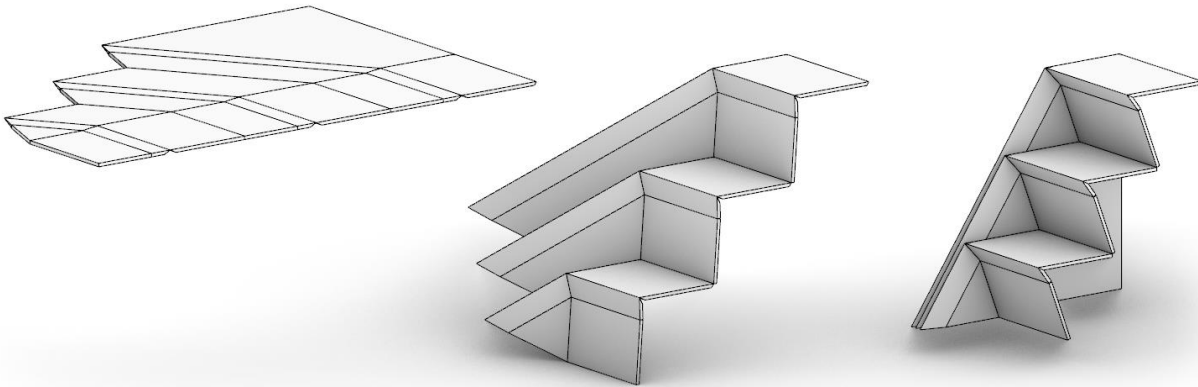


Figure 144: folding of the ladder thickened with "Double line" method.

We built the first prototype by 3D printing the tapered panels and assembling them by stitching them with common adhesive tape. After verified that it worked as expected, we built a full-size prototype by CNC milling wooden panels and gluing them on a thin membrane. The prototype gave us some hints about the stiffness of the structure and the possible problems that we will discuss in the next section.



Figure 145: thick rigid non-flat foldable developable ladder with one-DOF, study 3D printed preliminary prototype.

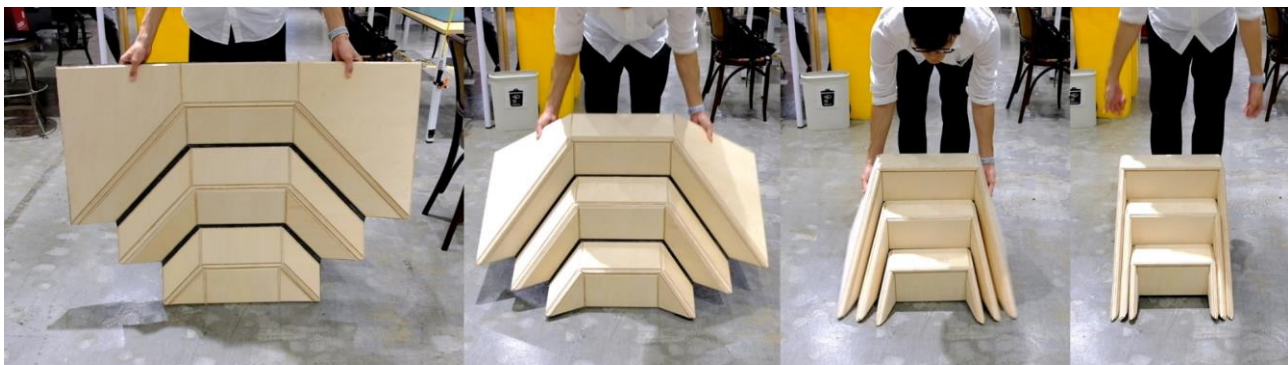


Figure 146: full-scale wooden prototype, folding test.

6.2.6. Stability Problems and Possible Solutions

The first problem we tried to solve was that the ladder tended to collapse when loaded. Because of its shape and its particular kinematics, surprisingly applying loads on the front two vertices of the first two steps did not interfere with the equilibrium state. However, when we applied two loads on the two back corners of the last step, it caused the collapsing of the whole ladder (as shown in Figure 147).

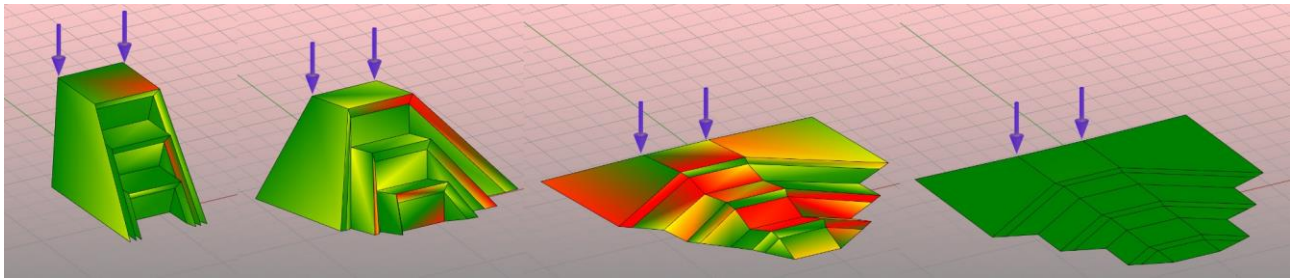


Figure 147: collapsing of the model of the ladder under given loads.

The three solutions in Figure 148 are possible locking systems that preserve the CP and prevent the collapsing of the ladder once loaded. All three systems: hooks, clips, and belt, are aimed to keep the ladder in position when loaded and they are all removable mechanisms which allow to fold and unfold the ladder fast. A different solution that helps keeping the ladder at blocked configuration is the solution proposed in Figure 149. This solution does not need any additional device but requires anchoring the ladder to a vertical support like a wall or a self-supported panel. This solution utilizes the gravity to keep the ladder at the blocked configuration. It is based on the fact that anchoring the side panel distributes the loads in a way that when a user steps on it the ladder tends to fold and to lock. The ladder so anchored once reached the blocked configuration, will tend to keep it as long as we apply a vertical force from the bottom directed upward. Another possible solution may be aimed to change a bit the pattern to angle the side faces and make them converge toward the base so that the forces transmitted to the side faces will point inward and will help keeping the ladder closed, however, this solution may fail with elastic panels and it would decrease the area of the footing making it less stable.

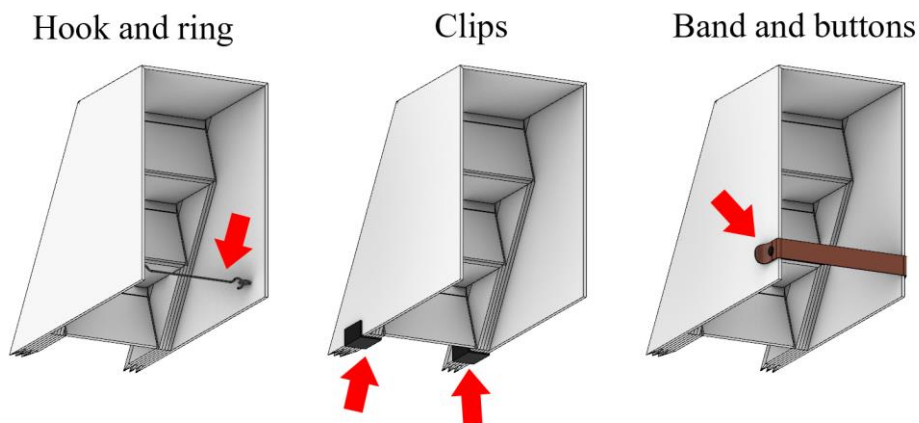


Figure 148: possible systems to keep the ladder at the blocked state even under load.

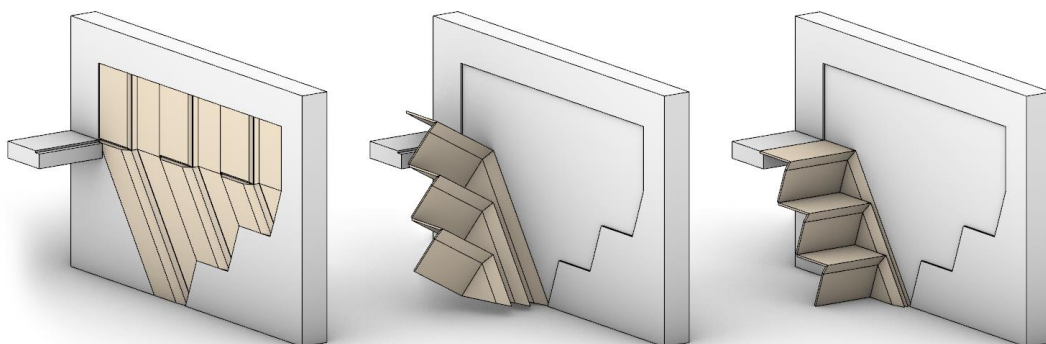


Figure 149: self-supporting ladder attached to a wall, it keeps the folded configuration by gravity.

Another issue, raised by the physical simulations, was a problem encountered while folding the ladder caused by the well-known pop-up and pop-down problem that we already mentioned in 4.8.3. This problem is critical, and it may cause the one-DOF mechanism to fold incorrectly or even to jam or break. This problem is caused by the fact that the degree-4

vertices have two possible folding modes where the mountain/valley assignment changes. At completely flat state there is no way to know whether a crease will start folding as a valley or a mountain crease. And even if a single crease starts folding with a wrong assignment it will cause a jam in the mechanism. A possible solution may be, for example, shaping the wall in a way that it would be impossible to unfold completely the ladder. This would solve the problem because there are no bifurcations in the motion except at the unfolded state, thus skipping the unfolded state will exclude the critical points where pop-up and pop-down problems occur. Another solution may be using non-developable non-flat-foldable vertices that skips the completely unfolded state⁹⁴ making it impossible to change the pop-up or pop-down assignment. However, these solutions have been both excluded for portable ladder because not having a completely flat configuration would have compromised the portability and the stocking efficiency. This design, thus, is preferable for ladders with a small number of steps where the pop-up/pop-down assignment can be controlled manually.⁹⁵

6.3. Case Study - One-DOF, Developable, Non-Flat Rigid-Foldable Chair⁹⁶

Designing an origami-like chair, presents some issues similar to the ones encountered while designing the ladder, like the rigid foldability, the DOF, the proportions, the thickness and stiffness of the panels, the centre of gravity and the equilibrium conditions, but in this case also the aesthetics and the ergonomics must be taken into account. For simpler designs, it is possible to modify directly the unfolded CP being able to foresee the folded result easily without necessarily using complex mathematical formulations, as we did for the ladder. However, while designing a piece of furniture, especially when there is ergonomics involved, it would be better for designers to develop a system to control the shape at the blocked configuration directly in three-dimensions, while preserving the developability, without necessarily needing to work on the unfolded CP. Nevertheless, modifying the folded state without losing the developability may not be trivial, because moving a single vertex of the model, without particular precautions, will change the planar angles summation at the vertex making the model no more developable instantly. Therefore, in the next sections, we show the workflow we followed that allowed us to realize a one-DOF developable rigid-foldable self-blocking chair working directly in three-dimensional space while preserving the developability of the unfolded planar CP.

6.3.1. Preliminary Paper Prototype

In section 6.2.6 we saw that, if not correctly designed, a pattern may be not suitable to self-lock under certain loads conditions. For the ladder we solved that problem by glueing the side face to a wall so that we were able to achieve a result where once added loads on the steps, the faces tended to push one against the other making it block firmly; or we studied some other portable solutions involving additional locking systems like clips, hooks, and belts. However, to simplify the usability of the chair, we tried to avoid external locking systems by exploiting the kinematics of the pattern itself and the force of gravity making it self-lockable⁹⁷. Thus, this time, we considered this necessity from the early stages, and, after a certain number of paper test prototypes, we found a solution that apparently was working as wanted.

⁹⁴ Because a planar unfolded configuration does not exist into non-developable vertices.

⁹⁵ We are still working on the upgrading of this design and we are achieving interesting results using non-developable single-flat-foldable vertices. This topic may be a future publication of the author of this thesis.

⁹⁶ The chair design is also published into the paper “Designing Self-Blocking Systems with Non-Flat-Foldable Degree-4 Vertices” written by the author of this thesis and Tomohiro Tachi, presented at the 7OSME (The 7th International Meeting on Origami in Science, Mathematics and Education). The meeting took place in Oxford between 5th and 7th September 2018. The paper is part of the results of the research carried out during the period abroad encouraged by the PhD course (Foschi & Tachi, 2018).

⁹⁷ We will show later that in the first full-size prototype this was not be possible, because we had to stabilise the chair with external locking systems. However, we still think that a perfect self-locking chair is possible with the right manufacturing process and selection of materials.



Figure 150: study models of the chair made with paper and cardboard.

In Figure 150 there is a selection of some of the preliminary study models. However, those models were not returning the results we expected, because even with very small forces the paper bent and the chair collapsed. Thus, to test the behaviour with rigid faces, we digitalized the model (Figure 151) we tested its rigid kinematics by folding and unfolding it with the same algorithm we presented in 4.8.1, then we added loads on the front vertices while keeping the faces planar and rigid as we did for the ladder. The simulation confirmed that the chair is very stable under vertical loads as shown in Figure 152, and as more loads, we add as more it tends to tighten at blocked configuration. We also tested the structural stability under rotating torsional movement around the Z-axis through the centre of gravity, but as far as the faces remain rigid the digital model of the chair does not collapse. Nevertheless, without properly rigid panels this perfect rigid behaviour may fail, thus the prototyping phase and the testing phase with different materials and thicknesses are crucial. A more specific analysis about the collapsing conditions under certain stresses, considering elasticity, and precise analysis of deformations may also be useful, but we decided to skip these digital simulations and test the resistance and the elastic deformations directly on the physical full-scale prototype.

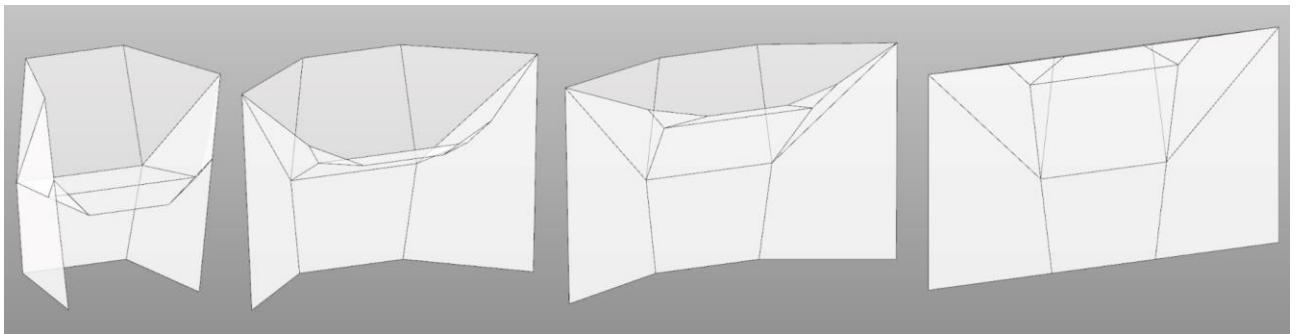


Figure 151: the unfolding of the preliminary digitalized model of the chair.

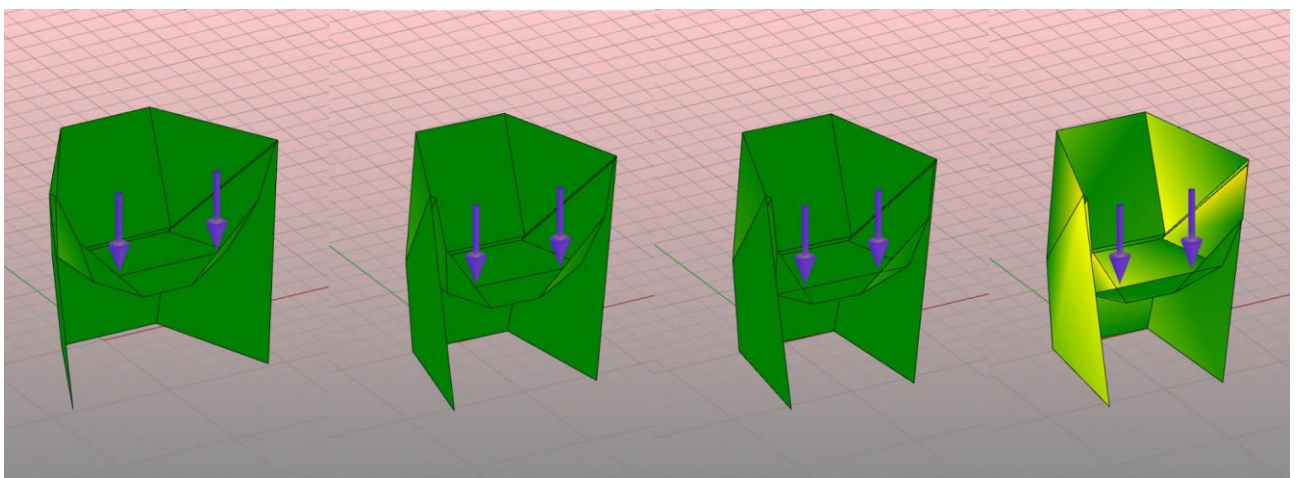


Figure 152: digital physical simulation of the chair under given loads; the more loads we add, the more the chair tightens at blocked configuration as far as the faces remain rigid.

6.3.2. Thickening – “Double Line” Method

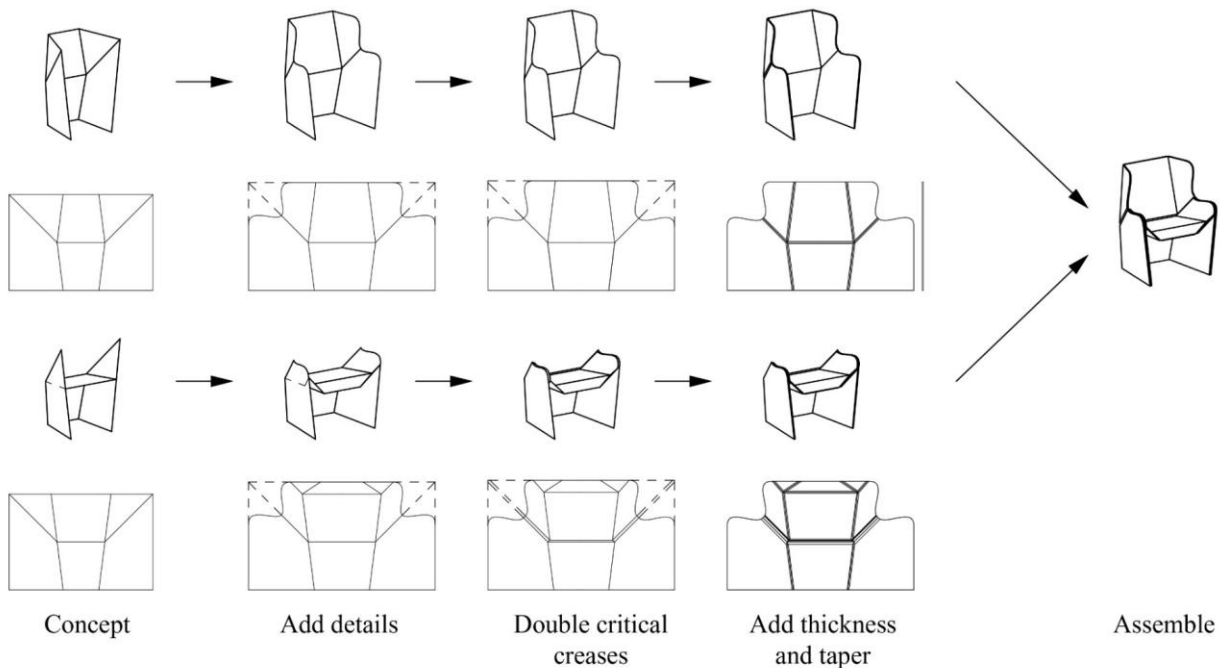


Figure 153: design process of the chair, from the concept to the model with thick panels.

To further enhance the ergonomics, to verify the stiffness and to correct the dimensioning of the chair we realized a prototype at human-scale. Thus, we converted the zero-thickness prototype to a thick prototype, and based on the experience with the ladder, we used the “Double line” method, which appeared to be the most suitable also for this application. The workflow we followed for thickening the chair is illustrated in Figure 153⁹⁸. In “Double line” method we need to double the critical creases and some connected creases, and the first prototype of the chair had only two blocking vertices in the seat, with only two blocking creases. Thus, we doubled the two blocking creases and we solved the two blocking vertices by doubling also the crease that connects them. Even if in this case it is not crucial, we designed the two resulting vertices as flat foldable vertices. The back part did not need any double crease because none of its creases blocks and the only double crease shared with the seat is one of the boundary creases of the glued faces, thus it is sufficient to offset that crease toward the unglued face to be able to not interfere with the back part. After doubled the creases, we refolded the model matching the original maximum fold angle of the model without double creases, and we added thickness to the panels. The maximum thickness of the panels that we can use without intersecting the panels, is half the distance between the blocking faces⁹⁹. However, the offset distance of the doubled creases in the CP does not correspond to the distance of the faces when doubled the creases¹⁰⁰, as shown in Figure 154. Because of that, in order to calculate the offset distance, given the thickness of the panels, we need to calculate or measure the fold angles of the two doubled creases¹⁰¹ (Figure 155) and apply the simple trigonometry formulations reported below.

⁹⁸ Even if it is possible to fold the chair from a single sheet of paper, we divided it in two pieces, one for the back and one for the seat, attached together by gluing the bottom three faces. To make it with just one sheet we can flip the seat upside down and stitch the bottom edges which will become a single linear mountain crease.

⁹⁹ Which are now spaced due to the added double lines, thus there is room for adding thickness.

¹⁰⁰ Unless both the fold angles of the doubled creases are equal to 90° .

¹⁰¹ Because the maximum fold angles of the doubled creases depend on the two new internal vertices, even if it is not crucial it is suggested to use flat-foldable vertices to simplify the formulations needed to calculate the fold angles starting from the unfolded CP (crease pattern). Although in our case we preferred to measure the angles directly from the folded three-dimensional model instead of calculating them.

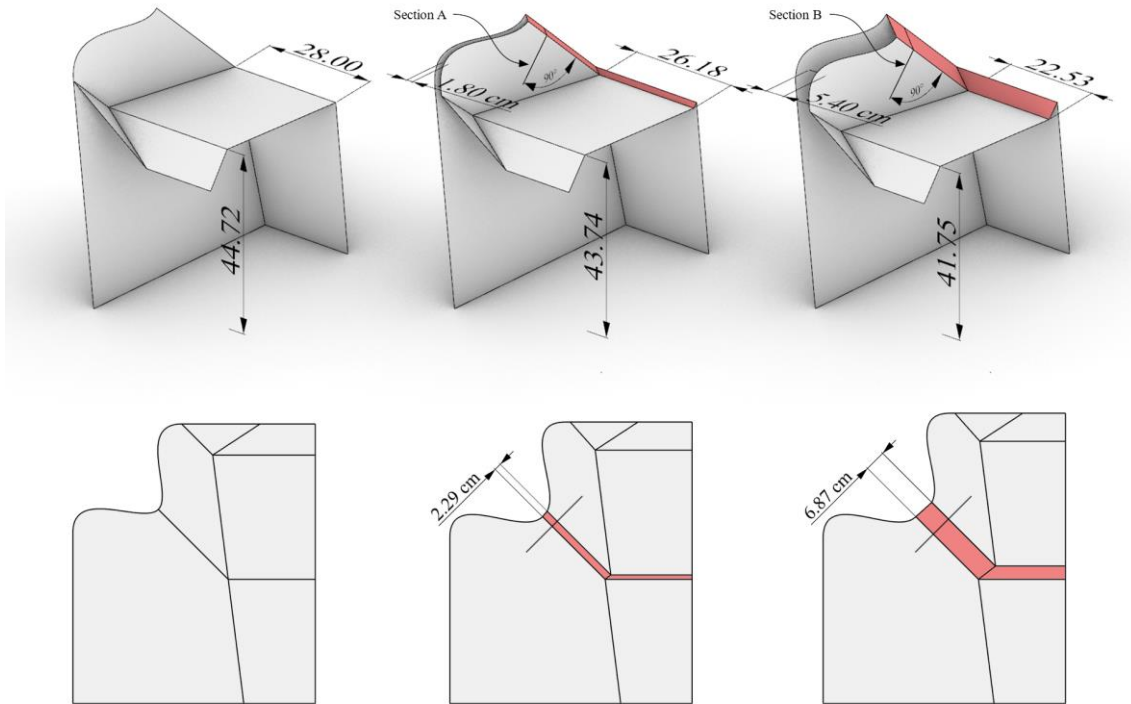
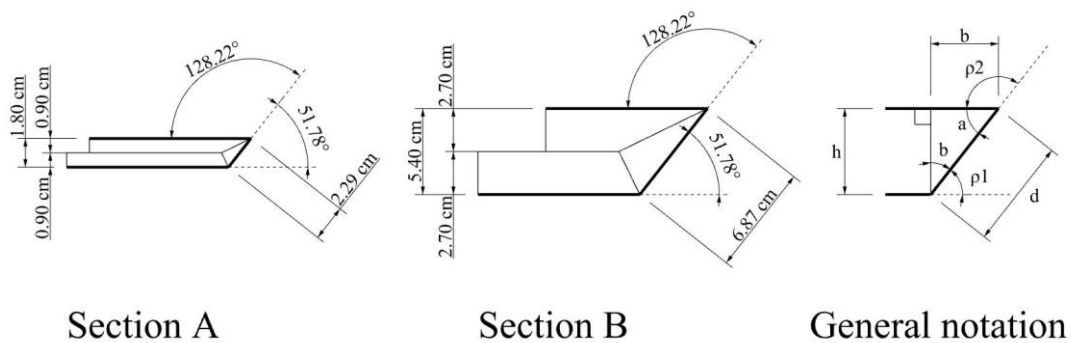


Figure 154: changing the offset of the double lines changes the space between the blocking faces.



Section A

Section B

General notation

Figure 155: section A and B, and general notation.

Apply the following formulation to calculate the offset distance d given the thickness of the panels $\frac{h}{2}$ and the fold angles ρ_1 and ρ_2 :

$$d = \frac{h}{\sin a} \tag{44}$$

Where:

$$a = 180^\circ - \rho_2$$

$$h = 2 \times \text{thickness of the panel}$$

$$d = \text{double line offset distance}$$

Once doubled the critical creases with the correct offset, we thickened the panels and tapered them. The tapering angle is given by half the fold angle at blocked state. The preliminary prototype shown in Figure 156 has been fabricated by 3D-printing the tapered panels that we glued to a sheet of plastic film (Tyvek). Subsequently, we glued the bottom three faces of the seat and the back. After verified the correct behaviour of the small-scale model, we realized a prototype at human-scale with a plastic sandwich panel with a thickness of 9 mm, that we folded and cut with CNC machine.

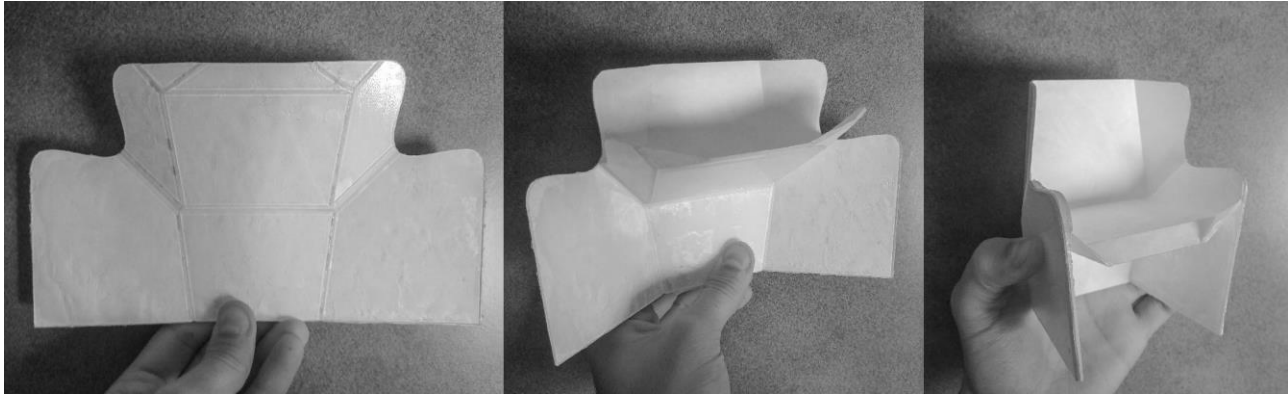


Figure 156: one-DOF thick rigid non-flat-foldable developable chair, prototype.

6.3.3. Blocked Degree-4 Vertex – From a Non-Developable Corner of 3 Faces

The tests we made on human-sized prototype highlighted some issues about the ergonomics, the weight, the portability, the stiffness and the size. We started correcting all these problems by re-modelling the zero-thickness digital model starting from the blocking vertices. To enhance the stiffness of the seat, we decided to change the pattern of the structure on the front making all the four vertices of the seat blocking at the same time, to do so we had to develop a method to work directly on the three-dimensional model while preserving the developability of the pattern.

The method we propose here is based on graphical constructions and a few trivial algebraic calculations. This method allows the designer to transform any non-developable corner of three faces into a developable degree-4 non-flat-foldable vertex. In this way, the designer can work directly on the three-dimensional folded model instead of working only on the unfolded CP. This method uses a zero-thickness mesh with planar faces, thus the thickness of the panels is not considered yet.

Any three-faces non-developable corner can be developed by cutting along any of the three edges splitting two faces. Thus, when we develop it, a gap will form between the two split faces.

Because we want to make it developable, we must fill that gap by extending one of the two split faces matching the bisector of the gap and adding an additional face in the remaining empty angle. Once refolded the three-faces corner the added face and the extended face will exceed outside the corner along the same plane of the extended faces. For each edge, there are only two possible directions to which the exceeding part can be oriented. Thus, the possible developable degree-4 single vertex patterns, into which any three-faces corner can be transformed, are six in total as shown in Figure 157.

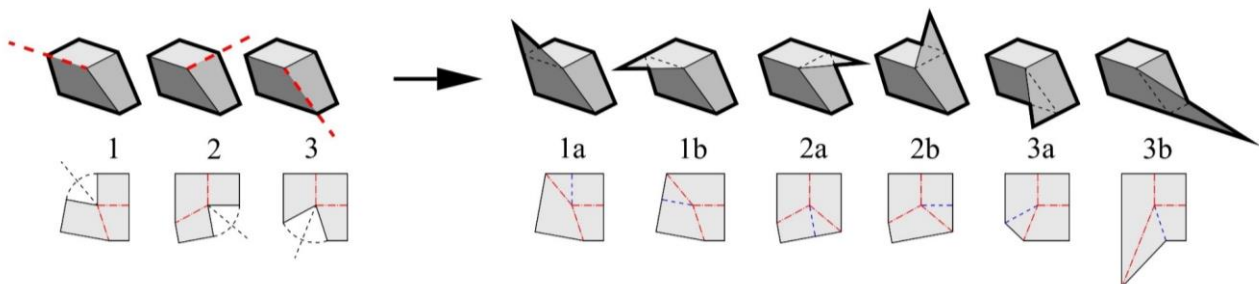


Figure 157: on the left: all the possible developments of the same three-faces corner cutting along the 3 edges; on the right: all the possible degree-4 single vertex patterns without cuts.

To transform any non-developable corner of three faces into a developable degree-4 vertex by graphical approach, apply the following steps. (1) Chose the edge to be cut, of a given three-faces three-dimensional corner (three possible choices). (2) Extend one of the faces adjacent to the chosen edge (two possible choices). (3) Measure the total angle at the corner of the 3 starting faces, subtract that angle to 360° , and divide the result by two. (4) Draw a reference line along the chosen edge. (5) Rotate the reference line around the corner of the calculated angle (the rotation happens in the same plane of the extended face, with the centre of rotation in the corner). (6) Cut the extended face with the rotated reference line. (7) Draw an overlapped triangle on the outside triangular extrusion to close the loop of 4 faces. (8) This poly-surface made by 4 faces can now be developed in-plane without ripping, stretching or bending it. The proposed method has been implemented using Grasshopper (Rutten, n.d.) and the full definition can be consulted in Appendix

6.3.5. Human-Size Prototype of the Chair - Critical Observations

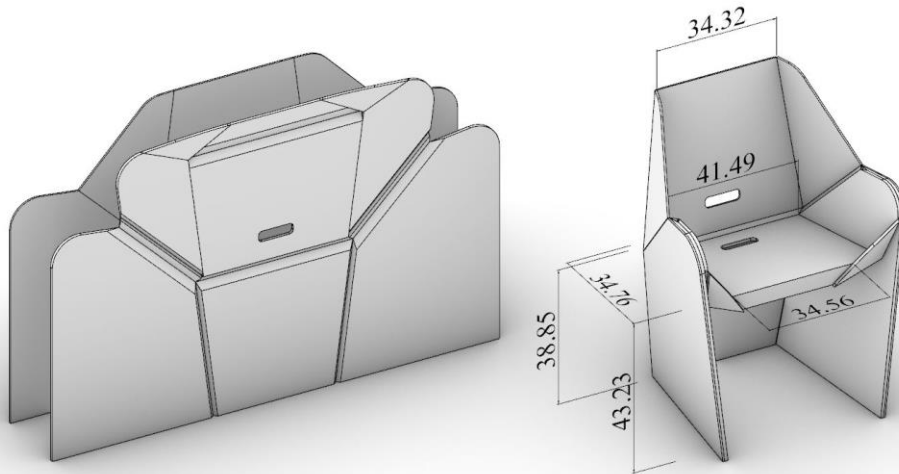


Figure 160: corrected design with better size, weight and ergonomics.

In Figure 160 we reported the final digital model which was subsequently produced by Kawakami Sangyo company by CNC cutting and attaching two plastic sandwich boards that they call “Plaperl”. This sandwich panel consists of two plastic boards with vacuum-formed cylinder in between. It has excellent rigidity and lightweight and it is made of polyolefin that does not create toxic gases such as hydrogen chloride and dioxin. Thus, it is environmentally friendly and excellent in recycling¹⁰². However, this material may not be the optimal choice for what concerns the aesthetics, because once creased or cut it exposes the inside core which is not very appealing. A close-up picture of exposed inside core of this material is shown in Figure 161. The final physical prototype at human-scale is shown in Figure 162 and Figure 163



Figure 161: detail of a section of the full-size prototype of the chair; to temporarily solve the limitations of the CNC machine, the company decided to take off one of the two protective layers to loosen up the hinges and partially solve a problem caused by the limited maximum angle of cut, when in use this area will be occluded to the view.

¹⁰² <http://www.putiputi.co.jp/en/>



Figure 162: unfolded and folded chair prototype at human-scale.



Figure 163: chair prototype in use.

The human-size prototype works almost as expected, but it has some critical points that should be studied further, discussed and improved. We report below some observations about the human-scale prototype that were also possible thanks to the comments of the users that examined the product¹⁰³.

- It has a unique original look that exposes the production process and folding function without losing the ergonomic shape and its elegant attractive simplicity. However, the sandwich panel exposes the core section at the edges of the panels, and in some other areas, which is acceptable for study experimental models or temporary use, but not for a final product and long-term use. The research of a better material is still in progress, we are thinking to use a semi-rigid felt-based material which is light enough, comfortable, but still rigid, easy to crease and durable even if folded and unfolded several times.
- The structural stability of the chair at folded state is satisfactory, it has no tendency of instability in rotational movement around the vertical axis, but when loaded it tends to generate a local buckling at the midpoint of the front mountain fold in the seat. We expected this kind of elastic/plastic deformations in some areas of the chair,

¹⁰³ In particular these observations were possible thanks to Prof. Yoshinobu Miyamoto who reviewed carefully the thesis and the chair.

the prototype was also made to verify this kind of problems in all day use. To solve it we could use a thicker panel for the seat or add a reinforced ribbon where the deformations occur¹⁰⁴.

- The minimal thickness when unfolded is remarkable, however, the overall dimension at flat state is three times larger than a typical foldable chair with armrests. To solve this problem the pattern may be improved by adding one or more transversal creases that activate only at flat state to be able to fold it in half once flattened. An additional crease in the middle may help to avoid the buckling effect mentioned earlier, however, it may also compromise the stiffens at folded state, more tests are needed before drawing any conclusions.
- The panels used are not perfectly rigid, thus the bending of the faces causes the chair to not behave like a perfect rigid one-DOF mechanism. Unfortunately, we have no examples of realized origami mechanisms that behave like perfect one-DOF rigid mechanisms as in the simulations, thus a non-perfect rigid behaviour was expected. Filipov, Tachi and Paulino studied an approach to improve the preservation of rigidity during folding and unfolding by over-constraining the faces, glueing more folded sheets together with particular orientations to counterbalance the dynamic deformations (Filipov, Tachi, & Paulino, 2015). However, this approach, for now, has been only tested on tubular structures, which are not comparable to the chair at its actual version. Nevertheless, in this project, there are a small number of internal vertices, and the actuation of the folding and unfolding can be easily helped by the user even if it is not a perfect rigid one-DOF mechanism. Thus, we considered acceptable a non-perfect rigid behaviour for now. In addition, the chosen material, and the manufacturing process are not optimal yet, thus improving these points would probably improve also the overall kinematics of the chair.
- Residual deformation tends to open the chair at flat state. This problem is probably also solvable changing the material, however, the residual deformation in this type of foldable furniture can be considered as an advantage because the memory of the material helps to avoid pop-up and pop-down problems at the beginning of the folding phase. We added a clip and a belt to keep the model flat, the same belt is used to stabilize the chair at the folded configuration
- Wrong cut angles make the adjacent panels to push one against each other causing a resistance when almost reached the folded configuration. This is a crucial problem, the tapering of the panels is strictly related to the fold angle at folded configuration, thus a wrong tapering angle may cause instability, or it may cause the mechanism to block before reaching the final configuration. Fortunately, even if the CNC machine used is not designed to cut at any angle, we were able to achieve a satisfactory result exploiting the elasticity of the material. However, there is still room of improvement, because the pushing panels causes the chair to hardly keep the folded configuration and it causes a misalignment of some panels (especially in the armrests), we solved this problem by adding external locking devices as we did for the ladder design, which help to stabilize and lock the chair at the correct folded configuration.

6.4. References – CHAPTER VI

Chen, Y., Peng, R., & You, Z. (2015). Origami of thick panels. *Science*, 349(6246), 396–400.
<https://doi.org/10.1126/science.aab2870>

Crampton, E. B. (2017). *Considering Manufacturing in the Design of Thick- Panel Origami Mechanisms*. Brigham Young University.

¹⁰⁴ To prevent, or at least limit, the occurrence of this kind of problems also to the first prototype the chair could have been modeled in advance with rigid architectural materials in 3D software such as Inventor or Fusion360.

- Edmondson, B., Lang, R. J., Morgan, M. R., Magleby, S. P., & Howell, L. L. (2015). Thick Rigidly Foldable Structures Realized by an Offset Panel Technique. *Origami 6: I. Mathematics*, 149–161.
- Filipov, E. T., Tachi, T., & Paulino, G. H. (2015). Origami tubes assembled into stiff, yet reconfigurable structures and metamaterials. *Proceedings of the National Academy of Sciences (PNAS)*, 112(40), 12321–12326. <https://doi.org/10.1073/pnas.1509465112>
- Foschi, R., & Tachi, T. (2018). Designing Self-Blocking Systems with Non-Flat-Foldable Degree-4 Vertices. *Origami 7: Engineering 1*, 795–809.
- Hoberman, C. S. (1988). Reversibly Expandable Three- Dimensional Structure. *Patent No. 4780344*. United States.
- Hull, T. C., & Tachi, T. (2017). Double-line rigid origami. *Asian Forum on Graphic Science (AFGS 2017)*.
- Klett, Y., & Drechsler, K. (2011). Designing technical tessellations. *Origami 5: Fifth International Meeting of Origami Science, Mathematics, and Education*, 5, 305–322.
- Ku, J. S., & Demaine, E. D. (2016). Folding Flat Crease Patterns with Thick Materials. *Journal of Mechanisms and Robotics*, 8(3), 1–6: 031003. <https://doi.org/10.1115/1.4031954>
- Lang, R. J., Howell, L. L., Magleby, S. P., & Nelson, T. G. (2017). Non-planar closed-loop hinge mechanism with rolling-contact hinge. *Patent No. US 2017/0219007 A1*. United States.
- Lang, R. J., Nelson, T., Magleby, S., & Howell, L. (2017). Thick Rigidly Foldable Origami Mechanisms Based on Synchronized Offset Rolling Contact Elements. *Journal of Mechanisms and Robotics*, 9(2), 021013 1-17. <https://doi.org/10.1115/1.4035686>
- Lang, R. J., Tolman, K. A., Crampton, E. B., Magleby, S. P., & Howell, L. L. (2018). A Review of Thickness-Accommodation Techniques in Origami-Inspired Engineering. *Applied Mechanics Reviews, TBD*, 70(1). <https://doi.org/doi:10.1115/1.4039314>.
- Pehrson, N. A., Magleby, S. P., Lang, R. J., & Howell, L. L. (2016). Introduction of monolithic origami with thick-sheet materials. *Proceedings of IASS Annual Symposia*, 2016(13), 1–10.
- Piker, D. (n.d.). Kangaroo Physics. Accessed June 27, 2018, from <https://www.food4rhino.com/app/kangaroo-physics>
- Rutten, D. (n.d.). Grasshopper official page. Accessed July 31, 2018, from <http://www.grasshopper3d.com/>
- Tachi, T. (2011a). One-DOF rigid foldable structures from space curves. *Proceedings of the IABSE-IASS Symposium*, 20–23.
- Tachi, T. (2011b) Rigid-Foldable Thick Origami. *Origami 5: Fifth International Meeting of Origami Science Mathematics and Education*, 253–264.
- Tedeschi, A. (2014). *AAD Algorithms-Aided Design. Parametric Strategies Using Grasshopper* (First ed.). Brienza (PO): Le Pensur Publisher.
- Trautz, M., & Kunstler, A. (2009). Deployable folded plate structures – folding patterns based on 4-fold-mechanism using stiff plates. In *Proceedings of the International Association for Shell and Spatial Structures (IASS) Symposium* (pp. 2306–2317). Valencia.
- Zirbel, S. A., Lang, R. J., Thomson, M. W., Sigel, D. A., Walkemeyer, P. E., Trease, B. P., Magleby, S. P., & Howell, L. L. (2013). Accommodating Thickness in Origami-Based Deployable Arrays 1. *Journal of Mechanical Design*, 135(11), 111005. <https://doi.org/10.1115/1.4025372>

Conclusions

As a first step into the field of origami applied to architecture and industrial design, we built a catalogue of projects and designs inspired by this universal art. This analysis confirmed that origami is often taken as a reference in architecture, furniture, manufacturing and fashion. Nevertheless, especially in the large-scale architectural projects, we observed that it is rarely used with functional intents. This may be caused by four main reasons: the lack of digital tools specifically designed for origami modelling; the fact that designing with origami is hard; the lack of specialized workforce that can build origami-like structures at architectonic scale; and the fact that kinetic architecture has higher costs of realization and maintenance than static architecture.

We focused on trying to solve the former two problems, which are a matter of drawing with the tools of descriptive geometry. Because origami has endless possibilities, and the available applications to design origami are limited in terms of design freedom, we aimed to extend the available tools without constraining them into a predefined set of new commands or into an application that performed a set of limited tasks. Thus, the new tools that we presented are in the form of a collection of original algorithms, procedures, examples and case studies that the designers can use as starting points or as references for their projects. These algorithms should help designers to understand what a good practice could be when designing with origami that requires to control shape and motion at the same time. To do that, we extensively investigated three main topics: solving the kinematics of given patterns, defining procedures to design a pattern working directly on the three-dimensional folded shape guaranteeing its developability, and solving some problems that may arise from the fabrication phase.

We studied these topics with the synthetic approach, which is the approach usually used by architects and designers, and which is the counterpart of the analytical approach. In most of the cases involving designing with origami, the synthetic method is highly preferable to the analytical method because it permits to visualise, and thus understand better procedures and results. Furthermore, it is easier to be used by who do not have a background in mathematics or computer science and, at the same time, we believe (supported by ancient and recent thinkers) that, in some cases, it has the same power and dignity of the analytical method. Therefore, it can be used not only as a visualization tool but also as a researching tool. To study and present the procedures solved with the synthetic method, we used Grasshopper (and relative add-ons), because it is one of the most used tools that architects and designers already use for parametric and computation modelling. Specific applications for designing origami exist, and we studied, used and reviewed most of them, but they usually absolve specific tasks that limit the design freedom. Contrariwise, with the parametrical approach, the possibilities are practically endless, and we can integrate the origami model directly into the environment where it is applied. In this way, we can directly extract pieces of information from other objects, like the distance from other buildings, the proportions and shape of the structure, the position of the sun and the direction of the light, the length of anchoring cables or support rails, and use them as design constraints or as references and inputs of our generative algorithms. We also highlighted the importance of working with software already used by professionals, because limiting the file conversions between different applications helps decreasing problems like incompatibility and data loss that may slow down or even obstruct the working process.

Before starting working on these topics, we put some effort into defining some fundamental aspects of origami theory that everyone who wants to approach this field should know. The fundamental aspects of origami that we carefully defined are the fold angle, the developability, the degree of freedom, the rigid-foldability, the flat-foldability and the non-flat-foldability. We reported the textual definition and the known algebraic formulations (where present and needed) of each subject, clarifying their meaning for a clearer and smoothing reading of the following chapters. These definitions are not only to be considered as an introductory part, but they were useful to carry out the comparison between the analytical algebraic method and the synthetic method. While studying known problems we also developed a new algebraic simplified approach that solves the problem of identifying the blocking crease and relative fold angles at blocked state in a non-flat-foldable degree-4 single vertex. This discovery was an original contribution for the study of the degree-4 non-flat-foldable vertices.

With these premises, we made a catalogue of algorithms aimed to generate and solve the kinematics of specific rigid-foldable patterns, starting from easiest cases (patterns with a single crease) up to more complex cases (patterns with multiple internal degree >4 vertices). These algorithms should help the designers solving the kinematics of the most known and useful patterns that they may want to use in their projects while designing kinetic structures inspired by origami. Subsequently, we verified the validity, robustness and usefulness of the presented catalogue of generative algorithms by exemplifying their use into possible design workflows of buildings, furniture and objects, reproducing some existing projects, choosing them among the ones that we collected. We used parametrical strategies for modifying the output folded shapes and obtaining new shapes and looks. The main purpose of these workflows was not to solve

the kinematics of the patterns, but to design a specific CP from some given framework conditions or reference shapes rails and structures, by following precise constructive procedures that guaranteed the generation of a folded developable surface.

Lastly, we focused on finding out which are the main problems that could arise from fabrication and how to solve them. We described the constructive processes of two original projects: a foldable chair and a foldable ladder. We presented them from start to finish describing carefully every generative step, from the idea to the prototyping, passing from the study of kinematics, stability, flexibility, anchoring, locking and thickening. We studied and tested many different thickening known methods, and we concluded that, for our cases, the “Double line” method by Tachi and Hull was the most efficient and versatile. It consists into doubling the critical creases (the blocking crease or creases, and one or more adjacent crease if needed) at every internal vertex and solving the intersections of the newly generated creases by making a closed loop of new creases that generates only flat-foldable degree-4 vertices. This method has three main characteristics. It guarantees material continuity without the need of adding holes at internal vertices and without needing any assembling. It preserves the original kinematics of the faces of the original zero-thickness pattern. Furthermore, it lies on the same plane when unfolded and all the creases can be marked by half cutting, carving or stamping generating grooves with specific tapering angles on the same side of the panel. For these reasons, the pattern, that results by applying the double line method, is easier to fabricate compared to other thickening methods, with automated processes like milling (with CNC machines) or folding (with folding machines). We highlighted the importance of designing by comparing the physical paper prototype with the digital model because both of them approximate some aspects of the final thick-panels prototype. Both the physical and the digital models are not self-sufficient, and we must always compare them to limit the risk of misinterpretation and bad designing.

Outlook

Future works may focus on non-developable degree-4 vertices. Their characteristic of being single-flat-foldable or double-flat-foldable has not been extensively studied yet. It may open new possibilities to solve the pop-up and pop-down problem in one-DOF mechanisms. At the same time, degree-4 non-developable vertices can preserve or even improve the compactness of the folded and unfolded pattern while still having a self-blocking configuration. Both the ladder and the chair designs could benefit from this type of vertices. The improvement of the chair and the ladder will probably be a future work of the author. In addition, some companies have demonstrated interest to produce them for commercial purposes. Furthermore, it may be challenging and inspiring to further develop the field of responsive folded surfaces, as we did not explore it in depth in this thesis, and it is a major topic in the field of architecture. Another interesting topic worthy of study is the implementation of accurate elastic deformations into the virtual simulations. We could implement it into Grasshopper (and relative plugs-ins like Karamba) or other software like Fusion 360, Merlin2 and Inventor.

In conclusion, our wish is that this thesis could help developing new origami-related projects more efficiently and, could inspire researchers who are just beginning their journey into this interesting scientific and artistic field.

Bibliography

Abel, Z., Cantarella, J., Demaine, E. D., Eppstein, D., Hull, T. C., Ku, J. S., Lang, R. J., & Tachi, T. (2016). Rigid Origami Vertices: Conditions and Forcing Sets. *Journal of Computational Geometry*, 7(1), 171–184.

<https://doi.org/10.20382/jocg.v7i1a9>

Akitaya, H. A., Cheung, K. C., Demaine, E. D., Horiyama, T., Hull, T. C., Ku, J. S., & Tachi, T. (2016). Box Pleating is Hard. *Discrete and Computational Geometry and Graphs*, 9943, 167–179.

Autodesk. (n.d.). Dynamo. Accessed February 4, 2019, from <https://dynamobim.org/>

Bateman, A. (n.d.). Tess. Accessed September 6, 2016, from <http://www.papermosaics.co.uk/software.html>

Belcastro, S. M., & Hull, T. C. (2002). Modelling the folding of paper into three dimensions using affine transformations. *Linear Algebra and Its Applications*, 348(1–3), 273–282. [https://doi.org/10.1016/S0024-3795\(01\)00608-5](https://doi.org/10.1016/S0024-3795(01)00608-5)

Bhooshan, S. (2015). *Interactive Design of Curved-Crease-Folding*. University of Bath.

Bhooshan, S. (2016). Upgrading Computational Design. *Architectural Design*, 86(2), 44–53. <https://doi.org/https://doi.org/10.1002/ad.2023>

Bhooshan, S., Bhooshan, V., El-Sayed, M., Chandra, S., Richens, P., & Shepherd, P. (2015). Applying dynamic relaxation techniques to form-find and manufacture curve-crease folded panels. *Simulation*, 91(9), 773–786. <https://doi.org/10.1177/0037549715599849>

Brandt-Olsen, C. S. (2016). *Calibrated Modelling of Form-active Structures*. The Technical University of Denmark.

Buffart, H., Hoffmann, S., Paris, J., Siebrecht, J., Corves, B., & Trautz, M. (2017). Non-flat folding mechanisms for structural purposes. *Proceedings of IASS Annual Symposia, 2017(13)*, 1-8.

Buffart, H., Hoffmann, S., Paris, J., Weigel, C., Siebrecht, J., Corves, B., & Trautz, M. (2018). Folding Mechanisms with Discriminate Extremal Configurations for Structural Purposes. *Origami 7: Engineering 1*, 685–697.

Buri, H., & Weinand, Y. (2008). ORIGAMI-folded plate structures, architecture. *10th World Conference on Timber Engineering*, 2–5.

Cardone, V. (2017). *Gaspard Monge, padre dell'ingegnere contemporaneo*. Rome: DEI Tipografia del genio civile.

Carlevaris, L., De Carlo, L., & Migliari, R. (2012). *Attualità della geometria descrittiva*. Gangemi editore.

Casale, A., & Calvano, M. (2012). House of cards. The fold for the construction of articulated surfaces. *Disegnarecon*, 9, 289–300.

Casale, A., Valenti, G. M., & Calvano, M. (2013). *Architettura delle superfici piegate: le geometrie che muovono gli origami*. Roma: Edizioni K.

Chandra, S., Bhooshan, S., & El-Sayed, M. (2015). Curve-Folding Polyhedra Skeletons through Smoothing. *Origami 6: I. Mathematics*, 231.

Chandra, S., Körner, A., Koronaki, A., Spiteri, R., Amin, R., Kowli, S., & Weinstock, M. (2015). Computing curved-folded tessellations through straight-folding approximation. *Proceedings of the Symposium on Simulation for Architecture & Urban Design*, 152–159.

- Chen, Y., Peng, R., & You, Z. (2015). Origami of thick panels. *Science*, 349(6246), 396–400. <https://doi.org/10.1126/science.aab2870>
- Crampton, E. B. (2017). *Considering Manufacturing in the Design of Thick- Panel Origami Mechanisms*. Brigham Young University.
- Demaine, E. D. (n.d.). .Fold file format. Accessed February 4, 2019 from <https://github.com/edemaine/fold>
- Demaine, E. D., Demaine, M. L., Huffman, D. A., Koschitz, D., & Tachi, T. (2015). Characterization of curved creases and rulings: design and analysis of lens tessellations. *Origami 6*, 209–230.
- Demaine, E. D., Demaine, M. L., Huffman, D. A., Hull, T. C., Koschitz, D., & Tachi, T. (2016). Zero-Area Reciprocal Diagram of Origami. *Proceedings of IASS Annual Symposia*, 2016(13), 1-10.
- Demaine, E. D., Demaine, M. L., Huffman, D. A., Koschitz, D., & Tachi, T. (2018). Conic crease patterns with reflecting rule lines. *Origami 7: Mathematics*, 573–589.
- Demaine, E. D., Demaine, M. L., Koschitz, D., & Tachi, T. (2011). Curved crease folding: a review on art, design and mathematics. *Proceedings of the IABSE-IASS Symposium: Taller, Longer, Lighter (IABSE-IASS2011)*, 20–23.
- Demaine, E. D., & O'Rourke, J. (2007). *Geometric folding algorithms: linkages, origami, polyhedra*. New York: Cambridge University Press.
- Demaine, E. D., & Tachi, T. (2010). Lecture 23 Video, Architectural Origami. Accessed October 1, 2018, from <http://courses.csail.mit.edu/6.849/fall10/lectures/L23.html>
- Dias, M. A., Dudte, L. H., Mahadevan, L., & Santangelo, C. D. (2012). Geometric mechanics of curved crease origami. *Physical Review Letters*, 109(11), 114–301. <https://doi.org/10.1103/PhysRevLett.109.114301>
- Edmondson, B., Lang, R. J., Morgan, M. R., Magleby, S. P., & Howell, L. L. (2015). Thick Rigidly Foldable Structures Realized by an Offset Panel Technique. *Origami 6: I. Mathematics*, 149–161.
- Epps, G. (n.d.). Robofold. Accessed February 14, 2016, from <http://www.robifold.com/>
- Epps, G. (2014). Robofold and Robots.Io. *Architectural Design*, 84(3), 68–69. <https://doi.org/https://doi-org.ezproxy.unibo.it/10.1002/ad.1757>
- Epps, G., & Verma, S. (2013). Curved Folding: Design to Fabrication process of RoboFold. *Proceedings of SMI/ISAMA2013 (Shape Modelling International): the Thirteenth Interdisciplinary Conference of the International Society of the Arts, Mathematics, and Architecture*, 75–83.
- Fallavollita, F. (2008). L'estensione del problema di Apollonio nello spazio e L'Ecole Polytechnique. *Ikhnos*, 1, 29–42.
- Fallavollita, F., & Salvatore, M. (2013). La costruzione degli assi principali delle superfici quadriche. *Disegnare Idee Immagini*, 46, 42–51.
- Feder, T. (2018). Q&A: Robert Lang, origami master. *Physics Today, People and History*, (January). <https://doi.org/10.1063/PT.6.4.20180108a>
- Filipov, E. T., Tachi, T., & Paulino, G. H. (2015). Origami tubes assembled into stiff , yet reconfigurable structures and metamaterials. *Proceedings of the National Academy of Sciences (PNAS)*, 112(40), 12321–12326. <https://doi.org/10.1073/pnas.1509465112>
- Foschi, R. (2017). Conformation of a Flexible Miura Pattern on a Double Curvature Surface. *Proceedings of the 11th Asian Forum on Graphic Science AFGS2017, (USB)*, 1–10.

- Foschi, R., & Tachi, T. (2018). Designing Self-Blocking Systems with Non-Flat-Foldable Degree-4 Vertices. *Origami 7: Engineering 1*, 795–809.
- Furuto, A. (2012). Resonant Chamber / rvtr. Accessed December 29, 2018 from <https://www.archdaily.com/227233/resonant-chamber-rvtr>
- Gattas, J. M., & You, Z. (2016). Design and digital fabrication of folded sandwich structures. *Automation in Construction*, 63, 79–87. <https://doi.org/10.1016/j.autcon.2015.12.002>
- Ghassaei, A. (n.d.). Origami Simulator. Accessed July 31, 2018, from <http://apps.amandaghassaei.com/OrigamiSimulator/>
- Hatori, K. (2011). History of Origami in the East and the West before Interfusion. *Origami 5: Fifth International Meeting of Origami Science, Mathematics, and Education*, 3–11.
- Hoberman, C. S. (1988). Reversibly Expandable Three- Dimensional Structure. *Patent No. 4780344*. United States.
- Huffman, D. A. (1976). Curvature and Creases: A Primer on Paper. *IEEE Transactions on Computers*, C-25(10), 1010–1019. <https://doi.org/10.1109/TC.1976.1674542>
- Huffman, D. A. (1977). Surface curvature and applications of the dual representation. *Workshop on Computer Vision Systems*, 213–222
- Hull, T. C. (n.d.). Tom Hull's page. Accessed February 4, 2019, from <http://mars.wne.edu/~thull/>
- Hull, T. C. (2003a). Counting mountain/valley assignments for flat folds. *Ars Combinatoria*, 67, 175–187.
- Hull, T. C. (2003b). Origami and Geometric Constructions: a comparison between straight edge and compass constructions and origami. Accessed February October 10, 2018, from <http://mars.wne.edu/~thull/omfiles/geoconst.html>
- Hull, T. C. (2006). *Project origami*. New York: A K Peters/CRC Press.
- Hull, T. C., & Tachi, T. (2017). Double-line rigid origami. *Asian Forum on Graphic Science (AFGS 2017)*.
- Jacques, J. (1989). Résolution par le pliage de l'équation du troisième degré et applications géométriques. *Proceedings of the First International Meeting of Origami Science and Technology*. Ferrara, Italy.
- Kawaguchi, K., Ohsaki, M., Takeuchi, T., Liu, K., & Paulino, G. H. (2016). MERLIN: A MATLAB implementation to capture highly nonlinear behavior of non-rigid origami. *Proceedings of IASS Annual Symposia (International Association for Shell and Spatial Structures)*, 2016(13), 1–10.
- Khademzadeh, H. R., & Mazaheri, H. (2007). Some results to the Huzita axioms. *International Mathematical Forum*, 2(14), 699–704.
- Kilian, M., Flöry, S., Chen, Z., Mitra, N. J., Sheffer, A., & Pottmann, H. (2008). Curved folding. *ACM Transactions on Graphics (TOG)*, 27(3), 75.
- Klett, Y., & Drechsler, K. (2011). Designing technical tessellations. *Origami 5: Fifth International Meeting of Origami Science, Mathematics, and Education*, 5, 305–322.
- Ku, J. S., & Demaine, E. D. (2016). Folding Flat Crease Patterns with Thick Materials. *Journal of Mechanisms and Robotics*, 8(3), 1–6: 031003. <https://doi.org/10.1115/1.4031954>
- Kuribayashi, K., Tsuchiya, K., You, Z., Tomus, D., Umemoto, M., Ito, T., & Sasaki, M. (2006). Self-deployable origami stent grafts as a biomedical application of Ni-rich TiNi shape memory alloy foil. *Materials Science and Engineering A*, 419(1–2), 131–137. <https://doi.org/10.1016/j.msea.2005.12.016>

- Lang, R. J. (2003). *Origami design secrets: mathematical methods for an ancient art*. Wellesley: A.K. Peters.
- Lang, R. J. (2008). The math and magic of origami. *TED talk*. ted.com. Accessed June 21, 2018, from https://www.ted.com/talks/robert_lang_folds_way_new_origami#t-156890
- Lang, R. J. (2011). *Origami design secrets: mathematical methods for an ancient art (Second ed.)*. Boca Raton, FL, USA: CRC Press.
- Lang, R. J. (2015a). Air Bag Folding. *Self-Published*. Accessed April 10, 2018, from <https://langorigami.com/article/airbag-folding/>
- Lang, R. J. (2015b). Origami and geometric constructions. *Self-Published*, 1–55. Accessed April 10, 2018 from http://langorigami.com/science/hha/origami_constructions.pdf
- Lang, R. J. (2015c). Treemaker. Accessed April 10, 2018, from <https://langorigami.com/article/treemaker/>
- Lang, R. J. (2016). Huzita-Justin Axioms. Accessed January 1, 2017, from <http://www.langorigami.com/article/huzita-justin-axioms>
- Lang, R. J. (2018). *Twists, Tilings and Tessellations. Mathematical methods for Geometric Origami. (First ed.)*. Boca Raton, FL, USA: K Peters/CRC Press.
- Lang, R. J., Howell, L. L., Magleby, S. P., & Nelson, T. G. (2017). Non-planar closed-loop hinge mechanism with rolling-contact hinge. *Patent No. US 2017/0219007 A1*. United States.
- Lang, R. J., Magleby, S. P., & Howell, L. L. (2016). Single-Degree-of-Freedom Rigidly Foldable Cut Origami Flashers. *Journal of Mechanisms and Robotics*, 8(3), 31005–31015. <https://doi.org/10.1115/1.4032102>
- Lang, R. J., Nelson, T., Magleby, S., & Howell, L. (2017). Thick Rigidly Foldable Origami Mechanisms Based on Synchronized Offset Rolling Contact Elements. *Journal of Mechanisms and Robotics*, 9(2), 021013 1-17. <https://doi.org/10.1115/1.4035686>
- Lang, R. J., Tolman, K. A., Crampton, E. B., Magleby, S. P., & Howell, L. L. (2018). A Review of Thickness-Accommodation Techniques in Origami-Inspired Engineering. *Applied Mechanics Reviews, TBD*, 70(1). <https://doi.org/doi:10.1115/1.4039314>.
- Le Klint, P. V. J. (n.d.). The story of LE KLINT. Accessed July 19, 2018, from <https://www.leklint.com/en-GB/About-LE-KLINT/History.aspx>
- Letellier, D. (2010). Tessel. Accessed November 29, 2018, from <https://www.davidletellier.net/TESSSEL>
- Liu, K., & Paulino, G. H. (2018). Highly efficient nonlinear structural analysis of origami assemblages using the MERLIN2 software. *Origami* 7, 4, 1167–1182.
- Loria, G. (1935). *Metodi matematici: essenza, tecnica, applicazioni*. (U. Hoepli, Ed.). Milano.
- McNeel (n.d.). Rhinoceros. Accessed August 20, 2010, from <https://www.rhino3d.com/>
- Migliari, R. (2008). Il problema di Apollonio e la Geometria descrittiva. *Disegnare Idee Immagini*, 36, 22–37.
- Migliari, R. (2008). Rappresentazione come sperimentazione. *Ikhnos, Analisi gr*, 11–28.
- Migliari, R. (2009a). *Geometria Descrittiva - metodi e costruzioni (Vol. 1)*. Novara: Città Studi edizioni.
- Migliari, R. (2009b). *Geometria Descrittiva - tecniche e applicazioni (Vol. 2)*. Novara: Città Studi edizioni.
- Migliari, R. (2012). Descriptive Geometry: From its Past to its Future. *Nexus Network Journal*, 14(3), 555–571. <https://doi.org/10.1007/s00004-012-0127-3>

- Mitani, J. (n.d.). Jun Mitani's page. Accessed March 12, 2018, from <http://mitani.cs.tsukuba.ac.jp/en/>
- Mitani, J. (2009). A design method for 3D origami based on rotational sweep. *Computer-Aided Design and Applications*, 6(1), 69–79. <https://doi.org/10.3722/cadaps.2009.69-79>
- Mitani, J., & Igarashi, T. (2011). Interactive Design of Planar Curved Folding by Reflection. *Pacific Conference on Computer Graphics and Applications - Short Papers*, 77–81. <https://doi.org/10.2312>
- Mitchell, D. (n.d.). A brief outline of origami design history. Accessed April 10, 2017, from <http://www.origamiheaven.com/origamidesignhistory.htm>
- Miura, K. (1985). Method of Packaging and Deployment of Large Membranes in Space. *The Institute of Space and Astronautical Science report No 618*. Sagamihara, Japan.
- Miura, K. (1997). Fold - its physical and mathematical principles. *Proceedings of the Second International Meeting of Origami Science and Scientific Origami*, 41–50.
- Pehrson, N. A., Magleby, S. P., Lang, R. J., & Howell, L. L. (2016). Introduction of monolithic origami with thick-sheet materials. *Proceedings of IASS Annual Symposia*, 2016(13), 1–10.
- Piker, D. (n.d.). Kangaroo Physics. Accessed June 27, 2018, from <https://www.food4rhino.com/app/kangaroo-physics>
- Resh, R. (1992). *The Ron Resch Paper and Stick Film*. Accessed April 10, 2017, from <http://www.ronresch.org/ronresch/gallery/paper-and-stick-film/>
- Roth, R., Pentak, S., & Lauer, D. A. (2013). *Design Basics: 2D and 3D* (Eighth ed.). Boston: Wadsworth.
- Rutten, D. (n.d.). Grasshopper official page. Accessed July 31, 2018, from <http://www.grasshopper3d.com/>
- Salvatore, M. (2012). *La stereotomia scientifica in Amédée François Frézier*. Firenze: Firenze University Press.
- Schmidt, P., & Stattmann, N. (2009). *Unfolded: Paper in Design, Art, Architecture and Industry*. Birkhäuser.
- Schwinn, T. (n.d.). Sandbox Topology. Accessed June 27, 2018, from <https://www.food4rhino.com/app/sandbox-topology>
- Seymour, K., Burrow, D., Avila, A., Bateman, T., Morgan, D. C., Magleby, S. P., & Howell, L. L. (2018). Origami-Based Deployable Ballistic Barrier. *Origami 7: Engineering I*, 763–777.
- Silverberg, J. L., Evans, A. A., McLeod, L., Hayward, R. C., Hull, T., Santangelo, C. D., & Cohen, I. (2014). Using origami design principles to fold reprogrammable mechanical metamaterials. *Science*, 345(6197), 647–650. <https://doi.org/10.1126/science.1252876>
- Stachel, H. (2015). Flexible Polyhedral Surfaces with Two Flat Poses. *Symmetry*, 7(2), 774–787. <https://doi.org/10.3390/sym7020774>
- Tachi, T. (n.d.-a). Tachi's web Page. Accessed September 6, 2017, from <http://www.tsg.ne.jp/TT/>
- Tachi, T. (n.d.-b). Tachi's Software. Accessed September 6, 2017, from <http://www.tsg.ne.jp/TT/software/>
- Tachi, T. (2009). Generalization of rigid foldable quadrilateral mesh origami. *Journal of the International Association for Shell and Spatial Structures*, 50(October), 2287–2294.
- Tachi, T. (2010a). Freeform rigid-foldable structure using bidirectionally flat-foldable planar quadrilateral mesh. *Advances in Architectural Geometry 2010*, 87–102. https://doi.org/10.1007/978-3-7091-0309-8_6
- Tachi, T. (2010b). Freeform variations of origami. *Journal for Geometry and Graphics*, 14(2), 203–215.

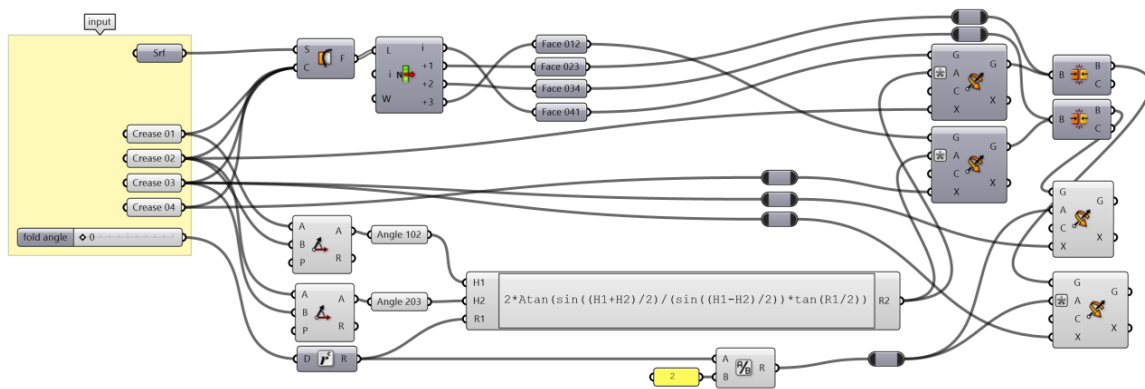
- Tachi, T. (2010c). Geometric Considerations for the Design of Rigid Origami Structures. *Proceedings of the International Association for Shell and Spatial Structures (IASS) Symposium 2010*, 12(2), 458–460. <https://doi.org/10.1016/j.mpaic.2011.07.005>
- Tachi, T. (2011a). One-DOF rigid foldable structures from space curves. *Proceedings of the IABSE-IASS Symposium*, 20–23.
- Tachi, T. (2011b) Rigid-Foldable Thick Origami. *Origami 5: Fifth International Meeting of Origami Science Mathematics and Education*, 253–264.
- Tachi, T. (2013). Composite rigid-foldable curved origami structure. *1st International Conference on Transformable Architecture*, 18–20.
- Tachi, T., & Epps, G. (2011). Designing One-DOF Mechanisms for Architecture by Rationalizing Curved Folding. *Proceedings of the International Symposium on Algorithmic Design for Architecture and Urban Design*.
- Tachi, T., & Hull, T. C. (2016). Self-foldability of Rigid Origami. *Journal of Mechanisms and Robotics*, 9(2). <https://doi.org/10.1115/1.4035558>
- Tachi, T., & Horiyama, T. (2018). 1-DOF Pattern to Fold into Multiple Polyhedra. In *7th International Meeting on Origami in Science, Mathematics and Education (7OSME)*.
- Tamasoft. (n.d.). Pepakura designer. Accessed September 6, 2016, from <http://www.tamasoft.co.jp/pepakura-en/>
- Tedeschi, A. (2014). *AAD Algorithms-Aided Design. Parametric Strategies Using Grasshopper* (First ed.). Brienza (PO): Le Penseur Publisher.
- Terzidis, K. (2006). *Algorithmic architecture*. Amsterdam [etc.]: Routledge.
- Terzidis, K. (2009). *Algorithms for visual design using the processing language*. Indianapolis: John Wiley & Sons.
- Thün, G., Velikov, K., Ripley, C., Sauv , L., & McGee, W. (2012). Soundspheres: Resonant chamber. *Leonardo*, 45(4), 348–357. https://doi.org/10.1162/LEON_a_00409
- Tolman, K., Crampton, E., Stucki, C., Mayenes, D., & Howell, L. L. (2018). Design of an Origami-Inspired Deployable Aerodynamic Locomotive Fairing. *Origami 7: Engineering 1*, 669–684.
- Trautz, M., & Kunstler, A. (2009). Deployable folded plate structures – folding patterns based on 4-fold-mechanism using stiff plates. *Proceedings of IASS Annual Symposia*, 2306–2317.
- WolframResearch. (n.d.). Mathematica. Accessed January 10, 2019, from <http://www.wolfram.com/mathematica-home-edition/>.
- Yin, S. (2009). The Mathematics of Origami. Accessed January 16, 2018, from www.math.washington.edu.
- Zirbel, S. A., Lang, R. J., Thomson, M. W., Sigel, D. A., Walkemeyer, P. E., Trease, B. P., Magleby, S. P., & Howell, L. L. (2013). Accommodating Thickness in Origami-Based Deployable Arrays 1. *Journal of Mechanical Design*, 135(11), 111005. <https://doi.org/10.1115/1.4025372>
- Zinelli, F. M. (1832). *Dei due metodi analitico e sintetico discorso dell'abate*. Venezia: Nella tipografia di Giuseppe Picotti.

Appendix A.

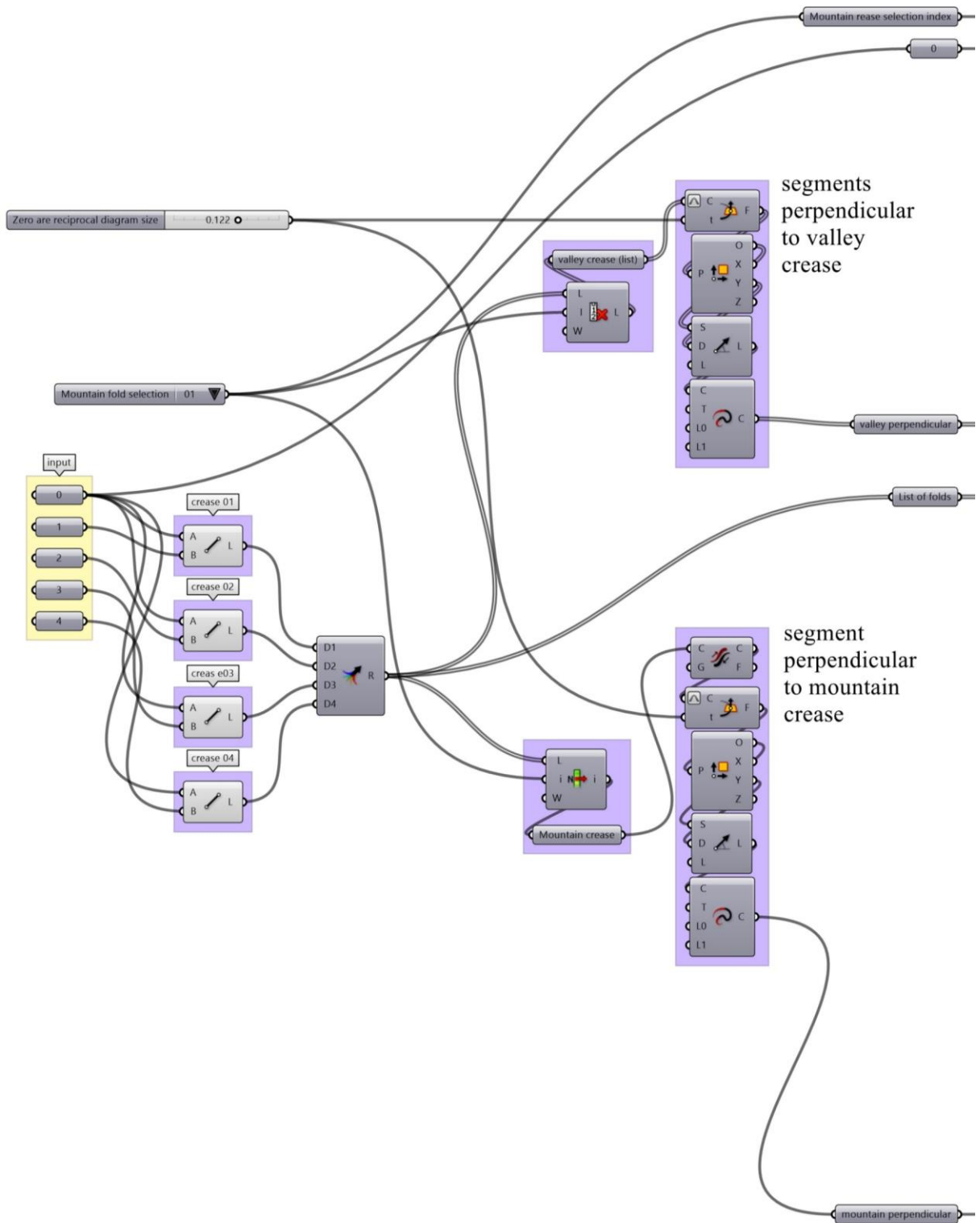
Definitions and Theorems – Generative Algorithms

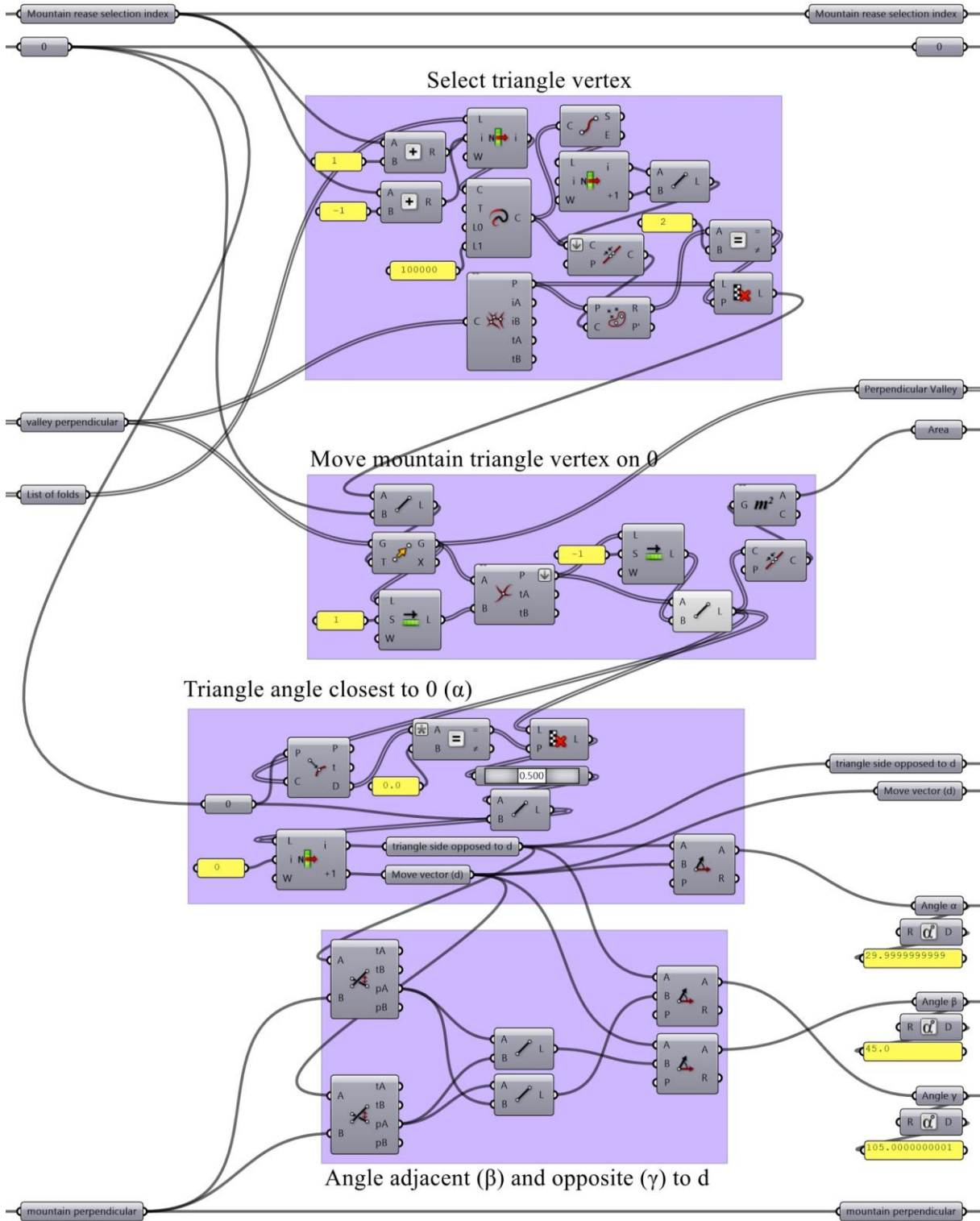
In this appendix are listed all the generative algorithms of the algorithms explained in CHAPTER III.

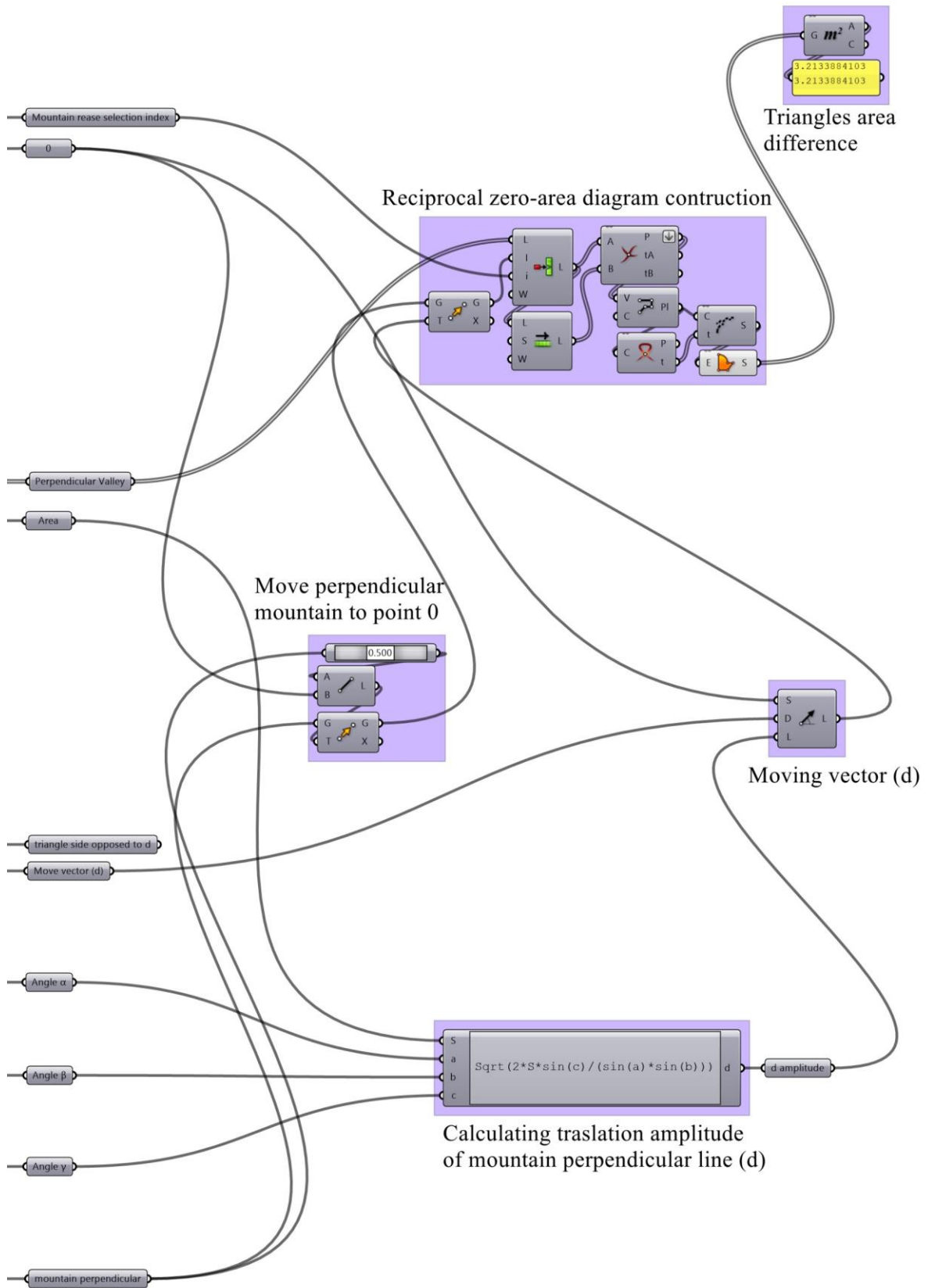
A.1. Flat-Foldable Degree-4 Single Vertex - Animation with Mathematical Formulations

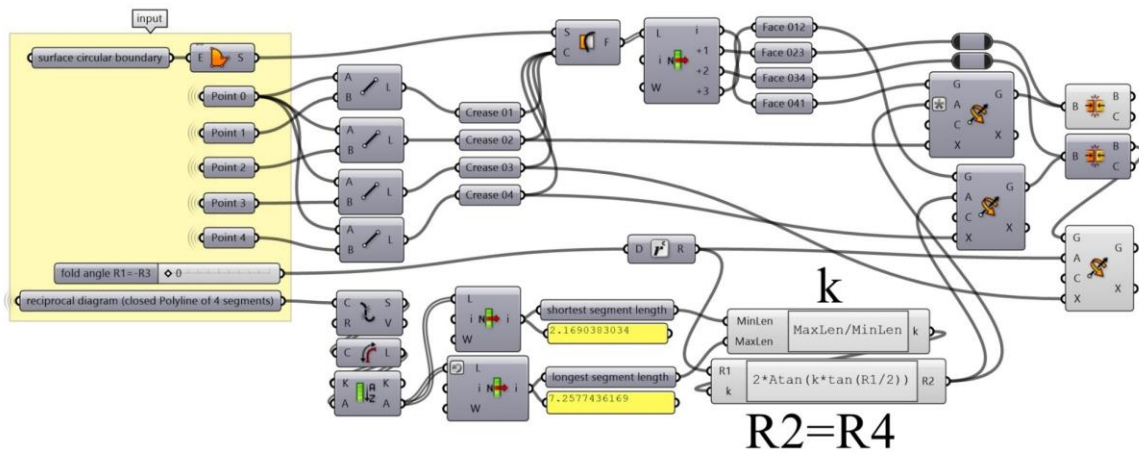


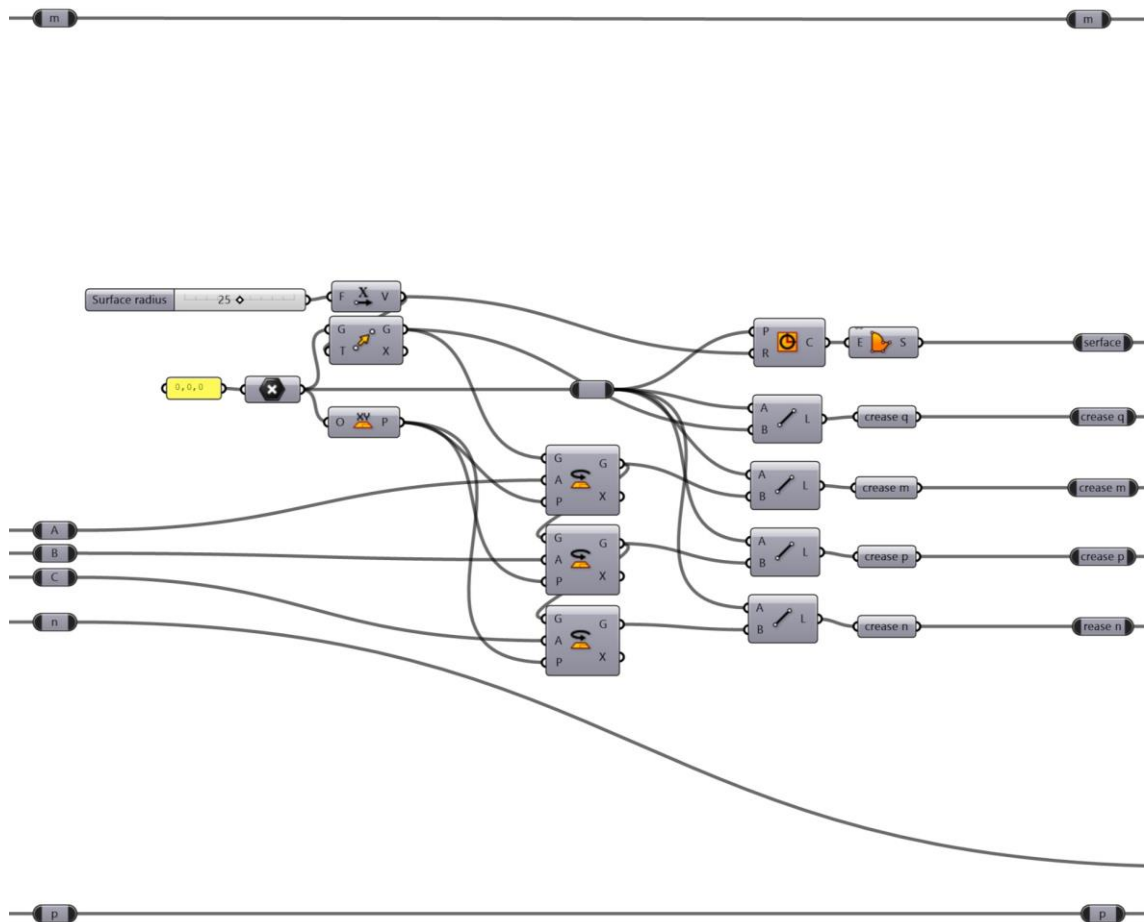
A.2. Flat-Foldable Degree-4 Single Vertex – Reciprocal Diagram Analysis as an Alternative Animation Method

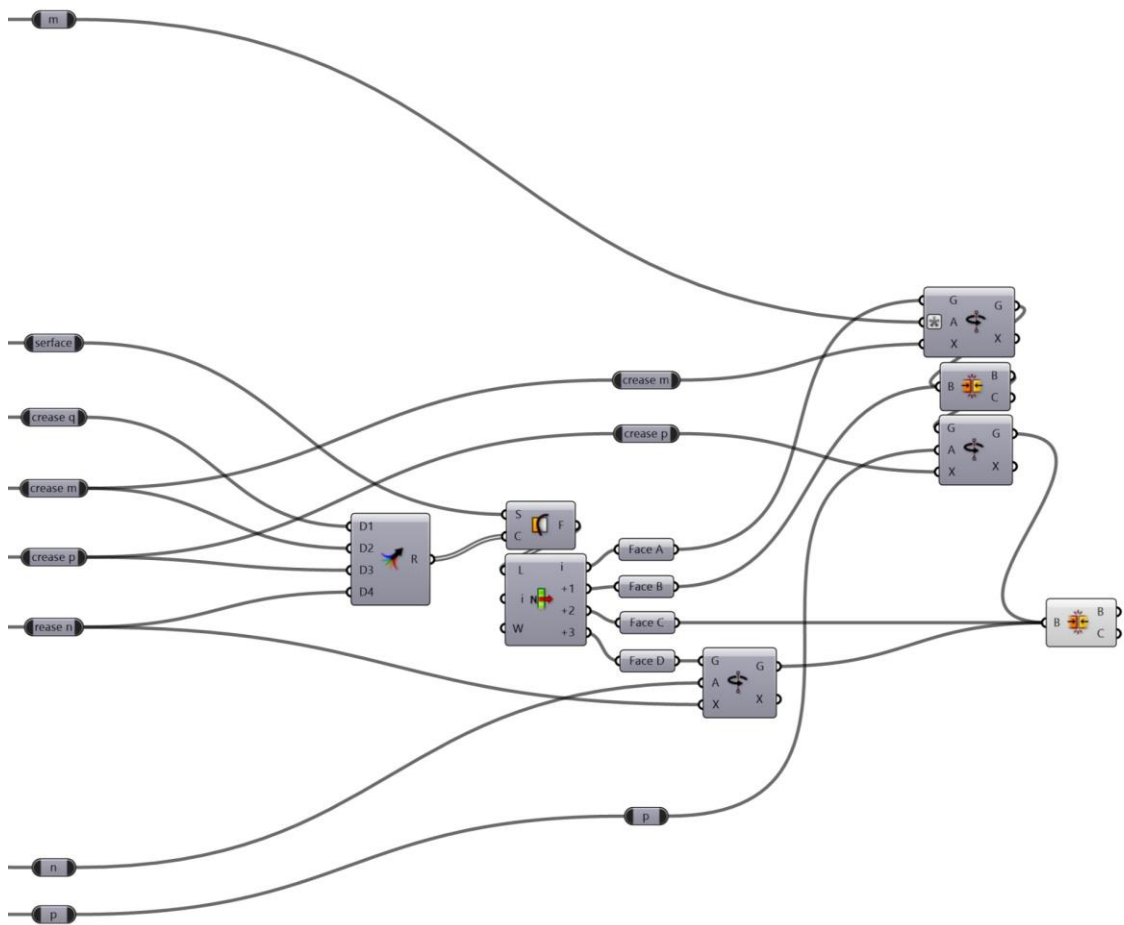




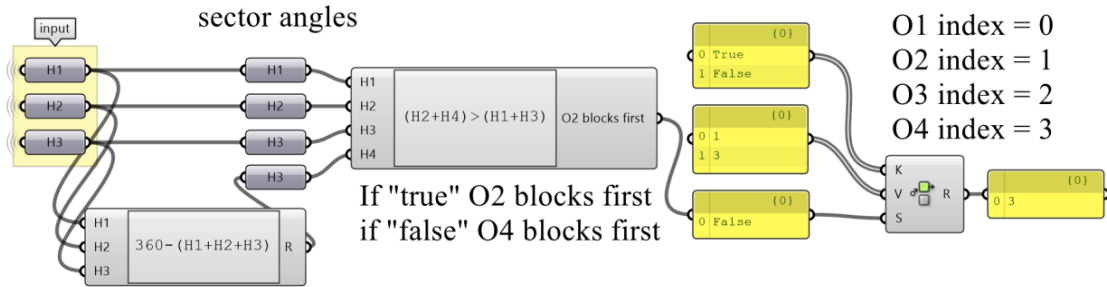








A.4. Identification of the First Blocking Crease in a Developable Degree-4 Vertex

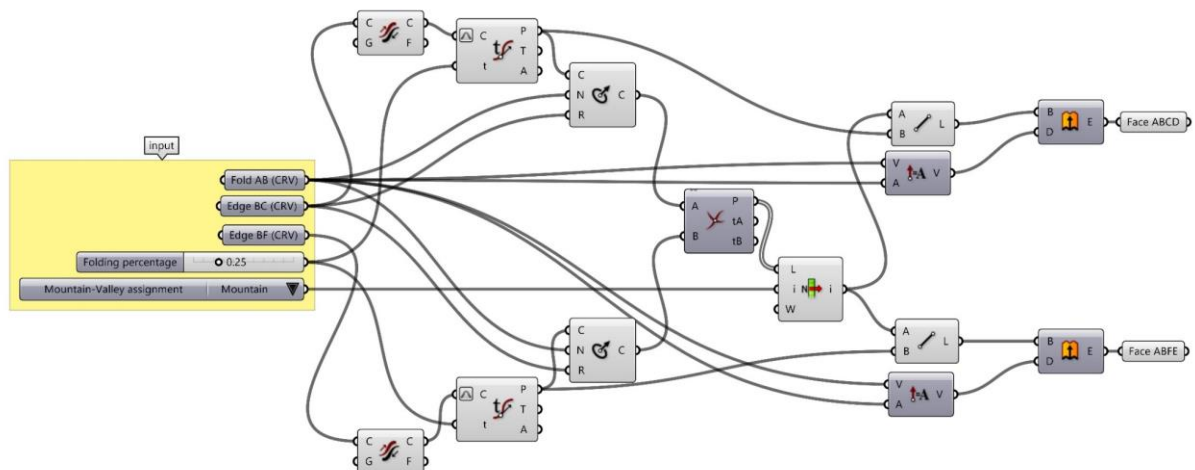


Appendix B.

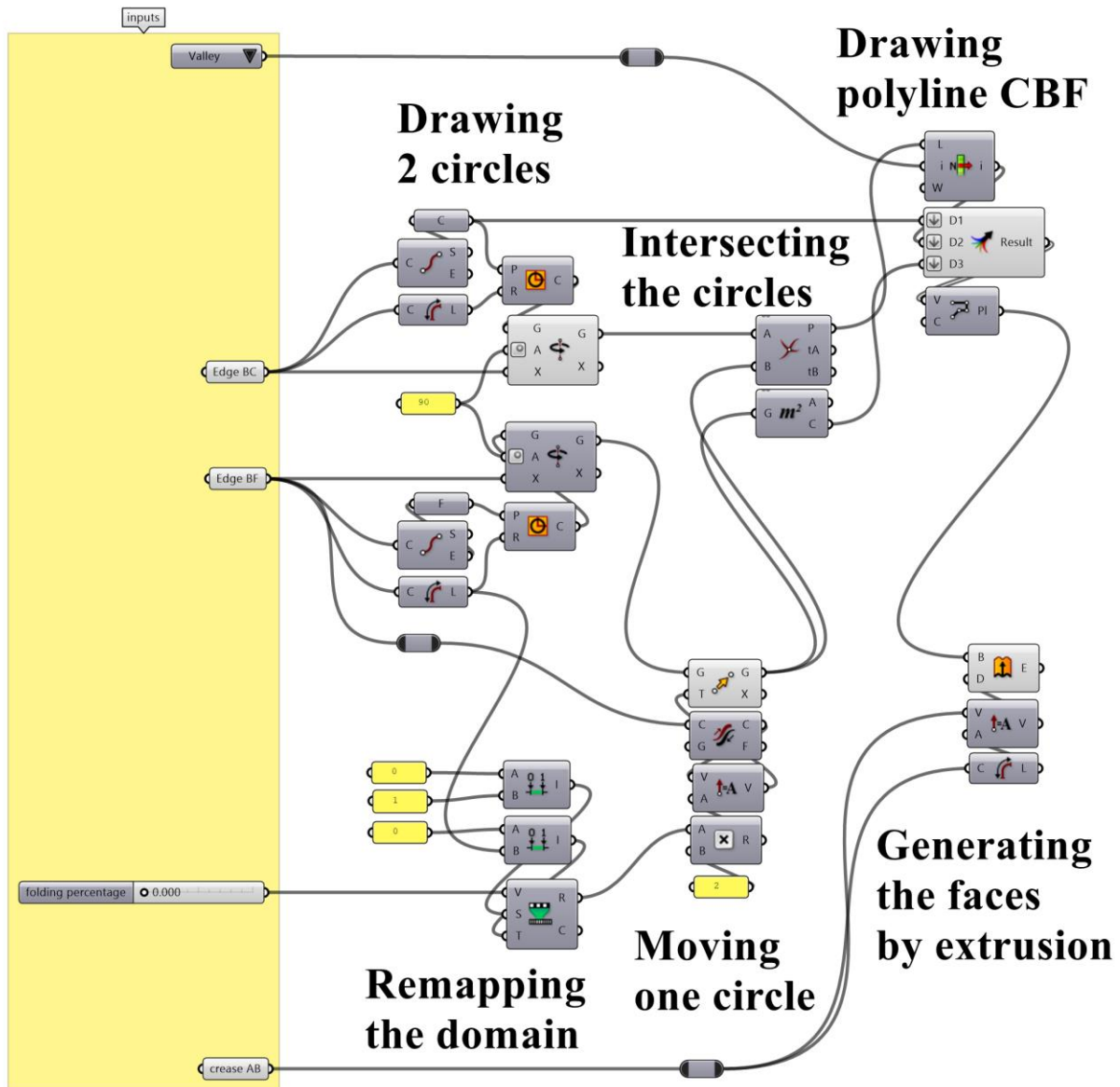
Constructive Methods for Solving the Kinematics of Origami – Generative Algorithms

The present appendix contains all the generative algorithms explained in CHAPTER IV, some of them are also inserted inside the text of the thesis, others appear for the first time in this appendix.

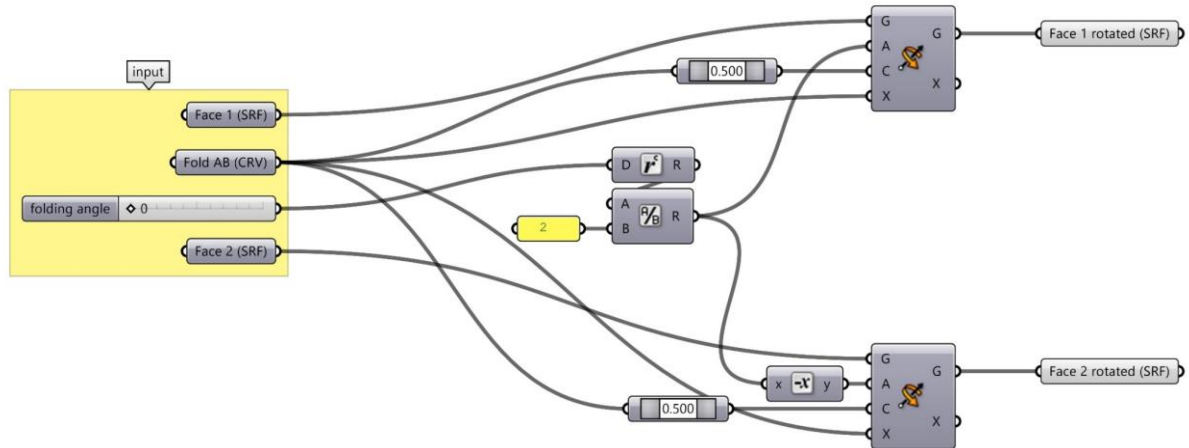
B.1. Single Linear Crease Between Equal Rectangular Faces, Two Edges Slide on Construction Plane – Intersecting Circles



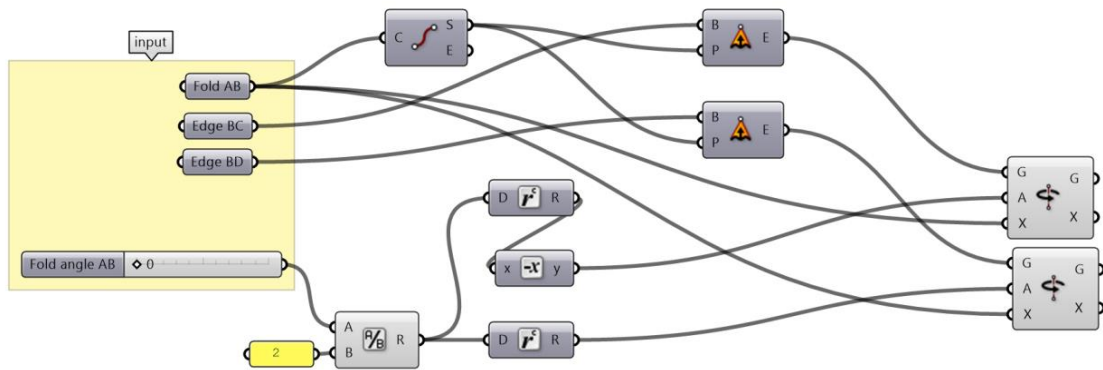
B.2. Single Linear Crease Between Asymmetric Rectangular Faces, Two Edges Slide on Construction Plane – Intersecting Circles



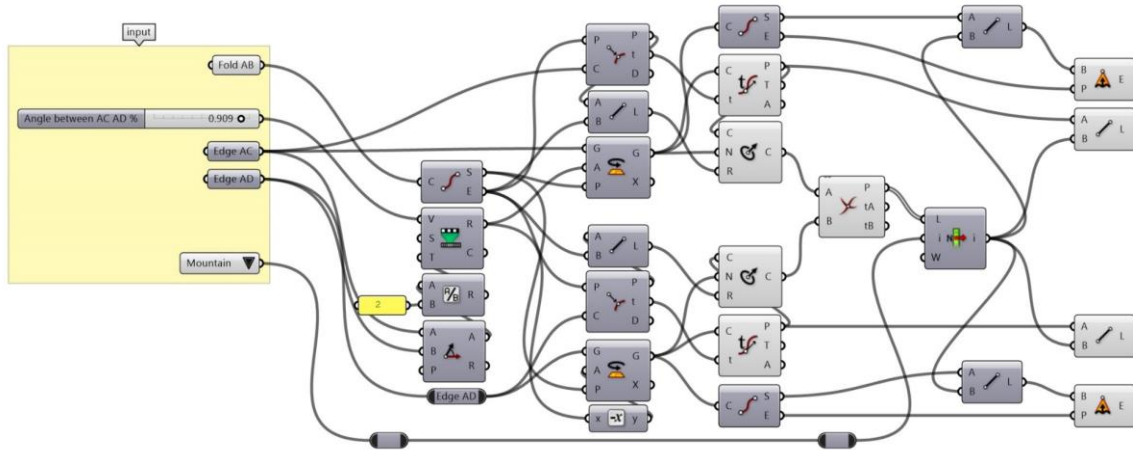
B.3. Single Linear Crease Between Rectangular Faces, Crease on Construction Plane – Varying Fold Angle



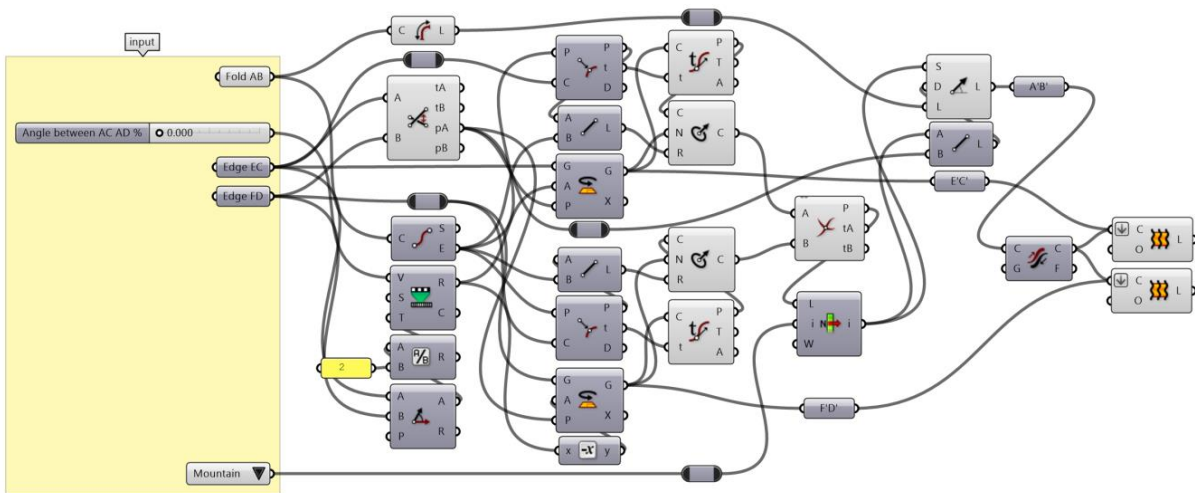
B.4. Single Linear Crease Between Triangular Faces, Crease on Construction Plane – Varying Fold Angle



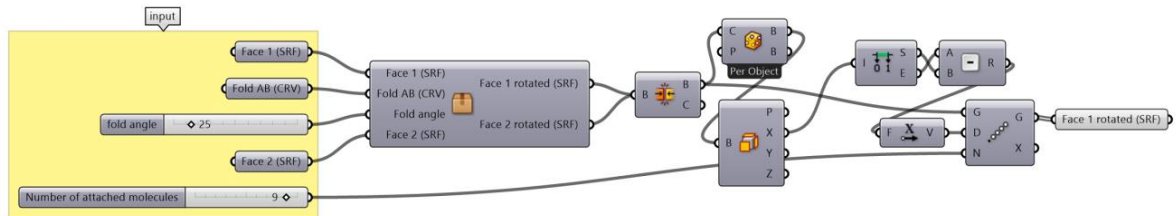
B.5. Single Linear Crease Between Triangular Faces, Two Edges Slide on Construction Plane – Intersecting Circles



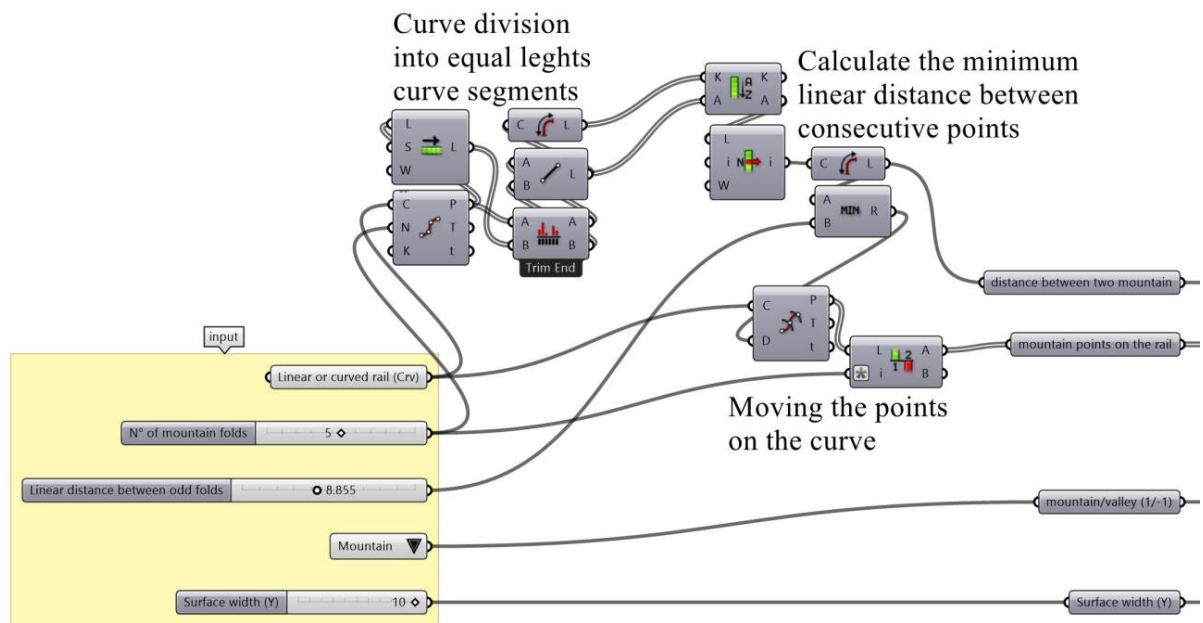
B.6. Single Linear Crease Between Trapezoidal Faces, Two Edges Slide on the Construction Plane – Intersecting Circles

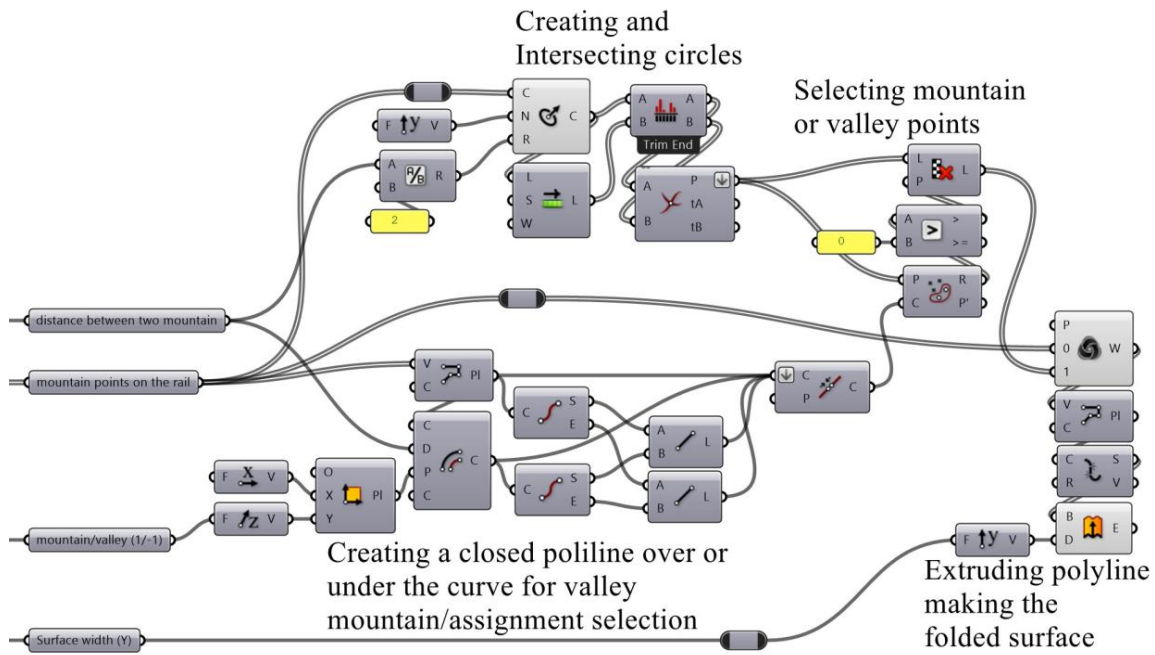


B.7. Straight Accordion – Array of “Single Linear Crease Between Rectangular Faces” Molecules

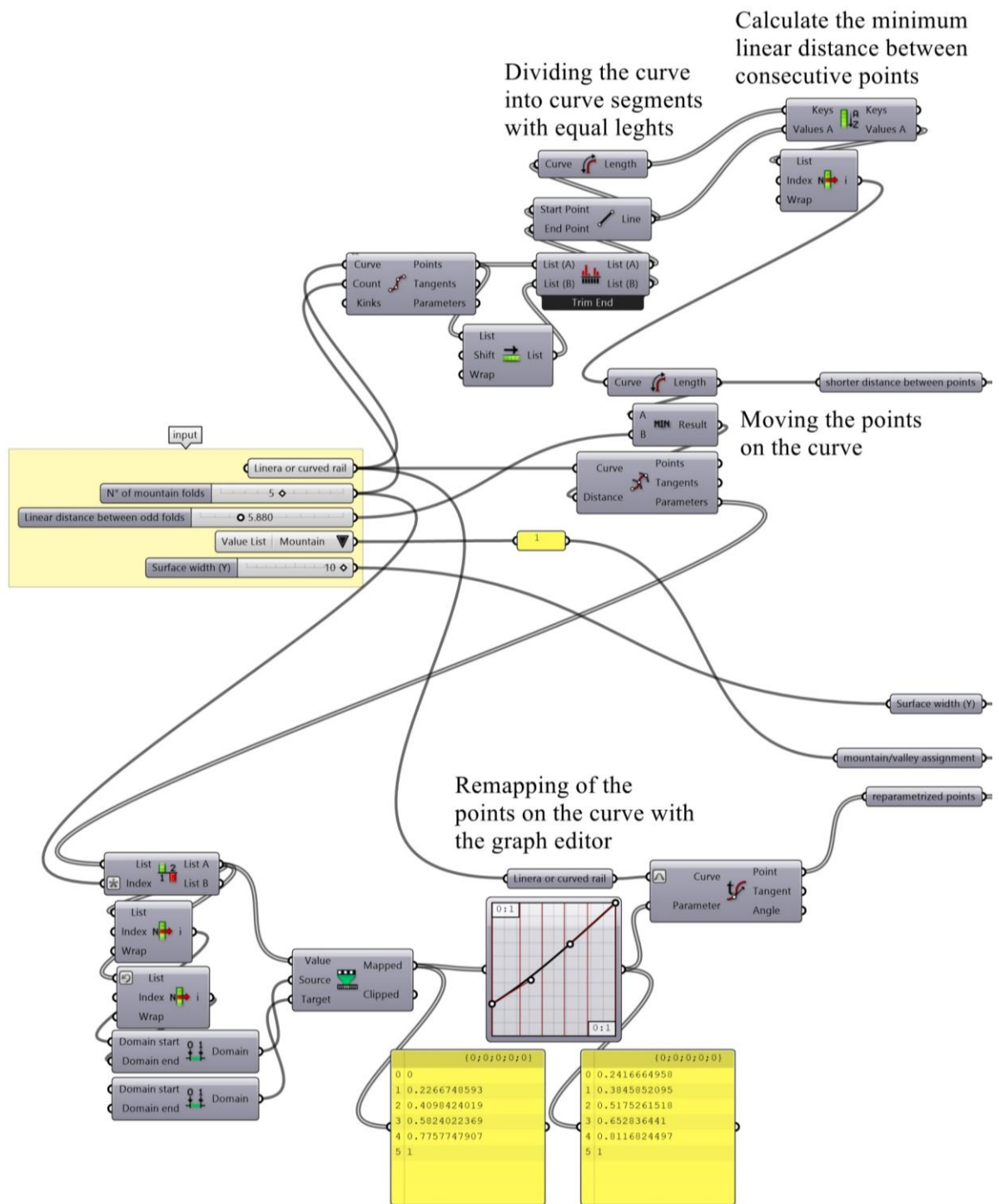


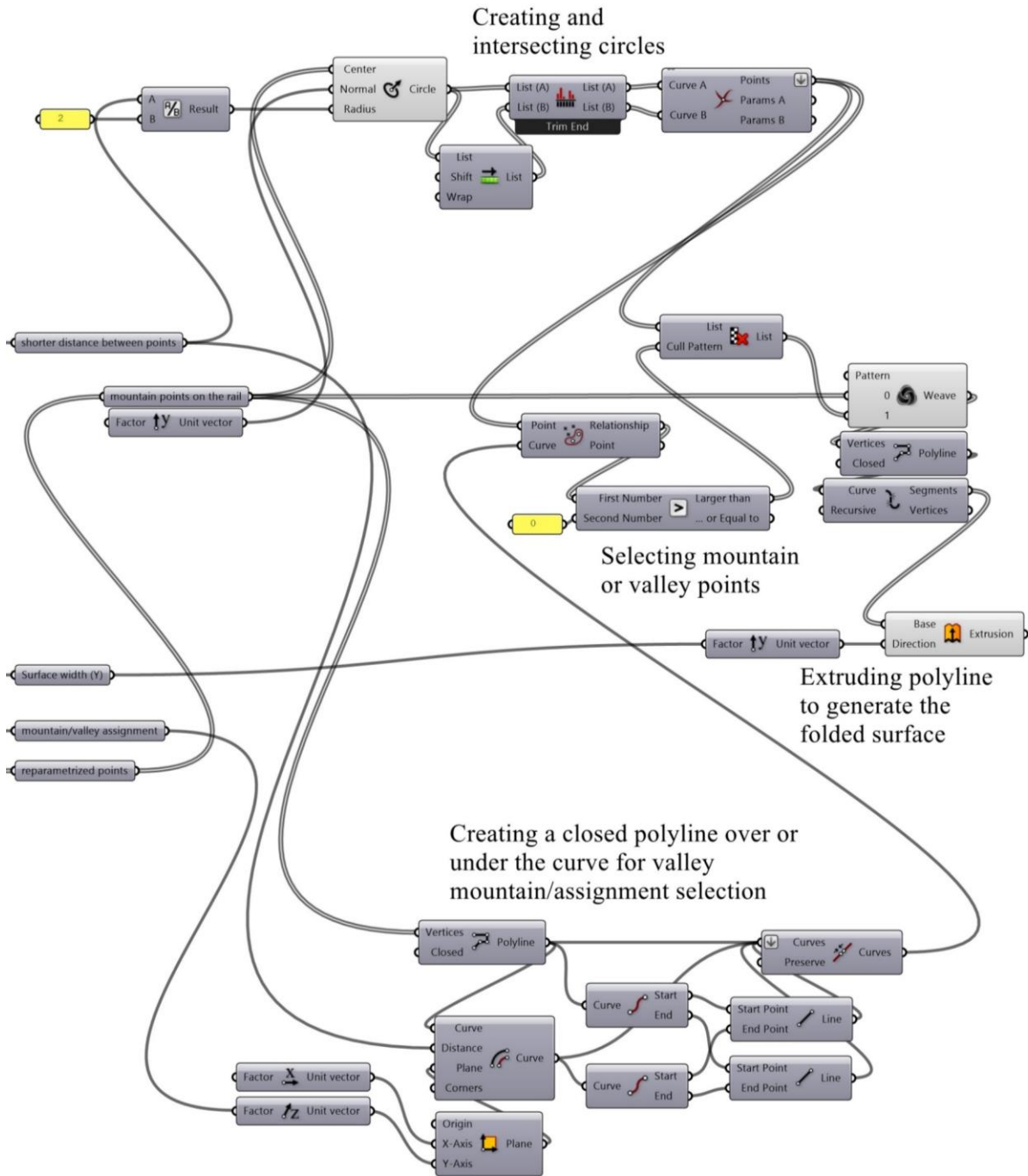
B.8. Straight Accordion Sliding on a Rail – Intersecting Circles



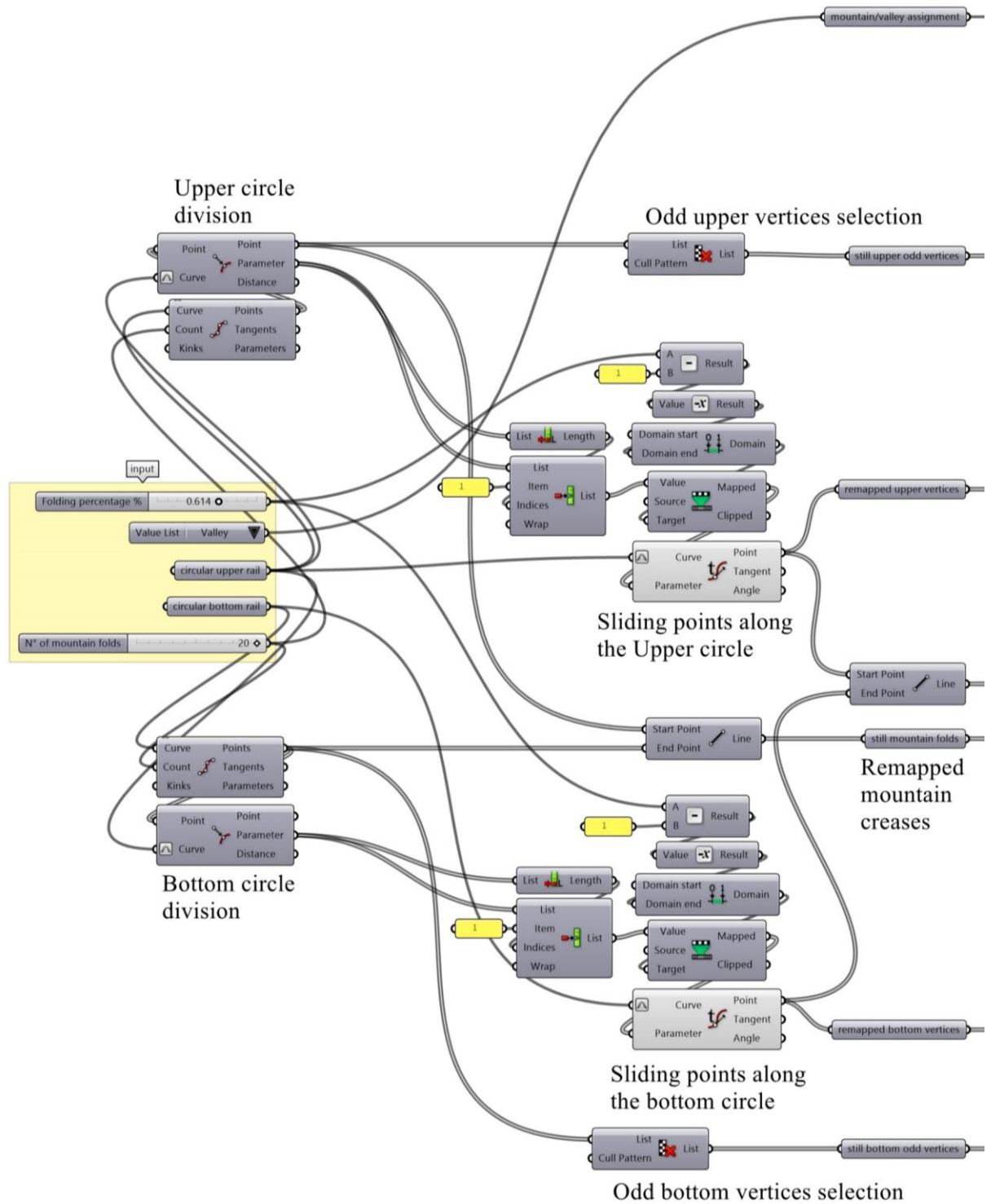


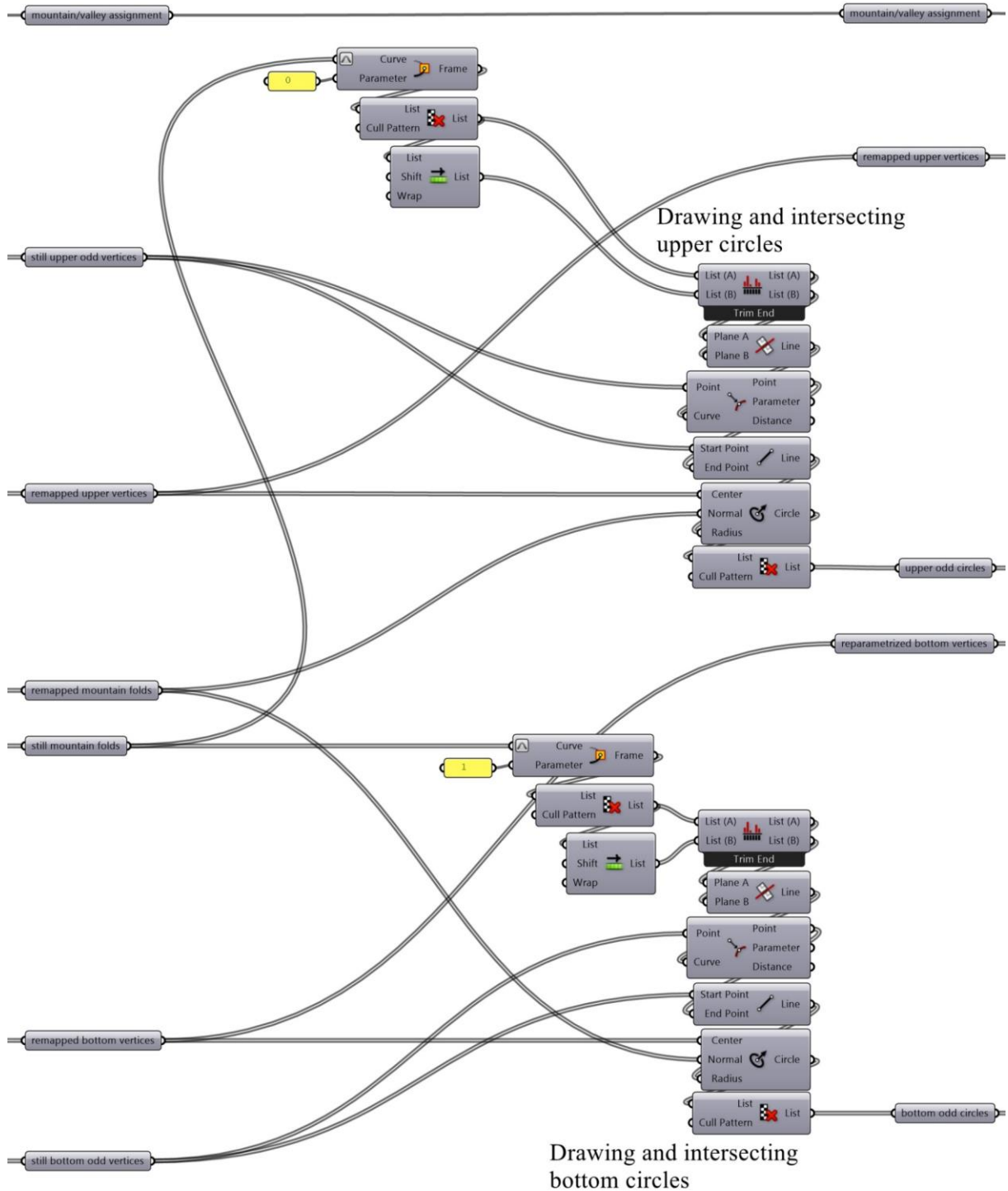
B.9. Straight Accordion on a Rail with Non-Uniform Fold Angle Distribution – Intersecting Circles and “Graph Mapper”

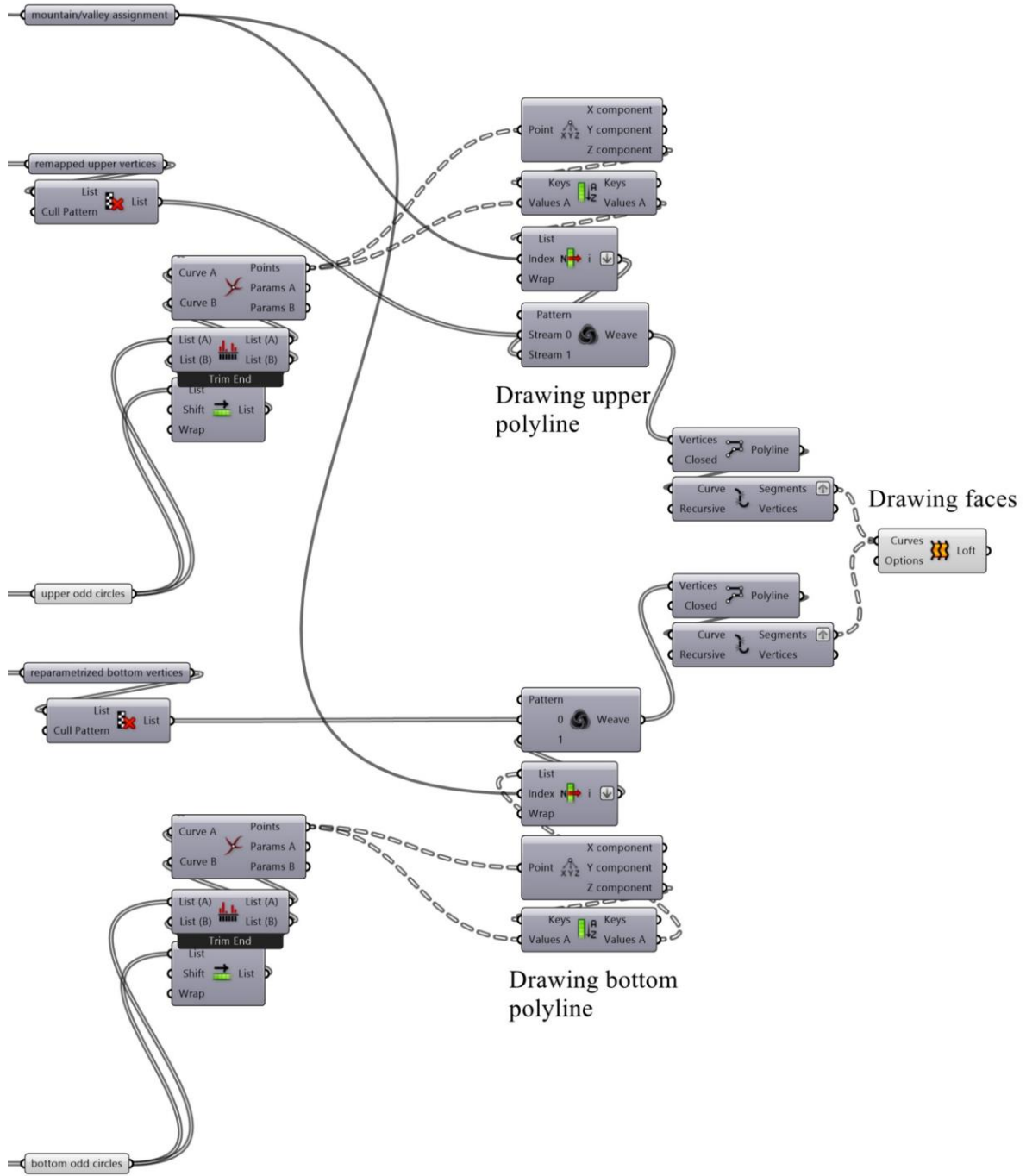




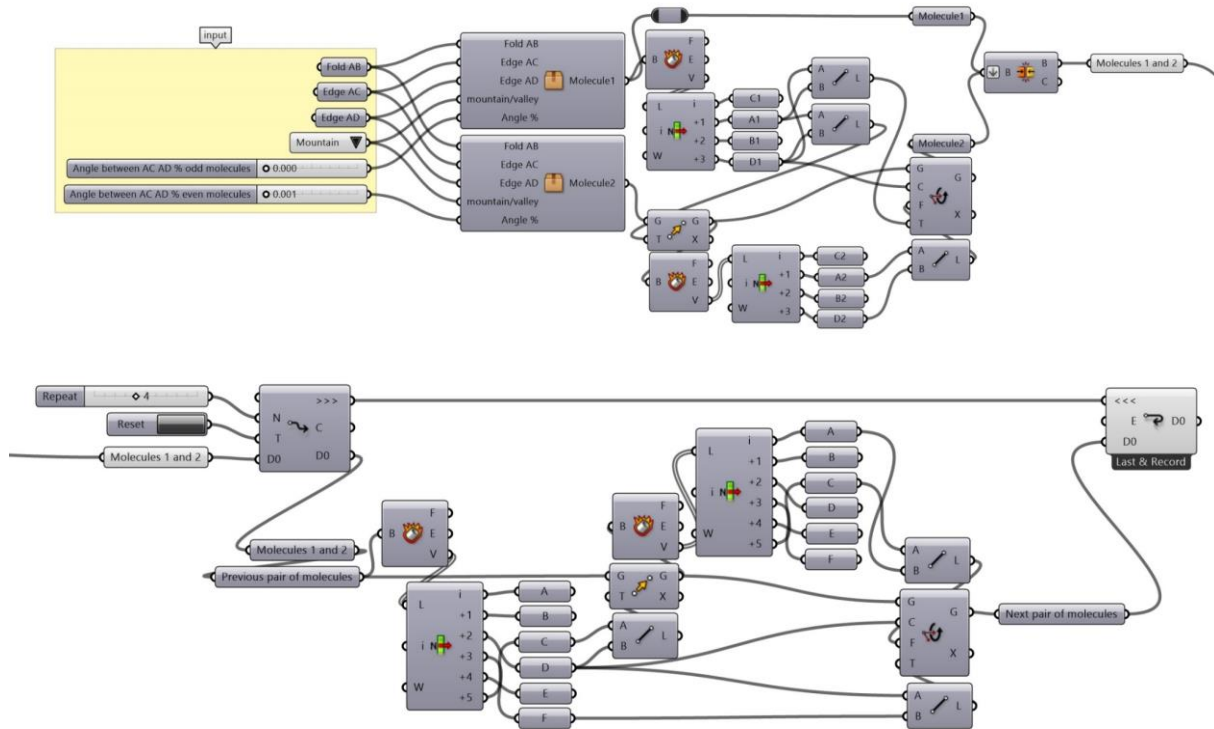
B.10. Accordion on Two Circular Rails – Intersecting Circles



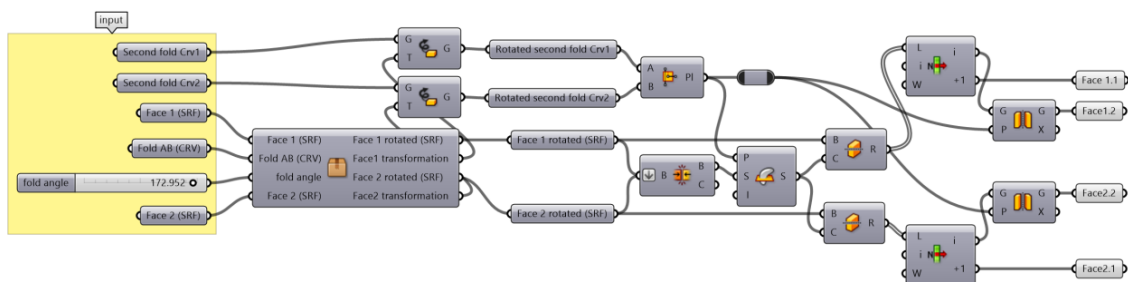




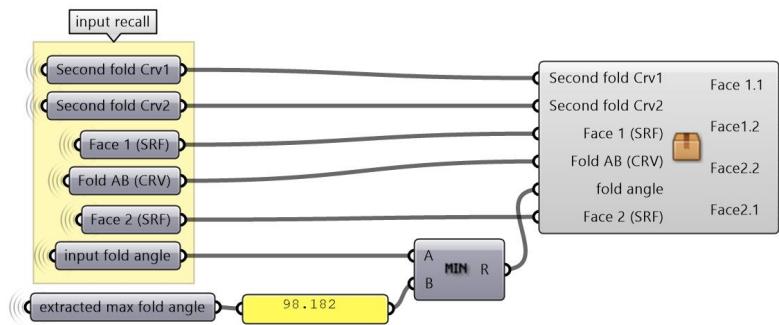
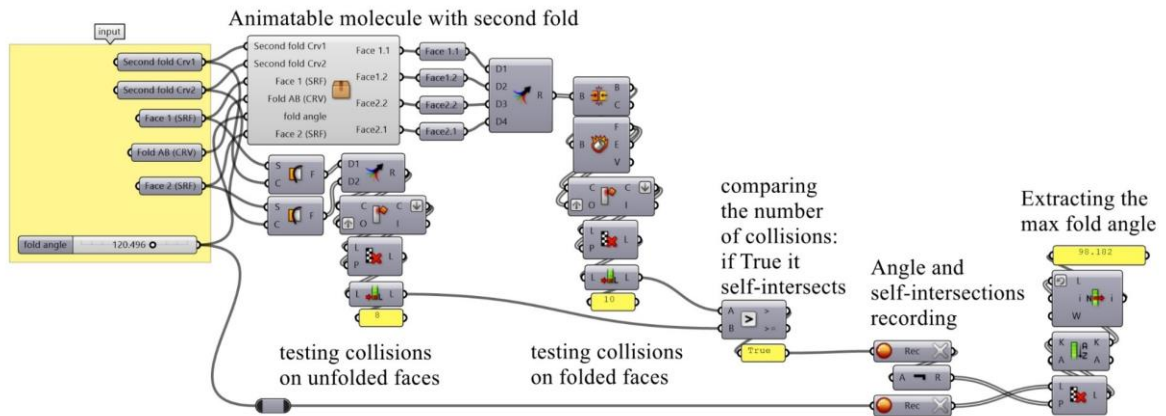
B.11. Triangulated Accordion – Joining Multiple “Single Linear Crease Between Triangular Faces” Molecules



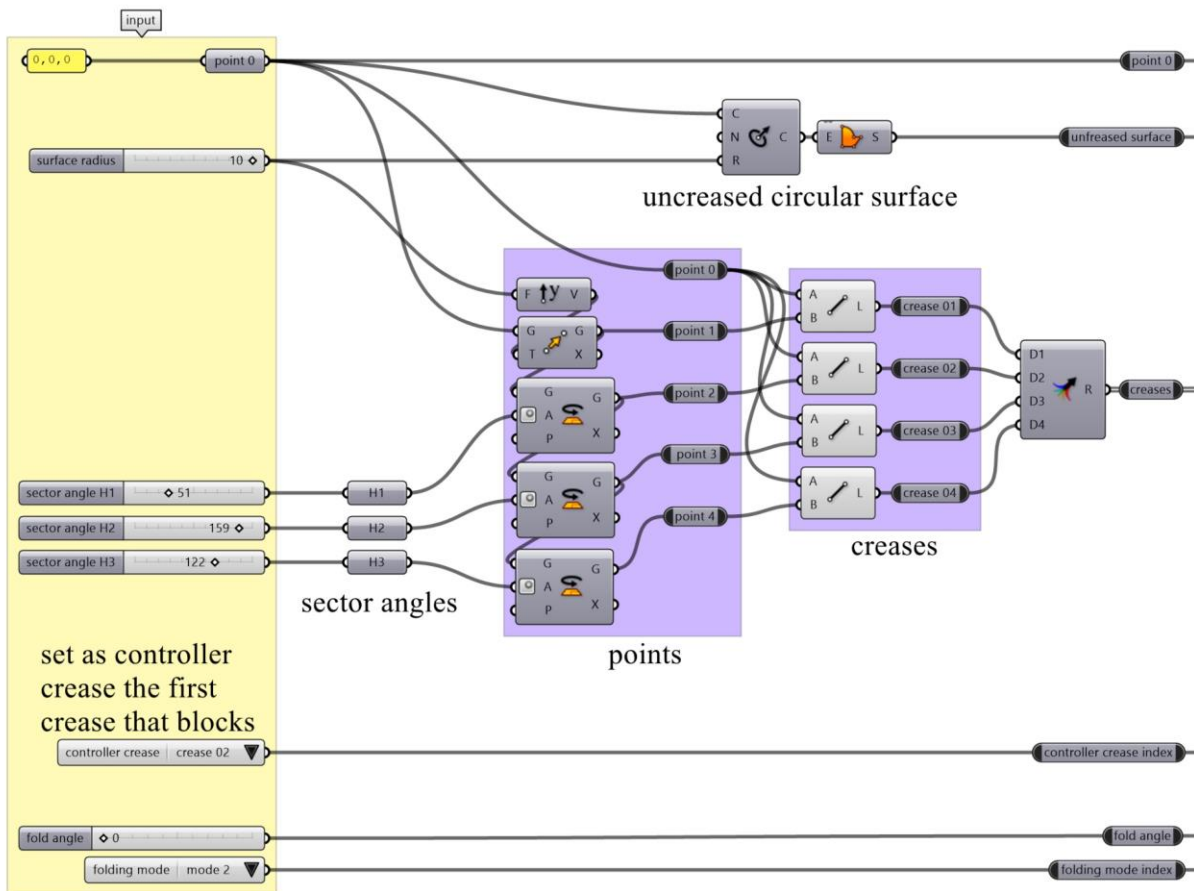
B.12. Symmetric Reverse Fold – Reflecting a Single Linear Crease

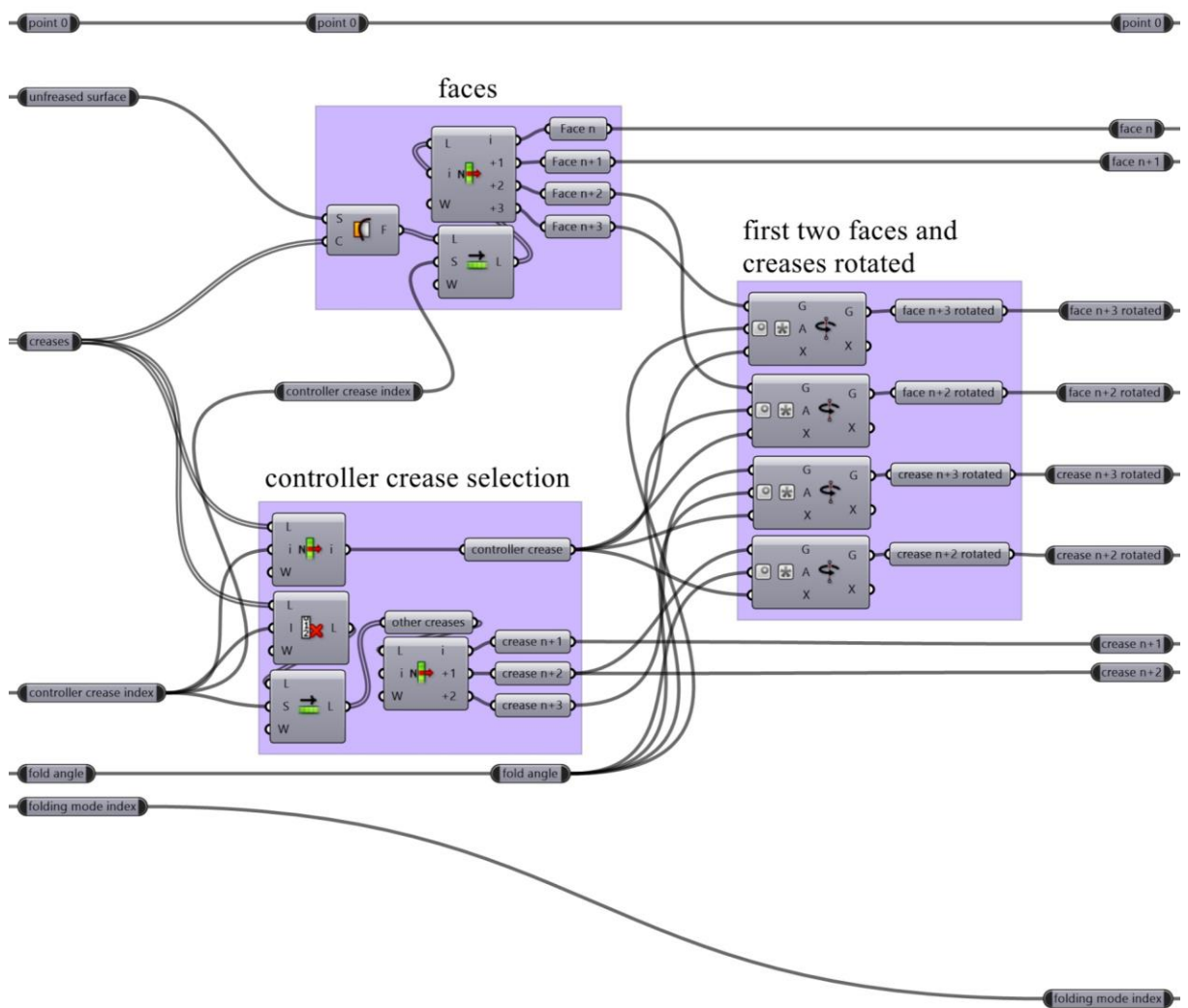


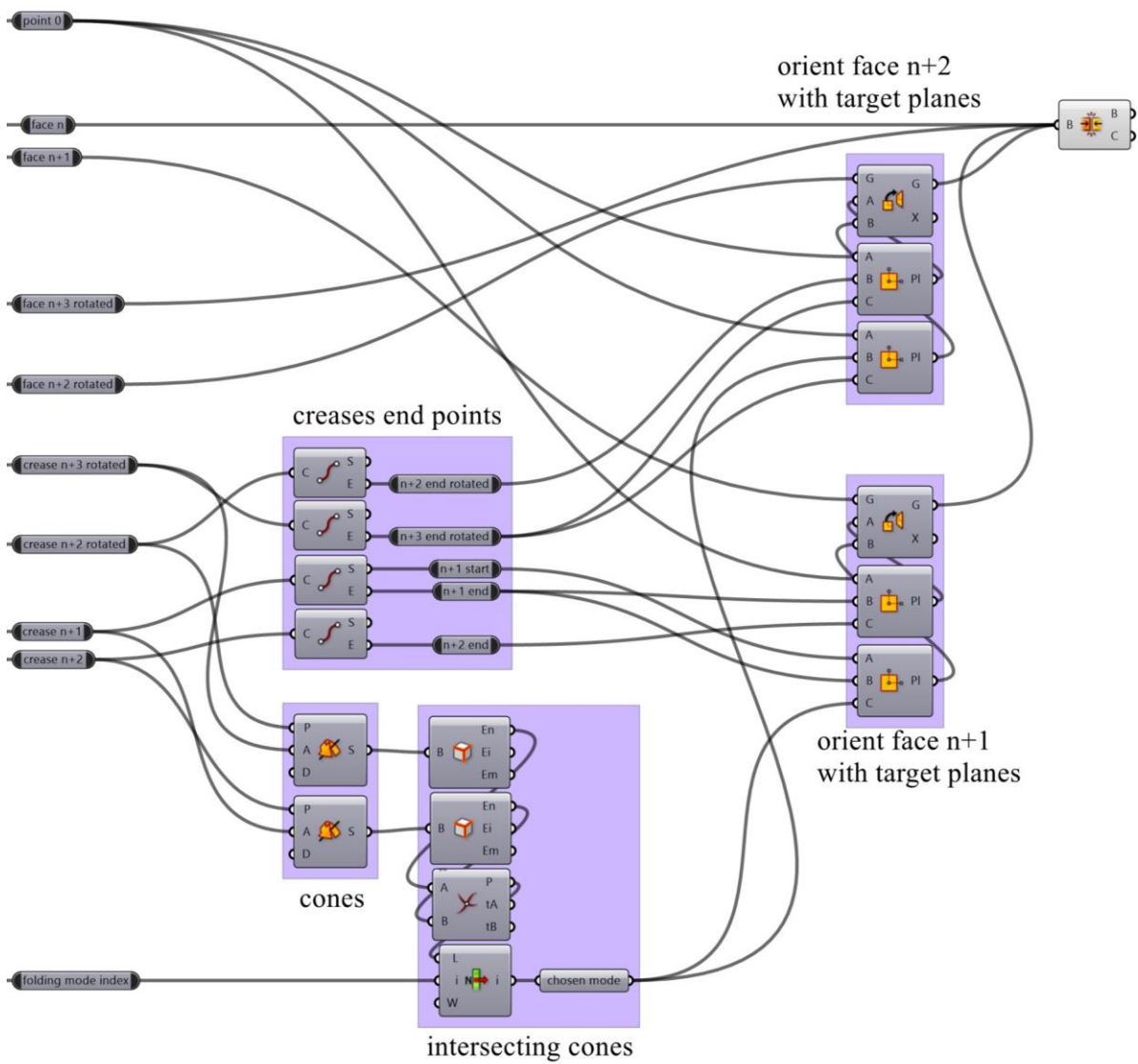
B.13. Asymmetric Reverse Fold – Reflection and Collision Detection



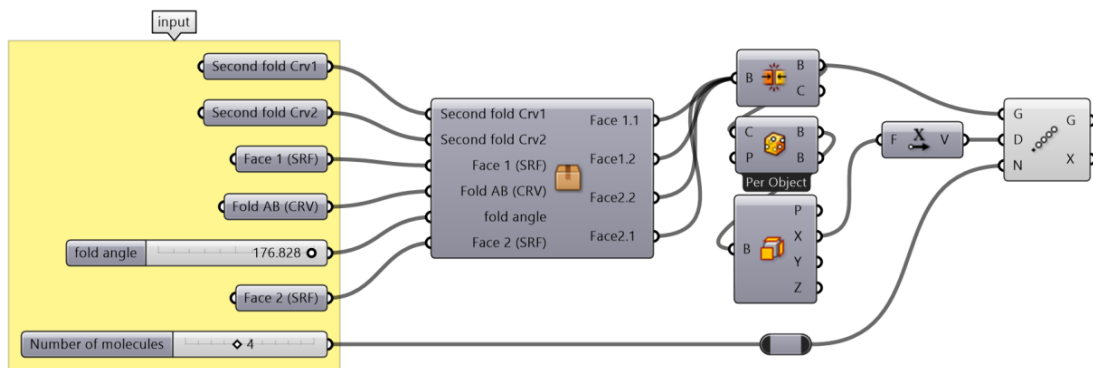
B.14. Generic Degree-4 Vertex – Intersecting Cones



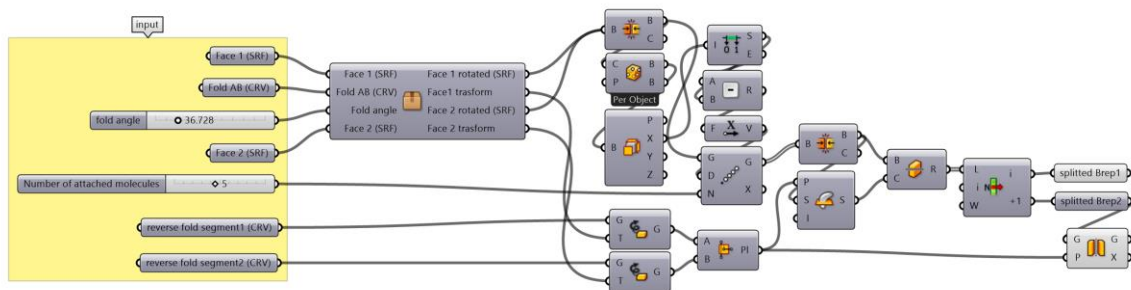




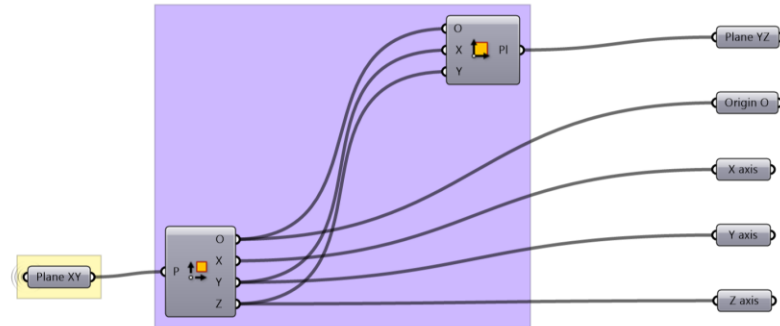
B.15. Joining “Symmetric Reverse Fold” Molecules – Critical Observations About Global Rigid-Flat- Foldability



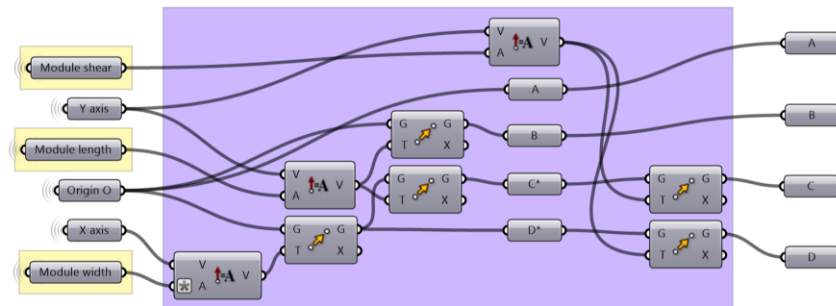
B.16. Joining “Asymmetric Reverse Fold” Molecules



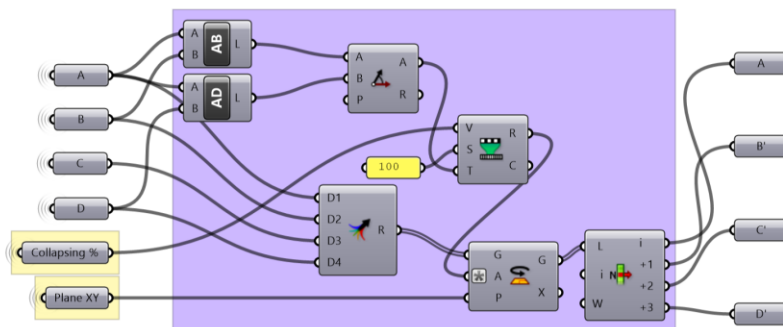
B.18. The Miura Pattern – Planar Rectangular Array of “Symmetric Reverse Fold” Molecules – Intersecting Circle with Plane of Symmetry



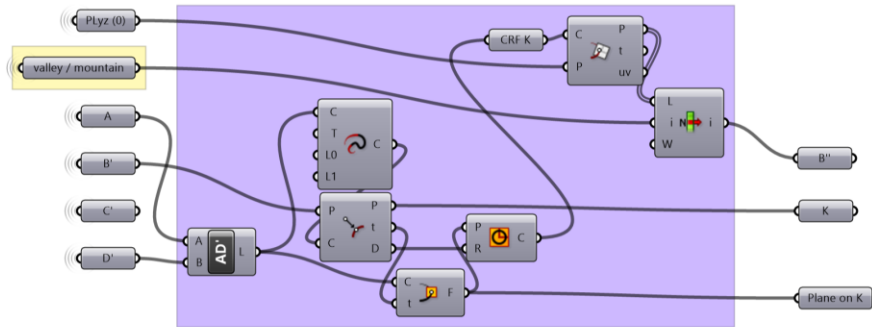
1) Plane YZ



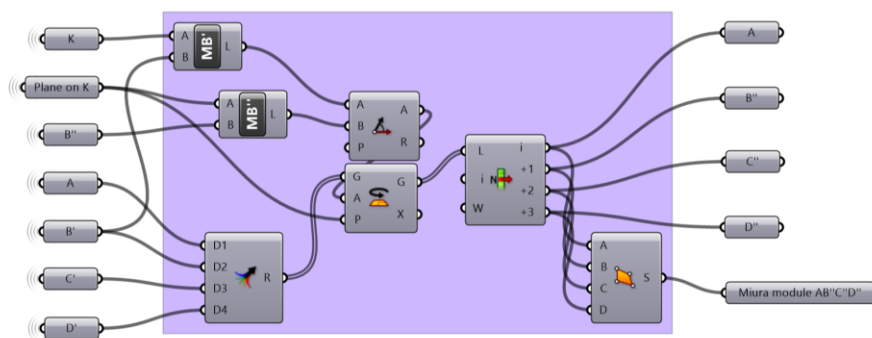
2) Miura Module (1 face)
Construction



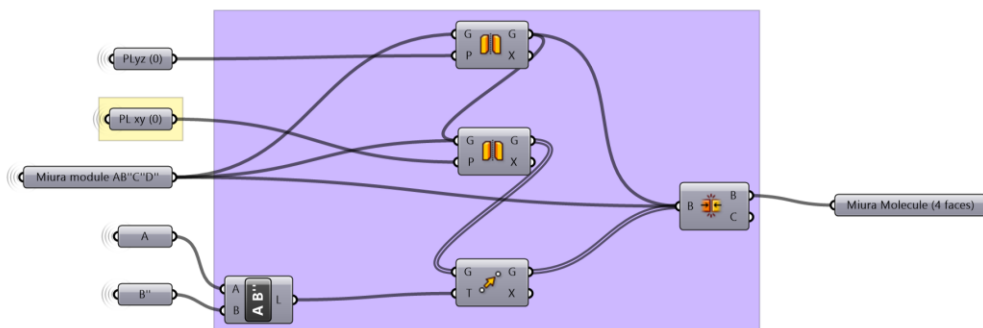
3) Miura Module
rotation from B to B'



4) CRF/Plane intersection

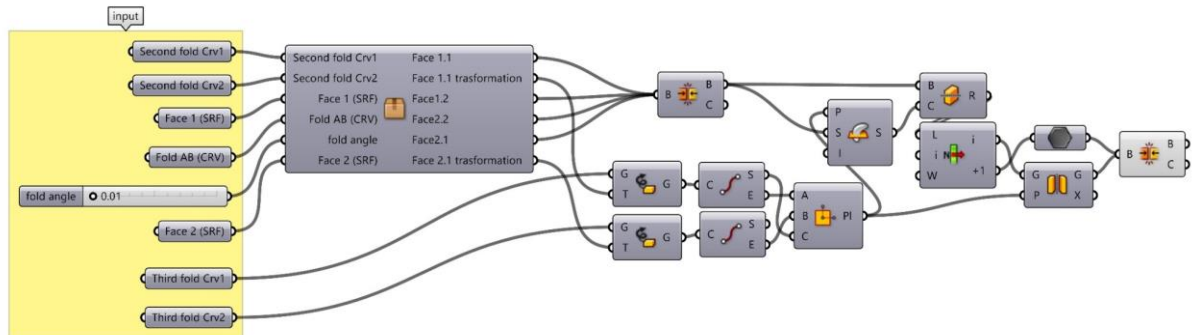


5) Miura Module rotation
from B' to B''

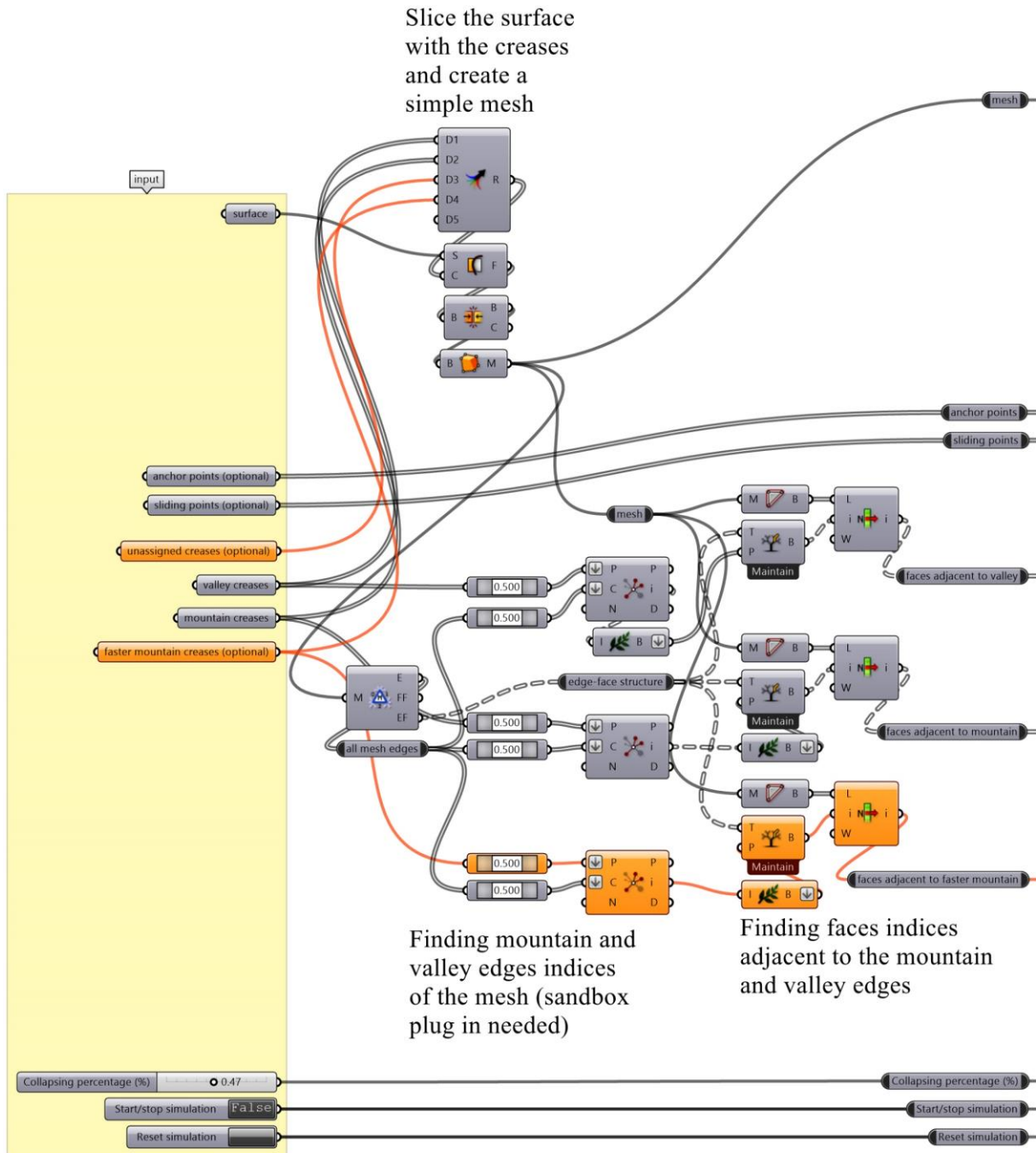


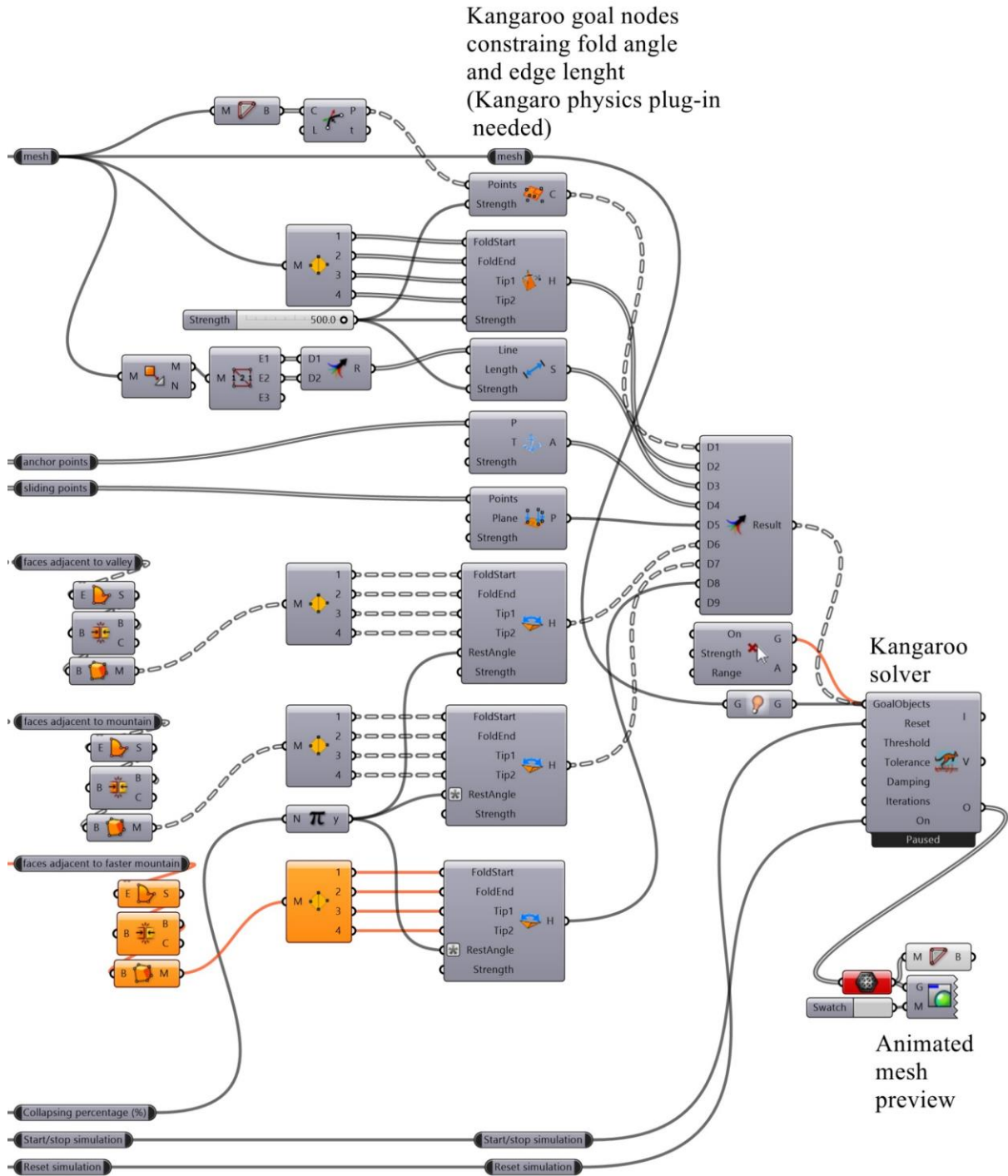
6) Miura Module
Reflexion and Translation

B.19. The sink fold – Reflecting the tip of a degree-4 vertex



B.20. Degree>4 Vertices – Physical Simulation



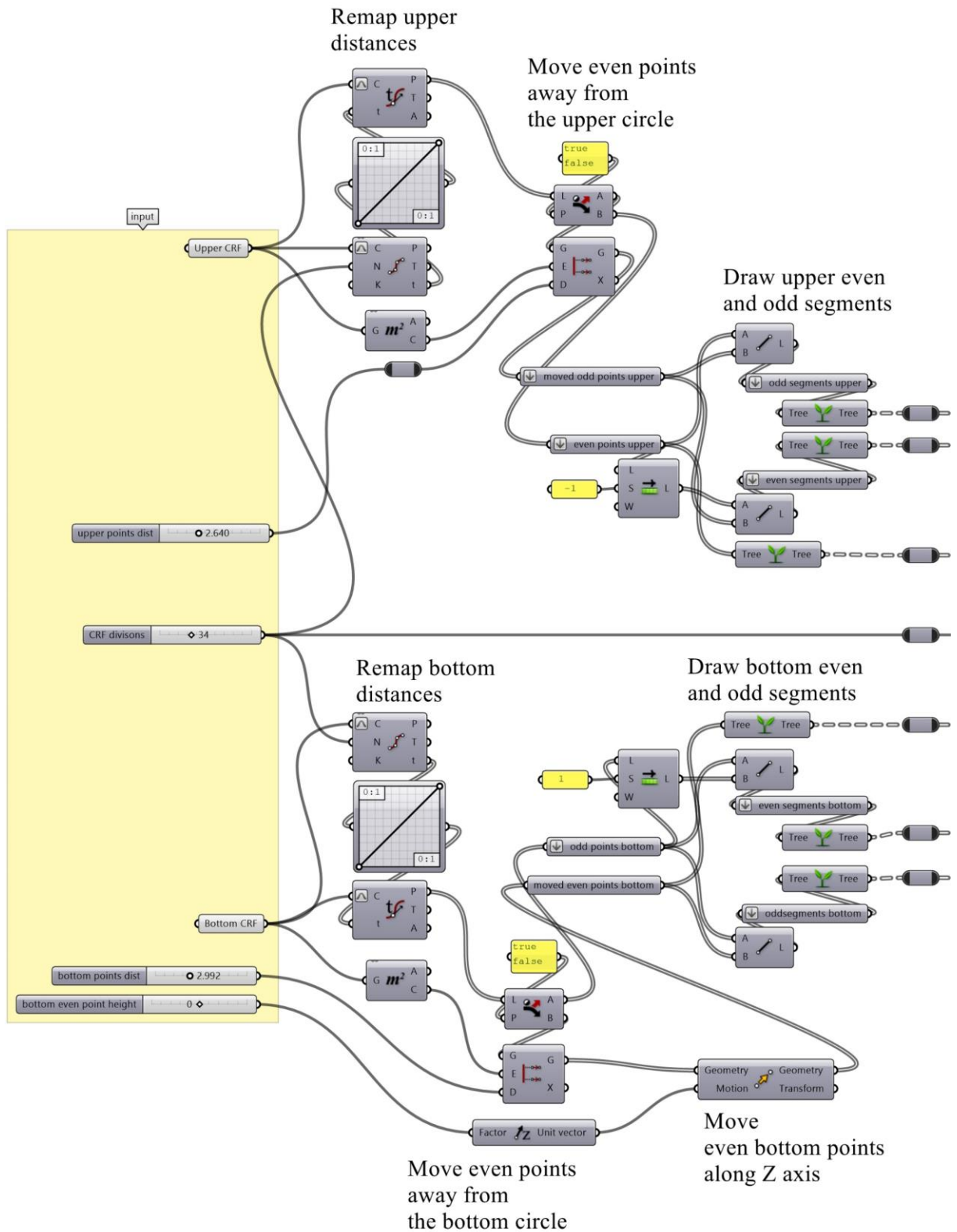


Appendix C.

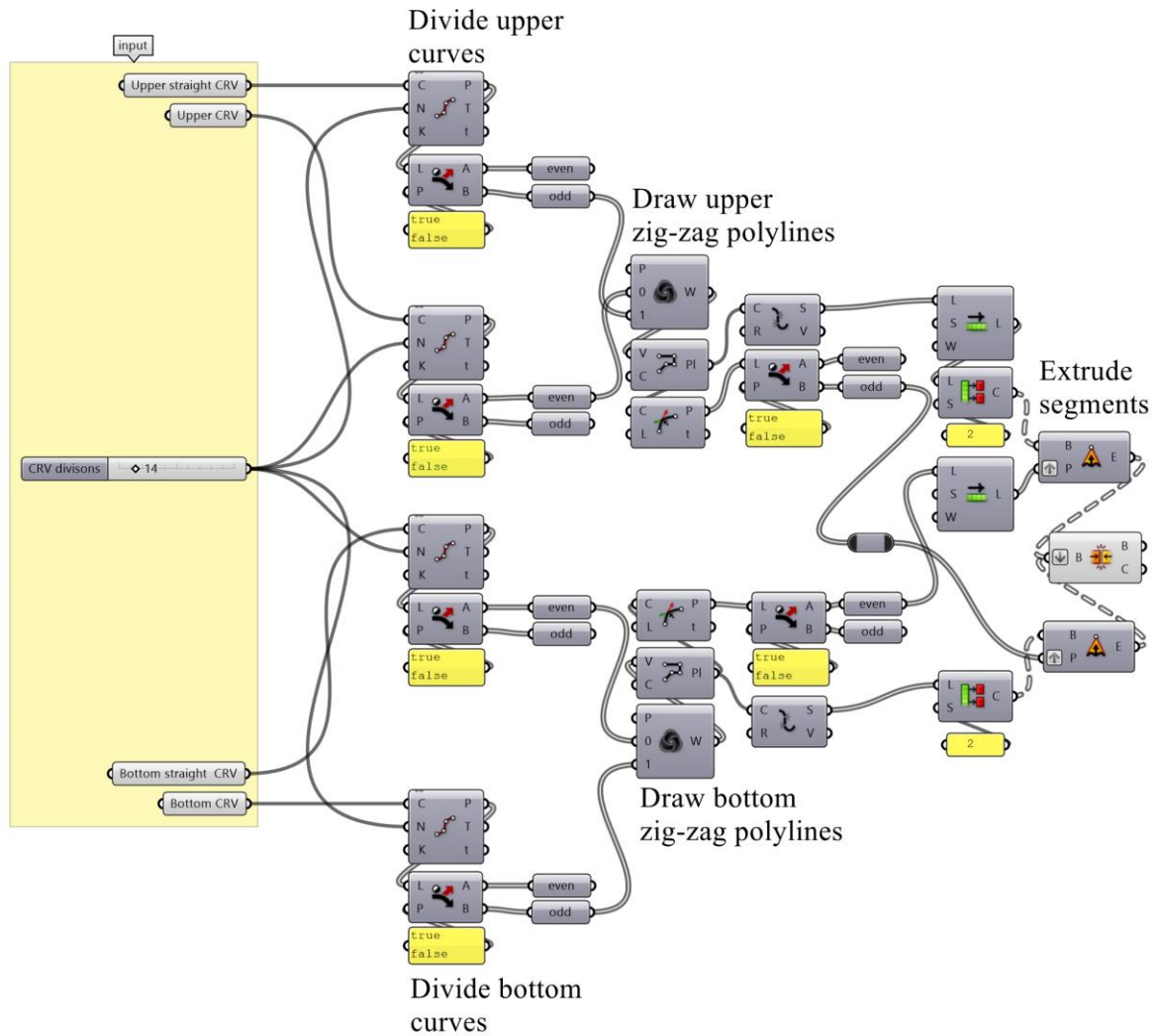
Pattern Design from a Given Shape – Generative Algorithms

In the present Appendix, we reported all the generative algorithm shown in CHAPTER V

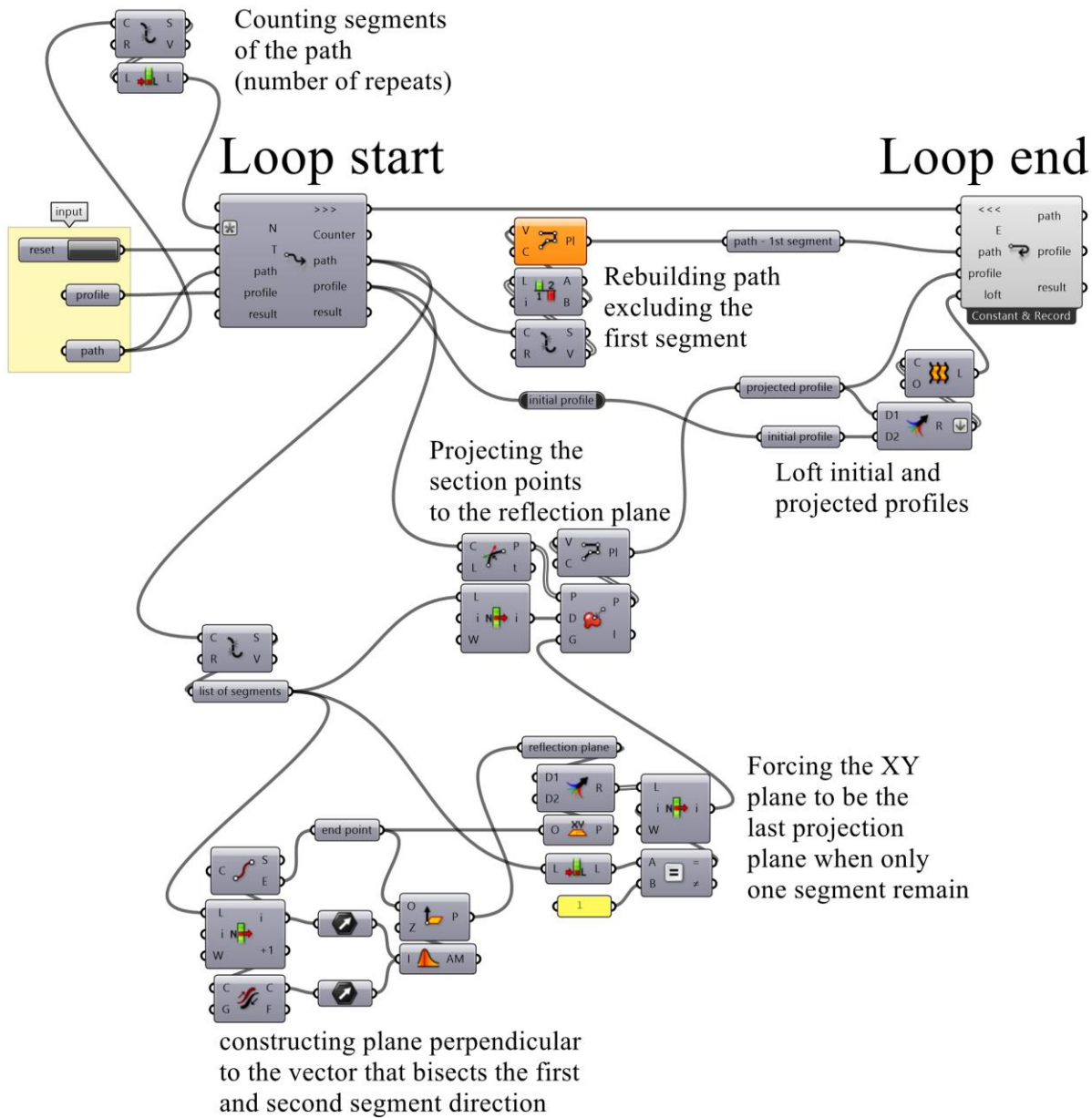
C.1. Lampshade – Vertices Extrusion and Reflection



C.2. Folded Facade – Vertices Extrusion from Reference Curved Rails

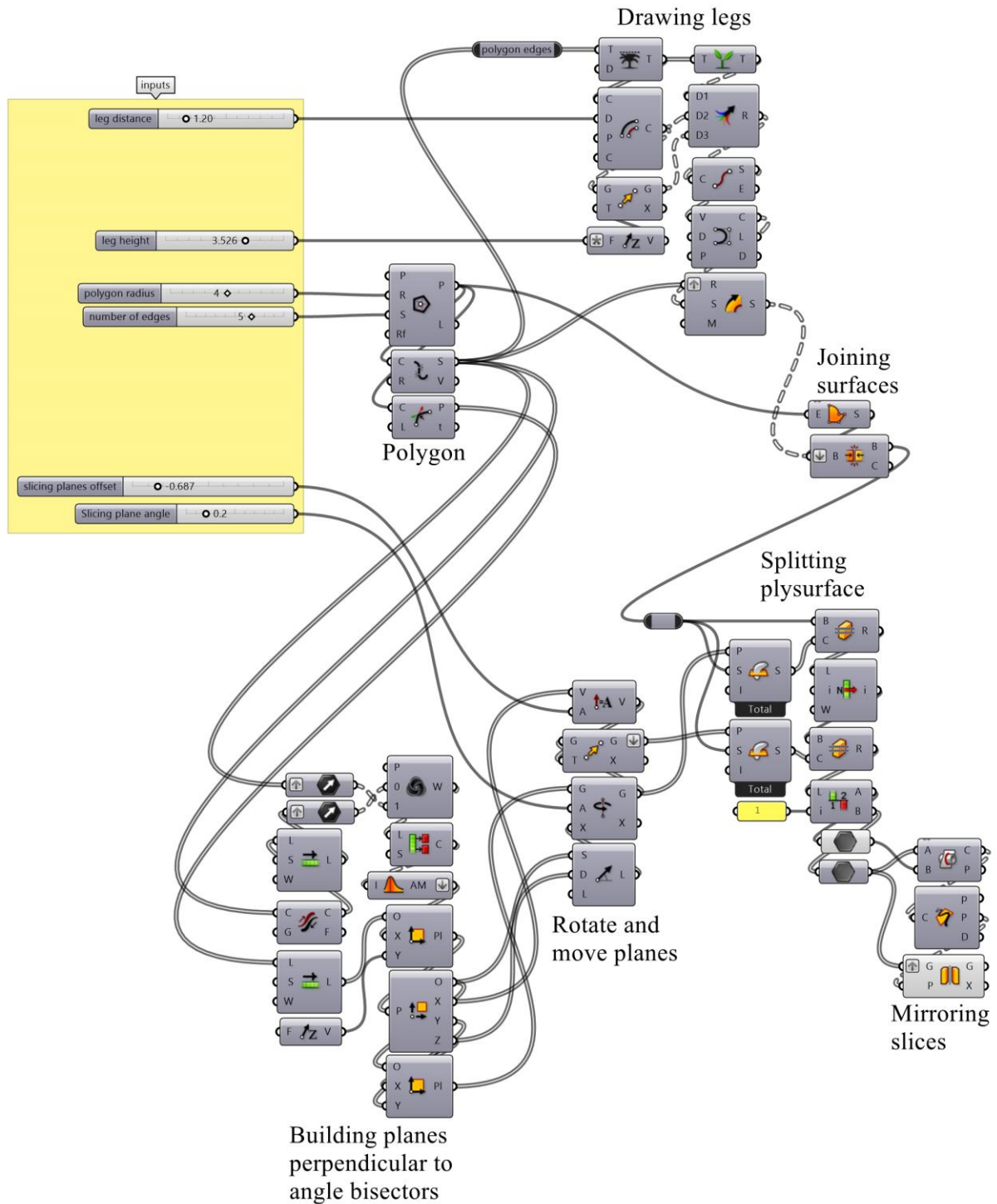


C.3. Building Envelope – Reflection of a Creased Developable Surface

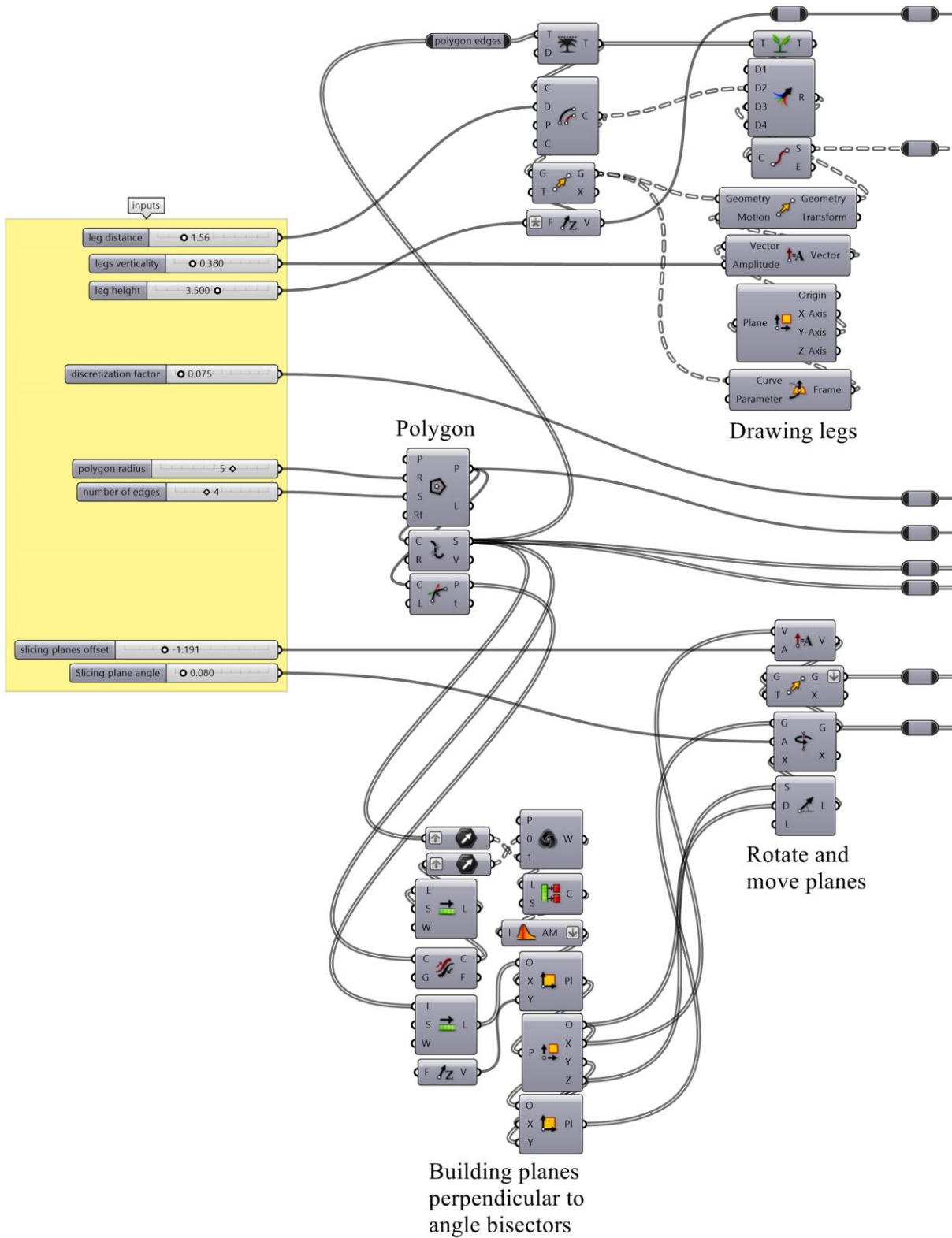


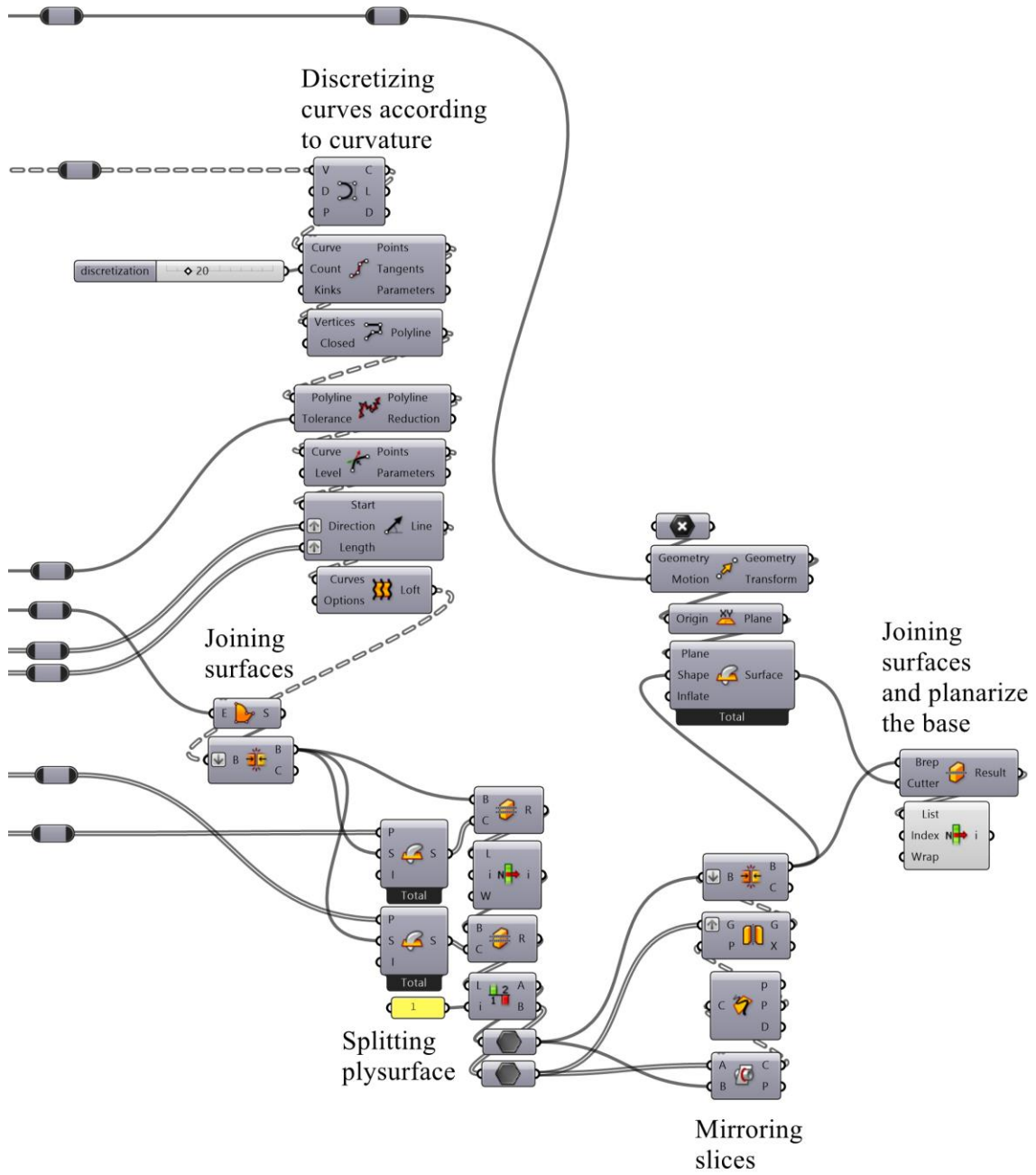
C.4. Curve-Folded Table

C.4.1. Reflection of a Developable Curved Surface



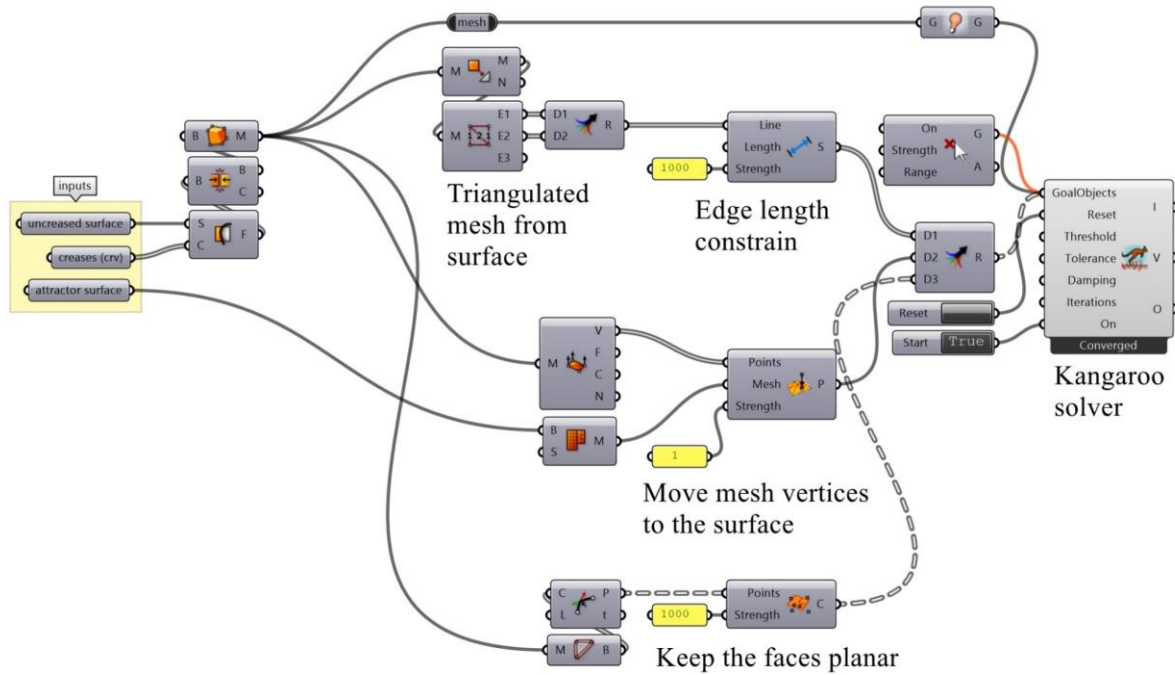
C.4.2. Discretization of the Curved Crease



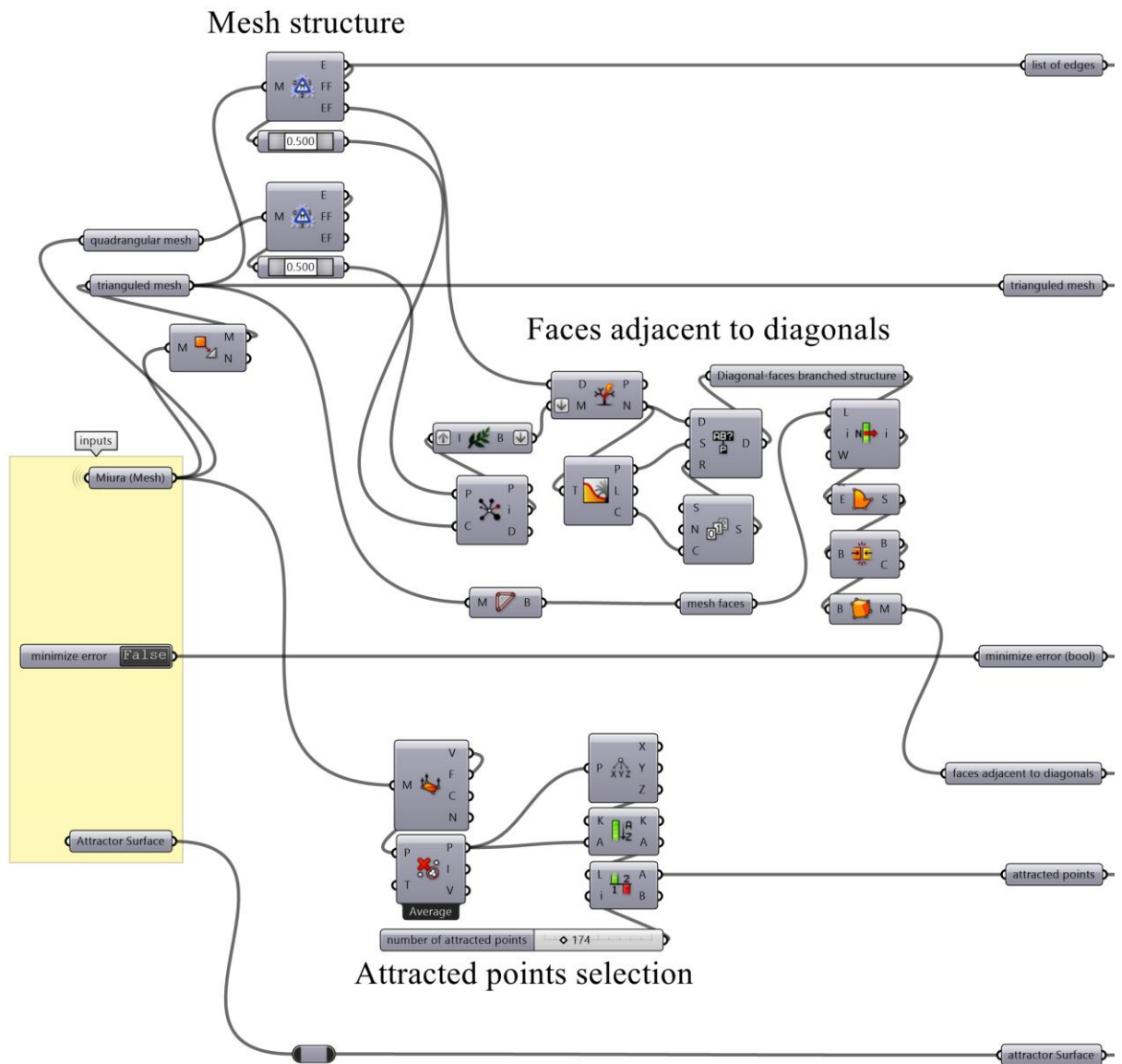


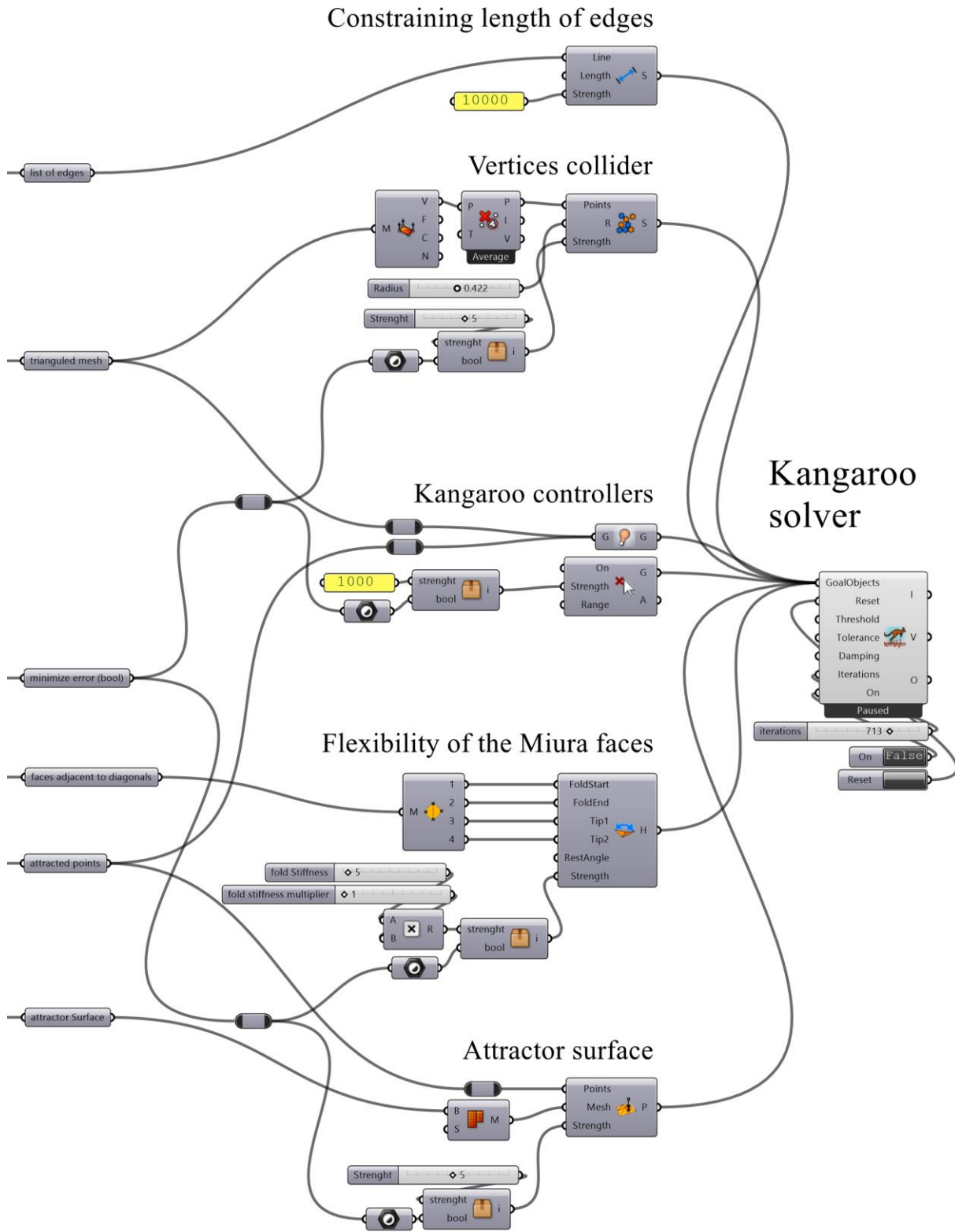
C.5. Conformable Corrugated Suspended Ceiling

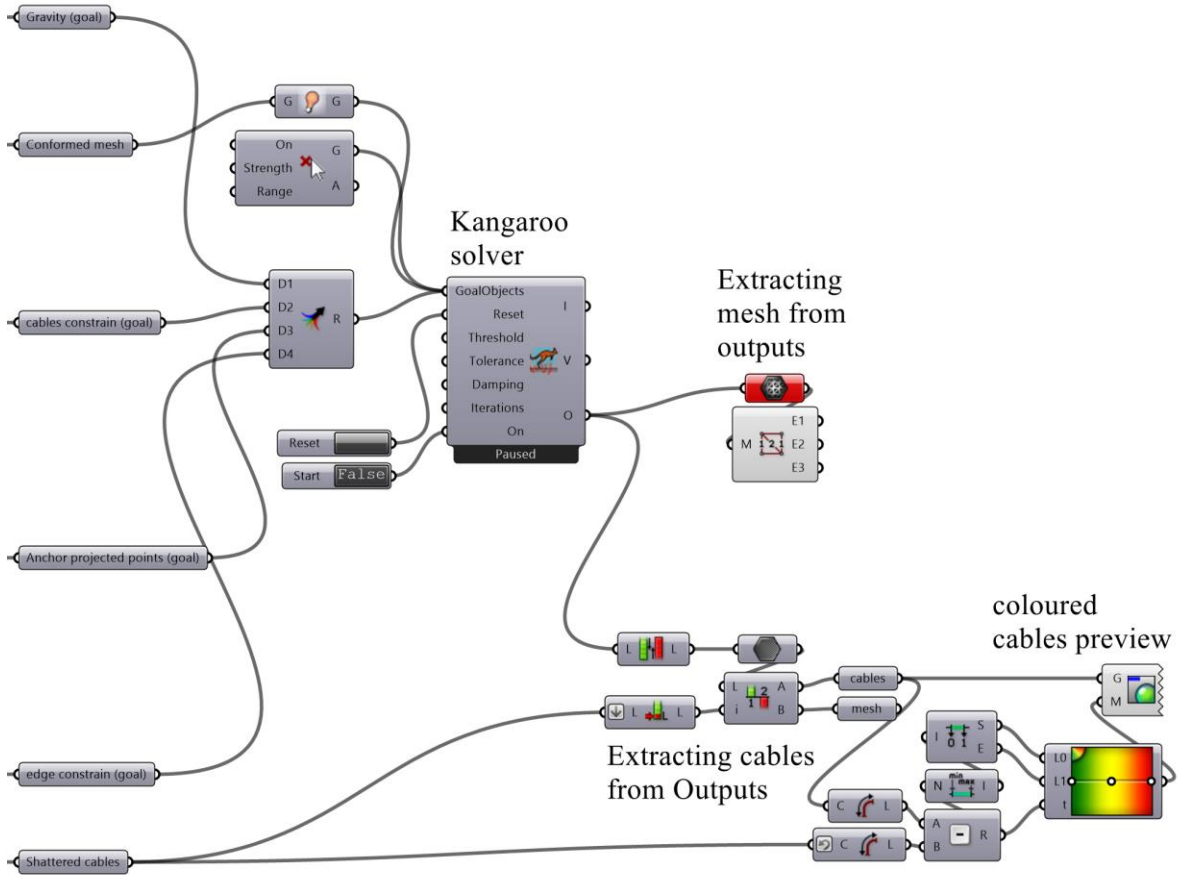
C.5.1. Conformation of a Rigid Creased Surface to a Curved Surface



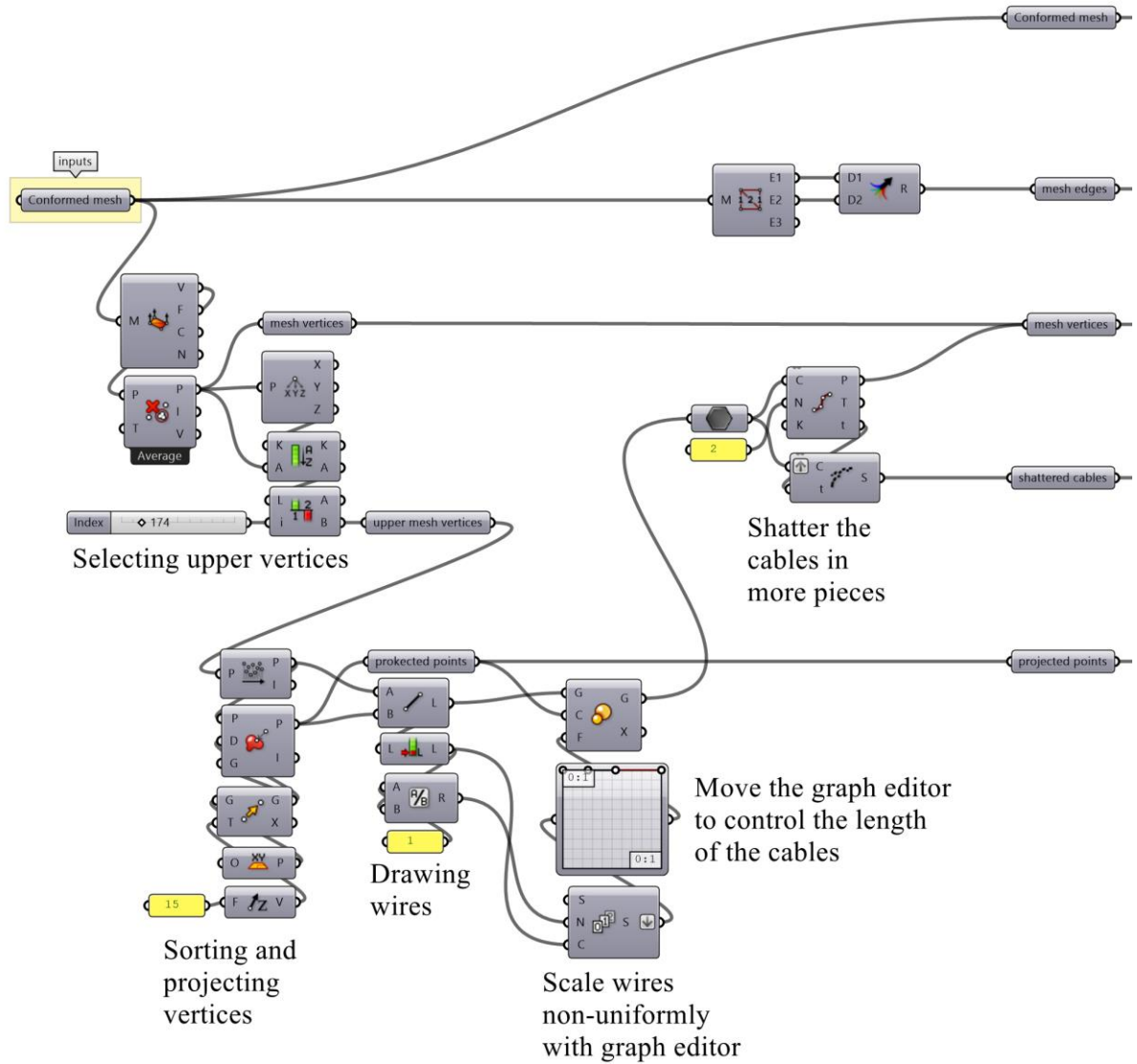
C.5.2. Conformation of a Flexible Miura-Ori to a Curved Surface

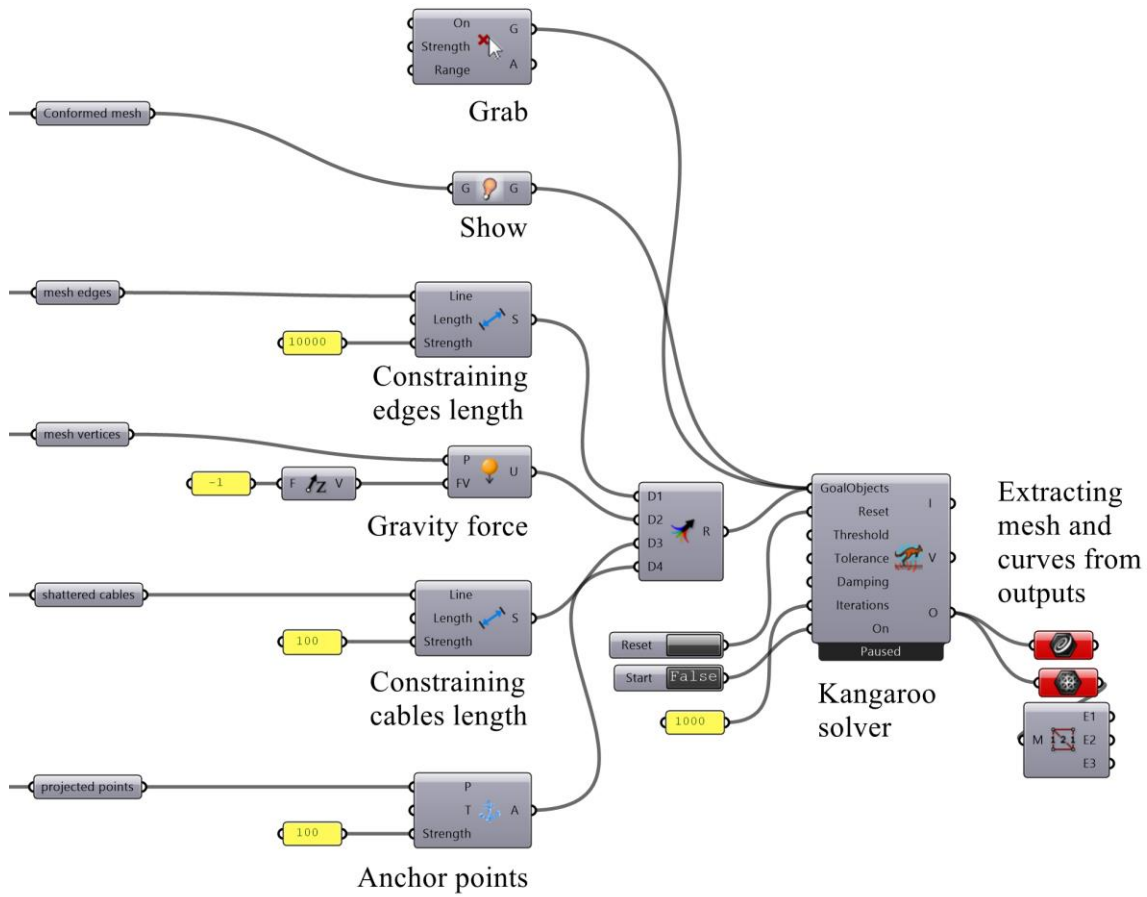






C.5.4. Changing shape to the Surface - Adjusting Cables Lengths



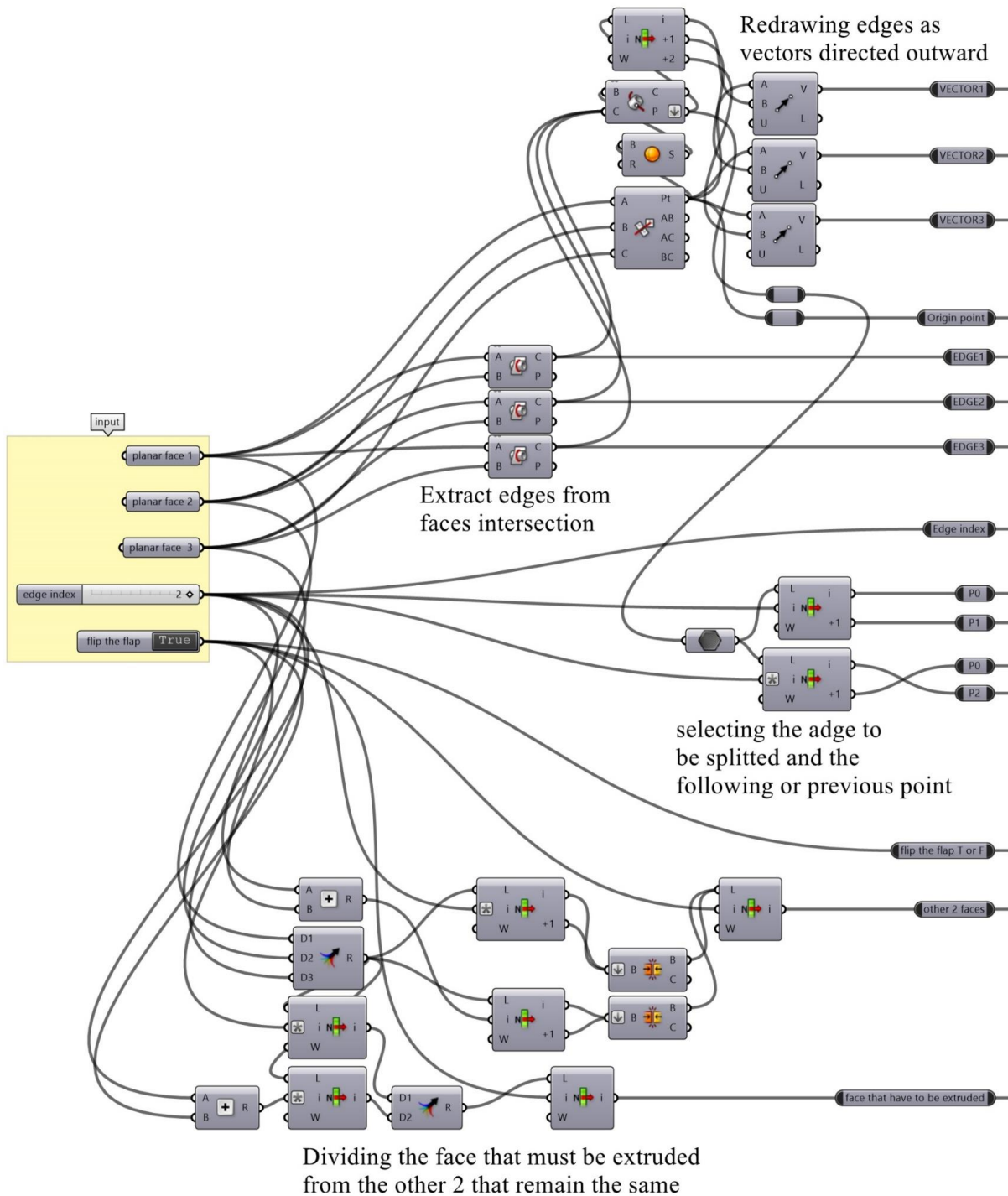


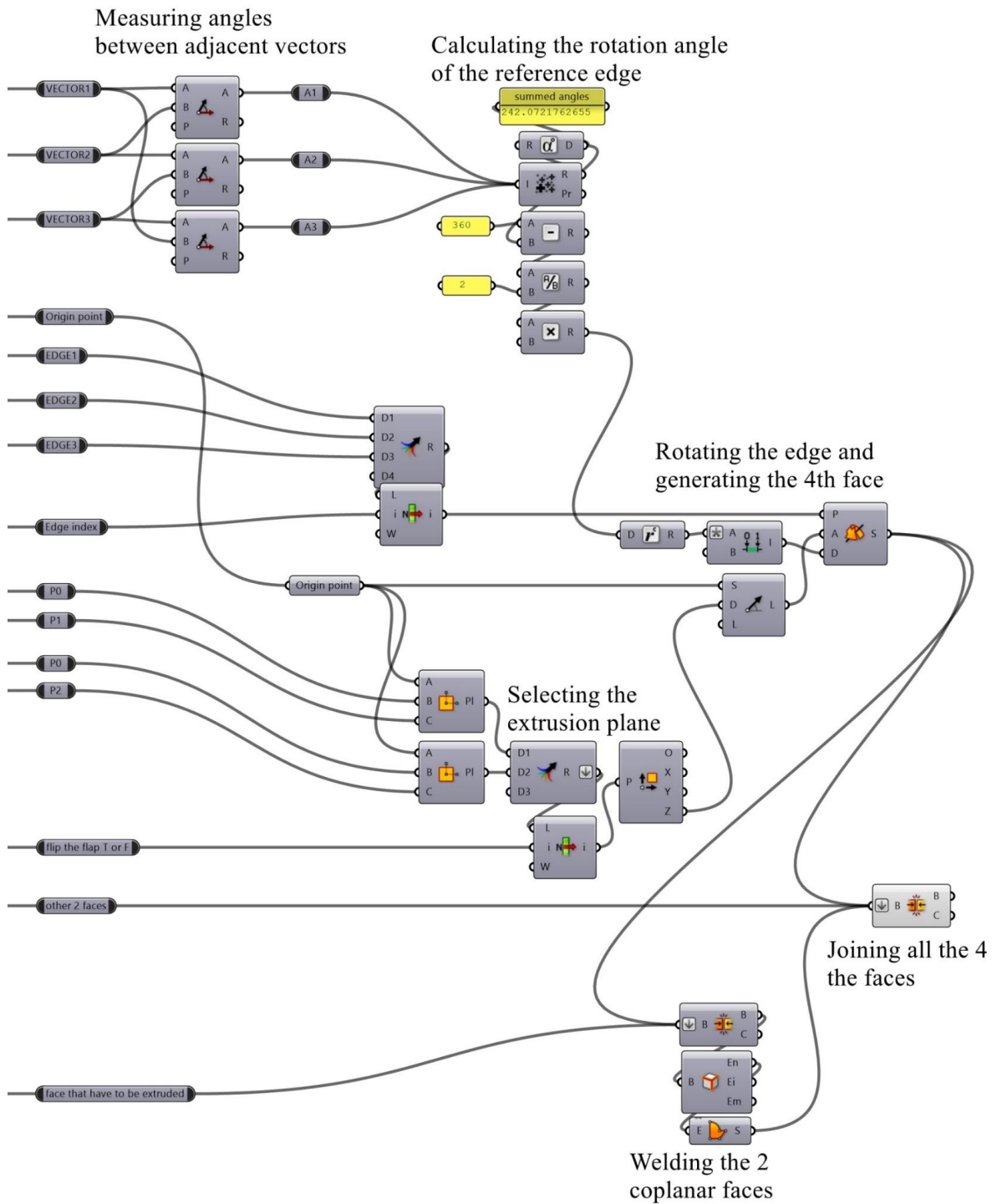
Appendix D.

Fabrication-aimed designs – Generative algorithms

In this appendix, we reported all the generative algorithms presented in CHAPTER VI.

D.1. Blocked Degree-4 Vertex – From a Non-Developable Corner of 3 Faces





Appendix E. Glossary

Accordion:	A sequence of alternated mountain and valley creases.
Algorithm:	A process or a set of rules to be followed to reach an expected result.
Array:	Collection of elements values or variables identified by an index.
Asymmetric reverse fold:	A reverse fold which is not flat-foldable.
Base:	A folded geometrical shape that has a structure which simplifies the desired subject.
Blocking crease:	The crease that hit 180° first in a pattern and arrests the motion of the whole mechanism. They can be more than one (e.g. in flat-foldable patterns all the creases hit 180° at the same time).
Boolean value:	A value which is “1” or “0” or reciprocally “True” or “False”.
Box pleating:	A folding technique which allows only the use of creases multiple of 45° , they are usually built on a grid.
B-rep:	B-rep stands for “Boundary representation”. In solid modelling and computer-aided design, it represents a collection of connected surfaces which defines the boundary between solid and non-solid.
Chaotic type:	It is a family of folded surfaces which has a crease pattern characterized by an irregular mesh of creases.
Circle packing:	Placing circles on a surface so that they do not overlap.
Circle river method:	A folding technique that constructs the crease pattern by packing non-overlapping circles and rivers into the surface which is usually a square.
Closed sink fold:	A sink fold which locks after folding. It usually cannot be performed rigidly, it needs to exploit the paper flexibility often crumpling or forcing the point while pushing it inside.
Cluster:	A group of items nested into a single new item.
Collapse:	This term describes the action of folding a crease pattern all at once to form the folded base.
Corrugation:	A particular type of tessellation that has no triple or more layers overlapped. The entire original surface of the paper is usually visible. The most common corrugations are in form of a wave with alternated peaks and valley.
CP:	Crease Pattern.
Crease:	The mark that appears on the paper after folding and unfolding it.
Crease assignment:	Determination if a crease is mountain or valley.
Crease pattern:	The scheme of creases on a flat sheet that is necessary to fold a particular base.

Crimp fold:	A sequence of symmetric valley and mountain creases with respects of a central pre-existing crease.
Curved fold:	A fold that starts from a curved crease and exploits the flexibility of the material to configure the surface into a curved shape. It can be performed only with a flexible sheet of material unless the ruling is predetermined, thus the curve has to be discretized into a polygonal chain.
Degree-4 vertex:	A point inside a crease pattern where only four creases meet.
Degree>4 vertex:	A point inside a crease pattern where more than four creases meet.
Developable:	That can be unrolled/unfolded on a plane.
Dihedral angle:	The angle between two faces adjacent to the same crease, it is defined as the angle between the normal vectors of the faces.
DOF:	Degree of freedom.
Edge:	A single linear segment which is on the perimeter of a face or a sheet of paper.
Flap:	A region paper which is usually attached to the rest of the base by a single edge. It can be composed of one or more layer of folded paper.
Flat-foldable:	A pattern that can be folded in the plane.
.fold:	Acronym of “Flexible Origami List Data-structure” is a file format (with extension .fold) for describing origami models with meshes. Developed by E. D. Demaine, J. S. Ku and R. J. Lang.
Fold angle:	The angle between the limbs of a fold. Usually, it is measured by measuring the angle between the normal vectors of the faces adjacent to the crease.
Folding mode:	Way to rigid-fold a pattern with a specific mountain/valley assignment. Any pattern usually has more than one folding mode.
Generative algorithm	A sequence of operations that generates a particular result
Generatrix:	A moving point, line, or surface forming a line, surface, or solid.
Grafting:	Modifying a crease pattern by slicing it along existing creases and adding a strip of new paper in order to add new features.
Hex pleating:	A design technique similar to box pleating but that uses only angles multiple of 30°. It usually starts from a grid made by equilateral triangles.
Hinge:	A movable joint which connects adjacent faces or flaps.
Huzita-Justin axioms:	A set of rules related to the mathematical principles of paper folding. They explain the operations that can be made while folding a piece of paper in the plane.
Inside reverse fold:	A type of reverse fold which changes the direction of the tip of a flap keeping its layers inside the rest of the flap.
List:	Several connected items that are written consecutively one below the other.

Macro-molecule:	A group of molecules.
Miura pattern:	Or Miura ori. It is a pattern made by rhomboid faces. It is famous to be one of the easiest one-DOF corrugations. It has been used by the engineer Koryo Miura to optimize the packing of solar panels for space travels.
Molecule:	Part of a crease pattern that can be attached to another molecule by matching the outer edges and vertices of the crease pattern with corresponding edges and vertices of a different molecule.
Mountain fold:	A crease that is convex from the observer point of view. It is usually drawn with a red dot-dot-dash line or dash-dotted line.
Node:	The endpoint of a line in a scheme structured as a tree. In Grasshopper, the nodes are the components which perform specific operations that can be connected one to each other with wires.
Nodal definition:	A group of linked nodes that make an algorithm in Grasshopper. Once set off, these definitions perform specific operations in a digital environment.
Non-developable:	That cannot be unrolled/unfolded on a plane.
Non-flat-foldable:	A pattern that can not be folded in the plane.
Nurbs:	Acronym for “Non-uniform rational basis spline”. It is a mathematical model commonly used in computer graphics for generating and representing curves and surfaces.
Offset base:	A base with a shifted crease pattern compared with the traditional. The shifting preserves the angle between the creases and it creates space in some location of the crease pattern which can be used to add features.
Origami:	Japanese word formed by “Ori” meaning “Folding” and “Kami” meaning “Paper”. It is the art of folding paper usually performed without cutting or glueing. It is usually associated with Japanese culture.
Open sink fold:	A sink fold which does not lock after folding. It can usually be performed without flexing or crumpling the paper.
Outside reverse fold:	A type of reverse fold which changes the direction of the tip of a flap keeping its layers outside the rest of the flap.
Petal fold:	A combination of two squash folds narrowed to form a rhomboid shape. It is used to fold the petals of the traditional iris flower.
Planar curved fold:	A curved fold that lies on a plane. It is usually performed by reflecting a developable ruled surface with respect of a slicing plane.
Pleat fold:	A sequence of alternated mountain and valley creases through one or more layers of paper.
Pre-creasing:	Folding and unfolding a crease before collapsing it. It is preferred to perform a pre-creasing before complex steps.
Rabbit-ear fold:	A type of folding that makes a flap from a triangular face by folding along the three bisectors of the triangle.
Reciprocal diagram:	A graphical tool for understanding and designing structural systems. In origami is used to investigate the first order approximation of rigid origami and other kinetic properties.
Recursive tessellations:	Is a particular type of tessellation where the same folds are repeated in a smaller scale following the principles of fractals figures. (The hydrangea of Fujimoto is one of the most famous).
Reverse fold:	A type of fold that changes the direction of a flap by partially inverting the direction of the central mountain or valley crease.

Rigid-foldable:	Something that is foldable without flexing or stretching the faces.
River:	A curved or rectangular constant-width region of paper that space the flaps in a crease pattern.
Self-arrests:	When a rigid origami structure reaches a state where at least one crease hit a fold angle of 180°, thus the two adjacent faces are colliding and co-planar.
Self-blocks:	See “Self-arrests”.
Semi-pre-folded:	It is said about origami patterns which are configured in an intermediate folding state which is not unfolded nor completely folded.
Shape-oriented type:	It is a family of folded surfaces which has a crease pattern characterized by creases arranged specifically to make a particularly shaped figure.
Shaping:	The act of sculpting the abstract geometric base to form the finished model. In shaping sometimes, the paper is stretched or folded with free-form or curved creases.
Single linear crease:	A non-curving crease that does not intersect any other crease.
Sink fold:	A fold performed on an internal vertex which forms a pointy flap. It consists in mirroring the point inside the model, by inverting the mountain valley assignment of the last tip of the point and pushing it inside while collapsing it.
Squash fold:	A type of fold where a single multi-layered-flap is opened and its layers are spread and flattened (usually) symmetrically.
Structured type:	It is a family of folded surfaces which has a crease pattern characterized by groups of equal tiles.
Swivel fold:	The asymmetric version of the squash fold, where usually there is a pivot point on one of the creases, around which the whole flap rotates while being spread and flattened.
Tessellation:	It is a particular type of origami made by equal molecules that can be spread in all the directions, the limit is only the dimension of the paper used. Tessellations are usually exhibited showing the front and back side or with backlight.
Tile:	A portion of a crease pattern that can be assembled into crease patterns by matching circles and river boundaries.
Tree structure:	The branched structure that contains lists or items at different hierarchy levels.
Triangulated accordion:	An accordion where all the quadrangular faces are divided along the diagonals and all the creases are redefined with an alternated mountain/valley assignment.
Unfold:	Open a folded model obtaining, as a result, a creased sheet of paper.
Unfoldable:	Something that cannot be folded.
Unsink:	Removing a sink fold.
Valley fold:	A crease that is concave from the observer point of view. It is usually drawn with a blue dashed line.
Vertex:	A point in a crease pattern where more than one crease converges.
Wire:	A line, thread or string that connects two nodes. In Grasshopper, wires are used to input into one or more nodes the outputs of other nodes. They move data in form of single items, lists, or trees.

Contacts:

riccardo.foschi2@unibo.it
riccardo.foschi28@gmail.com

Department of architecture,
University of Bologna,
Viale del Risorgimento, 2, 40136, Bologna (BO), Italy.

